TARGETED LIPID BASED DRUG DELIVERY SYSTEM OF β- CARYOPHYLLENE OXIDE USING NOVEL NANOCARRIER FOR TREATMENT OF BREAST CANCER

A Thesis

Submitted towards the Requirements for the Award of Degree of

Doctor of Philosophy
In

Pharmacy

Under the Department of Pharmacy

by

RENU DINKAR
(Enrollment No. 161555816239)

Under the Supervision of

Dr. Sobha Ram Sahu
Professor
P.K. UNIVERSITY



2026
P.K. UNIVERSITY
NH-27, Vill. Thanra (P.O. Dinara)
Shivpuri, M.P. India - 473665
www.pkuniversity.edu.in



This Piece of Work
is

Dedicated
To

My Beloved Parents

Whose blessings & love, brought me to this level.....

Renu Dinkar.....

DECLARATION BY THE CANDIDATE

I declare that the thesis entitles "**TARGETED LIPID BASED DRUG DELIVERY SYSTEM OF β-CARYOPHYLLENE OXIDE USING NOVEL NANOCARRIER FOR TREATMENT OF BREAST CANCER**" is my own work conducted under the supervision of Dr. Sobha Ram Sahu Sir at Department of Pharmacy P. K. University(MP) India.

Approved by Research Degree Committee. I have put more than 240 days of attendance with supervisor at the center.

I further declare that to the best of my knowledge the thesis does not contain part of any work which has been submitted for the award of any degree either in this University or in any other University, without proper citation.

Signature of the candidate

Date:

Place:

CERTIFICATE OF THE SUPERVISOR

This is to certify that the work entitled "**TARGETED LIPID BASED DRUG DELIVERY SYSTEM OF β- CARYOPHYLLENE OXIDE USING NOVEL NANOCARRIER FOR TREATMENT OF BREAST CANCER**" is a piece of research work done by Mrs. RENU DINKAR Under my Guidance and Supervision for the degree of Doctor of Philosophy of Faculty of Pharmacy, P.K. University (MP) India.

I certify that the candidate has put an attendance of more than 240 days with me. To the best of my knowledge and belief the thesis:

I. Embodies the work of the candidate herself.
II. Had duly been completed.
III. Fulfill the requirement of the ordinance relating to the Ph.D. degree of the university.

Signature of Supervisor

Date …….

15% Overall Similarity

The combined total of all matches, including overlapping sources, for each database.

Filtered from the Report

› Bibliography

Match Groups

148 Not Cited or Quoted 23%
Matches with neither in-text citation nor quotation marks

4 Missing Quotations 1%
Matches that are still very similar to source material

3 Missing Citation 0%
Matches that have quotation marks, but no in-text citation

0 Cited and Quoted 0%
Matches with in-text citation present, but no quotation marks

Top Sources

15% Internet sources
14% Publications
18% Submitted works (Student Papers)

P.K.UNIVERSITY
SHIVPURI (M.P.)

University Established Under section 2f of UGC ACT 1956 Vide MP Government Act No 17 of 2015

Ref. no.:- PhD/PKU/2026/03/40 Date: 31/03/2026

Pre – Ph.D Submission Presentation Certificate

This is to certify that **Renu Dinkar, Enrollment No: 161555816239,** research scholar in Pharmacy under the supervision of **Dr. Shobha Ram Sahu**, Faculty of Pharmacy has given her open pre- Ph.D. submission presentation on the approved topic "**Targeted Lipid Based Drug Delivery System of β-Caryophyllene Oxide Using Novel Nanocarrier For Treatment of Breast Cancer**" on Date 30/03/2026 at Time 02:00 PM in the P.K. University, Shivpuri (MP).

Dean Academic
P.K. University
Shivpuri (M.P.)

DEAN ACADEMIC
P.K.UNIVERSITY
SHIVPURI (M.P.)

ADDRESS: VILL: THANRA, TEHSIL: KARERA, NH-27, DIST: SHIVPURI, M.P. 473665,
MOB: 7241115088, Email:registrar.pkuniversity@gmail.com

P.K. University

Shivpuri (M.P.)

Enrolment Number: 161555816239

Result

Enrolment Number :	161555816239		
Candidate Name :	RENU DINKAR	**Course :**	Ph.D. in Pharmacy (Course Work)
Father's Name :	SHIV DAS DINKAR	**Year/Sem :**	1
Mother's Name :	DHAN DEVI	**Session :**	2021-22

Subject Name	Internal T	Internal T	Internal P	Internal P	External T	External T	External P	External P	
Research Methodology	N/A	N/A	N/A	N/A	50	42	N/A	N/A	42 / 50
Subject Specialization	N/A	N/A	N/A	N/A	100	77	N/A	N/A	77 / 100
Review of Literature	N/A	N/A	100	74	N/A	N/A	N/A	N/A	74 / 100

Marks Obtained 193 Result Pass Max Marks 250

Marks Obtained: 193

Result: Pass

Max Marks: 250

Notes:

• Student must pass in Theory and Practical separately.

• For pass the candidate is required to obtain 40% marks in each paper and 50% marks in aggregate.

• For pass the PhD candidate is required to obtain 65% marks in aggregate.

COPYRIGHT TRANSFER CERTIFICATE

Title of the Thesis: "**TARGETED LIPID BASED DRUG DELIVERY SYSTEM OF β-CARYOPHYLLENE OXIDE USING NOVEL NANOCARRIER FOR TREATMENT OF BREAST CANCER".**

Candidates Name: **Mrs. Renu Dinkar**

COPYRIGHT TRANSFER

The undersigned hereby assigns to the P.K.University ,Shivpuri (MP) all the copyrights that exist in and for the above thesis submitted for the award of the Ph.D. degree.

Date : **Mrs. Renu Dinkar**

Signature

Note: However, the author may reproduce/publish or authorized others to reproduce material extracted verbatim from the thesis or derivative of the thesis for author's personal use provided that the source and the University's copyright notice are indicated.

FORWARDING LETTER OF THE HEAD OF INSTITUTION

The Ph.D. thesis entitled "**TARGETED LIPID BASED DRUG DELIVERY SYSTEM OF β- CARYOPHYLLENE OXIDE USING NOVEL NANOCARRIER FOR TREATMENT OF BREAST CANCER**" Submitted by **Mrs. RENU DINKAR** is Forwarded to the university in six copies. The candidate has paid the necessary fees and there are No Dues outstanding against her.

Name …….. ……Seal ……

Date ……. Place …….

Signature of Head of Institution where

the Candidate was Registered for PhD degree

Signature of Supervisor

Date …… Address……..

Place……

ACKNOWLEDGEMENT

The Acknowledgement of a research endeavor opportunity to express appreciation for the joint effort of those who have been sources of motivation and support, and who have contributed invaluable knowledge towards achieving success in the pursuit of knowledge. With utmost humility and pride. I reflect on the inspiring individuals who have propelled my work forward, and I am filled with immense pleasure, gratitude and thanks for their unwavering dedication. First for most I would like to thank almighty god for perservence, courage and strength bestowed on me in undertake this project

For most. I extend my deepest appreciation to my esteemed Supervisor, **Dr. Sobha Ram Sahu**, Faculty of Pharmacy, P.K. University, Shivpuri, (M.P.) without whom this work would not have come to fruition 1 exceptional guidance, unwavering support kind cooperation and provision of a conductive work environmental have been invaluable beyond measure. I remain indebted to her instilling in me a relentless pursuit of excellence, a strong sense of honesty, and respect for ethical principles that govern our profession.

Furthermore, I extend my sincere thanks to the **Mr. Jagdeesh Prasad Sharma** Chancellor, PK University Shivpuri (M.P) for providing the necessary infrastructure and facilities that were essential during my research work. My profound sense of gratitude, faith, and we also go to **Prof. (Dr.) Mukesh Chansoriya** Vice Chancellor, P.K University Shivpuri (M.P) for his generous and valuable support throughout my research.

I take this pleasant opportunity to express my deep sense of gratitude and reverences to his holiness **Dr. Jitendra Kumar Mishra** Director, P.K University Shivpuri (M.P.) for his constant encouragement and providing me with the required facilities that enabled me to complete my project work.

Dr. Jitendra Malik Registrar, P.K University, Shivpuri (MP), who has inspired with his encouraging guidance and support right from the beginning of this work in spite of his busy schedule. I am short of words to thank him for his affectionate behavior and patience throughout the duration of research work.

I express my gratitude to **Dr. Aiman Fatima**, Dean Academics, of P.K. University, Shivpuri, (M.P.)

I would also like to extend my gratitude to and deep appreciation to respected **Dr. Ashish Vishwakarma**, Dean Research of P.K. University, (M.P.)

I owe a great deal of application and gratitude to entire faculty members of Faculty of Pharmacy P.K. University, **Dr. Vivek Gupta** (Principal). all teaching and all non-teaching staff of Faculty of Pharmacy without their support it would have been difficult to shape my research work.

I also express my gratitude to **Miss Nisha Yadav**, Librarian of P.K University along with **Mr. Anand Kumar**, Assistant Librarian and other staff of P.K. University I am also thankful to **Mr. Pankaj Singh. Mr. Alok Khare, and Mr. Prushottam Yadav** L.T. Cell of P.K. University.

I have no words to express my gratitude to my beloved parent's dear brother's and my husband for their love, support and constant encouragement during the entire course of my research work.

I have no words to express my gratitude to my beloved parent's dear brother's and my husband for their love, support and constant encouragement during the entire course of my research work.

Last but not least I would like to honestly appreciate the fact that it is my pleasure to have opportunity to pursue my higher education at P.K. University, Shivpuri (M.P). I owe my permanent deht towards it; this is having the special place in my heart for shaping my care.

1 must also express my love and affection to my family members for his understanding and unwavering love during my research tenure, Lastly, I am highly grateful to God, the almighty, for giving me courage and strength in face the most difficult times of life and for answering my prayers in a special way. 1 remain grateful for all that I have achieved in my life thus far.

Date…….. RENU DINKAR

Place…… Enrolment No: (161555816239)

Table of Contents

Chapter 1 Introduction 2
1.1 Breast Cancer 2
1.1.1. Statistics and Etiology 2
1.1.2. Breast cancer subtypes and classification 3
1.1.3. Diagnosis of Breast carcinoma 3
1.1.4. Management of Breast carcinoma and Treatment options 4
1.2. Triple Negative Breast Cancer (TNBC) 4
1.2.1. Challenges in treatment of TNBC 5
1.3. Anticancer agents of herbal origin 6
1.3.1. Caryophyllenes 7
1.3 Role of adjuvant therapy 14
Chapter 2: Literature survey 20
Chapter 3: Rationale 26
Chapter 4: Drug profile 31
Beta-caryophyllene oxide 31
Chapter 5: List of equipment and materials 34
Chapter 6: Formulation development and optimization 44
6.1 Introduction 44
6.1.1. Lipid nanocarriers: Solid Lipid Nanoparticles 44
6.1.2. Lipid nanocarriers: Nanostructured Lipid Carriers (NLC) 51
6.1.3. Applications in cancer therapeutics 53
6.2. PREFORMULATION 57
6.2.1. Identification and Standardization of API 58
6.2.2. Characterization of morphology and bulk crystallinity 58
6.2.3. Stability indicting analytical method development 59
6.2.4. Solubility profile in lipids and surfactants 64
6.3. Formulation development and optimization 66

6.3.1. Quality by Design (QbD) 66
6.3.2 Formulation of BCPO loaded solid lipid nanoparticles (BC-SLN) 72
6.3.3. Formulation and optimization of BCPO loaded nanostructured lipid carriers (BC-NLC) 74
6.3.4. Chemical conjugation of folic acid and stearic acid 76
6.3.5. Sterilisation of developed formulation 78
6.4. Characterization 80
6.4.1. Particle size and size distribution (polydispersity index) 80
6.4.2. Zeta potential 80
6.4.3. Scanning electron microscopy 80
6.4.4. Transmission electron microscopy (TEM) 80
6.4.5. Drug loading and Entrapment efficiency 81
6.4.6. In vitro drug release 81
6.4.7. In vitro release kinetics 82
6.4.8. Solid-state characterization 82
6.4.9. Evaluation of Folic acid-Stearic acid conjugate by FT-IR, NMR and mass spectrometry 82
6.4.10. Stability studies 83
6.4.11. In vitro haemolysis study 83
6.4.12. In vitro cytotoxicity studies on cancer cell lines 84
6.4.13. In vitro cytotoxicity on fibroblast cells 85
Chapter 7: Results and Discussion 89
7.1. Preformulation studies 89
7.1.1. Identification and Standardization of API 89
7.1.2. Characterization of morphology and bulk crystallinity 92
7.1.3 Stability indicting analytical method development 93
7.1.4. Solubility profile in lipids and surfactants 111
7.2. Formulation development and optimization 115

7.2.1. Formulation of BCPO loaded solid lipid nanoparticles (BC-SLN)..... 115
7.2.2. Effect of other processing parameters on Particle size 123
7.2.3. Formulation and optimization of BCPO loaded nanostructured lipid carriers (BC-NLC) 124
7.2.4. Optimization of level of DHA with full factorial design 125
7.2.5. Preparation of Folic acid-Stearic acid conjugate 131
7.2.6. Incorporation of Folic acid-Stearic acid conjugate in developed formulation 132
7.2.7. Sterilisation of developed formulation..... 133
7.3. Characterization 135
7.3.1. Particle size and Polydispersity index..... 135
7.3.2. Zeta potential..... 135
7.3.3. Scanning electron microscopy..... 135
7.3.4. Transmission electron microscopy (TEM)..... 136
7.3.5. Drug loading and entrapment efficiency..... 136
7.3.6. In vitro drug release 138
7.3.7. In vitro drug release kinetics 140
7.3.8. Solid state characterization..... 142
7.3.9. Evaluation of conjugate 144
7.3.10. In vitro haemolysis study 146
7.3.11. Stability studies..... 146
7.3.12. In vitro cytotoxicity studies on cancer cell lines..... 147
7.3.13. In vitro cytotoxicity studies on fibroblast cells 149
7.4. Summary and conclusion 151
Chapter 8: In vivo evaluation..... 155
8.1. Introduction..... 155
8.2. Experimental methodology..... 165
8.2.1. Acute Toxicity studies 165
8.2.2. In vivo biodistribution study 167

8.2.2.1. Radiolabelling studies of formulation and optimization 167
8.2.2.2. Animal experiments 168
8.2.3. In vivo efficacy study 170
8.2.4. Pharmacokinetic analysis 172
8.3. Results and discussion 174
8.3.1. Acute Toxicity studies 174
8.3.2. In vivo biodistribution study 176
8.3.2.1. Radiolabelling studies of formulation and optimization 176
8.3.2.2. Animal experiments 180
8.3.3. In vivo efficacy studies 185
8.3.4. Pharmacokinetic analysis 190
8.3.5. Summary of in vivo studies 197
Chapter 9 Summary and conclusions 199
10. Bibliography 204
11. Publications, Presentations and Achievements 227

List of figures

Figure 1.1 Biosynthesis of pathway of BCPO and its analogues 8
Figure 1.2 Schematic structure of caryophyllene 9
Figure 1.3: Derivatives of Caryophyllene 9
Figure 1.4 a) Eicosapentanoic acid b) Docosahexanoic acid 14
Figure 1.5 Structure of Folic acid 17
Figure 4.1 Structure of beta caryophyllene oxide 32
Figure 5.1 Structure of Glyceryl Di-behenate 39
Figure 5.2 Structure of folic acid 41
Figure 5.3 Structure of stearic acid 42
Figure 6.1Membrane contractor method for preparation of SLNC 46
Figure 6.2Models of drug incorporation for SLN 51
Figure 6.3Schematic of SLN and NLC crystal arrangement 52
Figure 6.4 Structural types of NLCs 53
Figure 6.5. Stearic acid-Folic acid conjugation scheme 77
Figure 7.1 DSC-TGA showing melting point of drug 90
Figure 7.2 Calibration curve of BCPO in 3% SLS solution 91
Figure 7.3 FT-IR spectra of BCPO 92
Figure 7.4 Microscopic appearance of BCPO 92
Figure 7.5 SEM image of BCPO particles 93
Figure 7.6 XRD pattern of BCPO 93
Figure 7.7 Chromatogram of BCPO 94
Figure 7.8 Contour plot for RT 98
Figure 7.9 Contour plot for peak area 98
Figure 7.10 Contour plot for NTP 99
Figure 7.11Perturbation plots for a) RT b) Peak area c) NTP 100
Figure 7.12Interaction plot for a) desirability b) RT c) peak area d) NTP 101
Figure 7.13 Overlay plot for Analytical method development 101
Figure 7.14 Calibration curve of BCPO by HPLC 103
Figure 7.15 Standard chromatogram of BCPO 103
Figure 7.16 Acid hydrolysis of drug 107
Figure 7.17 Alkali hydrolysis of drug 108
Figure 7.18 Oxidation of drug 109

Figure 7.19 Thermal degradation of drug 109
Figure 7.20 Microscopic observation of a) plain drug b) drug solubilised in solid lipid 111
Figure 7.21 Particle size and PDI for surfactants 114
Figure 7.22 Results of particle size for formulation trials with surfactants at 200 mg and 500 mg 117
Figure 7.23 Contour plot for Particle size 120
Figure 7.24 Contour plot for PDI 120
Figure 7.25 Correlation plots for predicted and actual for a) Particle size b) PDI 121
Figure 7.26 Perturbation plots for a) Particle size b) PDI 121
Figure 7.27 Interaction plot for a) Particle size b) PDI 122
Figure 7.28 Overlay plot 122
Figure 7.29 Effect of addition of increasing amount of DHA on particle size 125
Figure 7.30 Contour plot for %EE 128
Figure 7.31 Contour plot for particle size 128
Figure 7.32 Correlation plots for a) %EE and b) Particle size 129
Figure 7.33 Perturbation plots for a) %EE and b) Particle size 129
Figure 7.34 Interaction plots for a) %EE and b) Particle size 130
Figure 7.35 Overlay plot (ii) 130
Figure 7.36 Process of conjugation reaction 132
Figure 7.37 Effect of addition of conjugate on particle size 133
Figure 7.38 Results for Test for sterility (Aseptic area) 134
Figure 7.39 a) Particle size distribution b) Zeta potential 135
Figure 7.40 SEM images of a) Plain drug b) BC-NLC 136
Figure 7.41 TEM images of BC NLC 136
Figure 7.42 Ultracentrifuge samples without use of sodium sulphate 137
Figure 7.43 Effect of increasing amount of sodium sulphate on ultracentrifugation (from left to right) 137
Figure 7.44Effect of addition of liquid lipid on %EE and %DL 138
Figure 7.45 Drug release in pH 7.4 buffer 139
Figure 7.46 Drug release in 5% and 30% Ethanol release media 140
Figure 7.47 Release kinetics model fitting a) Higuchi model for SLN b) Higuchi model for NLC c) Korsemeyer-peppas model for SLN d) Korsemeyer-peppas model for NLC 142
Figure 7.48 DSC thermograms of a) BCPO b) Lipid c) BC-NLC 143
Figure 7.49 P-XRD diffractogram of a) BCPO b) BC-NLC C) Placebo 144

Figure 7.50 Dried Folic acid-Stearic acid conjugate 144
Figure 7.51 Mass spectra of Folic acid-stearic acid conjugate 145
Figure 7.52 FT-IR spectra of a) FA-SA conjugate b) Folic acid c) Stearic acid..... 146
Figure 7.53 Growth Curve: Human Breast Cancer Cell Line MCF-7 148
Figure 7.54 Growth Curve: Human Breast Cancer Cell Line MDA-MB-468..... 148
Figure7.55 Microscopic images of samples for cytotoxicity study a) BCPO b) DHA c) BCPO-DHA formulation d) Adriamycin e) Control 149
Figure 7.56 % inhibition vs conc. curve for a) BCPO, BC-NLC and b) Vincristine 151
Figure 8.1Linking of radionuclide to pharmaceutical entity via a targeting agent 159
Figure 8.2 Scheme for Acute toxicity study 165
Figure 8.3 Automated gamma ray counter 168
Figure 8.4 Histopathology of internal organs 175
Figure 8.5 Reduction products of Pertechnetate 176
Figure 8.6Representation of calculation of Rf value..... 177
Figure 8.7 Representative gamma count of TLC plate developed in acetone as mobile phase 178
Figure 8.8 Gamma count of TLC plate in Spectrum acquisition and analysis software (SAAS) a) ^{99m}Tc labelled complex b) Pertechnetate ($^{99m}TcO_4^-$) impurity..... 178
Figure 8.9 a) Female NOD SCID mice with orthotopic tumour model b) Administration of radiolabelled formulation to experimental animals..... 180
Figure 8.10 Biodistribution of radiolabelled formulations in various organs a) FA-SLN b) Vehicle control c) SLN..... 181
Figure 8.11 Biodistribution pattern of radiolabelled formulations in a) Liver b) Kidney c) Blood…182
Figure 8.12 Biodistribution of radiolabelled formulations in tumour over a period of 24 hours.... 183
Figure 8.13 a) Relative tumour volume b) Animal body weight 186
Figure 8.14 Survival curve..... 187
Figure 8.15 Comparison of tumour volume of all groups 188
Figure 8.16 PET scans of tumour bearing animals for treatment groups of a) FA-BC-NLC, b) n-3 PUFA NLC, c) BC-NLC, d) Blank NP, e) Adriamycin f) Control..... 189
Figure 8.17 Linearity graph 190
Figure 8.18 GCMS chromatogram of Caryophyllene standard 191
Figure 8.19 Chromatogram of plasma Blank and 500ppb standard..... 192
Figure 8.20 Pharmacokinetic analysis of plasma a) BCPO b) BC-NLC.....196

List of tables

Table 1.1 Reported Biological activities of BCPO 10
Table 1.2 Anti-proliferative and anticancer action mechanisms in *invitro* studies 11
Table 1.3 Fatty acid transporter and their sites of expression 16
Table 1.4 Folate receptors and their expression 17
Table 4.1 Profile of beta caryophyllene 31
Table 5.1 List of equipment 34
Table 5.2 List of software 35
Table 5.3 List of solvent/chemicals and their sources 36
Table 5.4 Excipient profile of Compritol 888 ATO 39
Table 5.5 Excipient profile of Gelucire 50/13 40
Table 5.6 Excipient profile of Folic acid 41
Table 5.7 Excipient profile of stearic acid 42
Table 6.1 Lipids and emulsifiers for solid lipid nanoparticles 45
Table 6.2 Passive targeting potential of lipidic Nanocarriers to tumorous tissues 55
Table 6.3 Examples of receptors overexpressed in tumours 56
Table 6.4 Instrumental and chromatographic conditions for HPLC method 59
Table 6.5 Matrix design for 2^3 Factorial design (Analytical) 60
Table 6.6 Experimental design for optimization of analytical method development 60
Table 6.7 List of samples for drug-excipient compatibility study 63
Table 6.8 Solid lipids with melting points 64
Table 6.9 Experimental design for screening of surfactants 65
Table 6.10 Quality Target Product Profile (QTPP) 66
Table 6.11 Critical Quality Attributes 68
Table 6.12 Levels of uncertainty and definitions 69
Table 6.13 Definition of Severity levels 70
Table 6.14 Uncertainty or probability risk prioritization matrix 70
Table 6.15 Initial risk assessment 71
Table 6.16 Experimental design for selection of solid lipid 72
Table 6.17 Matrix design for 2^3 Factorial design I 73
Table 6.18 Experimental design for Gelucire 50/13 74
Table 6.19 Experimental design for Gelucire 48/16 74
Table 6.20 Addition of increasing amount of DHA to formulation 74

Table 6.21 Matrix design for 2^3 factorial design III 75
Table 6.22 Coded values for Experimental design II 76
Table 6.23 Addition of increasing amount of n-3 PUFA in formulation 77
Table 6.24 Kinetic models and their plots 82
Table 7.1 Physico-chemical properties of drug 89
Table 7.2 Characteristic functional groups of BCPO 91
Table 7.3 ANOVA for RT, peak area and NTP 94
Table 7.4 Predicted and Observed responses for HPLC method validation 102
Table 7.5 Results of system suitability 102
Table 7.6 Results of Precision study 104
Table 7.7 Results of Accuracy study 104
Table 7.8 Details of forced degradation studies 105
Table 7.9 Visual observation of Drug-excipient compatibility studies 110
Table 7.10 Drug-excipient compatibility study by HPLC 111
Table 7.11 Microscopic evaluation of drug-lipid mixtures 112
Table 7.12 Formulation trials with surfactants level at 200 mg 115
Table 7.13 Formulation trials with surfactants level at 500 mg 116
Table 7.14 ANOVA for Particle size and PDI 118
Table 7.15 Predicted and Observed responses for validation batch (BC-SLN) 123
Table 7.16 ANOVA for %EE and Particle size 125
Table 7.17 Predicted and Observed responses for validation batch (BC-NLC) 131
Table 7.18 Optimized formula for FA-BC-NLC 133
Table 7.19 Results for %EE and drug loading of BC-SLN and BC-NLC 138
Table 7.20 Results of release kinetics with regression co-efficients 141
Table 7.21 Results of in vitro haemolysis study 146
Table 7.22 Results of stability studies for BC-NLC 147
Table 7.23 % cell inhibition and IC50 value for BCPO and BC-NLC 150
Table 7.24 % cell inhibition and IC50 for vincristine 150
Table 8.1 LD50 value and results of acute toxicity study 157
Table 8.2 Biomarkers and parameters used in assessment of acute toxicity 158
Table 8.3 Overview of various imaging modalities 160
Table 8.4 Radioisotopes used in PET and their half-lives 161
Table 8.5 Radioisotopes used in SPECT and their half-lives 162
Table 8.6 Details for Acute toxicity study 165

Table 8.7 Details groups for Biodistribution study 169
Table 8.8 Experimental details for in vivo efficacy study.....171
Table 8.9 Instrumental parameters for GCMS.....173
Table 8.10 R_f values of radiochemical components in acetone and saline mobile phase 177
Table 8.11 Effect of increasing concentration of stannous chloride 179
Table 8.12 Stability of radiolabelled formulation 179
Table 8.13 %Dose/organ for radiolabelled formulations in tumour 183
Table 8.14 T/C ratio of Adriamycin, FA-BC-SLN and n-3PUFA-SLN 185
Table 8.15 Tumour images for each formulation group.....188
Table 8.16 Summary of calibrants and QC response of Caryophyllene analysis 190
Table 8.17 Quantitative results of GC-MS method development.....192
Table 8.18 Summary of Plasma Caryophyllene concentration in BCPO 194
Table 8.19 Summary of Plasma Caryophyllene concentration in BC-NLC.....195
Table 8.20 Pharmacokinetic parameters of BCPO and BC-NLC 196

List of abbreviations

Abbreviation	Full name
ANOVA	Analysis of variance
ATCC	American Type Culture Collection
BCPO	Beta Caryophyllene Oxide
BRCA	BReastCAncer gene
CQA	Critical Quality Attributes
CT	Computerized Tomography
DHA	Docosahexanoic acid
DL	Drug loading
DMEM	Dulbecco's Modified Eagle Medium
EDC	1-Ethyl-3-(3-dimethylaminopropyl) carbodiimide
EE	Entrapment efficiency
EFSA	European Food Safety Authority
EPA	Eicosapentanoic acid
EPR	Enhanced permeation and retention
ER	Estrogen receptor
FA	Folic acid
FDA	Food and Drug Administration
FDG	Fluorodeoxyglucose (18F)
FEMA	Flavours and Extracts Manufacturers Association
FTIR	Fourier Transform Infrared
GC-MS	Gas chromatography–mass spectrometry
GRAS	Generally Regarded As Safe
HER	Human Epidermal growth factor Receptor
HPLC	High Performance Liquid Chromatography
IAEC	Institutional Animal Ethics Committee
ICH	International Conference on Harmonization
JECFA	Joint Expert Committee on Food Additives
LOD	Limit of Detection
LOQ	Limit of Quantification
MRI	Magnetic Resonance Imaging

MTT	3-(4,5-Dimethylthiazol-2-yl)-2,5-Diphenlytetrazolium Bromide
MWCO	Molecular weight cut off
NLCs	Nanostructured Lipid Carriers
NMR	Nuclear Magnetic Resonance
OECD	Organisation for Economic Co-operation and Development
PCS	Photon correlation spectroscopy
PDI	Polydispersity Index
PET	Positron Emission Tomography
PHA	Preliminary Hazard Analysis
PR	Progesterone receptor
PUFA	Polyunsaturated fatty acids
QbD	Quality-by-design
QTPP	Quality Target Product Profile
RCP	Radiochemical purity
RES	Reticuloendothelial system
RT	Retention time
RTV	Relative Tumour Volume
SEM	Scanning Electron Microscopy
SLNs	Solid Lipid Nanoparticles
SLS	Sodium Lauryl Sulphate
SPECT	Single-Photon Emission Computerized Tomography
TEM	Transmission Electron Microscopy
TLC	Thin Layer Chromatography
TNBC	Triple Negative Breast cancer
XRD	X-ray diffraction

ABSTRACT

Breast carcinoma is the heterogeneous tumour and considered as most prevalent female cancer worldwide. Current treatment regimen for breast cancer involves hormonal therapy, surgery, radiotherapy and chemotherapy. However, there are several limitations of the conventional approaches for treatment such as resistance of Triple negative breast cancer towards hormonal therapy, cytotoxicity to normal cells, high cost. This necessitates need of an alternative treatment which offers lesser side effects, targeted action and lower cost. The present investigation aims at developing a formulation that addresses such major concerns in treating breast cancer. The formulation strategies involve: 1] Use of an herbal principle, β-caryophyllene oxide (BCPO): easy availability, low cost, proven anticancer activity. 2] Solid lipid nanoparticle (SLN) system for drug delivery: SLN will lead to protection of drug from degradation, provide stability to the drug after IV administration and prevent leaching of drug at non-targeted sites. 3] Use of n-3Polyunsaturated fatty Acid (n-3PUFA), compound from natural origin: offers selective cytotoxicity towards cancer cells, acts as a lipid excipient with anticancer action. 4] Active Targeting of SLN with Folic acid: Targeting will aid in tumour site specificity resulting in reduced dose and side effects.

The developed SLN formulation will lead to significant improvement in available treatment options for breast cancer. The technology used is safe, scalable and has potential for clinical use. Also, it can act as platform technology for treatment of tumours at other sites.

Methodology:

The drug (BCPO) was standardized and authenticated by various methods such as FT-IR, HPLC, DSC and XRD. Solid lipid nanoparticles of BCPO were developed by melt emulsification method. In order to impart targeting properties to developed nanoparticles, a targeting ligand consisting of folic acid was separately developed by chemical conjugation method. Developed conjugate was further incorporate into nanoparticles and the formulation was optimized with the use of factorial design. Optimised formulation (FA-BCPO-SLN) showed the particle size of 178 nm with PDI of 0.4. FA-BCPO-SLN was observed to be showing sustained drug release (9% drug release over 24 hours) in contrast to plain drug which showed 60% drug release in 24 hours. To evaluate the anticancer potency of developed formulation, the formulation was exposed to in vitro cytotoxicity studies. FA-BCPO-SLN was observed to be showing enhanced cytotoxic effect on MDA-MB-468and MCF-7 cell lines. Further FA-BCPO-SLN was tested against normal fibroblast cell line consisting of healthy

cells. FA-BCPO-SLN was found to be showing fewer toxic effects towards healthy cells as compared to standard anticancer drug Vincristine. Acute toxicity study was performed on FA-BCPO-SLN with maximum possible drug loaded in formulation. The formulation was found to be safe to administer without any toxic effects at the dose of 37.5mg/kg. Distribution of FA-BCPO-SLN in body upon intravenous administration was studied in tumour bearing mice by the method of radiolabelling and gamma scintigraphy. FA-BCPO-SLN was found to accumulating in tumour at higher concentrations as compared to non-targeted formulation. Efficacy of FA-BCPO-SLN to arrest tumour was evaluated by in vivo efficacy study. The formulation was injected to tumour bearing mice and the tumour growth was measured over the period of 30 days. FA-BCPO-SLN was found to be arresting tumour growth with T/C ratio of 0.37 against T/C ratio of 0.63 for standard anticancer agent Adriamycin. Pharmacokinetic (pk) studies were performed and the pk profile of drug and formulation was compared. The formulation was found to be getting eliminated from blood stream faster as compared to plain drug indicating the accumulation of formulation at target site thus further confirming the results obtained by biodistribution studies.

Interpretation:

Lipid based drug delivery system was developed with the use of novel functional excipients namely n-3 PUFA for a natural origin active ingredient (BCPO). The developed formulation shows acceptable particle size, good particle surface morphology and entrapment efficiency. The formulation shows minimal and controlled drug release at pH of blood thus leading to minimal off target toxicity and wastage of drug. Incorporation of targeting ligand (Folic acid) further added the site specificity to the formulation. In vitro cytotoxicity studies provided the evidence of the synergistic action of drug (BCPO) and novel functional excipients (n-3 PUFA). Further, the dose of the drug used to develop optimized formulation was estimated to be safe as observed from Acute Toxicity Studies. In vivo tumour efficacy studies proved the anticancer effect of FA-BC-NLC. It can be concluded that, the robust, safe, site specific and efficacious formulation of FA-BC-NLC was successfully developed for treatment of breast cancer. The developed formulation serves as potential alternative for treatment of breast cancer by intravenous route.

Key words:

Beta caryophyllene oxide, breast cancer, solid lipid nanoparticles, folic acid, targeted drug delivery, biodistribution, radiolabelling, gamma scintigraphy, in vivo efficacy

Chapter 1

Introduction

Chapter 1 Introduction

1.1 Breast Cancer

1.1.1. Statistics and Etiology

Breast carcinoma is currently most prevalent cancer type in females worldwide. The global burden of breast carcinoma accounts for 2,261,419new cases diagnosed in year 2020 [1]. Currently, 7.8 million female patients are living with this disease worldwide [2]. In India, it is the leading malignant disease among women in metro cities like Delhi, Mumbai constituting more than 30% of all cancers in females. The standardised incidence rates of breast cancer among Indian female is from 6.2 to 39.5 per 100,000 women. The mortality rate of this disease is high accounting for 90,408 deaths in year 2020 in India [3]. Breast cancer related deaths are estimated to rise continuously with estimated deaths of 11.5 million by the year 2030. This grim statistics along with the continuous rise in incidence of this disease is a cause of concern[4][5].

Incidence of breast cancer cases were observed to be most prevalent in developed countries. However, the disease is now known to cause higher prevalence as well as high mortality in developing countries. In India, the rise in breast cancer cases is also accompanied by the occurrence of the disease in younger age group patients as compared to their counterparts in western countries. The age of onset of the disease in India is a decade earlier than western countries[5].

Breast cancer involves complex etiology and several risk factors have been identifies as possible causative agents for breast cancer. Several underlying causes may involve family history of the particular disease, age at first pregnancy, exposure to hormone replacement therapies, obesity, menstrual and reproductive history, early menarche, parity, breast density and also other factors such as alcohol consumption and diet[6][7][5]. There is also a strong correlation underlined between genetic mutations in BRCA 1 and BRCA 2 and increased risk of breast cancer[7].

1.1.2. Breast cancer subtypes and classification

Origin of breast cancer lies in breast tissues lining the milk producing lobules (lobular carcinoma) or lining the ducts that carry the milk to the nipples (ductal carcinoma). Cancers originating in lobules and ducts (in situ carcinoma) are classified as adenocarcinoma whereas cancers originating in connective tissues of breast are classified as sarcomas[7][5][8]. Ductal carcinoma (invasive and non-invasive) is known to be most prevalent type of cancer with invasive ductal carcinoma accounting for almost 80% of the cases[8]. Invasive ductal carcinoma carries the risk of metastasis to other body parts including bone, brain through bloodstream and lymphatic system[8].

Breast cancers are also classified based on their molecular characteristics and expression of hormonal receptors such as progesterone receptor (PR), estrogen receptor (ER) and human epidermal growth factor receptor (HER2 and HRE1)[8][9][10]. In newly diagnosed breast cancer cases, confirmation of ER, PR and HER2 status is mandatory in order to decide the treatment regimen. ER and PR positive cases roughly comprise of 75% of breast cancer and show better prognosis with hormonal therapy[11][9][12]. The cancer subtype which does not show any expression of hormonal receptors or HER2 protein is termed as Triple Negative Breast cancer (TNBC). TNBC comprises of almost 15% to 20% of the cases and is known to show poor prognosis, to be more aggressive subtype and is difficult to treat[13].

1.1.3. Diagnosis of Breast carcinoma

With the advancements in technology, there are multiple options available for detection of breast cancer in early stages. However, regular clinical breast examination and mammography still maintain their importance in early diagnosis in high risk patients[5]. For full focal diagnosis of breast cancer type and stage, patients need to undergo triple assessment which involves clinical evaluation followed by running various imaging tests and pathological examination. Various radiological imaging techniques including Ultrasound, Magnetic Resonance Imaging, CT scan, PET scan have been proven to be promising tools for identification of impalpable lumps in dense breast tissue as well as in monitoring the tumour response to treatment strategies. Pathological assessments including core biopsy, fine needle aspiration cytology (FNAC), surgical biopsy, punch biopsy give valuable information regarding the benign or malignant status of tumour, invasive or non-invasive nature of tumour as well as help in grading the stage

of tumour[5][8][14]. Tumour should also be assessed for its hormone receptor positive status and HER2/neu protein status during diagnostics stages[10].

1.1.4. Management of Breast carcinoma and Treatment options

Breast cancer patients need management on pathological, psychological and emotional levels. Treatment strategies for breast cancer patients majorly focus on relieving the symptoms, maintaining the good quality of life and preventing the recurrence of cancer. Depending on the stage and type of the tumour, various treatment options available include surgical removal of tumour, hormonal therapy or chemotherapy. Surgical removal of tumour involves mastectomy (removal of breast tissue) or lumpectomy, also known as breast conserving surgery (BCS)[7][5][11][8]. Patients with tumour size over 4 cm and local recurrence are treated with mastectomy. Mastectomy may be followed by breast reconstruction with the help of various oncoplastic techniques available[14]. Surgical removal of tumour is often followed by radiation therapy. Radiation therapy helps in destruction of any cancerous tissue left behind after surgery[5]. Systemic therapy can be administered either before the surgery (neo-adjuvant chemotherapy) to shrink the tumour size or after surgical tumour removal (adjuvant chemotherapy) to prevent the recurrence. In advanced stages of cancer, systemic therapies have additional roles of prevention of relapse, palliative care and maintaining overall quality of life. In case of metastasis, the goal is to choose the regimen with least toxicity[15].

Hormone receptor positive tumours are often treated with hormonal therapy. Estrogen is known to promote cell division in breast cancer. Thus, manipulation of hormonal levels in body is proven to be advantageous for treating breast cancer patients. Hormonal therapy includes use of selective estrogen receptor modulators (SERM) such as tamoxifen as well as aromatase inhibitors such as anastrozole. Choice of hormonal therapy also often depends upon the menopausal status of patient. In pre-menopausal women, surgical removal of ovaries is often undertaken in order to control the circulating levels of hormones. However in post-menopausal women, use of aromatase inhibitors is now proven to be a gold standard[15]. In metastatic stages, hormonal therapy is also used to lower the growth rate of already growing tumour[5].

1.2. Triple Negative Breast Cancer (TNBC)

Breast cancer subtype which does not express hormonal receptors including Progesterone receptor (PrR), Estrogen receptor (ER) as well as there is no or very less expression of HER2

receptor is termed as Triple Negative Breast cancer (TNBC). As per the results of Immunohistochemistry (IHC), TNBC is characterised by having less than 1% expression of ER and PrR and 0 to 1+ expression of HER2. TNBC is typically characterised as heterogeneous breast cancer subtype showing poor prognosis. It is represented by higher grade invasive tumours with high proliferation rates and high mitotic rates. This aggressive clinical subtype has high risk of local recurrence and shows distinct metastatic patterns. TNBC represents around 10% to15% of all breast cancer cases. As per the estimates, of total worldwide burden of 1 million cases of breast cancer per year, TNBC accounts for approximately 170,000 cases[16][17]. Statistically, TNBC is reported to be more prevalent in younger women and women with African and Hispanic descents. High prevalence of TNBC has also been observed in patients with mutation in BRCA1 gene[18][16]. TNBC shows high rates of recurrence within 3-5 years of diagnosis. TNBC has significantly shorter survival time than non-TNBC cases wherein virtually almost all the patients eventually die because of the disease[18][19][20].

1.2.1. Challenges in treatment of TNBC

TNBC does not respond to conventional hormonal therapy owing to the absence of expression of hormonal receptors and HER2 receptors, TNBC cannon be treated with conventional agents targeting hormone receptors including SERMs and aromatase inhibitors. The only treatment option that is the mainstream to treat TNBC is use of chemotherapeutic agents. TNBC is often managed by neoadjuvant chemotherapy followed by surgical removal of tumour. Common chemotherapeutic agents used to manage TNBC are anthracyclines (e.g. Doxorubicin), alkylating agents (e.g. Cyclophosphamide), taxanes and antimetabolites (e.g. 5-Flurouracil)[17][21]. Platinum based agents such as Cisplatin and Carboplatin are preferred in patients showing BRCA1/BRCA2 mutation. In advanced stages of disease, patients are treated with antimetabolites capecitabine and gemcitabine[19]. TNBC is known to be relatively highly responsive to chemotherapy than hormone receptor positive Breast cancer subtypes. However, response to chemotherapy lasts for short period of time followed by rapid relapse and resistance, commonly referred to as TNBC paradox[14][17][20]. There is more recent addition of eribulin to later line of treatment options. Despite use of effective chemotherapeutic agents as well as their combinations, overall outcome of the treatment regimen for TNBC remains disappointing. It is known that lesser than 30% of women with metastatic TNBC can remain alivefor5 years after diagnosis. There is a significant need to identify newer therapeutic targets for improved prognosis in TNBC[21][19][16].

1.3. Anticancer agents of herbal origin

For many years, chemotherapy has remained a gold standard for treatment of different types of cancers. Chemotherapy has proven efficacy and has shown betterment in life expectancy of patients. Even though, chemotherapies are obvious choice of treatments after the diagnosis of cancer, it comes at the cost of its own set of disadvantages. As most of the chemotherapeutic agents have low specificity and cannot differentiate between healthy cells and cancerous cells, patients must suffer through toxicity and side effects of drugs during the treatment. In many cases, toxic effects of the chemotherapeutic agents are severe and intolerable to patients and cause dose reduction or even discontinuation of the treatment[22]. Such gaps in treatment regimens lead to relapse of tumour cells. Most mainstream chemotherapeutic agents including topoisomerase inhibitors, alkylating agents, microtubule acting agents are active against a wide range of tumours. However, all these agents pose the challenge of severe toxic effects. Commonly observed side effects associated with chemotherapeutic agents include nausea, emesis, alopecia, anorexia, nephrotoxicity, myelosuppression, cardiotoxicity, neurotoxicity and haematologic toxicity. Other common limitations of chemotherapeutic agents include their complex synthesis and their higher cost, thus making the treatment regimen non-compliant to patients[22][23].

Plant derived medicines have been the part of therapeutic regimens since ancient times. Plants are known to have humongous potential and more than 3000 species from nature have been reported to have anticancer properties[24]. Growing evidence from many years of research has proven the anticancer potential of plant derived products. Vinca alkaloids (isolated from Catharanthus roseus), taxanes (derived from Taxus brevifolia), epipodophyllotoxins (derived from Podophyllum peltatum) and camptothecine derivatives (derived from Camptotheca acuminate) are examples of natural origin anticancer agents that are used in mainstream chemotherapy[22]. Vinca alkaloids, first developed in 1950s , are known as one of the oldest class and second most commonly used anticancer agents[24]. Different parts of plants including flowers, leaves, roots, rhizomes, stem, fruits, seeds can be used to isolate pharmacologically active components[23]. The anticancer activity of plant derived products is mainly attributed to secondary plant metabolites which include terpenes, flavonoids, alkaloids, lignans and glycosides[23]. Several years of research in the area of plant derived natural products has identified various mechanistic pathways responsible for their anticancer action. Various anticancer mechanisms involve inhibition of cell activating proteins and signalling pathways

including PI3K, Akt, MAPK/ERK, inhibition of enzymes such as topoisomerase, cyclo-oxygenase, activation of DNA repair mechanism and by induction of anticancer effect[23].

1.3.1. Caryophyllenes

Among natural products, essential oils have been used for multiple medicinal purposes since many years. Components extracted from Essential oils, especially terpenoids are of great commercial value in the areas of spices, agriculture, food, sanitary and pharmaceutical products[25]. Among many complex bioactives, caryophyllane class of compounds are commonly present in terpenoids obtained from wide variety of plants[26][27]. Caryophyllanes are a class of bicyclic sesquiterpenes which include constituents namely beta caryophyllene, iso caryophyllene, alpha humulene and beta caryophyllene oxide along with other minor metabolites[28][25][29][30][31]. These unique components are found be present in notable amounts in common dietary spices including clove (Syzygium aromaticum), basil (oscimm sp.), cinnamon (Cinnamomum zeylanicum), black pepper (Piper nigrum). These constituents are mainly isolated from respective plant parts by steam distillation. After many years of research, caryohyllenes have been found to be showing multiple pharmacological effects including anti-inflammatory, analgesic, antioxidant, antibacterial, antifungal and anticarcinogenic effects. Among different caryophyllenes, Beta caryophyllene and beta caryophyllene oxide are most researched compounds due to their interesting anti proliferative properties. BCP and BCPO have been traditionally used as food additives, taste enhancers and as flavouring agents. These two compounds have also been approved as flavouring agents by USFDA and EFSA (Identification numbers: BCP FL no 01.007 and BCPO FL no 16.043)[28][32][33].

a) Structural characteristics of Caryophyllenes:

The common biosynthetic pathway for caryophyllenes in plants involves cyclization of farnesyl pyrophosphate precursor. The reaction is catalysed by sesquiterpene cyclase Figure 1.1.

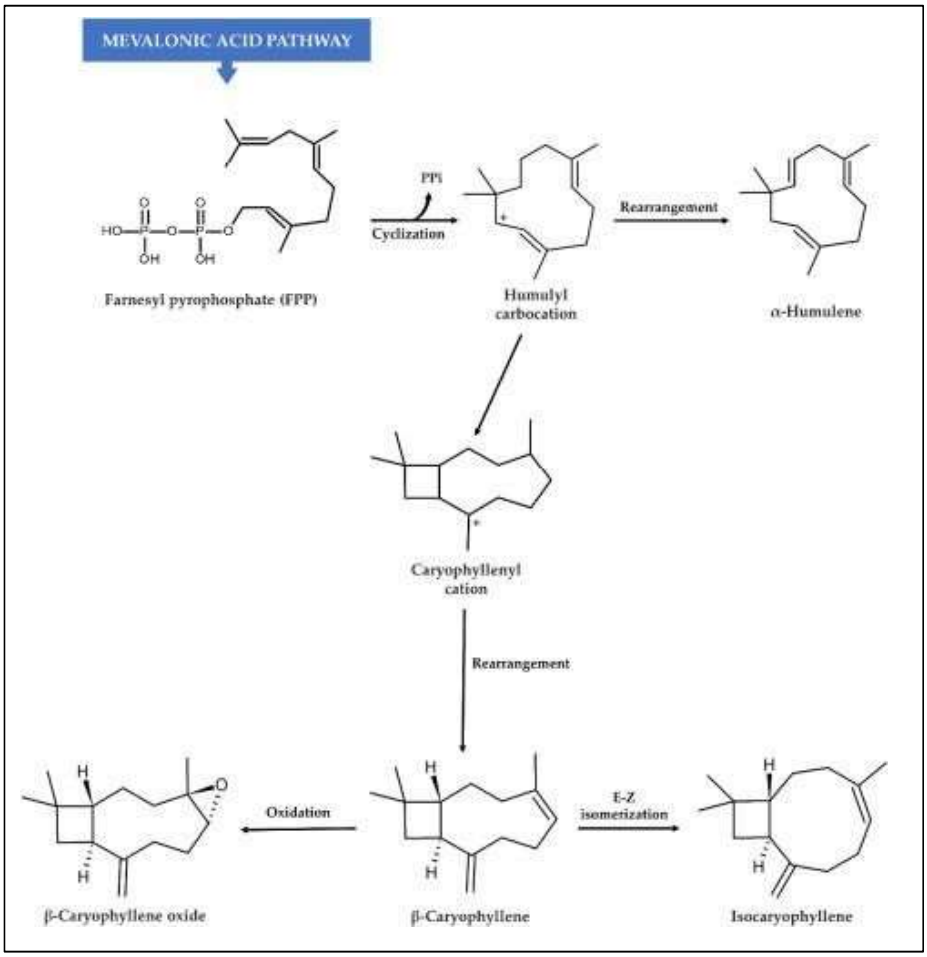


Figure 1.1 Biosynthesis of pathway of BCPO and its analogues

The common backbone skeleton of caryophyllenes is known as Caryophyllane. It possesses a characteristic structure of bicyclic undecane ring system in which a nine-membered ring is fused with dimethyl cyclobutene Figure 1.2.

Addition of an endocyclic double bond (at 4-5 position) leads to development of caryophyllene skeleton structure. Flexibility of nine-membered ring makes this structure prone to many rearrangements giving rise to multiple derivatives. (Figure 1.3).

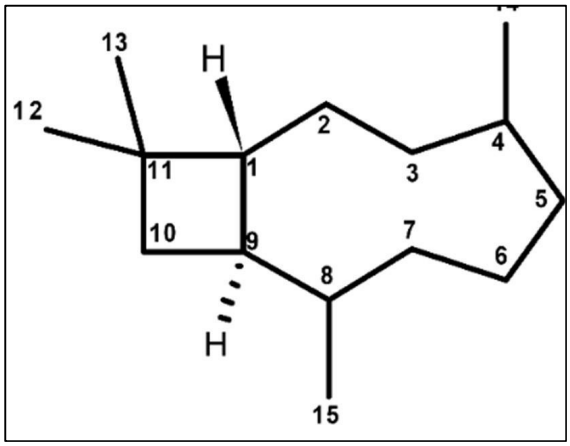


Figure 1.2 Schematic structure of caryophyllene

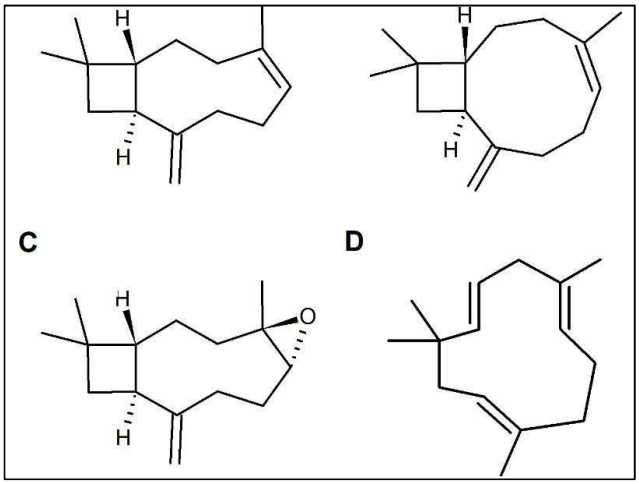


Figure 1.3: Derivatives of Caryophyllene

The endocyclic double bond (at 4-5) position in beta caryophyllene possesses higher reactivity than the exocyclic double bond. Both beta caryophyllene and iso caryophyllene can undergo oxidation at endocyclic double bond position to give rise to an endocyclic epoxide such as beta caryophyllene oxide[31].

b) Beta caryophyllene oxide:

BCPO has been extensively studied recently due to evidence of versatile pharmacological profile. Important biological sources for BCPO include guava (Psidium guajava), salvia (Salvia glutinosa), oregano (Origanum vulgare L.) basil (Ocimum sp.) and Syzygium cordatum [28].BCPO has been found to be showing antiviral; antibacterial, antifungal, anti-inflammatory antioxidant as well as anticancer activity. BCPO has been explored to show these activities as a single active as well as in combination with other caryophyllenes[28]. Beta caryophyllene

oxide has also been found to demonstrate chemo sensitizing, genoprotective and neuroprotective properties[31].

Table 1.1 demonstrates the reported biological activities f BCPO.

Table 1.1 Reported Biological activities of BCPO

Sr. no.	Reported activity	Studies giving evidence	Year	Reference
1.	Antifungal activity	In vitro study on simulated human nails	2000	[34]
2.	Antibacterial activity	In vitro antimicrobial activity In vivo studies of dental plaques of mongrel dogs	2016	[35]
3.	Analgesic activity	In vivo study using hot plate as stimulus	2010	[36]
4.	Anti-inflammatory activity	In vivo study by inducing inflammation in right hind paw of rats	2010	[36]
5.	Antiproliferative activity	In vitro study using MTT assay	2011	[37]
6.	Chemosensitive activity	In vitro study using caspase-GLO assay	2019	[38]

Extensive research studies have been undertaken to demonstrate anticancer activity of BCPO in several cancer cell lines. BCPO has been found to be showing cytotoxic action against cancer cell lines including HeLa (Human cervical adenocarcinoma cells), AGS (Human lung cancer cells), SNU-1 (Human gastric cancer cells), HepG2 (Human leukaemia cancer cells) showing IC50 values of 13.55, 16.79, 12.6, 3.95 uM respectively [28][29]. BCPO has also shown cytotoxic activity against the MDA-MB-468 triple negative breast cancer cell line. In vitro cytotoxic action of BCPO has been mainly ascribed to three different mechanisms namely induction of apoptosis, inhibition of metastasis and suppression of tumour growth [4]. BCPO has unique ability of modulating cell signalling pathways in cancer cells on account of the

presence of exocyclic functional groups namely methylene and epoxide groups. Presence of these functional groups enables BCPO to bind to DNA bases thus modulating the signal transduction pathways. BCPO has been found to be targeting PIK/AKT/m TOR / S6K1 pathway, STAT 3 pathway. BCPO also aids in reduction of procancer proteins namely Cyclin D1, COX-2, VEGF and reduction of apoptosis inhibitors such as bcl-2, IAP-1, IAP-2 and survivin. BCPO has also been found to be responsible for upregulation of proapoptotic genes such as bax, bak1, caspase 8 and caspase 9[28][31][4]. Potential antiproliferative and anticancer effects of BCPO are also ascribed to its effect of NF-kB signalling pathway[4].

Table 1.2 demonstrates various mechanisms responsible for antiproliferative and anticancer action of BCPO.

Table 1.2Anti-proliferative and anticancer action mechanisms in *invitro* studies

Sr. no.	Cell line	Mechanism	Reference
1.	MCF-7 and PC-3	Inhibition of PI3K/AKT/mTOR/S6K1 signalling pathway activation	[39]
2.	LNCaP and PC-3	Inhibition of PI3K/AKT/mTOR/S6K1 signalling pathway activation Induction of apoptosis	[40]
3.	M4BEU, CT-26, MCF-7 and PC-3	Enhancement of ROS production Depletion of cellular glutathione	[41]
4.	A-2780	Induction of apoptosis	[42]

One of the major limitations of cancer chemotherapy is associated toxic effects and damage to healthy cells. Beta caryophyllene oxide along with other caryophyllene analogues has been found to be exerting cytoprotective activity owing to their antioxidant and anti-inflammatory properties. BCPO has shown cytoprotective effect against damage by doxorubicin in hepatocytes. In vitro cell line research has also been focused on chemosensitizing properties of BCPO. BCPO has shown to be potentiating the effect of classic anticancer drugs as well as reversing the multidrug resistance. This synergistic chemosensitizing effect has been ascribed to the characteristic hydrocarbon arrangements in BCPO structure[27][26]. The cyclic

hydrocarbon based terpenoid structure of BCPO allows it to align in the cellular membrane of cancer cells thus improving the bilayer permeability of anticancer drugs. BCPO has been proven to be potentiating the activity of doxorubicin, paclitaxel and cisplatin in various cancer cell lines including U266, DU145, KBM-5. Co-treatment with BCPO was found to be improving the permeability of doxorubicin in Caco-2 cell line. BCPO also potentiated the cytotoxic effects of sorafenib in sensitive as well as resistant cell lines. BCPO has also been found to be increasing the intracellular concentrations of fluorouracil and oxiplatin in Caco-2 and SW-620 cells and improving their antiproliferative effect[31].

c) Safety profile of BCPO:

Beta caryophyllene oxide is Generally regarded as safe (GRAS) substance as per FEMA (flavours and extracts manufacturers association) and USFDA. BCPO is widely used in food and cosmetics industry as flavouring and taste enhancing agent. It is used in the concentration range of 25 ppm to 720 ppm in candies, chewing gums, puddings, beverages and other variety of food products with potential daily intake estimated to be around 10 mg. [33][31]. The reported value for acute oral lethal dose (LD50) is 5000mg/kg body weight[31][33]. The no-observed-adverse-effect level for BCPO was found to be 109mg/kg of body weight/ day as reported by European Food Safety Authority (EFSA)[31]. The reactivity of epoxide function in BCPO is hindered by vicinal methyl group, thus making the structure more or less inflexible to changes. Furthermore, BCPO may undergo ring opening in biological medium, however the derivatives formed are non-reactive towards DNA which explains the lack of genotoxicity of BCPO[31].

It has been hypothesized that, BCPO has shown dual action as sword and shield on in vitro cell lines. BCPO was found to be showing low toxicity towards non-cancerous and healthy cells including 3T3 fibroblasts and RGC-5 cells. Due to its low toxicity towards non-cancerous cells, it is suspected that BCPO acts on specific targets in cancerous cells while showing chemo preventive action on normal or healthy cells. This finding further supports the use of BCPO in clinical practice[32][31].

Beta caryophyllene oxide and its other analogues possess very little solubility in water or are practically insoluble in aqueous fluids. This limitation poses major barrier on exploration of these valuable natural ingredients for various biological actions. Another characteristic property of caryophyllenes is their volatile nature which presents yet another challenge of its stability in delivery systems as well as in biological fluids[28]. Research has been undertaken to address

this challenge by developing various alternatives for delivery of Beta caryophyllene oxide including beta-cyclodextrin complexes, liposomal drug delivery and nanoparticulate systems. Use of liposomes as delivery system with critical attention to lipid to drug ratio has been found to show multifold increase in in vitro cytotoxic action of caryophyllenes.

Even though, polypharmacological profiles of these natural ingredients have been established in *in vitro* studies, there is lack of clinical data supporting the claims. BCPO and other analogues have been proved to have chemopreventive as well as antiproliferative effects, however these ingredients are still humble in terms of exploration of their potential in *in vivo* studies. There are many pharmaceutical and pharmacologically unmet challenges to for these agents to reach the stage of clinical use. Consequently, there is a desperate demand to design suitable delivery system to explore the potential of BCPO in in vivo studies [43][28][32][25].

1.3 Role of adjuvant therapy

Polyunsaturated fatty acids (n-3 PUFA or ω-3 PUFA) also known as dietary essential fatty acids or bioactive lipids, have been known to play vital roles in cell growth, cellular metabolism, membrane function and structure since early age of development [44]. [DHA14]. The well-known nutritive role of n-3 PUFA has led to fortification of various bakery products with these bioactive lipids. n-3 PUFA are incorporated in variety of food products including milk, cheese and bread. [DHA10]. n-3 PUFA are also commercially available in encapsulated form as nutritive supplements.

A) Sources and structure of n-3 PUFA:

n-3 PUFA are commonly observed in cold-water fish and mainly comprised of particularly eicosapentanoic acid (EPA, 20:5n-3) and docosahexanoic acid (DHA, 22:6n-3) (Figure 1.4). Other examples of n-3 PUFA include alpha-linolenic acid (ALA) and (18:3) and stearidonic acid (SDA, 18:4) found in green leafy vegetables, flaxseed, walnuts etc. DHA is known to be the longest polyunsaturated fatty acid found in biological systems. These fatty acids are known as essential fatty acids as these are not naturally synthesized by human body and must be acquired through dietary sources[45].

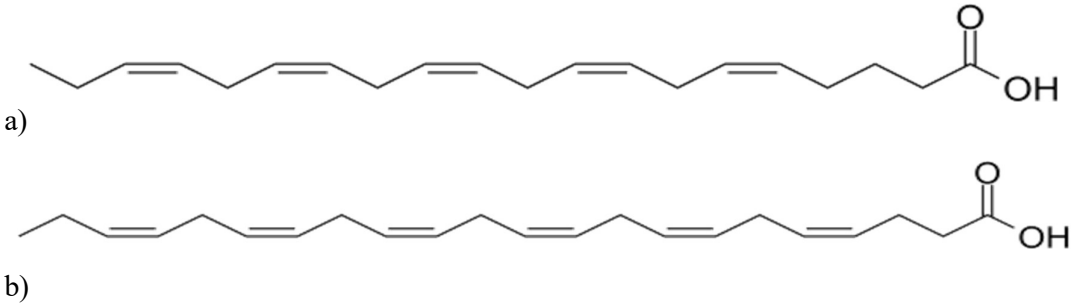


Figure 1.4 a) Eicosapentanoic acid b) Docosahexanoic acid

B) General functions of n-3 PUFA:

Highly flexible nature of n-3 PUFA leads to direct incorporation of these fatty acids in cell membranes. Apart from affecting membrane structures and dynamics, n-3 PUFA have also been known to influence energy production and storage, cell signalling pathways and inflammatory pathways. n-3 PUFA have also been known to possess immunomodulatory properties. n-3

PUFA has been hypothesized to act as adjuvant immunosuppressant in human clinical trials[44][45].

C) n-3 PUFA and inflammatory diseases:

Role of PUFA in inflammatory diseases is well researched. High incidence of inflammatory diseases including arthritis, metabolic disorders, asthma and cardiovascular diseases in western population has been correlated to lack of consumption of dietary essential fatty acids. Literature evidence suggests that n-3 PUFA has been correlated with the reduced risk of cancer over many years [DHA3]. Further, n-3 PUFA has been reported to play major roles in preventing and inhibiting cancer growth via different mechanisms. The mechanisms attributed to anticancer effect of n-3 PUFA when combined with other anticancer agents include alteration of membrane fluidity and accumulation of chemotherapeutic agent inside the cell, undergoing auto-oxidation and generation of reactive oxygen species, chemo sensitization of certain drugs owing to reduces expression of peroxisome proliferator activated receptor, and modulation of cell signalling pathway. Capacity of n-3 PUFA to change membrane fluidity and aid in accumulation of higher amount of drug inside cancer cell is particularly significant in case of drug resistance. Presence of high number of double bonds in PUFA structures makes them prone to oxidation. Such lipid peroxidation leads to generation of hydroperoxides and aldehydes which have shown to be playing active role in cytotoxic processes. Pertaining to these variable mechanisms, n-3 PUFA have been shown to be having synergistic potential when combined with other chemotherapeutic agents[44][46].

Apart from enhancing anticancer effect of other drugs, n-3 PUFA also possesses anticancer action of its own**.** n-3PUFA has ability to arrest cell proliferation, inhibit cell cycle and cell growth and induce cellular apoptosis by modulating various pathways such as mitogen-activated protein kinase (MAPK), JAK/STAT and PI3K/AKT/mTOR. It also causes down-regulation of EGFR, HER2 and up-regulation of Bax contributing to its proapoptotic effects. Additionally it has anti-inflammatory activity attributed to its antagonistic action to arachidonic acid and by the release of resolvins and protectins[47].

D) n-3 PUFA transporters and their up-regulation in cancer:

Recent research has thrown a light on involvement of specific transporters for uptake of long chain fatty acids. Earlier, cellular uptake of fatty acids was believed to be a passive process. Several transporter proteins have been found to be involved in trafficking the insoluble long chain fatty acids across the cell membrane as well as in their intracellular transport. These

transporters are present in the form of cytosolic and membrane lipid binding proteins. Examples of such lipid binding proteins include fatty acid binding proteins (FABP), fatty acid translocase (FAT) and fatty acid transporter protein (FATP). Table 1.3 gives the overview of fatty acid transporters and sites of their expression.

Table 1.3 Fatty acid transporter and their sites of expression

Sr. no.	Fatty acid transporter	Site of expression
1.	Fatty acid binding proteins (FABP)	Cardiac muscles, liver, endothelium, lungs, mammary gland
2.	Fatty acid translocase (FAT)	Liver, placenta
3.	Fatty acid transporter protein (FATP)	Liver, cardiac muscles, placenta

FABP, particularly FABP5 has gained focus during recent finding regarding its role in metastasis of prostate cancer. FABP5 is found to over expressed in colorectal, bladder, breast and oral squamous cell carcinoma. Further, poor prognosis in triple negative breast cancer has been strongly correlated to up regulation of FABP5.

1.4. Folic acid and its use as ligand:

Folic acid (FA), also known as vitamin B9, is one of the crucial water-soluble vitamins which carry out many vital functions in human body. Folic acid is not prepared naturally in human body and should be consumed through dietary sources such as green leafy vegetables, egg yolk, sunflower seeds or lentils or beans. Recommended dietary allowance of folic acid is 400 microgram per day. Folic acid is considered to be playing essential roles in DNA synthesis, DNA repair as well as in red blood cell production[48][49][50].

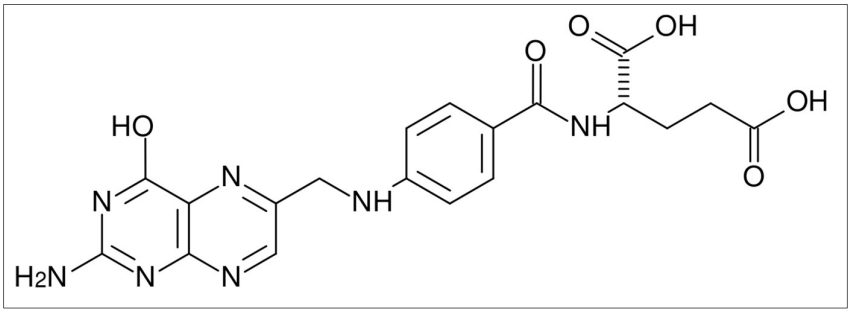


Figure 1.5 Structure of Folic acid

Folic acid cannot cross the cell membrane via simple diffusion and requires the aid of transporters and receptors expressed on cell surfaces. Folic acid is carried across the cell membrane by either reduced folate carrier or via folate receptors (FR). Folate receptors are a family of five different glycoprotein receptors expressed at different sites in human body. Among all folate receptors, folate receptor alpha (FRα) is known to possess high affinity for folate and is present on the surfaces of most cells[48][51][50][52].

Table 1.4 Folate receptors and their expression

Sr. no.	Name of folate receptor	Distribution in human body
1.	Folate receptor alpha (FRα/ Folr1)	Bronchial cells, retinal epithelial cells, kidney tubules, placenta
2.	Folate receptor beta (FRβ/ Folr2)	Placenta, spleen, bone marrow, thymus
3.	Folate receptor gamma (FRγ/Folr3)	Haematopoietic tissues
4.	Folate receptor delta (FRδ/Folr4)	T cells
5.	Retbindin protein (Rtbdn)	Secretory cells of retina

FA is transported across the cell's membrane by the process of receptor-mediated endocytosis. Upon internalization, receptor-ligand complex is separated from the membrane via the process of budding off and folate is released inside the cell[50][53].

Apart from DNA synthesis, FA plays vital roles in other biologic functions such as controlling the levels of blood homocysteine, synthesis of amino acids and protein metabolism. Deficiency of FA results in anaemia and it is recommended in higher amounts during pregnancy[48]. Considering the vital role played by FA in DNA synthesis, it is required by rapidly growingly

cells in higher amounts. Higher requirements of FA lead to over-expression of FR on surfaces of cancer cells. FR over-expression is well known in various types of tumours including kidney, breast, colorectal and ovarian tumours[52][49]. Over-expression of FR on cancer cells has also been correlated with the cancer growth and metastasis. Up regulation of FR on cancer cells leads to increased uptake of FA which leads to cell proliferation. It further leads to down regulation of cadherin thus promoting cell motility and cancer metastasis[50][51][54].

The phenomenon of over-expression of FR in cancer cells is used as one of the strategies of active targeting of drugs to tumour cells. Chemotherapeutic drugs are chemically conjugated to folic acid, wherein FA serves as a Trojan horse and carries the drug inside the cells after binding to cell surface receptors. FA does not lose its receptor binding ability after chemical conjugation with drugs and has been successfully used as a targeting ligand to transport the drugs to tumour sites[55][56][57].

Chapter 2

Literature survey

Chapter 2: Literature survey

1. Bhadran A et al., (2026) reported the development of advanced polymeric nanocarriers for Doxorubicin delivery using systems such as polymeric micelles, dendrimers, and polymersomes. These nanocarriers were designed to enhance drug targeting and reduce systemic toxicity, particularly cardiotoxicity. The study demonstrated improved drug encapsulation efficiency and controlled release profiles. Enhanced permeability and retention effect contributed to higher tumor accumulation. In vitro and in vivo evaluations showed improved anticancer efficacy. The system provided a promising approach for safer chemotherapy.

2. Imantay A et al., (2025) developed Doxorubicin-conjugated nanoparticles aimed at improving targeted drug delivery. The formulation showed high drug loading capacity and good stability under physiological conditions. These nanoparticles reduced off-target toxicity while increasing drug concentration at tumor sites. Cellular uptake studies confirmed enhanced internalization in cancer cells. Cytotoxicity studies demonstrated better anticancer activity compared to free drug. The study supported the role of nanotechnology in improving chemotherapy outcomes.

3. Recent researchers (2025) developed folic acid-functionalized iron oxide polymeric nanoparticles for targeted cancer therapy. The formulation used folate receptor-mediated endocytosis for selective delivery into cancer cells. The nanoparticles showed uniform particle size and high encapsulation efficiency. Sustained drug release was observed over an extended period. In vitro cytotoxicity studies confirmed enhanced anticancer activity. The study highlighted ligand-based targeting as an effective strategy.

4. Researchers (2024) focused on stimuli-responsive and ligand-targeted polymeric nanoparticles of Doxorubicin. These systems released drug in response to tumor-specific conditions such as pH and enzymes. The formulations showed high stability and drug loading capacity. Controlled release reduced systemic side effects. In vitro studies indicated selective toxicity toward cancer cells. These systems improved the therapeutic index of Doxorubicin.

5. A comprehensive review (2022) highlighted nanoformulations such as polymeric nanoparticles, liposomes, and micelles for Doxorubicin delivery. These systems improved

pharmacokinetics by prolonging circulation time. Reduced cardiotoxicity was a major advantage observed. Drug accumulation in tumor tissue increased due to the EPR effect. Controlled drug release improved therapeutic efficacy. The study emphasized the importance of nanocarriers in cancer therapy.

6. Cé R et al., (2021) developed folic acid-conjugated Doxorubicin polymeric nanocapsules for triple-negative breast cancer. The nanocapsules showed optimal particle size and high encapsulation efficiency. Targeting was achieved through folate receptor interaction. In vitro studies showed increased cellular uptake. Cytotoxicity assays confirmed improved anticancer activity. The study demonstrated effective targeted delivery.

7. Butowska K et al., (2021) reviewed polymeric nanocarriers as delivery systems for Doxorubicin. The study reported sustained and controlled drug release from polymer-based systems. Improved stability and reduced degradation were observed. Targeted delivery increased drug concentration in tumor tissues. Reduced systemic toxicity was a key benefit. The study supported polymeric systems as effective drug carriers.

8. Researchers (2020) developed PEGylated biodegradable polymeric nanoparticles of Doxorubicin. PEGylation helped avoid immune clearance and prolonged circulation time. The nanoparticles showed uniform size and high drug loading. Sustained drug release reduced dosing frequency. In vitro and in vivo studies showed improved anticancer activity. These systems enhanced safety and efficacy.

9. Studies (2018) focused on ligand-targeted nanoparticles using folic acid, transferrin, and antibodies. These ligands enabled selective binding to cancer cell receptors. The nanoparticles showed improved cellular uptake. Enhanced cytotoxic effects were observed compared to free drug. Targeted delivery reduced damage to normal cells. These studies strengthened targeted therapy approaches.

10. Early research (2016) established solvent evaporation and nanoprecipitation methods for polymeric nanoparticles of Doxorubicin. The formulations achieved nanoscale particle size and acceptable encapsulation efficiency. Sustained drug release profiles were reported. In vitro studies showed improved bioavailability. However, targeting ability was limited. These studies formed the foundation for later advancements.

11. **Celestial T. Yap *et al*** reviewed of practices in breast cancer treatment in different countries and presented the need for holistic approach in treatment of patients at various stages of recovery. Various approaches to provide support during breast cancer have been explored by authors especially from different perspectives such as family members and healthcare providers. This review provides the conclusive remarks regarding role of healthcare professionals in comprehending the complexity of breast cancers and the issues faced by patients and their family members [58].

12. **Massimiliano Cazzaniga and Bernardo Bonanni**, reviewed the evolving targets for breast cancer prevention on molecular level. The authors gave an overview of the recent findings in ER positive and ER negative breast cancer along with the involvement of various factors to act as carcinogens and their role in precancerous lesions [59].

13. **Lucas Antônio Miranda Ferreira *et al*** evaluated the role of docosahexaenoic acid (DHA) in enhancement of entrapment of an anticancer agent, doxorubicin. Solid lipid nanoparticles of doxorubicin were developed by addition of DHA with the postulate of enhancing the anticancer effect of doxorubicin. Developed nanoparticles were observed to have the particle size between the range of 127-94 nm with significantly enhanced entrapment efficiency. The formulation also showed higher cytotoxic action when tested against lung cancer cell line of A549 as compared to free doxorubicin and DHA. The research work proposed the vital role of DHA in enhancing the potential of anticancer agents and suggested it to be the important alternative for cancer treatment[60].

14. **Changhong Wei *et al***, assessed the effect of surface modification of polymeric nanoparticles for doxorubicin. The doxorubicin polymeric nanoparticles were surface modified by chemical conjugation with Folic acid-polyethyl glycol-propylene glycol (FA-PED-PG). Developed surface modified nanoparticles were found to have particle size of 229nm with drug loading of 86%. Authors observed that the surface modified polymeric nanoparticles showed enhanced cytotoxicity than non-modified nanoparticles. Authors concluded that the FA-PEGPG modified polymeric nanoparticles of doxorubicin showed site specific and improved cytotoxic action also improving the pharmacokinetic profile of the drug [60].

15. **M. Greenwell *et al*** reviewed the increasing demand for naturally derived principles from medicinal plants. The authors also discussed the properties of herbal principle which carry the potential to be developed as anticancer agents. The authors also commented on the emerging new drug delivery technologies including nanoparticles to enhance anticancer activities of herbal principles.

16. **Paolo Fiorenzani *et al*** assessed the analgesic effect of Beta-caryophyllene (BCP) and docosahexaenoic acid (DHA), alone and in combination in in vitro as well as in vivo studies. The in vitro toxicity of the compounds was evaluated in fibroblasts and astrocytes. As a result of research work, BCP was found to be changing the survival in astrocytes and fibroblasts. Further, co-administration of DHA was found to be counteracting this effect. I*n vivo* studies showed the reduction of pain response for combination of BCP and DHA. The research work proved the potential of combination of BCP and DHA and BCP alone at lower concentration for modulation of analgesic responses [61].

17. **Zhongguo Sui *et al***, worked on surface modified nanoparticles for systemic administration. The nanoparticles were prepared for the nuclear delivery of genetic material. The nanoparticles were modified with two ligands namely folate and transferring via linker of polyethylene glycol and phosphatidylethanolamine (PEG-PE). Developed nanoparticles showed gene loading capacity of 90% with particle size of 226nm. Authors proposed that the two ligands demonstrated excellent active targeting potential for targeted gene delivery[61].

18. **Angela M Rizzo *et al*** performed in vitro cell line studies to prove the potential of n-3 PUFAs to alter membrane permeability and modify cellular signalling in breast carcinoma cells. The study was carried out on two cancer cell lines showing different expressions of ER and EGFR receptors. The researchers observed that EPA and DHA lead to induction of cell apoptosis by reducing the cell viability. They were also found to be responsible for the expression of Bcl2 and procaspase-8 and reduction of EGFR activation. The research work underlined the role of n-3 PUFA in increasing the degree of fatty acid unsaturation and modification of cell membrane in breast cancer [61].

19. **Patricia D. Schley*et al***, carried out extensive research to study the effect of n- PUFA specifically DHA and EPA on breast cancer cell line MDA-MB-231. The combination of EPA and DHA was found to reduce the growth in MDA-MB-231 cells by 30-40%. Mechanism of reduced cell proliferation by EPA and DHA combination was postulated to be increased DNA fragmentation, increased caspase activity. n-3 PUFA was also found to be decreasing Akt phosphorylation and as NFjB DNA binding activity. Authors illustrated the apoptotic effect of n-3 PUFA by decreasing the cell signalling pathways [61].

20. **Anna Rita Bilia**, in an extensive review, proposed strategies for nanoencapsulation of essential oils. The authors have evaluated various advantages of nanoencapsulation such as improved stability, their capability of decreasing volatility, water solubility, and efficacy of essential oil-based formulations. The authors have also proposed two strategies of nanocarriers: Polymeric nanocarriers and lipid carriers. The article also reviews the applications of inclusion complexes in improving solubility and bioavailability of essential oils[61].

21. **Antonella Di Sotto *et al*** evaluated the genotoxic and mutagenic potential of beta-caryophyllene oxide. Potential of beta-caryophyllene oxide to get absorbed through cell membrane was assessed by the method of differential scanning calorimetry (DSC). To evaluate the same, the biomembrane model of dimyristoylphosphatidylcholine was used. The research work highlighted that, beta-caryophyllene oxide was devoid of genotoxicity and mutagenic effects, at both gene and chromosomal level. The research was shown to be an important stepping stone regarding safety profile of beta-caryophyllene oxide [61].

22. **Ashok Kumar Peepliwal** gave an extensive review regarding the status of breast cancer in India. Authors reviewed an etiology as well as the subtypes of breast cancer. Authors also gave an overview regarding the availability of diagnostic tools for detection of breast cancer at early stages. The review article also enlisted the available treatment options for improved prognosis and decreased morbidity. The review article is viewed to be beneficial to update the breast carcinoma information and research avenues [61].

23. **Hazra Avijit *et al*** extensively reviewed the therapeutic potential as well as the

pharmacology of n-3 PUFA, specifically EPA and DHA. Authors elaborated absorption, metabolism and biotransformation pathways for n-3 PUFA. Various activities of n-3 PUFA such as anti-thrombotic, anti-atherogenic, anti-proliferative have also been discussed. Special focus has been given to the ant-proliferative and cytotoxic influence of n-3 PUFA. Overall, it was concluded that n-3 PUFA, specifically EPA and DHA are desirable dietary supplements which show promising activities in cardiovascular and some non-cardiovascular diseases[46].

24. **Raj Kumar Salar, Naresh Kumar**, synthesized vincristine loaded nanoparticles with the use of method of ionic gelation. Developed nanoparticles were surface modified by Folic acid- Chitosan conjugation. The developed nanoparticles were found to have zeta potential of+11.2 ± 0.43 mV, particle size of 897.5 nm and polydispersity index of 0.738 ± 0.30. The structure of nanoparticles was found to be Face cantered cubic (FCC) which was confirmed by X-ray diffraction (XRD) studies. Developed formulation showed the encapsulation efficiency of 81.25% and loading capacity of 10.31%. The research work successfully demonstrated the effectivity of conjugated nanoparticles as a targeted drug delivery system owing to over- expression of folic acid receptors on cancer cell surface [62].

25. **Lekha Nair K *et al***, developed folic acid conjugated polymeric nanoparticles of Doxorubicin. Poly(δ-valerolactone)/poly (ethylene glycol)/poly(δ-valerolactone) (VEV) copolymer was used for synthesis of formulation. Solvent evaporation method was applied for development of nanoparticles. Nanoparticles showed the particle size of 97nm and high encapsulation efficiency. The nanoparticles also demonstrated the sustained nature of drug release. Developed nanoparticles were also tested against breast carcinoma cell line, MDA- MB-231. The nanoparticles showed increased cellular uptake and improved cytotoxicity in in vitro cytotoxicity studies. MTT assay and apoptosis assay revealed that Folic acid decorated nanoparticles showed significantly better cytotoxicity[63].

26. **Harish Pawar *et al*** developed folic acid functionalised long circulated co-encapsulated solid lipid nanoparticles for docetaxel (DTX) and cur cumin (F-DC-SLN). F-DC-SLNs were shown to have particle size of 247.5 ± 3.40 nm, zeta potential of 14.53 ± 3.6 mV and entrapment efficiency of 73.88 %. The cytotoxicity of developed nanoparticles was assessed in breast cancer cell lines, MCF-7 and MDA-MB-231. The targeting

efficiency of nanoparticles was established by Fluorescence microscopy. In addition, developed nanoparticles showed decreased accumulation in kidneys and heart in comparison with Taxotere®. The researchers concluded that F-DC-SLN enhance the targeting ability and pharmacokinetic profile of DTX [64].

Chapter 3

Rationale

Chapter 3: Rationale

3.1. Rationale for development of novel drug delivery system of BCPO

Currently available treatment options for breast cancer are known to be surgical removal of tumour, chemotherapy, hormonal therapy and radiation. However, each conventional treatment has its own limitations which further increase the complexity of the treatment. Limitations of each of the conventional therapies are elaborated as follows:

a. Hormonal therapy is a treatment option for hormone receptor positive tumours. However, it is ineffective in **'Triple negative breast cancer (TNBC)'**. TNBC lacks the expression of HER-2, Oestrogen receptors and Progesterone receptors, thus making therapy with the hormonal agents such as Tamoxifen, Raloxifen unsuccessful[65].

b. **Cytotoxicity**: Chemotherapy and radiotherapy exert severe toxic effects such as haemolysis, alopecia, thrombopenia due to non-targeted action. Hence novel formulation which will aid in tumour site specific delivery of the anticancer drugs is highly desired[65].

c. **Hydrophobicity of Anticancer agents**: Many of the newly developed cytotoxic molecules and bulk polycyclic molecules such as Paclitaxel, Etoposide are hydrophobic in nature which makes their IV administration a key obstacle in the cancer treatment.[66]

d. **High Cost**: The chronic nature of anticancer therapy and high cost of anticancer drugs becomes major concern to treat patients from lower economic strata and society. So availability of anticancer therapy at lower cost will be highly desired to treat such patients[67].

To overcome the limitations associated with conventional therapies, there is a pressing need for alternative treatments with lesser side effects and better target specific delivery. Active targeting of naturally derived principles in Novel Drug Delivery System can be a promising solution to this. Targeting of BCPO and n-3 PUFA nanoparticles using a suitable ligand such as Folic acid will immensely add value to the formulation by reducing side effects. Available literature supports the possibility of safe administration of BCPO or n-PUFA by i.v. route. However, very less work has been done to study anticancer activity of combination of BCPO and n-3 PUFA and its formulation for administration via intravenous route.

Thus, rationale for development of lipid-based nanoparticles of BCPO with the use of n-3 PUFA as functional excipient and folic acid as targeting agent is explained as follows:

a. **Use of herbal anticancer principle BCPO:** BCPO demonstrates anticancer activity by altering cellular pathways for tumour development, including mitogen-activated protein kinase (MAPK), STAT3 pathways and PI3K/AKT/mTOR/ S6K. It has also been correlated with suppression of angiogenesis, cellular survival and cell cycle progression[68]. However, lipophilicity of drug makes its i.v. administration challenging. A suitable lipid based nanoparticulate system for i.v. administration can be a solution to overcome this challenge.

b. **Use of n-3 PUFA as lipidic adjuvant with synergistic anticancer activity in lipid nanoparticles:** n-3 PUFA as lipid excipient of lipid nanoparticles can serve dual role. It will act as a formulation component of lipid nanoparticles aiding in formation of nanoparticles with reduced particle size. Further, n-3 PUFA will show synergistic effect along with its proven anticancer effect**.** n-3 PUFA has ability to inhibit cell cycle proliferation as well as arrest cell cycle and induce apoptosis by modulating various pathways such as PI3K/AKT/mTOR, mitogen-activated protein kinase (MAPK), and JAK/STAT. It also causes down-regulation of EGFR, HER2 and up-regulation of Bax contributing to its proapoptotic effects. Additionally, it has anti-inflammatory activity attributed to its antagonistic action to arachidonic acid and by the release of resolvins and protectins. Also, literature proves its potential as promising lipid excipient to enhance drug loading of hydrophobic drug in lipid nanoparticles. n-3 PUFA also shows tumour targeting potential owing to overexpression of fatty acid transporters in tumour.

c. **Use Active targeting method for delivery of lipid nanoparticles:** Conjugation of suitable ligand such as folic acid on the surface of SLN will improve its affinity towards cancer cells and the drug molecules will be delivered by Receptor mediated endocytosis. This approach will lead to improved efficacy of the treatment as well as reduced distribution of drug in non-targeted tissues.

d. Easy availability and low cost of BCPO and simple and scalable SLN formulation technology for i.v. administration offers cost effective alternative to the current anticancer regimen.

3.2. Novelty of the project:

Novelty of the project is envisaged as follows:

i. Establishment of BCPO as safe alternative for treatment of breast cancer by intravenous route.
ii. Development of validated analytical method and forced degradation conditions for BCPO.
iii. Development of pharmacokinetic profile of BCPO.
iv. Use of n-3 PUFA having proven cytotoxic activity as lipid adjuvant in lipid nanoparticles of anticancer agent BCPO.
v. Establishment of a novel lipid nanoparticulate formulation of BCPO for intravenous administration.

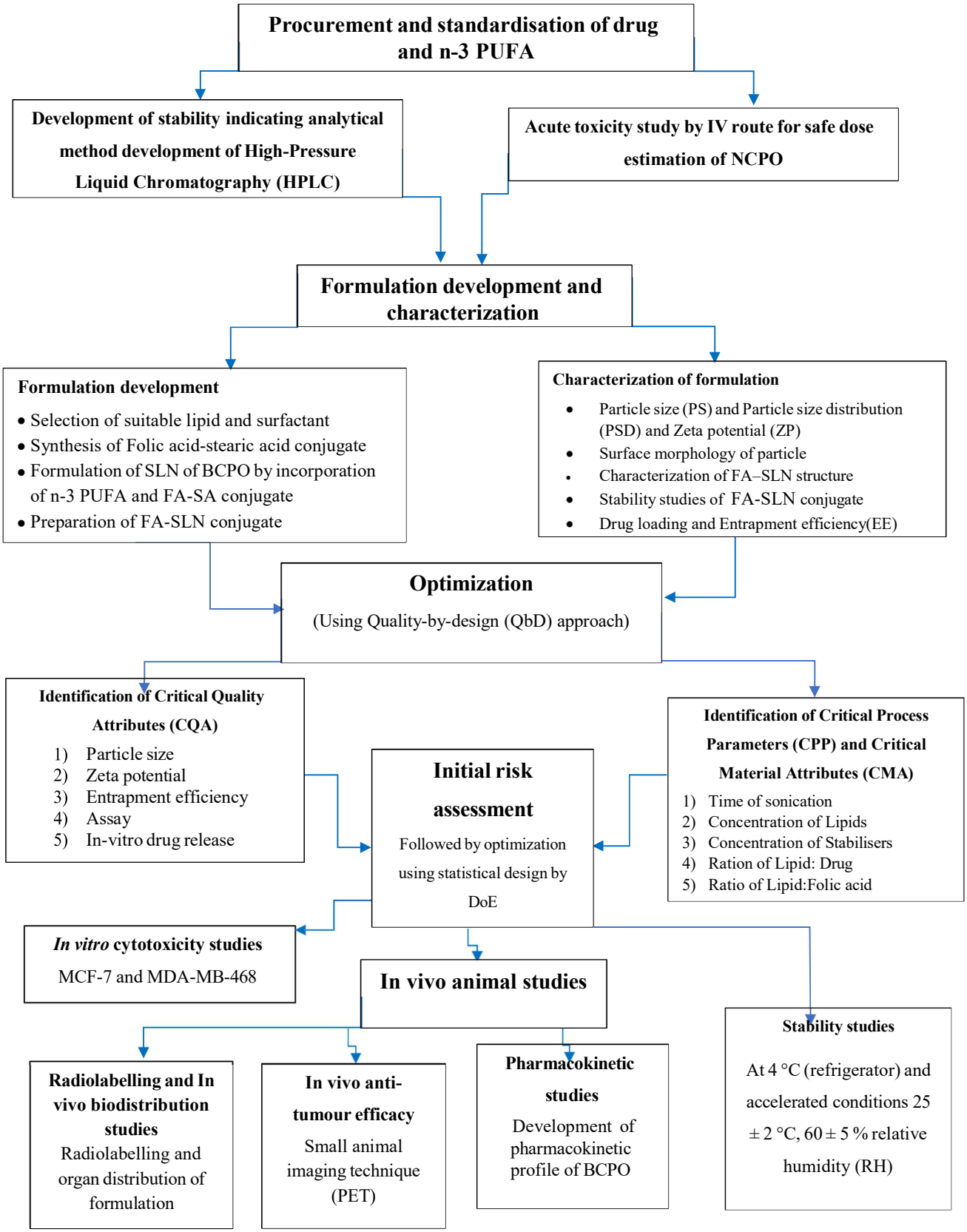
3.3. Objectives:

Objectives of the research work are stated as below:

- To develop Solid Lipid Nanoparticles (SLN) formulation of herbal principle, β-Caryophyllene oxide (BCPO) for intravenous administration.
- To establish role of n-3 Polyunsaturated Fatty Acid (n-3 PUFA) as lipid adjuvant in SLN formulation of BCPO.
- To target the developed SLN formulation to breast cancer cells by conjugating SLN with Folic acid (FA).
- To prove safety for I.V. administration, site specificity and anticancer activity of novel FA conjugated SLN formulation containing BCPO and n-3 PUFA by in vitro cell line studies and in vivo preclinical studies.

Thus, aim of present investigation is to design and develop a safe, scalable and cost effective intravenous SLN formulation for breast carcinoma including Triple Negative Breast Cancer (TNBC).

3.4. Plan of work:



Chapter 4

Drug profile

Chapter 4: Drug profile

Beta-caryophyllene oxide

The general and physicochemical properties of beta-caryophyllene oxide are enlisted in Table 4.1.

Table 4.1 Profile of beta caryophyllene

Name of Drug	**Beta-caryophyllene oxide**
Chemical name	(1*R*,4*R*,6*R*,10*S*)-4,12,12-trimethyl-9-methylidene oxatricyclo [8.2.0.04,6]dodecane
Appearance	White crystalline solid
Odour	Sweet, fresh, dry, woody, spicy
Molecular formula	$C_{15}H_{24}O$
Molecular weight	220.3
CAS registry	1139-30-6
Melting point	62.5 ^{0}C
Boiling point	279.68 ℃
Solubility	Soluble in ethanol, Insoluble in water
Log P	4.57
Use	Flavour enhancer, flavouring agent or adjuvant

	Used in soaps, detergents, fine fragrances and incense sticks
FEMA* No.	4085
JECFA# Flavour No.	1575

*Flavour and Extract Manufacturers Association

#Joint Expert Committee on Food Additives

General information:

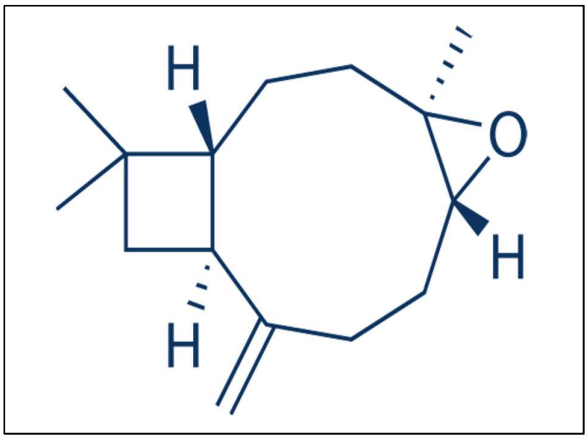
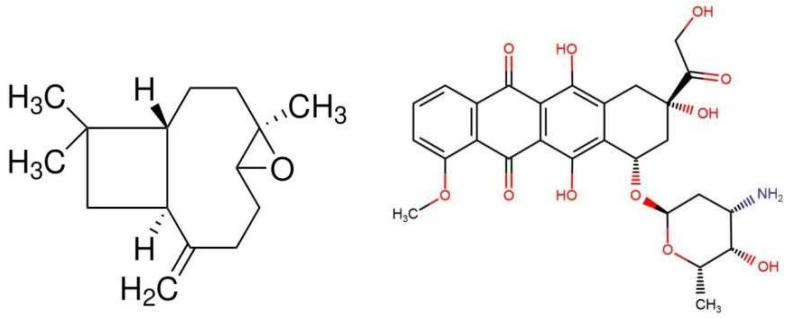
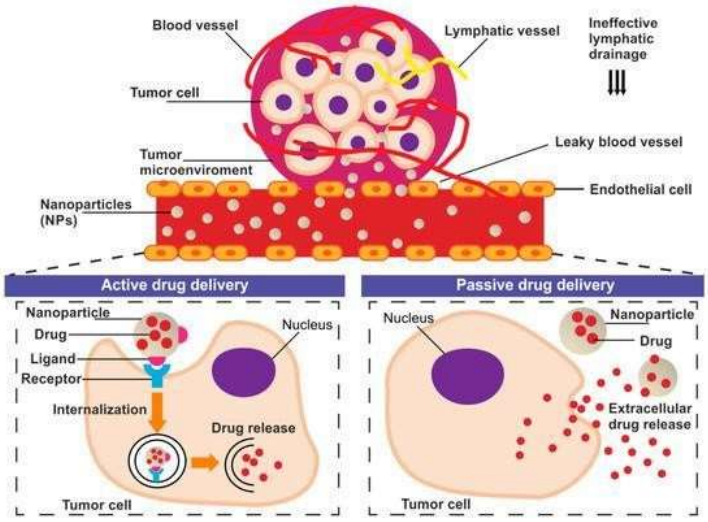


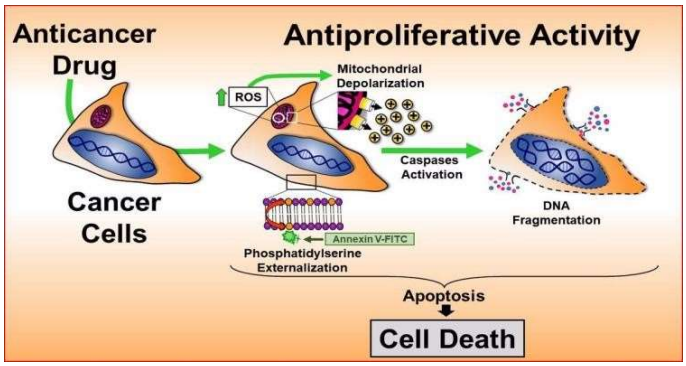
Figure 4.1 Structure of beta caryophyllene oxide

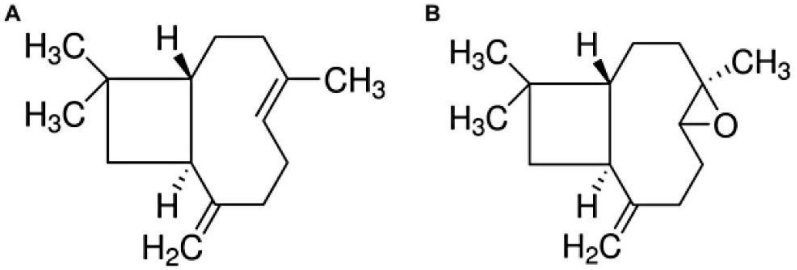
Beta caryophyllene oxide is naturally occurring bicyclic sesquiterpene epoxide. It is known to be a major element of most essential oils especially clove oil. The general applications of BCPO include as flavouring agent, adjuvant and food additive. BCPO has been found to possess certain biological properties including wide spectrum antifungal effect, antibacterial effect, and analgesic and anti-inflammatory effect. The BCPO has shown potential as an anticancer agent in in vitro cell line studies. Even though, the metabolic profile of BCPO remains poorly understood, the studies have been undertaken to establish the toxicity profiles of BCPO. BCPO is found to possess LD50 values of > 5mg/kg and > 2mg/kg for oral and dermal routes respectively.

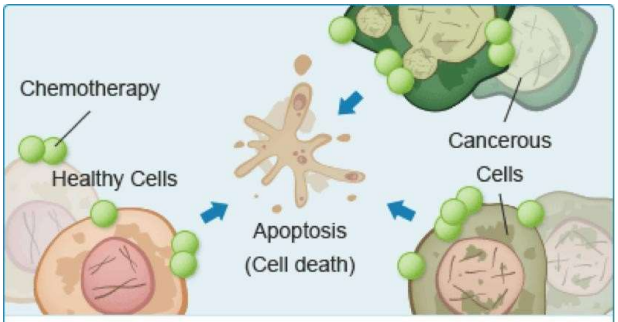
Beta-caryophyllene oxide in comparison with conventional anticancer drugs











Chemotherapy Side Effect Cause

Beta-caryophyllene oxide was selected for the present study due to its comparable anticancer activity with conventional chemotherapeutic agents, along with a significantly improved safety profile. Standard anticancer drugs such as Doxorubicin are widely used in clinical practice due to their strong cytotoxic effects against rapidly dividing cancer cells. However, these drugs lack selectivity and often damage normal healthy cells, leading to severe side effects such as cardiotoxicity, myelosuppression, and immunosuppression. In contrast, beta-caryophyllene oxide demonstrates selective toxicity toward cancer cells, thereby reducing harmful effects on normal tissues.

Unlike conventional drugs that primarily act through a single dominant mechanism, beta-caryophyllene oxide exhibits multiple mechanisms of anticancer action. It induces apoptosis through activation of caspase pathways, disrupts mitochondrial function, and causes cell cycle arrest. Additionally, it inhibits key signaling pathways such as NF-κB, which are involved in tumor growth, inflammation, and metastasis. This multi-targeted approach increases its effectiveness and reduces the likelihood of resistance development, which is a common limitation seen with drugs like Doxorubicin.

Another major limitation of conventional anticancer drugs is the development of multidrug resistance (MDR), where cancer cells become less responsive to treatment over time. Beta-caryophyllene oxide has shown the ability to overcome or reduce this resistance by enhancing drug sensitivity and modulating cellular pathways involved in resistance mechanisms. Moreover, it has demonstrated synergistic effects when used in combination with standard drugs such as Doxorubicin, thereby improving overall therapeutic efficacy and allowing dose reduction of toxic drugs.

From a formulation and drug delivery perspective, beta-caryophyllene oxide offers additional advantages. Its lipophilic nature facilitates easy incorporation into nanoparticle-based delivery systems, which enhances its bioavailability and enables targeted delivery to tumor sites. In contrast, conventional drugs often require complex modifications to achieve

similar targeting efficiency. Nanoformulations of beta-caryophyllene oxide can provide sustained drug release, reduced systemic exposure, and improved accumulation at the tumor site, which further enhances its therapeutic performance.

Furthermore, beta-caryophyllene oxide possesses antioxidant and anti-inflammatory properties, which help in reducing tumor-promoting inflammation and protecting normal cells from oxidative damage. Conventional anticancer drugs generally lack these protective effects and may even increase oxidative stress in healthy tissues. This dual role of beta-caryophyllene oxide, acting as both an anticancer and protective agent, makes it a more balanced therapeutic option.

In comparison to conventional chemotherapeutic agents, beta-caryophyllene oxide presents a promising alternative due to its natural origin, lower toxicity, multi-targeted mechanism, and compatibility with advanced drug delivery systems. These advantages justify its selection in the present study as a safer and potentially more effective anticancer agent.

Chapter 5

List of equipment and

Materials and Method

Chapter 5: List of equipment and materials

List of equipment used for undertaking present research work is depicted in Table 5.1.

Table 5.1 List of equipment

Sr. no.	Equipment Name	Manufacturer
1.	High performance liquid chromatography (HPLC)	1) Shimadzu LC2010HT with UV-Vis detector 2) Jasco with PDA detector
2.	Double beam UV-Vis Spectrophotometer	Shimadzu 1800
3.	Fourier Transform Infrared (FTIR)	Shimadzu IR infinity, Japan
4.	Probe Sonicator	Oscar Ultrasonic Processor Sonapros PR250
5.	Particle size analyzer	Malvern ZS90
6.	Ultracentrifuge	Beckman Optima max XP
7.	Differential Scanning Calorimetry	DSC 6220, SII Nanotechnology, SEIKO
8.	Transmission Electron Microscope	JEM 2100F FEG-TEM, JEOL, Tokyo
9.	X-ray Diffraction	PAN analytical X'Pert PRO MPD
10.	Freeze drier	Martin Christ
11.	Deep freezer	Vestforst
12.	Electronic weighing balance	Premier Weighing Systems
13.	Precision balance	Wensor, XB220A (2007)
14.	Melting Point Apparatus	Labline Instruments
15.	Microscope	Labline Instruments

16.	pH meter	DBK Digital pH meter
17.	Magnetic stirrer	REMI 1MLH, REMI Lab
18.	Microcentrifuge	REMI 120-C, REMI Labs
19.	Cold centrifuge	Spinwin MC05-R, Tarsons
20.	Bath Sonicator	Oscar Ultrasonic
21.	Hot air oven	Labline Instruments
22.	Milli-Q Water Purification System	Millipore, USA
23.	Stability Chamber	Thermolab, India
24.	Gamma well Counter	1240 GSPEC-USB, Para Electronics
25.	Positron emission tomography (PET)	Eye series, β -eye, Bioemtech, Greece

5.2. List of software used:

Table 5.2 List of software

Sr. no.	**Instrument/ Application**	**Software**
1.	Shimadzu HPLC software	Lab solutions
2.	Jasco HPLC software	Chromnaav
3.	Zetasizer	Malvern software version 7.11
4.	Statistical design	Design-Expert Version 13, Stat-ease
5.	Referencing and citation	Mendeley Desktop Elsevier
6.	Gamma scintigraphy	Spectrum acquisition and analysis software (SAAS)
7.	Positron emission tomography (PET)	β -eye Bioemtech, Amide, CASToR image reconstructor

5.3. List of solvents, chemicals and their sources:

Table 5.3 List of solvent/chemicals and their sources

Sr. no.	Name of solvent/chemical	Source
1.	Acetonitrile HPLC grade	Loba Chemie
2.	Beta caryophyllene oxide	Prasad organics
3.	Docosahexanoic acid (DHA)	Redox Pharmachem
4.	Folic acid	Loba Chemie
5.	Stearic acid	Loba Chemie
6.	Glyceryl monostearate	Loba Chemie
7.	Polysorbate 20	BASF, Mumbai
8.	Gelucire 48/16	Gattefosse India Pvt Ltd,
9.	Gelucire 50/13	Gattefosse India Pvt Ltd,
10.	Ethyl-3-(3-dimethylaminopropyl) carbodiimide (EDC)	Loba Chemie
11.	Dimethyl formamide (DMF)	Loba Chemie
12.	Pyridine	Loba Chemie
13.	Soyabean-Casein Digest Medium	HiMedia
14.	Thioglycollate Medium	HiMedia
15.	Sodium sulphate	Loba Chemie
16.	Trypsin	HiMedia
17.	Glucose	Loba Chemie
18.	Sulphorhodamine B	HiMedia
19.	Dimethyl sulphoxide	Loba Chemie
20.	Stannous chloride ($SnCl_2$)	Loba Chemie

21.	[18F]-2-fluoro-2-deoxy-D-glucose (^{18}F-FDG)	TATA Memorial Centre
22.	Sodium pertechnetate	TATA Memorial Centre
23.	Compritol 888 ATO	Gattefosse India Pvt Ltd,
24.	Methanol AR Grade	Loba Chemie
25.	Hydrochloric acid	Loba Chemie
26.	Hydrogen peroxide	Loba Chemie
27.	Polyethylene glycol 400	Loba Chemie
28.	Polyethylene glycol 200	Loba Chemie
29.	Sodium hydroxide	Loba Chemie
30.	Sodium chloride	Loba Chemie
31.	Polyethoxylated castor oil (Kolliphor EL)	BASF, Mumbai (Gift sample)
32.	Potassium dihydrogen orthophosphate	Loba Chemie
33.	Disodium hydrogen phosphate	Loba Chemie
34.	Dialysis Membrane-70	Himedia
35.	Membrane filter (0.22 µ)	Pall corporation
36.	Poloxamer 188	BASF, India
37.	Poloxamer 407	BASF, India
38.	Polysorbate 80	BASF, Mumbai
39.	TPGS	BASF, Mumbai
40.	Solutol HS 15 (Polyethylene glycol15-hydroxy stearate)	BASF, Mumbai
41.	Precirol ATO 5 (Glyceryl palmitostearate)	Gattefosse India Pvt Ltd,
42.	Sodium Hydroxide	Loba Chemie
43.	Sodium Lauryl Sulphate	Loba Chemie

44.	Mannitol	Loba Chemie
45.	Trehalose	Loba Chemie

5.4. Excipient profile:

1) Compritol 888 ATO:

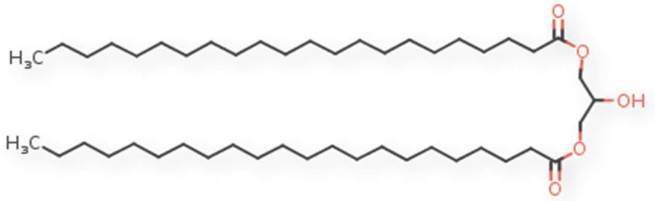


Figure 5.1 Structure of Glyceryl Di-behenate

Table 5.4 Excipient profile of Compritol 888 ATO

Attributes	**Description**
Name	Compritol 888 ATO
Generic name	Glyceryl Di-behenate
Chemical Composition	Consists of mono-, di- and triesters of behenic acid
Molecular formula	C25H50O4
Molecular Weight	414.7
Appearance	fine white powder
Melting Point	65 – 77°C
HLB	2
Solubility	Soluble in chloroform and dichloromethane when heated, practically insoluble in cold ethanol, slightly soluble in hot ethanol insoluble in mineral oil, and water.
Use	1) Sustained release matrix for tablet. 2) Binder, coating agent for tablet 3) Solid lipid for lipidic nanoparticles 4) Taste masking of APIs.

2) Gelucire 50/13:

Table 5.5 Excipient profile of Gelucire 50/13

Attributes	**Description**
Name	Gelucire50/13
Generic name	Stearoyl polyoxyl-32 glycerides
Chemical Composition	Consists of mono, di- and triglycerides and PEG-32 mono- and diesters of palmitic (C16) and stearic (C18) acids
Appearance	fine white powder
Melting Point	46-51
HLB	11
CMC	100 mg/L
Solubility	Freely soluble in methylene chloride, soluble in warm ethanol;
Use	Solubilizer for poorly soluble APIs and bioavailability enhancer. Self-emulsifies in Type III (SMEDDS). Drug release modifier, Dissolution enhancer; non-ionic surfactant; penetration agent.

3) Folic acid

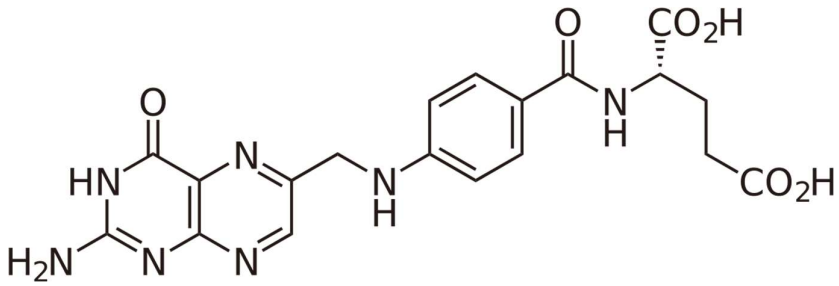


Figure 5.2 Structure of folic acid

Table 5.6 Excipient profile of Folic acid

Attributes	**Description**
Name	Folic Acid
Molecular Formula	$C_{19}H_{19}N_7O_6$
Molecular Weight	441.4
Appearance	odourless orange-yellow needles
Melting Point	50°C
Log P	-2.5
pKa	3.5
Solubility	Slightly soluble in methanol, less in ethanol, insoluble in chloroform, acetone. Solubility n water: 1.6 mg/L at 25 °C;
Use	Supplement to treat low folate levels

4) Stearic acid

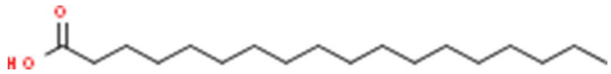


Figure 5.3 Structure of stearic acid

Table 5.7 Excipient profile of stearic acid

Attributes	**Description**
Name	Stearic Acid
Chemical composition	Octadecanoic acid
Molecular Formula	$C_{18}H_{36}O_2$
Molecular Weight	284.5
Appearance	Hard, white, glossy, crystalline powder
Melting Point	68.8 °C
Log P	8.23
pKa	4.75
Solubility	In water 0.597 mg/L (at 25 °C)
Use	Lubricant, binder, solubilising agent and emulsifying agent.

Chapter 6

Formulation development and Optimization

Chapter 6: Formulation development and optimization

6.1Introduction

6.1.1. Lipid nanocarriers: Solid Lipid Nanoparticles

Researchers were introduced to lipid based nanoparticles, earlier known as nanopelletes, during 80s[71]. The lipidic mixture of nano as well as microparticles was later also named as lipospheres[72]. Nano-sized particles prepared with the aid of particle size reduction technology such as ultrasound and high-pressure homogenization caught the attention of researchers owing to their multiple advantages. The technology went on to get advanced and has received an impetus during last few decades leading to rising number of publications in the area.

Solid lipid nanoparticles (SLN) and nanostructured lipid carriers (NLC) are variables of lipid based nanocarriers which are colloidal in nature with the size range between 50 nm to 1000nm. Lipid based particles use the lipids from natural origin and are stabilised in water as a dispersion medium with the aid of surfactants and/or stabilisers.

a) Advantages of SLN [73][74]**:**

Advantages of SLN as a nano-particulate system are enlisted as follows.

- Site-specific delivery owing to their small particle size and narrow size distribution
- Controlled drug release with use of solid-state lipids
- Use of biocompatible and natural origin lipids making the articles devoid of any toxicity issues
- Greater stability after lyophilisation or spray-drying
- Sterilization by autoclaving or by gamma irradiation
- Cost-effective and non-complex production technology
- Possibility of loading both lipophilic and hydrophilic drugs

b) Methods of production of SLNs:

Solid lipid particles are typically made up of solid lipids. To stabilise the lipid particles in aqueous environment, surfactants and stabilisers are used. Methods of preparation of SLNs

are extensively reviewed in literature [74][75][76]. The important methods of preparation are highlighted as below:

1) High shear homogenization with the aid of ultrasound

The size of the lipid particles is reduced with the aid of high shear or by providing the acoustic energy. These are most commonly used methods for preparation of SLN [71][72]. These methods suffer from the disadvantages of reduced quality of particles and metallic impurities after ultrasonication.

Table 6.1Lipids and emulsifiers for solid lipid nanoparticles

Lipids	Triglycerides, Hard fat types, Fatty Acids
Emulsifiers	Lecithins, Poloxamers, Phosphatidylcholines, Polysorbates, bile salts

2) High-pressure homogenization (HPH)

To prepare SLN by high pressure homogenization method, the particle are subjected to very high pressure (approx. 100-2000 bar) at very high velocity (approx. 1000km/h). The particles are passed through a small orifice at high pressure and high velocity thus converting the particles into nanoparticles[77]. HPH methods fall into two categories, hot homogenization (performed at high temperatures) and cold homogenisation (performed at low temperatures, effective for heat sensitive lipid excipients).

3) Microemulsion technology

First tried by Gasco et al [78], this technique involves thermodynamic stabilisation of lipidic nanoparticles to form an isotropic dispersion. The amount of surfactants and stabilisers required in this method are relatively higher and it leads to formation of relatively dilute dispersion which requires concentration.

4) Solvent emulsification and evaporation method

Under this method, SLN are prepared by solubilising the lipid phase in an organic solvent followed by addition of lipid phase to water phase. The organic solvent is further evaporated under constant stirring or high temperature to precipitate the nanoparticles[79]. Even though

this method yields the particles with smaller size, it suffers from the disadvantage of existence of small quantities of organic solvent.

5) Solvent emulsification and diffusion method

This method was previously established and used for preparation of polymeric nanoparticles [80]. In this method, the lipid phase and aqueous phase are melted separately at high temperature and mixed under continuous stirring. This method offers advantage over solvent evaporation method by avoiding the use of toxic organic solvents.

6) Solvent injection method

The method was earlier used in preparation of liposomes and the modification was proposed by Muller-Goymann[81] for production of SLN. Briefly, the lipid phase id injected in a solvent that is miscible with water in presence or absence of surfactants. Further evaporation of organic solvent leads to precipitation of nanoparticles.

7) W/O/W double emulsion method

W/O/W double emulsion method was proposed by Zhang et al for loading insulin in SLN [82]. This method offers an advantage of high loading for hydrophilic or peptide-based drugs.

8) Membrane contractor method [83]

This method is represented schematically in Figure 6.1.

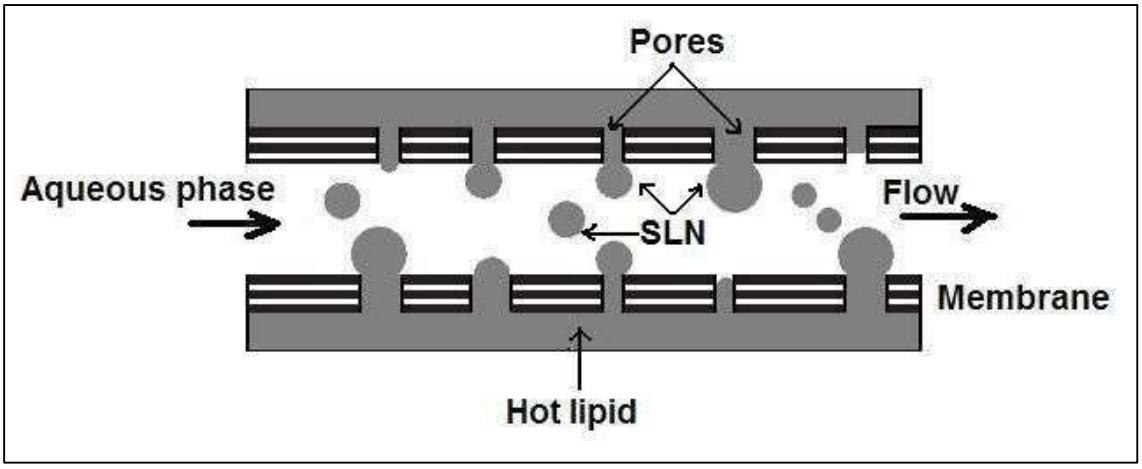


Figure 6.1Membrane contractor method for preparation of SLNC

C) Characterization of SLNs

SLNs are complex colloidal systems which are subjected to variations owing to lipid polymorphism and simultaneous existence of other colloidal carriers. To optimize the process technology for SLN, careful characterization is necessary. The important characterization parameters are enlisted below:

1) Particle size and particle size distribution

The particle size is an important optimization parameter for SLNs. Particles larger than nano-size range may lead to blocking of capillaries upon intravenous administration. Further, nano-size particles are important for enhanced skin penetration in topical and transdermal drug delivery, enhanced solubility and bioavailability in oral delivery, enhanced permeation and retention effect and escaping the reticuloendothelial system (RES) in case of intravenous drug delivery. Further, uniform size distribution is important as larger or bimodal distribution of particles will affect the performance of SLNs. Commonly used techniques to measure particle size and size distribution include laser diffraction (LD) technique and photon correlation spectroscopy (PCS).

2) Zeta potential

Measurement of zeta potential is important in characterization of SLN as it gives the idea about the particle aggregation during storage. Higher zeta potential value indicates higher charge on particle surface preventing the aggregation. Zeta potential value close to zero suggests the possibility of particle aggregation. In case where non-ionic surfactants or steric stabilisers are used, zeta potential value close to zero does not always suggest the aggregation.

3) Particle shape and morphology

Techniques utilised for determination of particle size mostly use the principle of light scattering. However, light scattering techniques do not give any indication regarding the shape of the particle. To visualise the particle shape as well as to measure the size of particles various advanced microscopic techniques are used. Such techniques include scanning electron microscopy (SEM), atomic force microscopy (AFM), transmission electron microscopy (TEM) and field-emission scanning electron microscopy (FESEM).

4) Crystallinity and polymorphism

Solid lipids exist in various polymorphic states during storage such as α, β, and β'. modification of lipids is considered most stable polymorphic state for solid lipids. During preparation

process of SLN, solid lipids may assume different polymorphic states during cooling stage. The stability of lipid polymorphic states is as follows:

Supercooled melt > α-modification > β'-modification > β-modification

During preparation, lipids may cool down in the form of supercooled melts. However, during storage, lipids slowly tend to convert into to most stable form i.e.,β. The stable crystalline stage is achieved by perfectly ordering the crystal lattice structure of the lipids in particle thus leading to expulsion of the drug.

To understand the storage stability of drug loaded SLN, characterization of lipid polymorphism is very important. Commonly used techniques to study lipid crystallization and polymorphism include differential scanning calorimetry (DSC) and x-ray diffraction study (XRD)[84].

5) Assessment of alternate colloidal structures

To study the presence of several other colloidal structures, advanced techniques such as nuclear magnetic resonance (NMR) are used[74].

6) Assay for drug content

During the preparation of SLN, drug may get exposed to various conditions including high temperature, high shear, sonication and interaction with the excipients. Such harsh processes may lead to chemical degradation or instability of the drug. Thus, it becomes mandatory to evaluate the drug content of final developed formulation and match the reading with theoretical value. Various techniques used to determine drug content include-visible spectrophotometry, high performance liquid chromatography (HPLC) and LC-MS.

7) Encapsulation/ Entrapment efficiency (EE)

For the matrix systems such SLN, drug is said to be uniformly dispersed in lipid matrix. Determination of the quantity of drug that is present inside the nanoparticles is known a entrapment efficiency. Entrapment efficiency can be determined by various methods such as centrifugation, dialysis and size-exclusion chromatography.

To determine the entrapment efficiency by ***centrifugation***, nanoparticles are centrifuged at very high speed. At the end of the centrifugation process, lipids particles are separated as precipitate from the clear aqueous phase as supernatant. The supernatant is separated carefully to analyse

the amount of free drug. Larger particles typically settle down faster in centrifugation process. To separate nanoparticles, ultracentrifuge with very high centrifugation speed

(1,50,000 rpm) is used[85][86]. The process is sometimes aided with addition of salts such as sodium chloride or sodium sulphate to enhance the lipid precipitation.

To determine the entrapment efficiency by dialysis method, the SLN solution is filled inside a dialysis bag having very small pore size. The free drug dissolves in the eternal phase and develops equilibrium on both sides of dialysis bag. The time required to develop the equilibrium is recorded to take out an aliquot. By analysing the drug fraction in aliquot, amount of free drug can be determined[87][88].

In size exclusion chromatography, the SLN solution is passed through silica column through which a mobile phase is run. The nanoparticles being larger is nature than unentrapped drug molecules, elute out first. The free drug elutes from the column at the end and can be separated from the entrapped drug in the particles [89].

The formula used for calculation of %EE is as follows:

%EE = (Total drug added-total free drug)*100/Total drug added

8) In vitro drug release studies

In vitro release is conducted to understand the in vivo fate of the lipid nanoparticles. Drug release from lipid nanoparticles is impacted by various factors such as pH at the site of release, temperature, presence of enzymes at the site of release. Such conditions can be mimicked in in vitro release studies to develop the drug release profile. These studies for lipid nanoparticles are commonly carried out with the use of flow-through cell, magnetic stirrers, water shaker baths or modified USP type-II apparatus.

10) In vitro cell line studies

Cytotoxicity studies are mainly important during development of colloidal carriers for anticancer agents. Cytotoxicity studies are carried out on both pure drug and its colloidal formulation to assess their cytotoxic potential against selected cancer cell lines. Among various methods to perform cytotoxicity studies, MTT assay and SRB assays are most used. In these methods, the test samples are serially diluted to different concentrations and incubated with the cancer cells in suitable media. The principle of MTT assay uses the phenomenon of conversion of MTT dye (3-(4, 5-Dimethylthiazol-2-yl)-2, 5-Diphenlytetrazolium Bromide) to violet coloured crystals of formazan. Formazan crystals are further dissolved in solvents such as dimethyl sulphoxide(DMSO) to measure their concentration. Conversion of MTT to formazan

crystals is undertaken by live cells mitochondrial enzymes. The concentration of formazan crystals can be correlated to % cell viability.

11) In vivo efficacy studies

The in vivo stability, efficacy and site specificity of the drug loaded nanocarriers is evaluated by in vivo studies. Fate of the drug after administration into the body via specific route of administration can be evaluated by pharmacodynamic studies, pharmacokinetic studies, in vivo tumour efficacy studies and biodistribution studies to name few.

i) Pharmacokinetic studies:

Evaluation of pharmacokinetic parameters such as volume of distribution, AUC, time to reach maximum plasma concentration (Tmax) and maximum plasma concentration (Cmax), help to confirm the in vivo fate of lipid nanoparticles. Pharmacokinetic profile of nanocarriers can be compared with the standard drug product of with plain drug to understand the improvement in absorption, distribution and elimination of drug. For targeted drug delivery systems, biodistribution studies help to understand the site specificity of targeted formulation [90].

ii) Pharmacodynamic studies:

In case of lipid nanocarriers for anticancer drugs, tumour models are developed in order to evaluate the efficacy of anticancer agent. Xenograft models are developed in rodents such as rat or mice, by implanting the cancer cells at specific anatomical location such as flank region. The parameters which are evaluated in efficacy studies include measurement of tumour volume, tumour growth rate, measurement of angiogenesis and histopathology of excised tumour [86][91].

Drug incorporation models of SLN

Amongst all the methods of preparation used to prepare SLN, melt-emulsification is the most widely used method. During preparation of SLN by melt emulsification method, the solid lipid is congealed under constant stirring while the temperature drops down to room temperature. The entrapment of drug in solid lipid nanoparticles developed by melt-emulsification method is dependent on multiple factors including solubility of drug in lipid, temperature of emulsification, rate of cooling the emulsion and melting points of drug and lipid. Based upon the various factors affecting drug entrapment in SLN, Muller et al proposed three different

models to depict the drug incorporation in SLN[73]. The three drug incorporation models are as depicted in Figure 6.2.

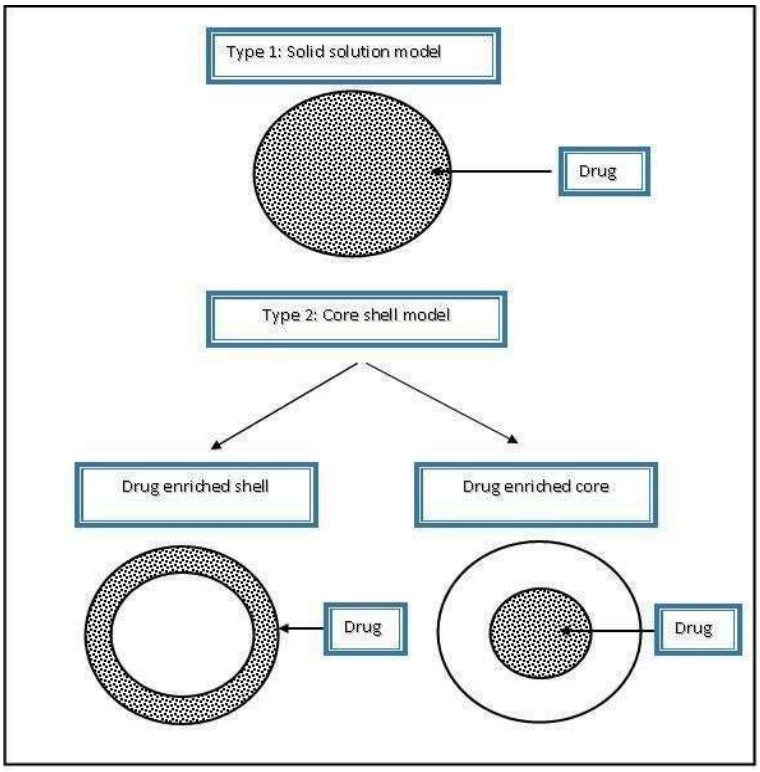


Figure 6.2Models of drug incorporation for SLN

6.1.2. Lipid nanocarriers: Nanostructured Lipid Carriers (NLC)

Nanostructured lipid carriers are known as second generation lipid nanosystems. NLCs are advanced in structural aspects over SLNs and are prepared by replacing some proportion of solid lipid in SLN by liquid lipids or oils. NCLs are known to enhance the drug loading and more controlled drug release profile. NLCs are also known to ameliorate the stability of the nanosystems with lesser evidences of drug expulsion[92].

 Theory of NLC formation

All the methods of preparation of SLN involve formation of colloidal dispersion of nanoparticles either by solidification or by evaporation of solvents. Solid lipids assume their crystal structures during the formation of nanoparticles and may crystallize in their stable βform or unstable α form. Use of stabilisers in SLNs keeps the nanoparticles stable in their α form for certain period. However, the lipids tend to get converted into their naturally stable β-

modification by perfectly ordering the crystal structure leading to drug expulsion. This leads to poor stability of SLN systems and shorter shelf life.

The crystal lattice arrangement in SLNs also depends upon the nature of solid lipids used for preparation of SLNs. Use of solid lipids of only one type and shorter chain triglycerides leads to formation of highly ordered crystal lattice with very less imperfections. Highly ordered crystal lattice leads to very less space available for drug loading. On the other hand, use of spatially different lipids and lipids with longer chain of triglycerides leads to formation of less ordered crystal lattice with more imperfections and improved drug loading. Figure 6.3 shows the schematic representation of crystal lattice structures of SLN and LNC.

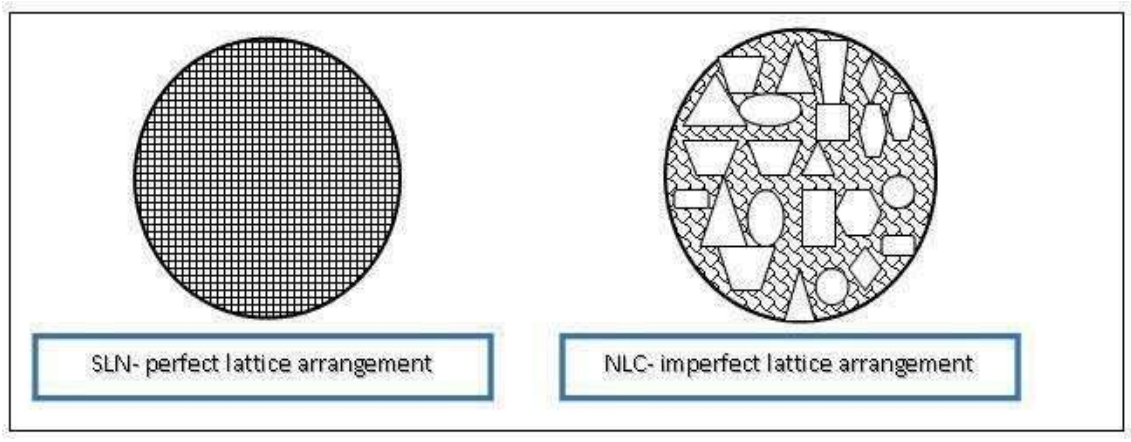


Figure 6.3Schematic of SLN and NLC crystal arrangement

- ***Types of NLCs***

Based on the co-existence of solid lipids and oils in nanoparticles, NLCs are classified in three different types (Figure 6.4).

1. Type I (The imperfect type NLC)

2. Type II (The multiple oil/fat/water type NLC)

3. Type III (The structureless type NLC)

The imperfect type NLC consist of the mixture of both solid lipids and liquid lipids (oils). Any two solid and liquid lipids can be mixed to form nanoparticles if the lipids are compatible with each other. Mixing of spatially different types of lipids leads to creation of imperfections in nanoparticles thus making the space available for drug loading.

The imperfections in the crystal structure increase with the structural difference in the participating lipids [73]. When the two lipids with large difference in their structure are mixed to form nanoparticles, liquid lipids precipitate in the form of small oil compartments inside solid lipid. Such structural arrangement gives rise to Type II NLC system. These types of systems are also known as lipid nanocapsules. Lipid nanocapsules are prepared by phase inversion method to precipitate the liquid lipid in solid lipid. This method has been previously reported for Paclitaxel [93] and Tamoxifen [94] NLC preparation.

To prepare type III NLCs, the nanoparticles are composed of such lipids, which will not lead to crystallization. Such lipid mixtures are carefully chosen in order to prevent crystallization and develop stable nanoparticles [73].

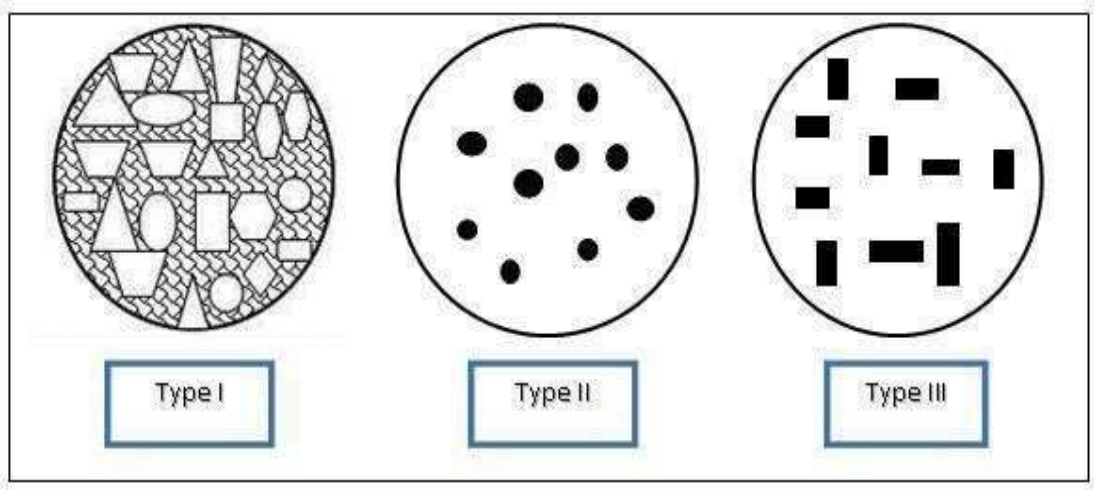


Figure 6.4 Structural types of NLCs

6.1.3. Applications in cancer therapeutics

1. Improved Bioavailability

A vast majority of newly developed chemical agent suffer from the disadvantage of poor oral bioavailability. Multiple reasons reported for poor bioavailability include low aqueous solubility, susceptibility to enzymes leading to their degradation, poor oral absorption as well as susceptibility to P-gP efflux proteins [95][73][96][97][98][99].

Lipids are reported to be improving the bioavailability of drugs by various mechanisms [100][101][102][103][104]. Lipids undergo enzymatic digestion first in stomach and afterwards in intestine forming micelles. Micellar solubilisation of drug leads to improved

solubility and absorption. Several other mechanisms of lipids to improve bioavailability include enhanced permeability across GI membrane, enhanced lymphatic uptake and inhibition of P-gP efflux pumps. Various lipidic systems reported to improve the bioavailability of drugs include LeciPlex®, GeluPearl®, proliposomes, and lecithin based systems[86][100][105][106].

2. Improved targeting potential

Currently available anticancer delivery systems face the disadvantages of a range of side effects patients must suffer. The current drug delivery systems are not target specific and deliver the drug to all other parts of body apart from the site of action. The non-targeted approaches used in current medicine led to off-target delivery, wastage and unwanted toxicity of drugs. Many years of research work has been invested to develop the drug delivery systems that are more target specific thus avoiding the off-site toxicity. Targeted drug delivery systems offer following advantages in cancer treatment:

1) Improved delivery of drug at cellular level and increased drug payload

2) Reduced systemic toxicity and reduced drug wastage

3) Reduced cost of therapy

Lipid based nanosystems offer an ample potential to develop targeted delivery systems. There is abundant amount of literature indicating the results of chemically conjugating targeting ligands to lipid nanoparticles for site specific drug delivery. The targeted delivery systems are broadly categorised as active targeting and passive targeting systems.

Passive Targeting

Lipid based nanosystems possess the potential for passive targeting by the virtue of their small size. The nano-sized particles can extravasate the fenestrated leaky tumour vasculature and accumulate in the tumour mass. The impaired lymphatic drainage in tumour cells further keeps the particles trapped inside the tumour cells, a phenomenon known as enhanced permeability and retention (EPR) effect. To possess effective passive targeting ability, the size of nanoparticles should be in range of 10nm to 400 nm. Particles larger than 400nm would be unable to cross the leaky tumour vasculature. Larger particles also have the risk of getting cleared by the RES system in the body. Efforts also should be taken to make the surface of the particles sufficiently hydrophobic in order to escape phagocytosis and opsonisation. Further,

pH sensitive lipids can be used in preparation of nanoparticles which release the drug at the acidic pH of tumour site thus avoiding the drug wastage and toxicity in systemic circulation.

Table 6.2depicts the literature evidence of passive targeting of anticancer drugs.

Table 6.2Passive targeting potential of lipidic Nanocarriers to tumorous tissues

Sr. No.	**Nanocarrier type and related information**	**Advantages offered**	**References**
1.	Surface modified liposome of Doxorubicin (PEGylated liposomes)	Improved circulation time in plasma Reduced cardiotoxicity	Elbayouni T.A. et al,2008. Berry G. tumour bearing, 1998
2.	Doxorubicin and cyclophosphomide liposomes (non-PEGylated)	Longer half-life Improved therapeutic index	Mross K. et al, 2004
3.	Tamoxifen citrate SLN	Longer systemic circulation	Reddy L.H et al, 2006
4.	5-Fluorouracil and stearyl chloride conjugate SLN	Enhanced targeting of liver	Yu B.T. et al, 2003

Active targeting

Active targeting properties can be imparted to lipid-based nanoparticles by anchoring the targeting ligands on the particle surface. Tumour cells multiply at faster rate than normal cells and over express certain receptors in order to acquire more amount of nutrients. The ligands binding to these overexpressed receptors are exploited as targeting agents. Examples of such targeting ligands include folic acid, transferrin, immunoglycoproteins, asialoglycoproteins etc. The ligands are added to lipid nanoparticles either by chemical conjugation or by physical interaction. The functional groups in lipids utilised in chemical conjugation of ligand include –COOH, -$NH_2$and –SH leading to esterification, amidation and thiolation reactions. Researchers have also hypothesized the use of a linker between lipid and the ligand in order to

impart more flexibility to ligand [107].Table 6.3[108][109]depicts the examples of receptors and proteins overexpressed in different types of tumours.

Table 6.3Examples of receptors overexpressed in tumours

Overexpressed Targets	**Tumours overexpressing targets**	**Ligands**
Folate Receptor	Brain, kidney, lung, ovarian and breast tumours	Folic acid
Transferrin Receptor		RGD peptide
Sigma Receptor	Breast, lung and Prostate tumours	Benzamide derivatives
LDL Receptor	Almost all types of solid tumours	Cholesterol
Carbohydrate Receptors	Liver	Mannose, Fucose, and Asialogycoproteins

3. Improved permeation for topical preparations

Lipid nanocarriers are known to enhance the skin permeation of various active ingredients. SLN and NLC systems have been reported to be explored for the treatment of numerous skin ailments such as psoriasis, keratitis, acne etc.

Lipid based nanocarrier systems have been proven to advantageous for treatment of various conditions including cancer. Lipid nanocarriers have been reported to be administered by various routes including oral, intravenous, topical as well as nasal. These systems offer advantages such as low particle size, enhanced permeation across membranes, enhanced solubilisation, and prolonged systemic circulation. These nanocarrier systems also possess the potential to chemically conjugate with ligands and surface modification thus imparting them the site specificity and sustained drug release. The well demonstrated effectiveness of lipid nanocarrier systems thus provides a great scope for exploring their potential for newer chemical ingredients.

6.2. PREFORMULATION

Pre-formulation studies are undertaken to obtain thorough idea of the physicochemical properties of drug and excipients to develop a stable and optimised formulation system. BCPO was analyzed and standardized with the help of techniques including Differential scanning calorimetry (DSC),UV-Visible spectroscopic techniques, Fourier transform infra-red (FTIR) spectroscopy and Analytical method was developed for analysis and standardization of BCPO and for analysis of drug release in presence of its degraded products.

Pre-formulation studies are enlisted as below:

I. Identification and Standardization of API: Physico-chemical properties, Melting point of drug, FT-IR spectroscopy, UV-Visible spectroscopy

II. Characterization of bulk Crystallinity and polymorphism: Microscopic characterisation (morphology, particle characteristics by light microscopy, Scanning Electron Microscopy), Thermal characterization (DSC, TGA) and X-ray Diffraction

III. Analytical method development for stability: Analysis of stability at different stress conditions (thermal/acid/base/light/oxidation), solution state and solid-state stability, excipients compatibility.

IV. Solubility profile if lipids and surfactants

6.2.1. Identification and Standardization of API

A. Physico-chemical properties of drug:

BCPO was described for colour, nature, odour and crystalline or amorphous form.

B. Melting point determination:

Melting point of BCPO was determined by an open capillary method.

C. Differential Scanning Calorimeter (DSC):

The melting temperature range of BCPO was determined with the use of differential scanning calorimeter (DSC), using alumina as a reference. The BCPO was scanned from the temperature range of 30^0C to 250^0C per minute[110].

D. UV-Visible spectroscopic method development:

UV-Visible method of BCPO was developed with the use of 3% Sodium Lauryl Sulphate (SLS) solution as a solvent. BCPO weighing 10 mg was solubilised in 10 ml of 3% SLS solution and volume was adjusted to 100ml (stock solution).From the stock solution, 10ml solution was added to a volumetric flask of 100 ml capacity and the volume was adjusted to100ml with 3% SLS solution. The obtained drug solution was further scanned in UV range of 200-400 nm on UV-visible Spectrophotometer.

E. Fourier Transform Infrared Spectroscopy (FTIR):

The Infrared spectrum of the BCPO was acquired by FTIR. The assembly was cleaned with acetone to avoid traces of impurities. The sample was placed on the crystal lens. The spectrum was recorded from 4000cm^{-1} to 400cm^{-1}. The corresponding groups were identified to confirm the purity of drug.

6.2.2. Characterization of morphology and bulk crystallinity:

A. Appearance and particle size by microscopy:

The physical appearance of the BCPO was observed with the use of light microscopy. Particle size was evaluated under 45X magnification using an optical microscope (Labline, India).

B. Scanning electron microscopy:

Scanning electron microscopy was performed to determine shape and surface morphology of BCPO crystals.

C. Powder X-ray diffraction (PXRD):

The X-ray diffractogram of BCPO was obtained with the use of an X-ray diffractometer at 40kV at 0.02°/min. The uninterrupted scanning was continued over an angular range of (2Ɵ) of 5°-40° with step size of 0.017° and Xe-filled counter rate detector[110].

6.2.3. Stability indicting analytical method development

A. High Pressure Liquid Chromatographic (HPLC) method development:

An in-house stability indicating HPLC method was established for quantification of BCPO. The method was further optimized and validated. The mobile phase for analysis was developed by mixing Acetonitrile (ACN) and water in ratio of 90:10. It was filtered through 0.45 um membrane filter and degassed by sonication for 20 min. prior to use. The analysis was carried out on C18 analytical column Zorbax Eclipse XDB (Agilent technologies), 250mmX4.6mm, 5um. The HPLC system used for analysis was Shimadzu HPLC LC2010. The HPLC system was provided with the UV/Vis detector and detection wavelength of 210 nm. Run time of the method was set as10 min., injection volume was set as 20 ul and column temperature was set at 30^0 C. Lab solutions software was used for data processing and analysis. Table 6.4 depicts the instrumental and chromatographic conditions for HPLC method[111][112][113][114].

Table 6.4 Instrumental and chromatographic conditions for HPLC method

Mobile phase	ACN : water (90:10)
Column	C18, (100 mm × 4.6 mm, 5µm or equivalent)
Column temperature	25°c
Elution mode	Isocratic
Flow rate	1.0 ml/min
Detection wavelength	210 nm
Injection volume	20ul
Expected retention time	About 6.3 minutes
Run time	10 minutes

Optimum flow rate and ratio of mobile phase components was determined with use of 2^3 factorial design. Two factors viz. flow rate and composition of mobile phase were screened at three levels each. The dependent variables selected for the design included peak area, retention time (RT) (min.) and NTP value (Table 6.5). Other parameters including column temperature,

injection volume and detection wavelength were kept constant. Design-Expert (Version 10, Stat-ease. Inc, USA)software was used for deriving statistical model including parameters such as best fitting model, polynomial equation, perturbation plots, interaction plots and 3-D response curve. The optimum combination of the set factors was determined by setting the p-value at <0.05.

Table 6.5Matrix design for 2^3 Factorial design (Analytical)

Independent parameters	Levels (Coded)		
	Low	Medium	High
X1: Mobile phase (MP) composition	-1	0	1
X2: Flow rate (ml/min)	-1	0	1
Dependant parameters			
Y1= Peak area			
Y2= Retention time (RT)			
Y3= NTP			

Description of independent parameters and coded levels for experimental design for analytical method development is as described in Table 6.6.

Table 6.6Experimental design for optimization of analytical method development

Levels	**Low**	**Medium**	**High**
1) Composition of mobile phase (Acetonitrile: water)	70:30	80:20	90:10
2) Flow rate (ml/min)	0.5	1	1.5

The effect of each independent parameter was studies for each dependent parameter. The design space was constructed and analysed to derive the optimum product quality. The streamlining was performed to lessen the retention time by analysing desirability criteria

(numerical) as well as overlay plot (graphical). The established model as further validated by evaluating the observed and predicted response values.

B. Preparation of Standard Solution:

A stock solution of BCPO(100 µg/mL) was prepared by weighing 10 mg of BCPO and transferring it to a volumetric flaskof100ml capacity. The volume was adjusted with mobile phase (ACN : water, 90:10).From this, 2 ml of solution was placed in a 10 ml volumetric flask. The volume of the solution was adjusted to 10 mL with the mobile phase to create a standard solution of 20 µg / mL.

C. HPLC Method Validation[115][116][117][118][119]

The HPLC method was developed and validated as per the guidelines by International Conference on Harmonization (ICH). Parameters for validation included linearity, precision, system suitability, accuracy, range, limit of detection and quantification limit.

1) System suitability:

System suitability of the method was ascertained by analysing five replicates of the standard solution (20µg/mL). The parameters including column efficiency assessed by the number of theoretical plates (N); BCPO retention time (tR) and tailing factor (Tf) were calculated.

2) Linearity:

To determine the linearity, peak area was plotted against the concentrations of BCPO for a sequence of concentrations of standard solutions (1, 5, 10, 15, 25 and 50 µg/mL) and Calibration curve was obtained. The linearity was assessed by analysis of linear regression with the use of least squares methodology.

3) Precision:

To determine the precision the standard solutions with different BCPO concentrations (15, 20 and 25µg/ml) was assayed. For intra-day precision the samples were analyzed at three concentration levels of BCPO in the same day. Inter-day precision was performed by analysing the solutions on three consecutive days.

4) Accuracy:

Accuracy is known as the closeness of the results with their theoretical value. Accuracy is established after determination of linearity, precision and specificity. Accuracy of HPLC

method for BCPO was assessed by calculating the percentage of recovery of known amounts of BCPO from three different concentrations standard solutions (15, 20 and 25µg/mL). Samples were evaluated in triplicate and the results were analysed by comparing the amount of BCPO added with the results acquired by the HPLC assay.

5) Range: was established from the results of linearity, precision and accuracy test.

6) Limit of Detection (LOD) and Limit of Quantification (LOQ):

LOD was established with the use of calibration curve and following equation (1):

$$\boldsymbol{LOD = 3.3\sigma/S} \quad (1)$$

where, σ = standard deviation of the response and

S = slope of the curve

LOQ is a significant parameter in case of colloidal carrier systems. Very low value of drug should be detectable for the given carrier system with the use of established method. The LOQ was determined by the calibration curve and applying the equation (2):

$$\boldsymbol{QL = 10\sigma/S} \quad (2)$$

where σ = standard deviation of the response and

S = slope of the curve.

D. Forced degradation study[120][121]***:***

In order to validate the developed HPLC method, the drug was exposed to different degradation conditions. Stability of the samples exposed to various extreme conditions was determined with the use of HPLC method. Frequently encountered degradation mechanisms include oxidation, acid and base hydrolysis, thermal and photolytic degradation.

1) Acid, base and neutral hydrolysis:

Hydrolysis of BCPO at acidic, basic and neutral p H conditions was analysed by undertaking series of trials. BCPO solution (5 ml, 200µg/mL) was delivered to a 50mL round bottom flask. The samples were refluxed with 5mL of 1 N HCL and 0.1 N HCl as acid hydrolysis, and 1.0N NaOH and 0.1 N NaOH as basic hydrolysis for 2 hours. BCPO solution at same concentration as acid and base hydrolysis was also mixed and refluxed with distilled water as neutral

hydrolysis at 80°C for 1 hour. At the end of the reflux reaction, samples were sufficiently diluted with the use of mobile phase to get 20µg/mL solution.

2) Preparation of samples for Oxidative degradation:

For oxidative degradation, 5 ml of BCPO solution (200 µg/mL) was mixed with 3 %, 10% and 30% v/v of H2 O 2 solution. The reaction mixtures were further stored at room temperature (RT), protected from exposure to light for 24 hours. The samples were then sufficiently diluted with the use of mobile phase, yielding a concentration of 20µg/mL and analyzed using HPLC.

3) Thermal degradation:

Degradation of drug after exposure to high temperature was studied by keeping the samples of BCPO in hot air oven at 60^0C and80°C for 2 hours, 4 hours and 24 hours. At the end of the exposure, BCPO solution (20µg/mL) was prepared with mobile phase and analyzed using HPLC.

4) Photolytic degradation:

Photolysis of BCPO was evaluated by exposing the BCPO sample to sunlight for 8 hours. A stock solution of BCPO(200µg/mL) was developed by adding 20mg of accurately weighed BCPO to a volumetric flask of 10mLcapacity.Thevolume was adjusted by addition of mobile phase. The sample was suitably diluted with the mobile phase, yielding a final solution of 20µg/mL and analyzed using HPLC.

E. Drug excipient compatibility studies:

BCPO was subjected to compatibility study with each excipient in order determine the stable combination of drug and suitable excipients. To perform compatibility studies, drug was mixed with each excipient in equal ratios and the blend was packed in glass vials. The mouth of the vial was closed with aluminium foil with perforations and vials were kept at the conditions of40°C/75% RH for 1 month. During the study, the vials were observed for any visual and physicochemical changes including discoloration and liquefaction. The stability of BCPO in all the blends was further analysed by HPLC. Table 6.7 depicts the blends of samples exposed to compatibility study.

Table 6.7 List of samples for drug-excipient compatibility study

Sr no.	Sample	Drug: Excipient ratio

1.	Pure drug	1
2.	Compritol 888 ATO	1:10
3.	Gelucire 50/13	1:10
4.	Docosahexanoic acid	1:10
5.	Folic acid	1:10
6.	Stearic acid	1:10

6.2.4. Solubility profile in lipids and surfactants

Different components of formulation included solid lipid, liquid lipid, surfactant, drug (BCPO) and vehicle (water). A systematic scientific approach was utilized for selection of individual component of the formulation.

1) Solubility in solid lipid:

Solid Lipid component of the formulation was chosen based on the solubility of drug in given solid lipids which is evaluated by microscopic techniques along with the visual observations. Various lipids screened under this study included Compritol 888ATO, Precirol ATO5, Stearic acid, Glyceryl monostearate. To observe the outcome of increasing amount of lipid on drug solubility, drug and lipid were melted together in drug: lipid ratios of 0.5:1, 1:1, 1:2, 1:8 and 1:20. Smear of melted Drug-Lipid mixture was made on glass slide and observed under microscope for free drug crystals. List of solid lipids screened along with the melting points is given in Table 6.8.

Table 6.8Solid lipids with melting points

Sr no.	**Solid lipid**	**Melting point (^{0} C)**
1.	Glyceryl monostearate	78-81
2.	Stearic acid	69-70
3.	Precirol ATO 5	50-60
4.	Compritol 888 ATO	65-77

2) Solubility in surfactants:

Surfactant component of the formulation was selected by addition of surfactant to Drug-Lipid mixture. The mixture was further melted, and water was added to the mixture at same temperature. Particle size of the resulting emulsion was measured with the use of zeta sizer (*MalvernZS90*). Suitability of the surfactant was assessed based on the particle size. Various surfactants screened included Gelucire 50/13, Gelucire 48/16, Tocopherylpolyethyleneglycol1000succinate (TPGS), Polysorbate 20 (T20), Kolliphor P188 (P188), Kolliphor RH40 (RH40), Kolliphor P407 (P407), Polysorbate 80 (T80), Kolliphor EL (EL). Combinations of solid lipids (200 mg) with each surfactant were prepared at three different levels of surfactant (200 mg, 350 mg, 500 mg). The experimental design for the same is as depicted in Table 6.9.

Table 6.9 Experimental design for screening of surfactants

Set / Surfactant	**TPGS**	**T20**	**P188**	**RH40**	**P407**	**T80**	**EL**
Lipid I: Compritol 888 ATO 200mg							
Set I*	200	200	200	200	200	200	200
Set II*	350	350	350	350	350	350	350
Set III*	500	500	500	500	500	500	500
Lipid II: Precirol 200mg							
Set I	200	200	200	200	200	200	200
Set II	350	350	350	350	350	350	350
Set III	500	500	500	500	500	500	500

Set I: Level of each surfactant at 200 mg

Set II: Level of each surfactant at 350 mg

Set III: Level of each surfactant at 500 mg

6.3. Formulation development and optimization

Targeted delivery systems of solid lipid nanoparticles (SLN) and nanostructured lipid carriers (NLC) were developed for intravenous administration. For preparation of these delivery systems in sequential and scientific manner, Quality-by-design (QbD) method was undertaken.

6.3.1. Quality by Design (QbD)

Quality by design is a scientific tool used in pharmaceutical industry which is based on in-process quality control of the products being developed. QbD approach does not rely on the finished product testing and focuses on identifying the critical parameters affecting the product quality during development stages. With the use of QbD approach, the process is streamlined and a deeper understanding is developed regarding the all the components affecting the quality of the finished product. While adopting QbD approach, as a first step, critical process parameters (CPP) are identified. Further, critical quality attributes (CQA) are established as the parameters that have substantial impact on the quality of finished product. With use of statistical design software such as Design-Expert, the optimized product is established from minimum number of trials[122][123][124][125][126].

1) Quality target product profile (QTPP):

Quality target product profile (QTPP) is established as a first step of QbD approach. Quality characteristics to be achieved to establish desired quality of the product are summarised in QTPP.

For the formulation of BCPO lipid nanoparticles, QTPP was decided as described in the Table 6.10.

Table 6.10 Quality Target Product Profile (QTPP)

element of QTPP	**Target**	**Justification**
Dosage form	Targeted Lipid based nanoparticles	To improve bioavailability at tumour site and to reduce off-target toxicity

Route of administration	Intravenous		
Dosage strength	To be founded on the outcomes of *in vitro* cytotoxicity and acute toxicity studies		B-caryophyllene is a natural origin drug which has not been explored for its anticancer potential. There is no marketed formulation available.
Indication	B-caryophyllene is natural origin active ingredient, originally being used for its flavouring properties in cosmetic industry. It has been found to possess anticancer potential in recent Literature		As per the literature reports, B-caryophyllene has shown anticancer effect in in vitro cell line studies
Dosage regimen	To be founded on the outcomes of *in vitro* cytotoxicity and acute toxicity studies		B-caryophyllene is a natural origin drug which has not been explored for its anticancer potential. There is no marketed formulation available.
Patient population	Patients suffering with breast cancer including the subtype of hormone receptor negative breast cancer		Based on literature information.
Shelf- life	Minimum 24-months of shelf-life at refrigeration temperature		Equivalent to or better than the shelf-life of standard anticancer agent.
Quality attributes of drug product	Physical	Lipid nanoparticles suspended in aqueous vehicle	Meeting the compendial quality standards

	Identification	By FT-IR, HPLC, XRD, DSC	
	Assay	% Of label claim (by HPLC): 90-110% w/w	
	Drug release	Type of apparatus: Dialysis bag Rotation speed: 100 rpm Media: 100 ml of ethanolic phosphate buffer (p H 7.4)	Based on drug product development data
Container and closure system	Container and closure system considered suitable for such type of formulation system		Necessary to keep the product stable for target shelf-life

2) Critical quality attributes (CQA):

Critical quality attributes (CQA) are the quality parameters which should fall within the appropriate range or limits to guarantee the required quality in established product. CQAs are identified with the help of QTPPs.

Table 6.11describes the critical quality attributes for the desired formulation.

Table 6.11 Critical Quality Attributes

Quality attributes of drug product	**Target**	**Is this a CQA?**	**Justification**
Appearance	No visual defects to ensure patient acceptability	No	Appearance of nanoparticles is not connected to safety as well as efficacy.
Size	To be decided based on development	Yes	Inconsistency in particle size will affect the efficacy. Therefore, particle size will be evaluated at the intermediate step and at the final stage for the finished product.

Odour	No appreciable odour	No	Odour of the formulation is not connected to safety and efficacy.
Assay	% Of label claim (by HPLC): 90-110% w/w	Yes	Inconsistency in assay will disturb safety and efficacy. Therefore, assay will be evaluated at intermediate step and at the final stage for the finished product.
% Entrapment efficiency (EE)	50 % or above	Yes	Low entrapment efficiency will adversely affect the efficacy. Therefore, EE will be evaluated at the intermediate step and at the final stage for the finished product.
Drug release	Not more than 15 % in 24 hours in phosphate buffer pH 7.4	Yes	Failure to achieve the dissolution specifications may have an adverse impact on Pk/Pd of drug and thus affect efficacy of the product. Hence, the attribute will be monitored all the way through the formulation development process

3) Initial risk assessment of formulation variables:

Initial risk assessment was performed to identify potential high risk formulation variables based on preliminary hazard analysis (PHA). PHA method is based on the use of uncertainty and severity scores to understand the level of risk of formulation variables. Scores for uncertainty (u) and severity (s) are assigned based on the understanding of formulation development and available literature data.

Table 6.12 and Table 6.13 describe the uncertainty levels severity levels.

Table 6.12Levels of uncertainty and definitions

Levels	Uncertainty	Probability
1	**Full knowledge** The parameter has been thoroughly assessed previously for this product	**Negligible** <1 in 200 chances of failure.

2	**Prior experience** The parameter has been thoroughly measured on other products depicting sufficient similarity (which may include similarity in API, similar process of formulation or similar dosage form), or the product is evaluated based on previously confirmed statistical or mechanistic models.	**Low** <1 in 50 chances of failure.
3	**Published literature** Impact of the parameter can be deduced from literature data as well as from general knowledge of pharmaceutical process and technology.	**High** <1 in 20 chances of failure.
4	**Insufficient knowledge** The impact of this parameter is not properly understood.	**Very high** >1 in 20 chance of failure.

Table 6.13 Definition of Severity levels

Levels	Severity
1	**Zero impact.** when the parameter has no influence on product quality.
2	**Impact on non-CQA.** When the parameter does not affect CQAs of the product but may affect other product or process related attributes.
3	**Impact on CQA.** When the parameter influences a CQA, however, outcomes can be appropriately corrected or balanced in downstream processes to avoid a failure of the process.
4	**Critical impact on CQA.** When the parameter influences a product CQA resulting in a failed batch.

Based on the above scoring system risk prioritization matrix was made and is given in below in Table 6.14.

Table 6.14 Uncertainty or probability risk prioritization matrix

	Uncertainty			
	1	**2**	**3**	**4**

Severity	1	Low	Low	Medium	High
	2	Low	Low	Medium	High
	3	Low	Medium	High	High
	4	Medium	High	High	High

For each formulation variable the combination for severity and uncertainty is referred from the above risk prioritization matrix to carry out the initial risk assessment and is as follows: -

- When the ensuing criticality is **low,** no follow-up action is required. However, the ALARP principle still pertains(ALARP – as low as reasonably possible).

- When the ensuing criticality is **medium,** follow-up action is suggested, applying the ALARP principle.

- If the subsequent criticality is **high,** mandatory follow-up action to reduce the risk.

The initial risk assessment matrix (Table 6.15) is constructed based on above scoring criteria and references from pharmaceutical database.

Table 6.15 Initial risk assessment

CQA	**Drug substance**	**Level of lipid**	**Level of Surfactant**	**Level of conjugate**
	U S risk	U S risk	U S risk	U S risk
Particle size	2 3 Medium	2 4 high	2 4 high	4 4 high
PDI	2 3 Medium	2 4 High	2 4 High	4 4 High
Entrapment efficiency	2 4 High	2 4 High	2 4 High	3 1 Medium
Drug release	4 4 medium	2 3 high	2 3 high	4 4 high

6.3.2 Formulation of BCPO loaded solid lipid nanoparticles (BC-SLN)

The drug loaded SLN were prepared by melt emulsification method (FAC.1, cross ref!). To prepare drug loaded SLN, solid lipid and surfactant were mixed in ratio of 1:2.5 and heated to 65^0 C. Aqueous phase (distilled water) was heated separately at same temperature. To molten mixture of solid lipid and surfactant, 20 mg of BCPO was added just before addition of aqueous phase to avoid its exposure to high temperature for longer duration. Aqueous phase was mixed with lipidic phase at once and under continuous stirring. The resultant hot emulsion was subjected to probe sonication at 40% amplitude for 10 min. Temperature was sustained at 60^0 C during sonication. Towards the end of the sonication process, the mixture was immediately subjected to low temperature (2-8^0 C) to obtain SLN[25][127].

A) Selection of suitable solid lipid:

Solid lipid component of the formulation system was selected based on miscibility of BCPO in melted lipid. Smear of melted Drug-Lipid mixture was observed under microscope as described in 3.6.Out of all solid lipids evaluated (Stearic acid, Compritol 888ATO, Glyceryl Monostearate and Precirol ATO5), Compritol 888ATO and Precirol ATO5 showed good solubilisation capacity for Drug.

Compritol 888ATO and Precirol ATO5 were further evaluated in combination with various surfactants based on particle size. The experimental design for the combinations of Compritol 888ATO and Precirol ATO5 in as given in Table 6.16.

Table 6.16 Experimental design for selection of solid lipid

Component	**F1**	**F2**	**F3**	**F4**	**F5**	**F6**	**F7**	**F8**
Drug (mg)	20	20	20	20	20	20	20	20
Compritol 888ATO	200	200	200	200	-----	-----	-----	-----
Precirol (mg)	-----	-----	-----	-----	200	200	200	200
Tween 80 (mg)	500				500			
Cremophor EL		500				500		

Gelucire 48/16			500				500	
Gelucire 50/13				500				500
Distilled water (ml)	20	20	20	20	20	20	20	20

B) Selection of suitable surfactant and optimization of lipid: surfactant ratio:

Initial experimental results provided insights into efficiency of different surfactants in particle size reduction. Among the various surfactants screened, Gelucire 50/ 13 and Gelucire 48/16 showed better particle size reduction in combination with Compritol 888 ATO. For further optimization of lipid: surfactant ratio and volume of aqueous phase, 2^3Factorial design was adapted. For this study, influence of independent process parameters viz., Lipid: surfactant ratio (X1) and volume of water (X2) on dependent parameters viz., particle size (Y1) and PDI (Y2) was evaluated at three levels (**Table 6.17**). The experimental design was separately applied to each of surfactant Gelucire 50/13 and Gelucire 48/16 to select suitable surfactant. Sonication time (10 min) and processing temperature were kept constant throughout the experimental design. Design-Expert(Version 10, Stat-ease. Inc, USA) software was used to derive the statistical model including parameters such as best fitting model, polynomial equation, perturbation plots, interaction plots and 3-D response curve. The optimum combination of the set factors was determined by setting the p-value at <0.05.

Table 6.17 Matrix design for 2^3 Factorial design I

Independent parameters	Levels (Coded)		
	Low	Medium	High
X1: Lipid: Surfactant ratio	-1	0	1
X2: Volume of water (ml)	-1	0	1
Dependant parameters			
Y1= Particle size (nm)			
Y2= PDI			

Description of independent parameters and coded levels for experimental design for Gelucire 50/13 and Gelucire 48/16 are given in Table 6.18 and Table 6.19.

Table 6.18 Experimental design for Gelucire 50/13

Levels	Low	Medium	High
1) Compritol 888ATO: Gelucire 50/13ratio	1:5	2:5	4:5
2) Volume of Water	10ml	20ml	30ml

Table 6.19 Experimental design for Gelucire 48/16

Levels	Low	Medium	High
1) Compritol 888ATO: Gelucire 50/13 ratio	1:5	2:5	4:5
2) Volume of Water	10ml	20ml	30ml

The design space is constructed by analysing the effect of each independent parameter on each dependent parameter. Further, the formulation process was streamlined in order to lessen the results of dependent parameters to fit the desirability criteria. Overlay plot was used to arrive at the optimized formula which dictates the balance between set ranges of dependent parameters. The model was further validated by assessing the observed and predicted values.

6.3.3. Formulation and optimization of BCPO loaded nanostructured lipid carriers (BC-NLC)

Nanostructured lipid carriers of BCPO were formulated by the method similar to SLN as describes in 3.7.2. Liquid lipid i.e., docosahexanoic acid (DHA) was added to lipid phase just before addition of drug to avoid its exposure to high temperature. To understand the effect of amount of DHA added to formulation on particle size, increasing amount of DHA was added to lipid phase by replacing parts of solid lipids as depicted in Table 6.20[128][129].

Table 6.20 Addition of increasing amount of DHA to formulation

Ingredients	F1	F2	F3	F4	F5

Drug (mg)	20	20	20	20	20
Compritol 888 ATO (mg)	175	150	125	100	50
DHA (mg)	25	50	75	100	150
Gelucire 50/13 (mg)	500	500	500	500	500
Water (ml)	20	20	20	20	20

From the preliminary trials, it was understood that, increasing amount of liquid lipid (DHA) in formulation led to decrease in particle size. NLC is also known to enhance the loading capacity of formulation system [128][130]. The level of DHA in NLC was thus optimised with the use of 2^3Factorial design[131][132][133]. The independent parameters used for this study included % amount of DHA (X1) and amount of drug (X2). The effect of independent parameters was evaluated on dependent parameters viz. particle size (Y1) and entrapment efficiency (Y2). Rest other experimental parameters were kept constant. Design-Expert (Version 10, Stat-ease. Inc, USA) software was utilised to derive the statistical model including parameters such as best fitting model, polynomial equation, perturbation plots, interaction plots and 3-D response curve. The optimum combination of the set factors was determined by setting the p-value at <0.05. Table 6.21design for 2^3 Factorial design II.

Table 6.21 Matrix design for 2^3 factorial design III

Independent parameters	**Levels (Coded)**		
	Low	Medium	High
X1: % amount of DHA	-1	0	1
X2: amount of drug (mg)	-1	0	1
Dependant parameters			
Y1= Particle size (nm)			
Y2= Entrapment efficiency (%)			

Description of coded values of independent parameters is given in Table 6.22.

Table 6.22 Coded values for Experimental design II

Levels	Low	Medium	High
1) % Amount of n-3 PUFA	10%	30%	50%
2) Amount of drug	25mg	50mg	75mg

The design space is constructed by analysing the effect of each independent parameter on each dependent parameter. Further, the formulation process was streamlined to lessen the results of particle size and increase the results of entrapment efficiency to fit the desirability criteria. Overlay plot was used to arrive at the optimized formula which dictates the balance between set ranges of dependent parameters. The model was further validated by assessing the observed and predicted values.

6.3.4. Chemical conjugation of folic acid and stearic acid

Chemical conjugate of Folic acid-Stearic acid was prepared by slight modification of previously reported method[134][135][55].To conjugate folic acid and stearic acid, 800 mg of stearic acid was dissolved in DMF. Further, 800 mg of 1-Ethyl-3-(3-dimethylaminopropyl) carbodiimide (EDC) was added to stearic acid and DMF solution as a catalyst and the mixture was further reacted for 1 hour. Secondly, 1200 mg of Folic acid dissolved in 5 ml of pyridine was mixed with stearic acid, DMF and EDC mixture. The reaction was further continued for 24 hours. At the end of reaction, 50 ml of water was added to precipitate folic acid and stearic acid conjugate. To remove un-reacted reagents and other water-soluble products, the conjugate was dialysed against distilled water with the use of cellulose acetate membrane for 24 hours. Final conjugate was collected by filtration and air dried for further use. Figure 6.5 [134]shows the scheme for chemical reaction between stearic acid and folic acid.

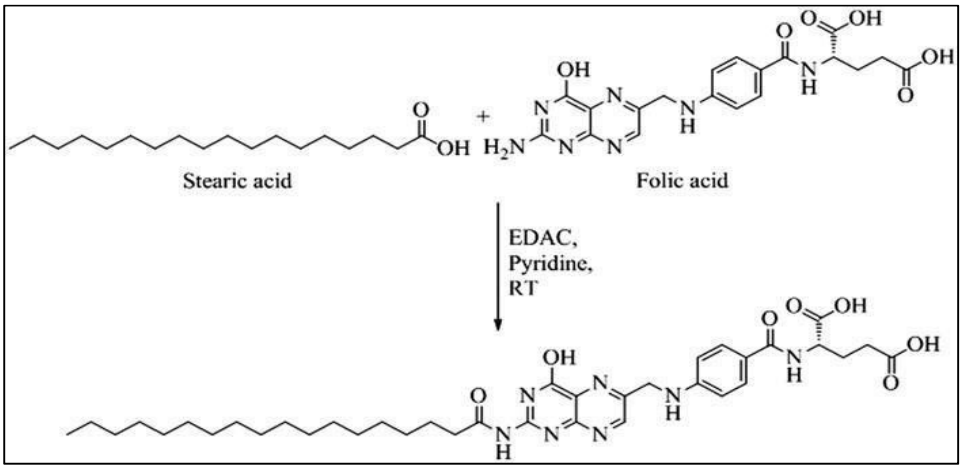


Figure 6.5. Stearic acid-Folic acid conjugation scheme

A) Incorporation of Folic acid-Stearic acid conjugate in developed formulation(FA-BC-NLC):

A part of solid lipid was further replaced with developed conjugate of Folic acid and Stearic acid. Folic acid-Stearic acid conjugate was added in increasing amount in the formulation by replacing part of solid lipid. Folic acid conjugated BCPO NLC (FA-BC-NLC) was prepared by similar method as described in 3.7.3. Folic acid-stearic acid conjugate was added to lipidic phase just before the addition of drug and along with DHA. Effect of addition of increasing amount of conjugate (Table 6.23) was further evaluated on the basis of particle size.

Table 6.23 Addition of increasing amount of n-3 PUFA in formulation

Ingredients	**F1**	**F2**	**F3**	**F4**
Drug (mg)	20	20	20	20
Compritol 888 ATO (mg)	140	130	115	100
Liquid lipid (mg)	60	60	60	60
Lipid conjugate (mg)	00	10	25	40
Gelucire 50/13 (mg)	500	500	500	500
Water (ml)	20	20	20	20

6.3.5. Sterilisation of developed formulation

To make the formulation suitable for intravenous administration, various methods including membrane filtration, autoclaving, and preparation aseptic area were explored for preparation of sterile formulation. Formulations developed by each of these methods were further subjected to Test for sterility to check suitability of each method. Other parameters including particle size, PDI and % assay were also considered for finalising the method for sterilisation of formulation[136][137][138].

1) Sterilisation by Membrane filtration:

FA-BC-NLC was prepared with the method described in 3.7.4. The formulation was further filtered through 0.22 µm membrane filter under vacuum in aseptic area in sterile container. The container was sealed with sterile aluminium cap and further subjected to test for sterility.

2) Sterilisation by autoclaving:

FA-BC-NLC formulation was filled in a clean glass vial making sure to leave some headspace. The vial was capped airtightly with aluminium caps and subjected to autoclaving at 120^0 C and 15 psi for 20 min. At the end of the autoclaving cycle, the content of the vial was subjected to test for sterility.

3) Preparation of formulation in aseptic area:

The glass apparatus and water required for preparation of formulation was autoclaved at 120^0 C and 15 psi for 20 min. beforehand. All the other material including water bath, tripod stand were wiped with ethanol and exposed to UV light for 20 min. All the material was aseptically transferred inside aseptic area. The formulation was prepared as described in 3.7.3. The prepared formulation was filled in sterile vial and sealed. It was further subjected to test for sterility.

A) Test for sterility:

Formulations sterilised by different sterilisation methods were subjected to test for sterility. Test for sterility was performed by direct inoculation method. The culture media used for the test included Soyabean-Casein Digest Medium and Fluid Thioglycollate Medium.Formulation amounting to 1 ml was carefully removed from the sealed containers with a sterile pipette. It was aseptically transferred to the test tubes containing 9ml of culture media. The liquids were mixed carefully taking care not to aerate excessively. Positive and negative controls were also

maintained along with the test samples. The inoculated media was incubated 30–35°C for 'Fluid ThioglycollateMedium'and at 20–25°C for 'Soyabean-Casein Digest Medium' for 14 days. After 14 days, all samples were subcultured on fresh media and incubated for another 14 days. At the end of the test, test tubes were observed for growth in form of turbidity in test tubes.

6.4. Characterization

Developed nanosystems were evaluated for particle size, % drug release, %entrapment efficiency and size distribution (PSD). Chemical structure of Folic acid-Stearic acid conjugate was evaluated by FT-IR and Mass spectrometry[139].

6.4.1. Particle size and size distribution (polydispersity index)

The mean diameter of particles and size distribution of developed nanosystems were obtained by particle size analyser. To measure the particle size, 10-fold diluted samples were used with distilled water as dilution medium. 1ml of sample after dilution was filled in the cuvette and particle size and PDI were analysed at 25^0C by the principle of dynamic light scattering at the angle of 90°.

6.4.2. Zeta potential

Zeta potential of developed formulation was determined with the use of same instrument as that of particle size (Malvern Zetasizer-ZS90). Sample was diluted in the ratio of 1:10 before zeta potential measurement. To measure zeta potential by the principal of dynamic light scattering, samples were filled inside the folded capillary cells. The cell creates an electric field. The particles get attracted towards the opposite charge and travel with the velocity proportional to their zeta potential. Velocity the further measured with the aid of principle of light scattering and converted to zeta potential with the use of software.

6.4.3. Scanning electron microscopy

Morphology of particle surfaces of developed nanosystems was observed by scanning electron microscopic technique (JEOL JSM IT 200 SEM).

6.4.4. Transmission electron microscopy (TEM)

TEM technique (JEM-1400Plus Electron Microscope, Jeol Co, Japan) was used to evaluate the morphological characteristics of FA-BC-NLC formulation. The suitably diluted sample as placed on carbon-laminated coper grid and air-dried before measurement of particle size and morphology.

6.4.5. Drug loading and Entrapment efficiency

Entrapment efficiency and capacity of drug loading was established by ultracentrifugation method. Briefly, 3 ml of formulation was subjected to ultracentrifugation (Beckmann Optima Max Ultracentrifuge) at 75,000 RPM at 40^0 C for 1 hour. In order to precipitate the lipid nanoparticles, pre-optimized amount of Sodium sulphate was added to the formulation. At the end of the ultracentrifugation, supernatant was separated and analyzed for free drug content with the use of HPLC by the method described above[140][141][142][143]. Entrapment efficiency was determined with the use of equation (3).

$$\%\, EE \;=\; weight\ of\ BCPO\ in\ SLN / weight\ of\ BCPO\ added\ X\ 100 \qquad (3)$$

Drug loading capacity was determined with the use of equation(4).

$$\%\, DL \;=\; weight\ of\ BCPO\ in\ SLN \;/\; weight\ of\ BCPO\ loaded\ SLN\ X\ 100 \qquad (4)$$

6.4.6. In vitro drug release

In vitro drug release study was undertaken to establish the sustaining effect of developed nanosystems on drug release. To perform in vitro release of BCPO, FA-BC-SLN and FA-BC-NLC, dialysis bag method was used with magnetic stirrer for 24 hours. Dialysis bag (Cellulose acetate membrane, MWCO 12kDa, HiMedia) was soaked in release media (7.4 buffer) for 12 hours prior to study. Accurately measured drug solution and respective formulation (2 ml) were individually filled in dialysis bag. Dialysis bag was positioned in beaker consisting of 100 ml of release media. Rotational speed of the stirring of media was maintained at 100 rpm on magnetic stirrer. During study, 1 ml of aliquot was removed and immediately substituted with same volume of fresh release media at pre-determined time interval. Aliquots were further centrifuged and injected to HPLC system to determine the % drug release. Similarly, drug release of drug solution (drug dissolved in ethanol) was performed and treated as control. Drug release profile for both drug solution and formulations were developed for 24 hours by making the graph of % cumulative drug release vs time. The release profiles were also analysed for determination release kinetics and drug release mechanism by analysing the data by various release models[141][144][145][146].

6.4.7. In vitro release kinetics

In vitro release kinetics of developed formulation was analyzed with an aim to understand the drug release model and pattern of drug release after intravenous administration. Various kinetic models analysed are enlisted in Table 6.24.

Table 6.24 Kinetic models and their plots

Kinetics Plots	Kinetics Plots
Zero order	The cumulative amount of drug release vs Time
First order	Log cumulative % of drug remaining vs. Time
Higuchi	Cumulative% drug release vs. square root of time
Korsmeyer Peppas	Log cumulative %drug release vs. Log time
Hixson Crowell cube root law	Cube root of drug % remaining vs. Time

6.4.8. Solid-state characterization

A) Differential Scanning Calorimetry (DSC):

Blend of formulation excipients (placebo), drug and BC-NLC were analysed by DSC. Drug sample was weighed accurately (5mg) and wrapped in aluminium pans. The sample was further exposed to a temperature range of 25–280°C at the rate of10°C/min[110].

B) Powder X-ray diffraction (XRD)

Developed formulation along with placebo and pure drug were analysed by XRD (X'PERT MPD, Philips, Holland). The uninterrupted analysis was continued over the angular range of (2Ɵ) of 3°-50°[110].

6.4.9. Evaluation of Folic acid-Stearic acid conjugate by FT-IR, NMR and mass spectrometry

Infrared spectrum of folic acid-stearic acid conjugate was obtained with FTIR (Shimadzu, Japan). The spectrum of the dried sample was recorded from 4000 cm $^{-1}$ to 400 cm^{-1}. Distinctive

peaks corresponding to amide bond formation were identified to confirm the identity of drug. Developed conjugate was identified and confirmed by Mass spectrometry and NMR.

6.4.10. Stability studies:

At the end of the optimization and characterization steps, the formulation was subjected to stability studies. Predetermined number of batches of formulation were filled in glass vials. The vials were sealed with aluminium caps and stored at the temperature of 4°C. The samples were evaluated after 3 months and 6 months for particle size, PDI and entrapment efficiency.

6.4.11. In vitro haemolysis study

In vitro haemolysis study was carried out on whole human blood sample. The first step of haemolysis study consisted of separation of RBCs by centrifugation. The blood sample was centrifuged at 5000 rpm for 10 min. After centrifugation process, the supernatant plasma was removed, and pellets of erythrocytes settled at the bottom were collected. The erythrocytes were further rinsed three times with saline phosphate buffer (pH 7.4) and further resuspended in same buffer to form 10 haematocrit suspension. The second step of haemolysis study consisted of incubation of test samples with RBCs for predetermined period. To evaluate the haemolytic potential of developed formulation, following sets were incubated with RBC suspension (0.5ml):

1) 1 ml of 1% Triton X solution (100% haemolytic standard)

2) 1 ml formulation (equivalent to 1mg/ml of drug concentration)

3) 1 ml of phosphate buffer saline (negative control)

The final volume of the solutions was made up to 10 ml with saline. Solution was incubated at 37^0 C for 1 hour. At the end of 1 hour, solutions were centrifuged, and the supernatant was collected. Absorbance of the supernatant was noted at 540nm. % Haemolysis as calculated with the use of following equation(5):

$$\% \, Haemolysis = \frac{(A_{test} - A_{neg\ control})}{(A_{pos\ control} - A_{neg\ control})} x\ 10 \qquad (5)$$

6.4.12. In vitro cytotoxicity studies on cancer cell lines:

Anticancer potential of drug, synergistic action of drug and n-3 PUFA and anticancer action of FA-BC-NLC was evaluated by in vitro cytotoxicity study[143][147][148][149].

A) Cell lines and culture medium:

In vitro evaluation of cytotoxic effect was done in two breast cancer cell lines viz. MDA-MB-468 and MCF-7. Both cancer cell lines were procured from ATCC. In order to culture the cell lines DMEM medium was used. The medium was also supplemented with penicillin and streptomycin (100IU/ML and 100ug/ml respectively) and Fetal Bovine Serum (FBS)(10% inactivated). The conditions used for cell culture were 5% CO_2, 37^oC and humidified atmosphere. After achieving the confluence, cells were detached from each other and from surface of cell culture flask, with the use of dissociating solution. The composition of dissociating solution consisted of 0.02 % EDTA, 0.2 % trypsin and 0.05 % glucose in PBS. Cells were further observed under the microscope to check cell viability and centrifuged. Seeding of the cells was performed in 96-well cell culture plates as 50,000 cells/well. The plates were further incubated at 37^oC in 5 % CO_2 incubator for 24 hours.

B) Procedure:

Cytotoxicity of developed nanosystems was evaluated by Sulphorhodamine B (SRB) assay method. Two cancer cell lines, MCF-7 which shows over expression of folate receptors[56]and MDA-MB-468, a TNBC cell line, were used for cytotoxicity determination. Briefly, $5X10^3$ cells of each cell line were inoculated in96 well microtiter plates. The plates were kept 37^0 C, 5% CO_2incubator and 100% relative humidity for 24hours before start of the experiment. At the end of 24 hours, seeding medium was discarded and fresh experimental medium with varying concentrations of BCPO solution (in ethanol), SLN containing BCPO (BC-SLN), SLN containing n-3PUFA (n-3PUFA-SLN) and SLN containing BCPO+ n-3PUFA (BC-NLC) was added. After addition of sample solutions, plates were incubated for the period of 48 hours. Adriamycin was used as standard in the study. At the end of 48 hours, 50 µl of SRB solution (0.4% w/v in 1% acetic acid) was added to cell culture plates. Culture plates were incubated at room temperature for 1 hour. At the end of 1-hour, unbound dye was removed, and absorbance of the plates was recorded on a plate reader (Spectramaxi3X) at a wavelength of 540 nm. The wavelength of 690 nm was treated as reference wavelength.

C) Statistical calculation:

%Growth at each concentration level was calculated with the use of equation (6):

$$\%\ Growth\ =\ average\ absorbance\ of\ test\ well\ /\ average\ absorbance\ of\ control\ wells\ *\ 100 \quad (6)$$

% Cell inhibition was calculated as equation (7) :

$$\%\ cell\ inhibition\ =\ 100\ -\ \%\ cell\ growth \quad (7)$$

6.4.13. In vitro cytotoxicity on fibroblast cells

To establish the non-toxic nature of drug as well as developed formulation on non-cancerous or healthy cells, cytotoxicity study was also performed against fibroblast cells[150][151][152].

Materials & Methods

1. MTT Powder (in form of solution passed through a 0.2µm filter and stored at 2–8 ℃)
2. Dimethyl sulphoxide (DMSO)
3. CO_2 incubator (5%)
4. Spectramaxi3X Plate reader

Development of standard solution and test solutions:

Standard: Vincristine

Vincristine stock solution was prepared with the concentration of 1.24mM. The stock solution was serially diluted to attain the concentration of 1.56µM. DMEM plain media was used as dilution solvent.

1.24mM

↓ (24µl of 1.24mM + 276µl of Plain DMEM media)

100µM

↓ (150µl of 100µM + 150µl media)

50µM

↓

(150µl of 50µM + 150µl media) 25µM

(150µl of 25µM + 150µl media)

12.5µM

(150µl of 12.5µM + 150µl media)

6.25µM

(150µl of 6.25µM+ 150µl media)

3.125µM

(150µl of 3.125µM+ 150µl of media)

1.56µM

Development of test solution:

The stock solution of concentration 32mg/mL was prepared using DMSO as a solvent. From the stock solution, sequential dilutions were prepared to arrive at the concentration of 10µg/mL. DMEM was used as dilution solvent for treatment.

32mg/mL

(20µl of32mg/mL+180µlof media)

3.2mg/mL

(30µl of3.2mg/mL+270µl of media)

320µg/mL

(150µl of320µg/mL+150µlof media)

160µg/mL

(150µl of160µg/mL+150µlof media)

80µg/mL

(150µl of80µg/mL+150µl of media)

40µg/mL

(150µl of40µg/mL+150µl of media)

20µg/mL



(150µlof20µg/mL+150µl of media)

10µg/mL

Details of cell lines and cell culture medium:

In vitro fibroblast study was performed in3T3L-1 mouse fibroblast cell line. Cell line was received from ATCC. DMEM medium was used to culture the cell lines. The medium was also supplemented with penicillin and streptomycin (100IU/ML and 100ug/ml respectively) and Fetal Bovine Serum (FBS)(10% inactivated). The conditions used for cell culture were 5% CO_2, 37°C and humidified atmosphere.

Procedure:

After achieving the confluence, cells were dissociated with the use of dissociating solution (0.2 % trypsin,0.05 % glucose in PBSand0.02 % EDTA). Cells were further observed under microscope to check cell viability and centrifuged. Seeding of the cells was performed as 50,000 cells/well in cell culture plates which were further incubated at 37°C, 5 % CO_2 for 24 hours.

After incubation period of 24 hours, the solution from the 96-well plates was discarded and replaced with 100 µl of MTT (0.5mg/1ml of MTT in PBS). The cells were further incubated with MTT solution for 4 hours. At the end of 4 hours, MTT solution was discarded and replaced with DMSO solution (100µl). Plates were shaken with DMSO solution to dissolve the crystals of formazan. The absorbance reading of the plate was measured with plate reader at the wavelength of 590nm to calculate IC_{50} value. % Cell growth inhibition was calculated as follows:

Calculating Inhibition (equation (8)**):**

$$\%\ \boldsymbol{Inhibition} = ((OD\ of\ Control - OD\ of\ sample)/OD\ of\ Control)\ x\ 100. \qquad (8)$$

Chapter 7

Results and discussion

Chapter 7: Results and Discussion

As previously mentioned in the chapter 6, various tests were performed to characterise the drug and to develop lipid-based formulations of BCPO. The results the experimental methodologies are as described below:

7.1. Preformulation studies

Under preformulation studies, various tests were performed to establish and ascertain the fundamental properties of the drug product as well as excipients. Results of the preformulation studies are as described below:

7.1.1. Identification and Standardization of API

A. Physico-chemical properties of drug:

The drug was described for colour, nature, crystalline/ amorphous form, LogP. The properties are as enlisted in Table 7.1[153][154].

Table 7.1Physico-chemical properties of drug

Sr. no.	Parameter	Specification
1.	Colour and Nature	White crystalline powder
2.	Odour	Characteristic
3.	Class	Bicyclic sesquiterpene
4.	Molecular weight	220.356 g/mol
5.	Melting point	61 to 63°C
7.	Boiling point	279.68 °C
8.	LogP	4.4

B. Melting point determination:

Determination of melting point of BCPO was performed by capillary method. The melting point of BCPO was observed to be 62^0 C. Melting point value was found to be matching with the value found out from literature (60-62^0 C)[153][154]. As the melting point of a particular material is an indication of purity, even the low amounts of impurities in the sample can be detected by variability in melting point.

C. Differential Scanning Calorimeter (DSC):

The DSC-TGA thermogram of pure drug is as shown in Figure 7.1. Pure drug shows sharp peak at 63.5^0 C. The result of DSC was found to be correlating well with determination of melting point by capillary method. Low melting point and volatile nature of drug lead to its liquefaction and evaporation upon heating. Broad peak near 273^0 C indicates the boiling point of BCPO[154][153][110].

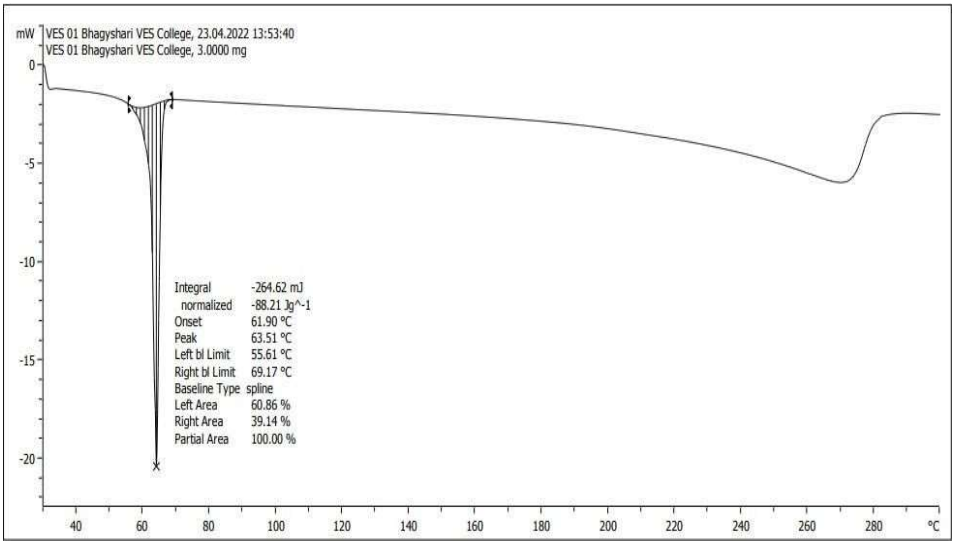


Figure 7.1 DSC-TGA showing melting point of drug

D. UV-Visible spectroscopic method development[155]***:***

UV-Visible spectroscopic method was developed for BCPO at the wavelength of its maximum absorption. BCPO was found to be insoluble in aqueous vehicles and in other conventional surfactants at their low concentrations. Further, use of organic solvents such as ethanol was observed to be interfering with λmax value of drug. Thus, 3% SLS solution was used as vehicle for drug for UV spectroscopy. The λmax of BCPO in 3% SLS solution was found to be 210 nm.

Calibration curve was developed for drug in 3%SLS solution (Figure 7.2). The curve as found to be obeying the Beer-Lamberts law in the range of 4-40 ug/ml. Equation for calibration curve by UV was found to be: $y = 0.0225x + 0.0509$ with R^2 value of 0.997.

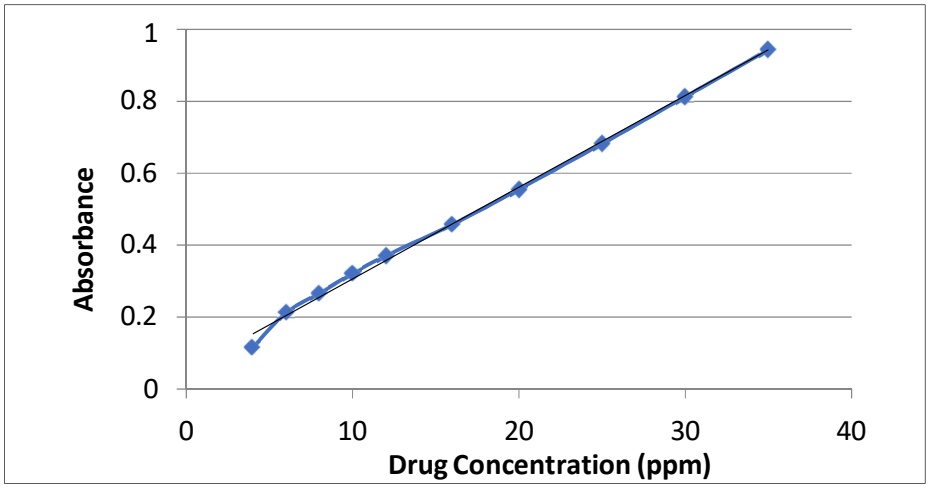


Figure 7.2 Calibration curve of BCPO in 3% SLS solution

E. Fourier Transform Infrared Spectroscopy (FTIR):

Authenticity of drug sample was evaluated by Fourier Transmission Infra-red (FTIR) spectroscopy (Shimadzu). FTIR spectrum of BCPO was recorded for a range of frequencies 4000-400 cm-1 (Figure 7.3). It showed significant peaks confirming its identity including 1645 (C=C nonaromatic stretching) and 2887 (-CH_2 – stretching).Table 7.2 shows characteristic functional groups identified for BCPO.

Table 7.2 Characteristic functional groups of BCPO

Wavenumber (cm^{-1})	**Functional group**
1645	C=C nonaromatic stretching
2887	-CH_2 – stretching

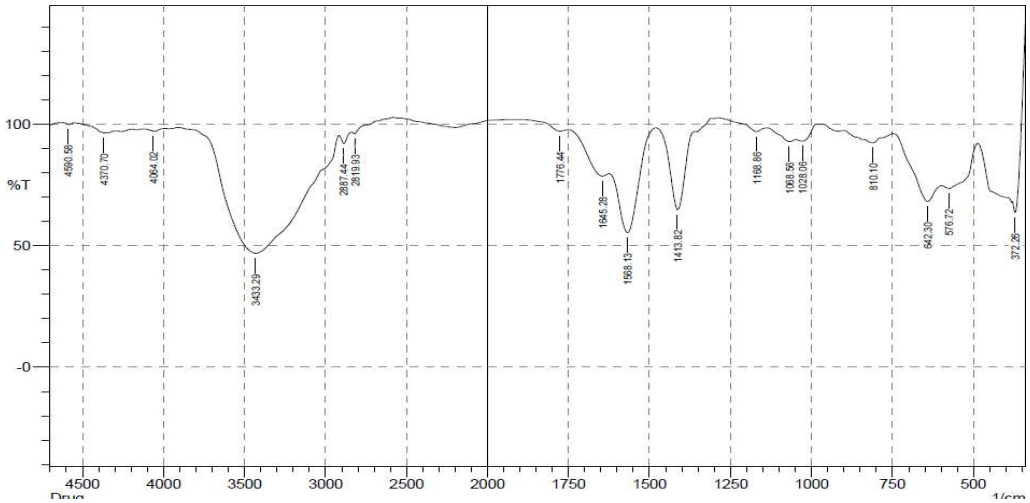


Figure 7.3 FT-IR spectra of BCPO

7.1.2. Characterization of morphology and bulk crystallinity

A. Appearance and particle size by microscopy:

Drug was observed to be white irregular shaped crystals as observed under light microscope. The particle size was found to be between 500um to 1 cm as observed under 45X magnification.

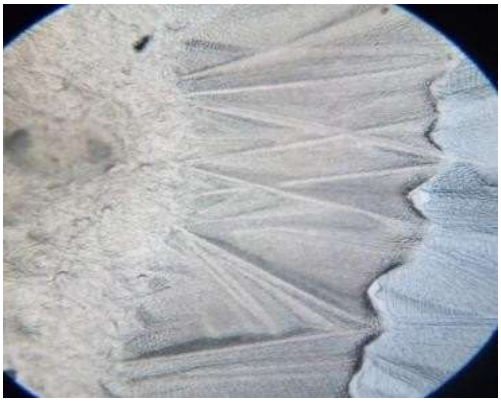


Figure 7.4 Microscopic appearance of BCPO

B. Scanning electron microscopy:

The Scanning electron microscopic study was undertaken to evaluate surface morphology and particle diameter of the optimized formulations. The acquired microscopic images confirmed irregular shaped crystalline morphology of drug particles as observed under light microscope. Figure 7.5shows SEM images of drug particles.

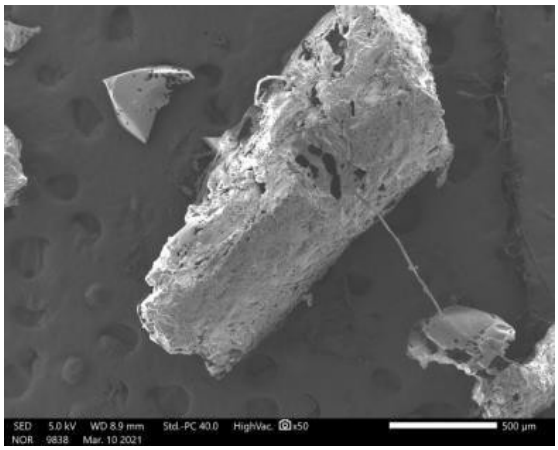


Figure 7.5 SEM image of BCPO particles

C. Powder X-ray diffraction (PXRD*[110]*):

The X-ray diffraction studies were undertaken to establish the crystalline nature of drug. The diffraction patterns Figure 7.6obtained from the graph of 2 Theta (degree) versus Intensity (Counts) showed intense peaks which confirmed the presence of crystalline form of drug. Intense peaks were observed between 2θ values of 10.52, 13.03,14.69, 17.58, 19.97 and 28.89^0.

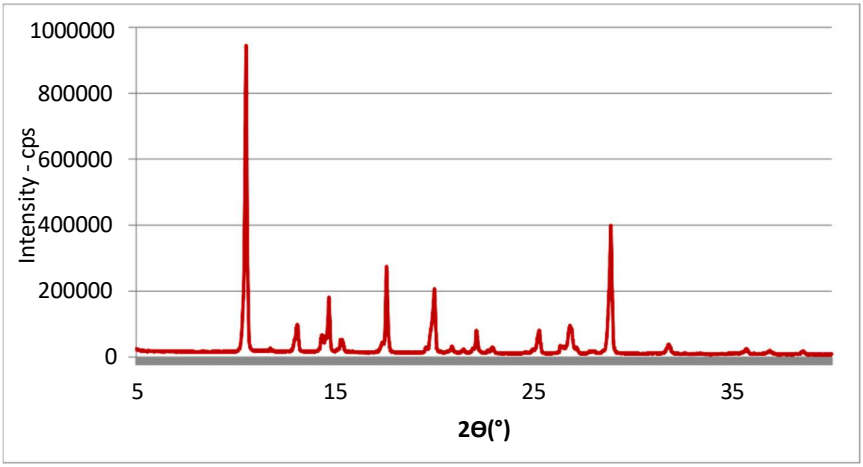


Figure 7.6 XRD pattern of BCPO

7.1.3 Stability indicting analytical method development

A. High Performance Liquid Chromatographic (HPLC) method development and optimization [111][114][113][156]***:***

Stability indicating analytical method was established for quantitative analysis of BCPO from in vitro samples. BCPO eluted at 6.01 min. and the method was found to be selective between linearity range of 2-50 ppm. LOD and LOQ were obtained with the use of the calibration curve

(Figure 7.2). Further, the drug was subjected to various stress conditions such as acidic, alkaline, temperature and oxidative stress to develop stability indicating assay method. Parameters of stress conditions were altered to achieve 10-15% of degradation of drug molecule. Analytical method was validated to separate the degradant peaks from drug peak. Figure 7.7shows the typical chromatogram of depicting peak of BCPO.

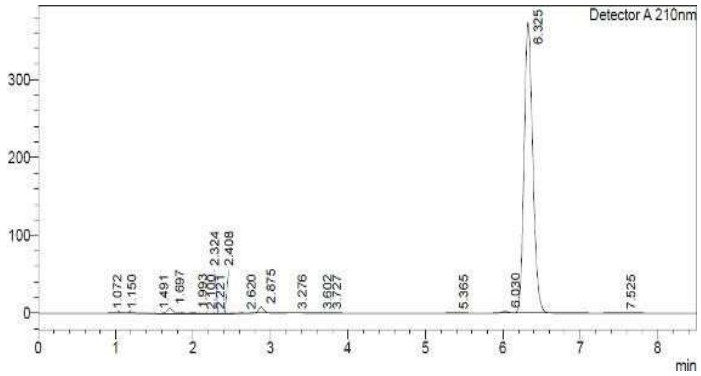


Figure 7.7 Chromatogram of BCPO

Optimum level of flow rate and the mobile phase composition were optimised with use of 2^3Factorial design. Two factors namely composition of mobile phase (ratio of ACN: water) and flow rate were varied at three levels. Peak area, retention time and NTP were measured as responses to check the effect of these variables.

A total of 13 trials were taken as suggested by Design-Expert software in order to fit the data to build a suitable statistical model and contour plots. Based on the fit summary, ANOVA, and the model graphs, the design space was identified to attain the desired intents of optimum peak area, RT and NTP. The model that was found to best fitting for the dependent variables of RT and peak area was Quadratic. The best fitting model for the dependent variable of NTP was 2F1. Table 7.3depicts the Analysis of variance (ANOVA) for three dependent variables of RT, peak area and NTP.

Table 7.3 ANOVA for RT, peak area and NTP

Response	**Source**	**Sum of Squares**	**df**	**Mean Square**	**F-value**	**p-value**	
Retention time	**Model**	573.06	5	114.61	213.14	< 0.0001	**significant**
	A-MP Composition	151.60	1	151.60	281.94	< 0.0001	

	B-Flow rate	322.67	1	322.67	600.06	< 0.0001	
	AB	34.34	1	34.34	63.86	< 0.0001	
	A^2	6.04	1	6.04	11.23	0.0122	
	B^2	37.58	1	37.58	69.88	< 0.0001	
	Residual	3.76	7	0.5377			
	Cor Total	576.82	12				
Peak area	**Model**	1.196E+12	5	2.392E+11	666.56	< 0.0001	**significant**
	A-MP Composition	2.693E+08	1	2.693E+08	0.7503	0.4151	
	B-Flow rate	1.032E+12	1	1.032E+12	2876.14	< 0.0001	
	AB	1.921E+05	1	1.921E+05	0.0005	0.9822	
	A^2	1.747E+09	1	1.747E+09	4.87	0.0631	
	B^2	1.268E+11	1	1.268E+11	353.29	< 0.0001	
	Residual	2.512E+09	7	3.589E+08			
	Cor Total	1.199E+12	12				
NTP	**Model**	1.267E+07	3	4.224E+06	10.88	0.0024	**significant**
	A-MP Composition	1.160E+06	1	1.160E+06	2.99	0.1178	
	B-Flow rate	6.309E+06	1	6.309E+06	16.26	0.0030	
	AB	5.201E+06	1	5.201E+06	13.40	0.0052	
	Residual	3.492E+06	9	3.880E+05			
	Cor Total	1.616E+07	12				

A: Composition of MP, B: Flow rate

The **Model F-values** 213.14, 666.56 and10.88 imply the model is significant also indicated by **P-values** of less than 0.0500. In case of RT and peak area, A, B, AB, A^2 and B^2 are observed to be significant model terms. In case of NTP, B and AB are observed to be significant model terms.

Polynomial equations for RT, area and NTP are as depicted in equation (9), (10) and (11).

$$\begin{aligned} Retention\ time \\ = +8.93897 - 5.02667(MP\ Composition) - 7.33333(Flow\ rate) \\ + 2.93000(MP\ Composition) * (Flow\ rate) \\ + 1.47862(MP\ Composition)^2 + 3.68862(Flow\ rate)^2 \end{aligned} \quad (9)$$

$$\begin{aligned} Area = +5.14241E + 05 + 6699.00002(MP\ Composition) - 4.14760E \\ + 05(Flow\ rate) + 219.16668(MP\ Composition) * (Flow\ rate) \\ + 25150.05753(MP\ Composition)^2 + 2.14253E \\ + 05(Flow\ rate)^2 \end{aligned} \quad (10)$$

$$\begin{aligned} NTP = +10404.48718 - 439.77778MP\ Composition - 1025.44445Flow\ rate \\ - 1140.33333MP\ Composition * Flow\ rate \end{aligned} \quad (11)$$

Figure 7.8, Figure 7.9 and Figure 7.10show contour plots of RT, peak area and NTP respectively. The contour plots depict the effects of changing levels of flow rate and ratio of mobile phase on the response factors. As seen in Figure 7.8, retention time of the drug was observed to be affected by both composition of mobile phase and flow rate. Retention time decreases as the % of ACN in mobile phase increases. Polarity of mobile phase increases with increasing percent of the polar component i.e. water. Increasing polarity leads to more retention of the drug on stationary phase. Increasing the non-polar component in mobile phase leads to faster elution of drug from column. Retention time also decreases with increase in the flow rate of mobile phase owing to the faster elution of the drug [157][158].

Figure 7.9 depicts the effects of mobile phase composition and flow rate on peak area. As observed from Figure 7.9, peak area does not get affected with the change in the composition of mobile phase. However, change in flow rate has considerable effect on the peak area. Peak area is found to decreasing with increase in flow rate of the mobile phase[157].

Figure 7.10 depicts the effects of changes in independent variables on NTP value. As depicted in Figure 7.10, both independent variables do not show considerable effect on NTP value. However, NTP value is observed to be decreasing at higher levels of both the factors.

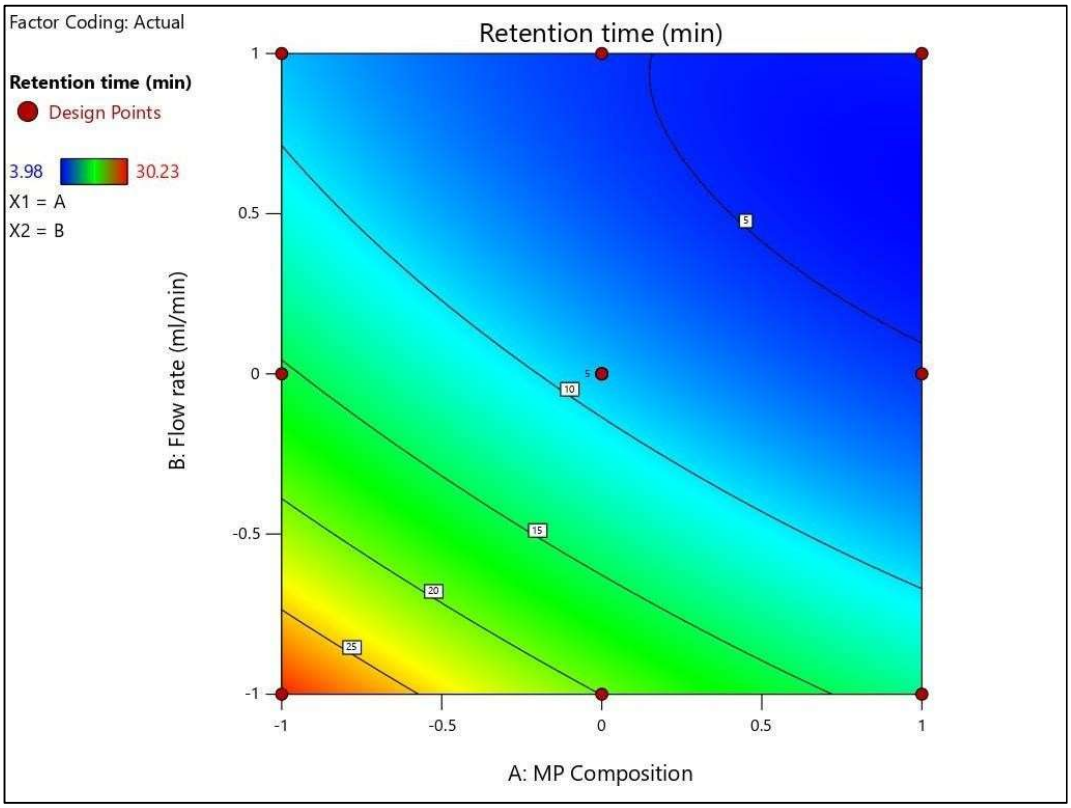


Figure 7.8 Contour plot for RT

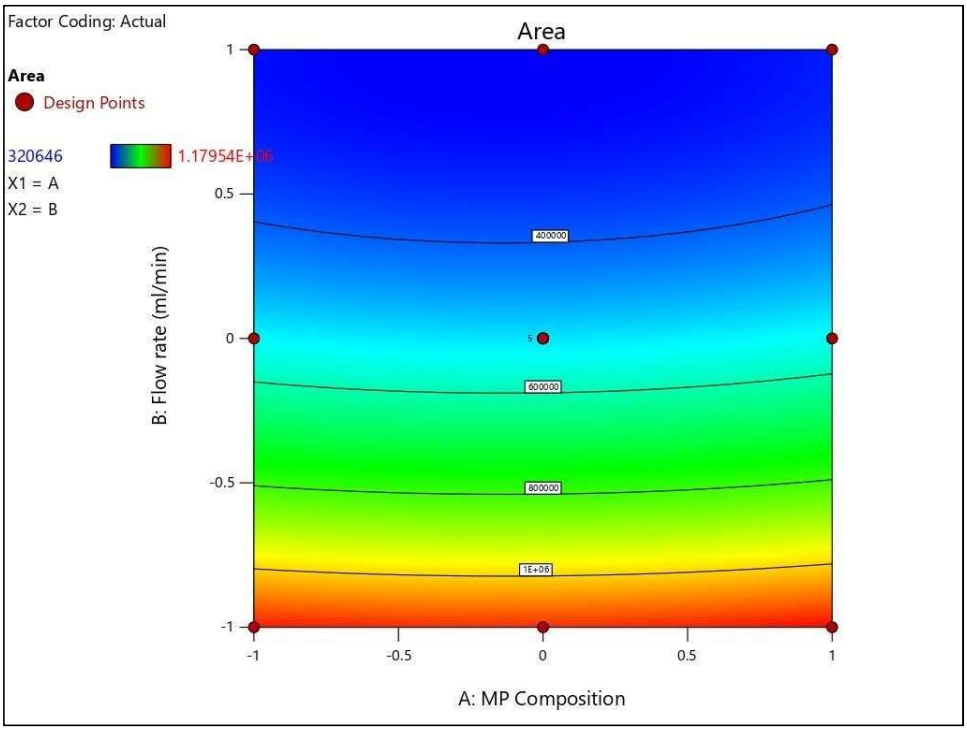


Figure 7.9 Contour plot for peak area

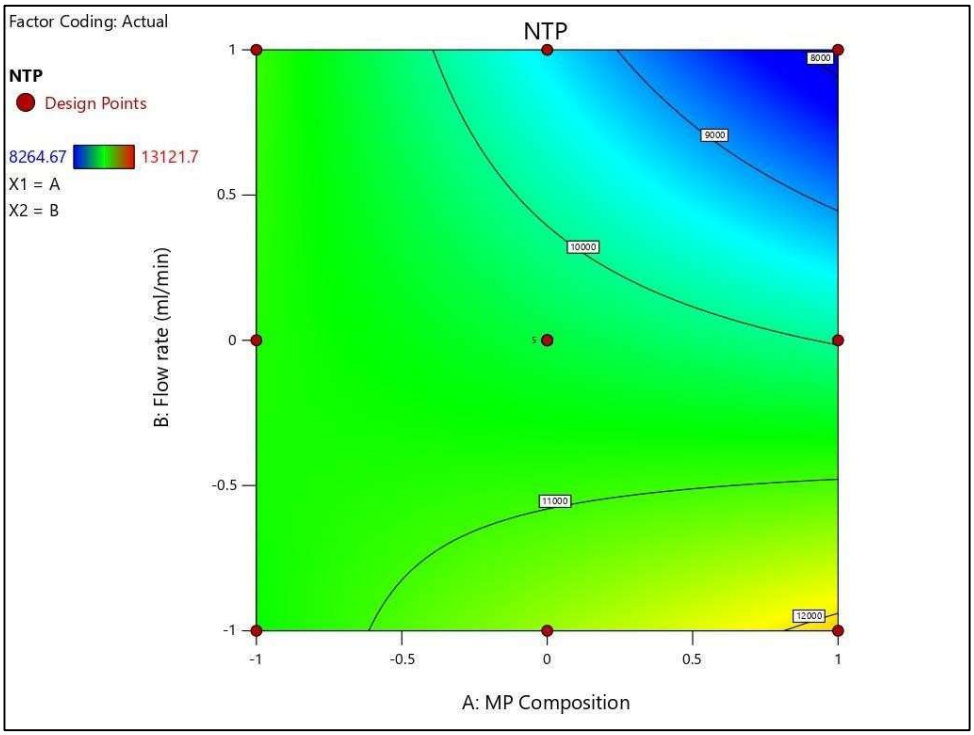


Figure 7.10 Contour plot for NTP

Perturbation plot originates at the centre of the experimental space and measures the response of the factor in three dimensions while keeping other factors constant. It is an important diagnostic tool for assessing comparative effects of all the factors and for selection of axes in 3D response surface and contour plots. The steeper slope or greater curvature in the plot signifies greater sensitivity of response to respective factor, whereas flat line in the plot indicates insensitivity of the response to given factor.

Figure 7.11 (a), (b) and (c) depict the perturbation plots for three dependent variable of RT, peak area and NTP. As seen in Figure 7.11, steeper curvature in plot of factor B (flow rate) suggests greater sensitivity of peak area to flow rate. Further, relatively lesser curvature and flatter nature of plots for both factors show insensitivity of NTP to both flow rate and mobile phase composition. In case of RT, the response is observed to be slightly more sensitive to flow rate than to composition of mobile phase.

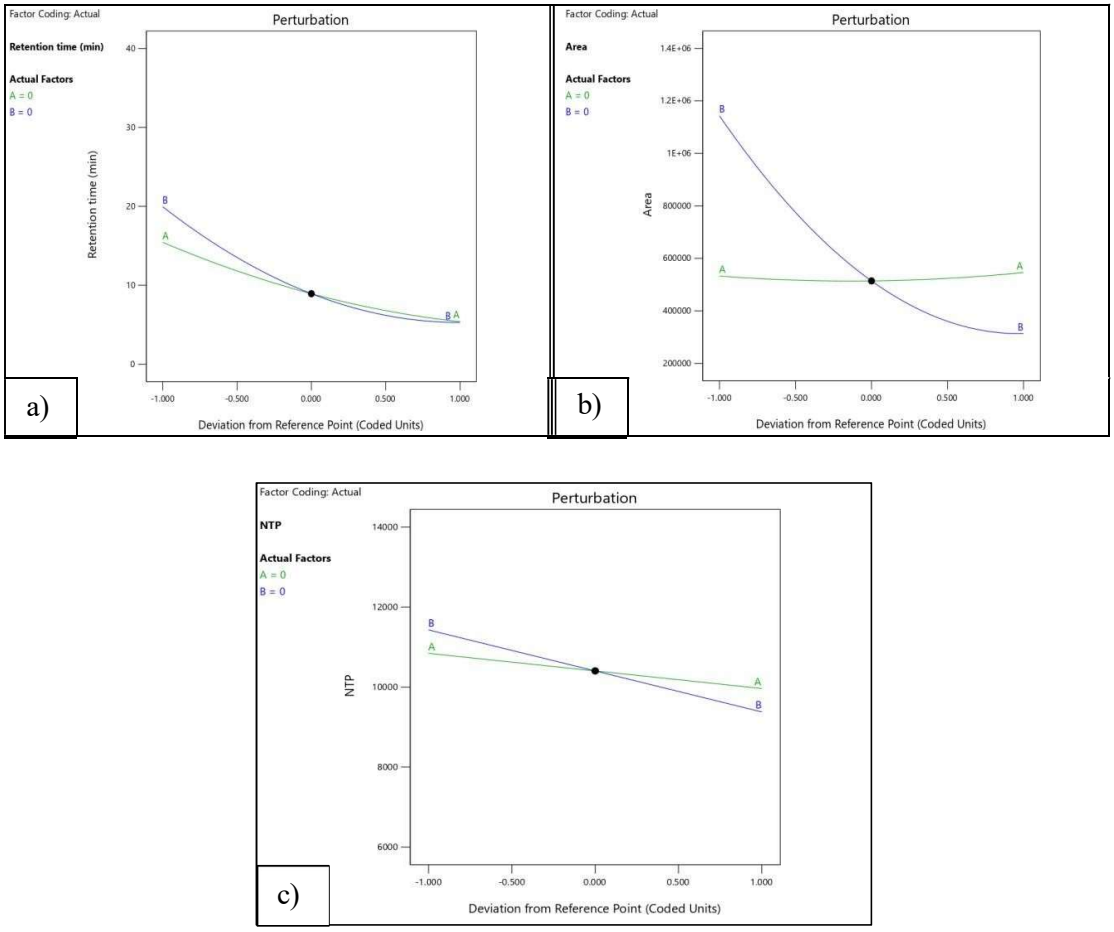


Figure 7.11Perturbation plots for a) RT b) Peak area c) NTP

As seen in interaction plots (Figure 7.12), no interaction is observed among the factors for the response of peak area. Further in case of RT, basal level of interaction can be observed between mobile phase composition and RT. For the response of NTP, higher level of interaction is observed between both factors.

Data optimization and validation of model:

Overlay plot shows two distinguishing regions, a region that depicts the space the significant response value (yellow in colour) and a region depicting the response values not meeting the desired criteria for finished product (grey in colour).

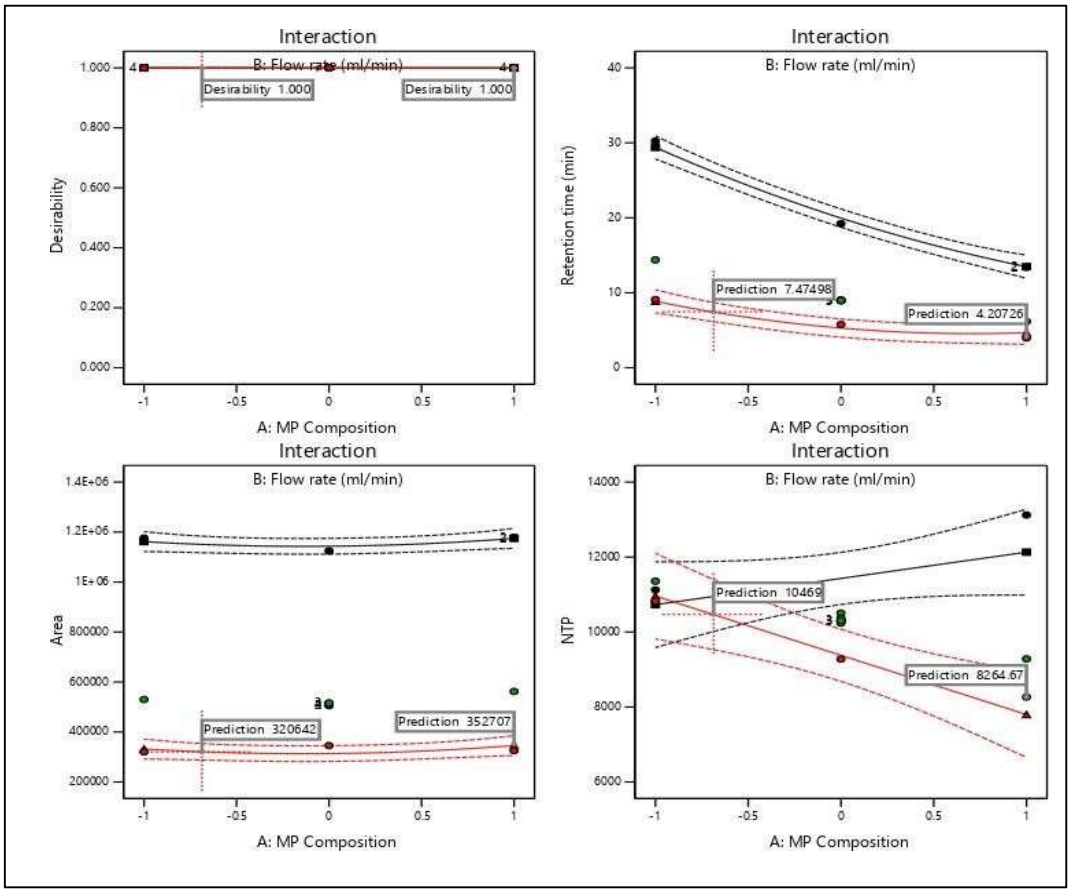


Figure 7.12Interaction plot for a) desirability b) RT c) peak area d) NTP

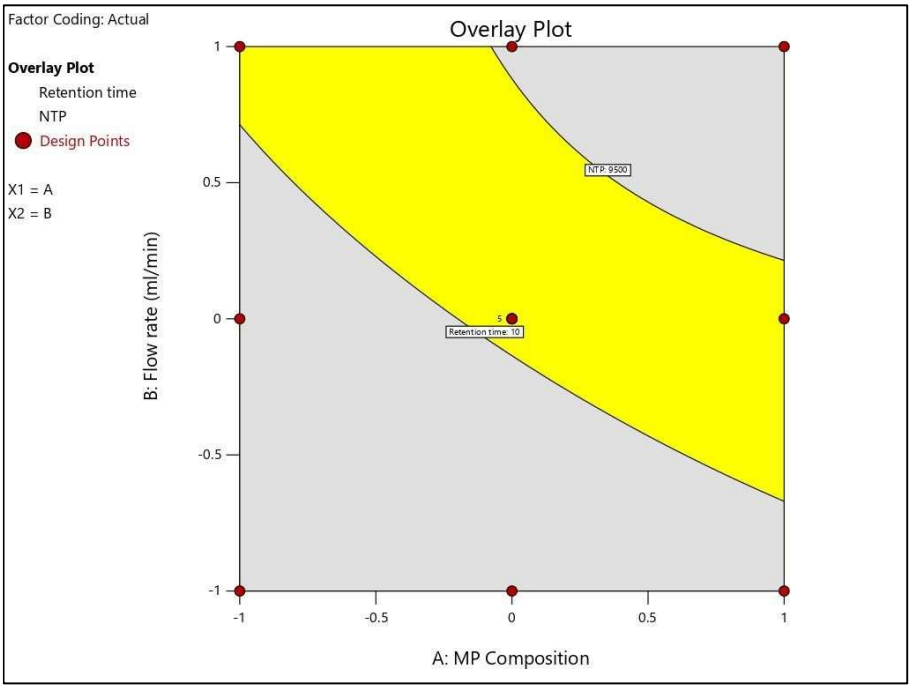


Figure 7.13 Overlay plot for Analytical method development

Based on the full factorial design and overlay plot, mobile phase composition of 90:10 and flow rate of 1ml/min were selected as optimum and the risk was mitigated to low. Table 7.4depicts parameters of the developed method with the predicted and observed response values for RT, peak area and NTP.

Table 7.4 Predicted and Observed responses for HPLC method validation

Parameter	Value	Predicted response			Observed response		
		RT (min.)	Area	NTP	RT (min.)	Area	NTP
Composition of MP	90:10	6.17	562059	9283	6.040	552191	13337
Flow rate	1ml/min						

B) HPLC Method Validation [159][115][160]***:***

1) System suitability:

The outcomes of system suitability developed analytical method are as depicted in Table 7.5.

Table 7.5 Results of system suitability

Parameter	Value	Acceptance criteria
Retention time (RT)	6.2 ± 0.03 min.	-
Tailing factor (T_f)	1.094± 0.009	≤2
Number of theoretical plates (NTP)	13361± 415	≥2,000

The chromatographic conditions were found to be meeting the desired criteria for the parameters to be tested. Thus, the developed method was established to be appropriate for the quantification of drug.

2) Linearity:

A method is said to be linear when the results are found to in direct proportionality with the concentration of analyte. Calibration curve was plotted with concentration of BCPO for different dilutions on X-axis and peak area on Y-axis. BCPO showed a linear calibration curve across concentration range of 0.5-10.00µg/ml (Figure 7.14). Equation for the developed calibration curve was observed as y = 29419x – 5069 with an R^2 value of 0.999. Figure 7.15 shows the standard chromatogram of BCPO (20ug/ml).

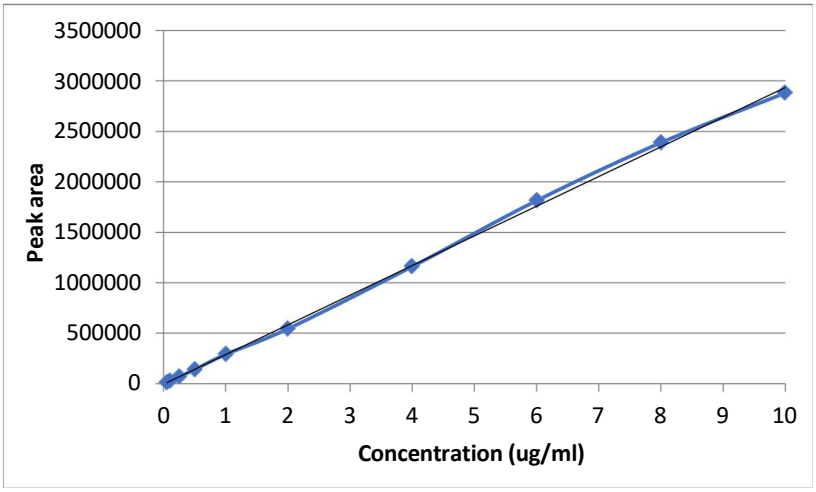


Figure 7.14 Calibration curve of BCPO by HPLC

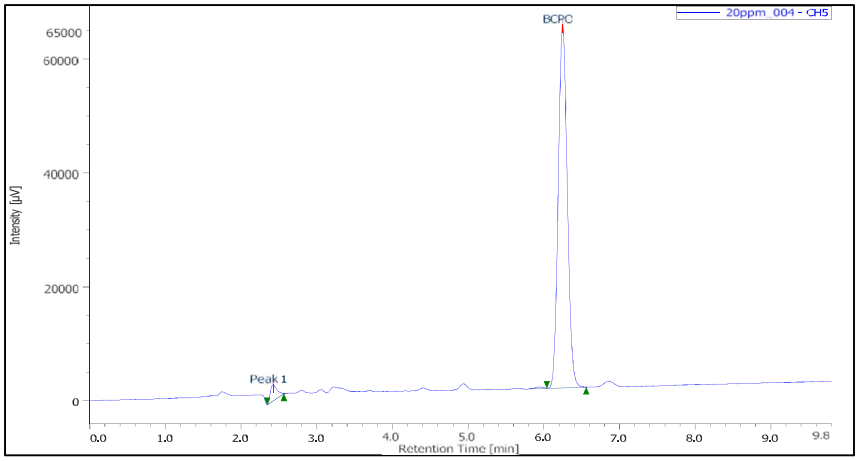


Figure 7.15 Standard chromatogram of BCPO

3) Precision:

Precision is the repeatability of the response acquired for a sequence of concentrations. Precision of the established method was assessed by performing six independent injections of working concentration. It is expressed in the form of %relative standard deviation. Results of Precision study are as depicted in Table 7.6.

Table 7.6 Results of Precision study

Sample number	**RT**	**Area**
1	6.04	552191
2	6.043	554476
3	6.047	541110
4	5.993	552433
5	5.987	553735
6	5.98	556211
Mean	6.015	551692.7
SD	0.031388	5387.442
%RSD	0.521827	0.97653

4) Accuracy

The accuracy of the developed method is known as the closeness of the results with the standard. Table 7.7 depicts the accuracy of the HPLC method developed for BCPO.

Table 7.7 Results of Accuracy study

Recovery level	**Recovery of concentration (ug/ml)**	**% Recovery**	**% RSD**
15	14.83	98.8	0.21
20	19.4	97	0.13
25	25.2	100.8	0.08

5) Range

Range of the developed HPLC method for BCPO was found to be from 0.5ug/ml–10ug/ml.

6) Limit of detection (LOD) and Limit of Quantification (LOQ):

Limit of detection is the lowermost concentration that can be identified with the developed method above the noise from baseline. Typically, the lowest concentration that can be determined should be at least three times the noise level. Quantification Limit is lowermost concentration which can be detected and shows the reproducibility. LOD and LOQ values for developed method were observed to be 3.27 ug/ml and 9.9 ug/ml respectively.

D) Specificity and Forced degradation study:

BCPO was exposed to stress testing at conditions specified in ICH guidelines[161][159]. The stress conditions were changed systematically to arrive at the conditions leading to 5-20% degradation[121].Table 7.8 depicts different conditions of stress testing and sequence of change of conditions. Table also refers the figures of drug chromatograms obtained at respective conditions.

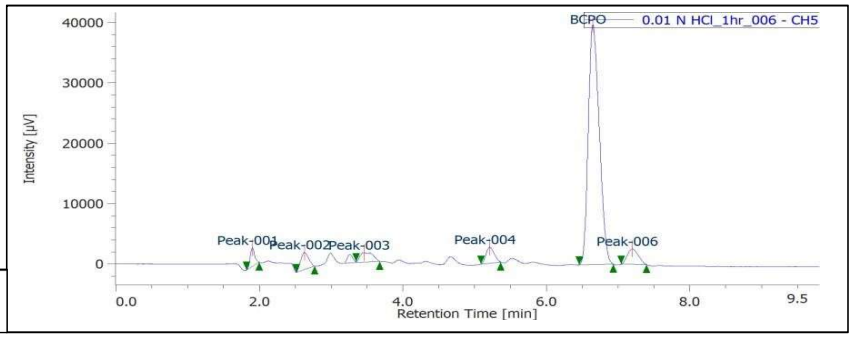
Table 7.8 Details of forced degradation studies

Sr. no.	Stress condition	Specification	Duration	%Degradation	Cross-reference to chromatogram figures
1.	Acid hydrolysis	0.01 N HCL	1 Hr	ND	Figure 7.16(a)
		0.01 N HCL	2 Hrs	ND	Figure 7.16(b)
		0.1 N HCL	2 Hrs	74%	Figure 7.16(c)
		0.1 N HCL	1 Hr	25%	Figure 7.16(d)
2.	Alkali hydrolysis	0.1 N NaOH	2 Hrs	ND	Figure 7.17(a)
		0.1 N NaOH	1 Hr	ND	Figure 7.17(b)
		1 N NaOH	2 Hrs	ND	Figure 7.17(c)
3.	Oxidation	10% H_2O_2	2 Hrs	ND	Figure 7.18(a)
		30% H_2O_2	2 Hrs	ND	Figure 7.18(b)
		30% H_2O_2	24 Hrs	27%	Figure 7.18(c)

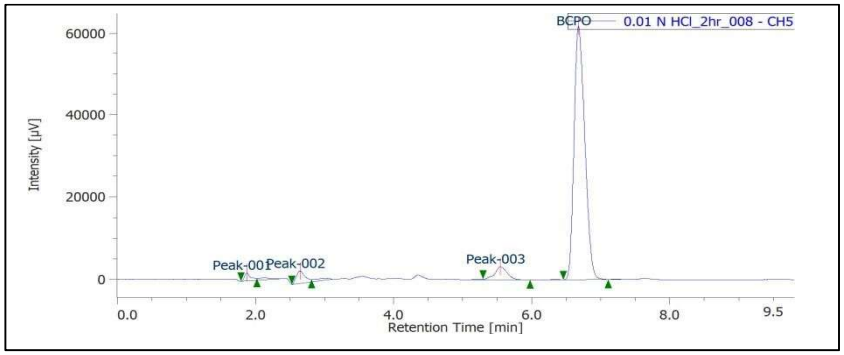
4.	Temperature	60^0 C	2 Hrs	ND	Figure 7.19(a)
		80^0 C	2 Hrs	ND	Figure 7.19(b)

ND: Not detected

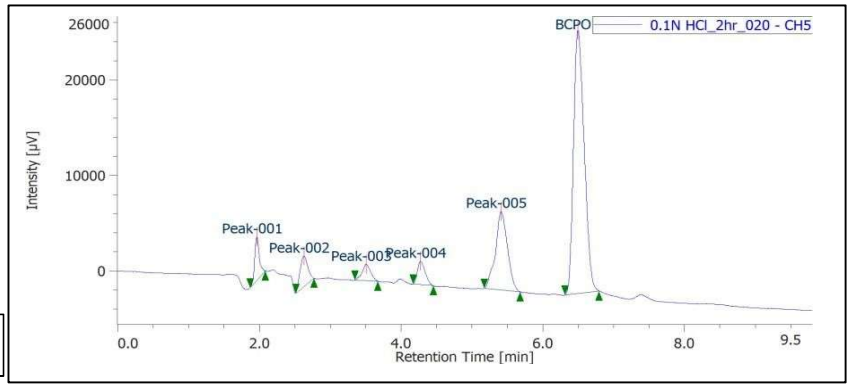
a)



b)



c)



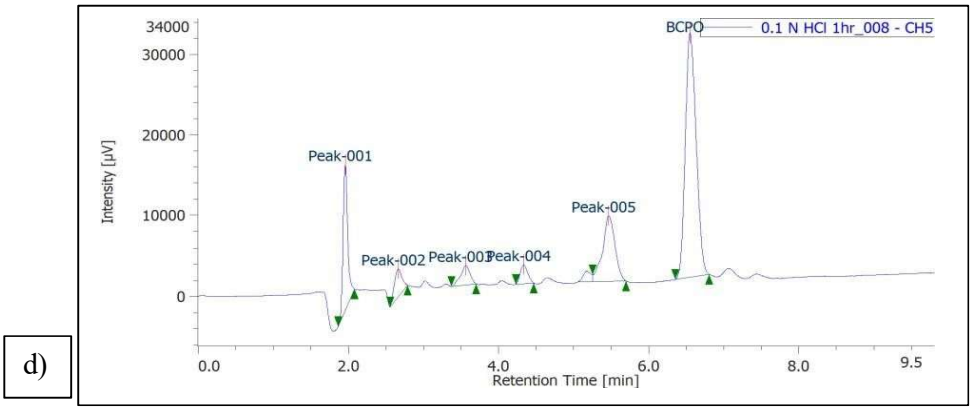
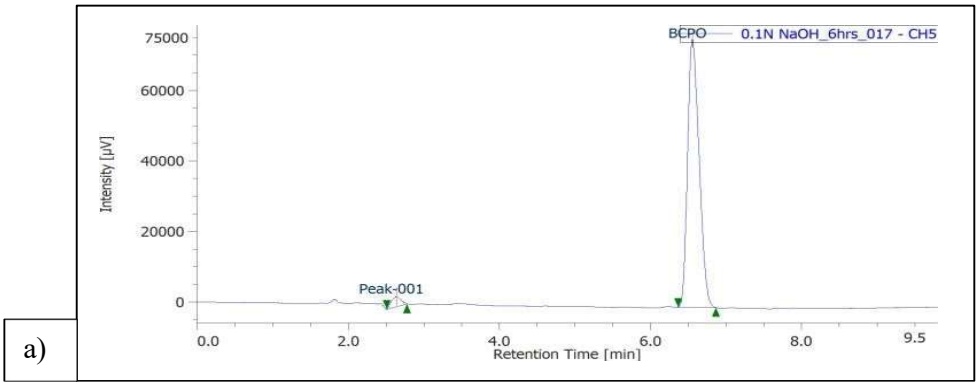
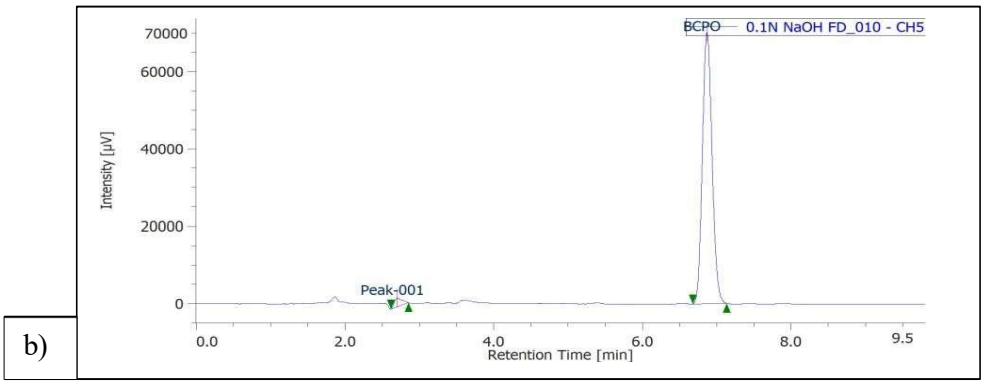
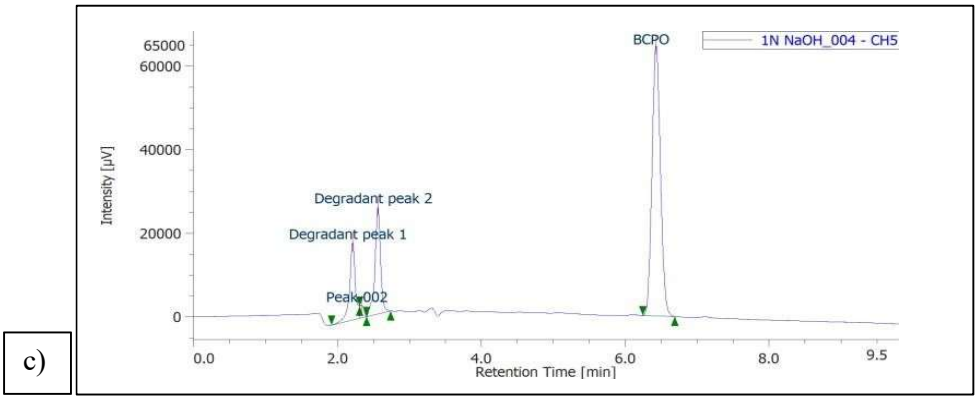


Figure 7.16 Acid hydrolysis of drug

a) 0.01N HCL 1 Hr b) 0.01N HCL 2Hrs c) 0.1N HCL 2Hrs d) 0.1N HCL 1Hr



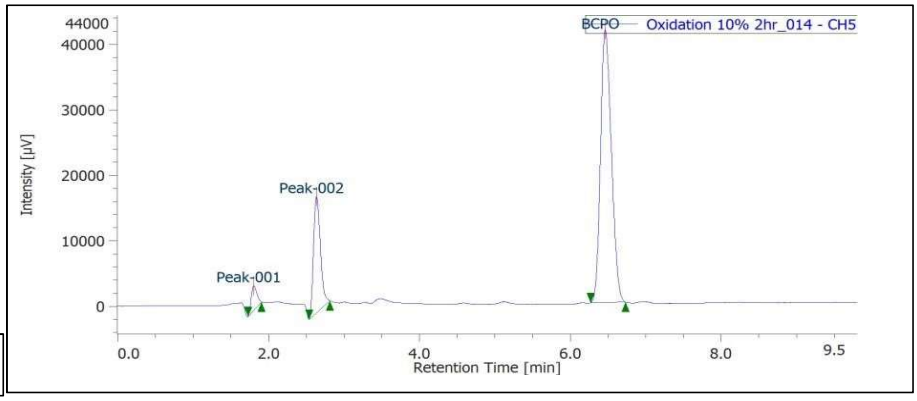




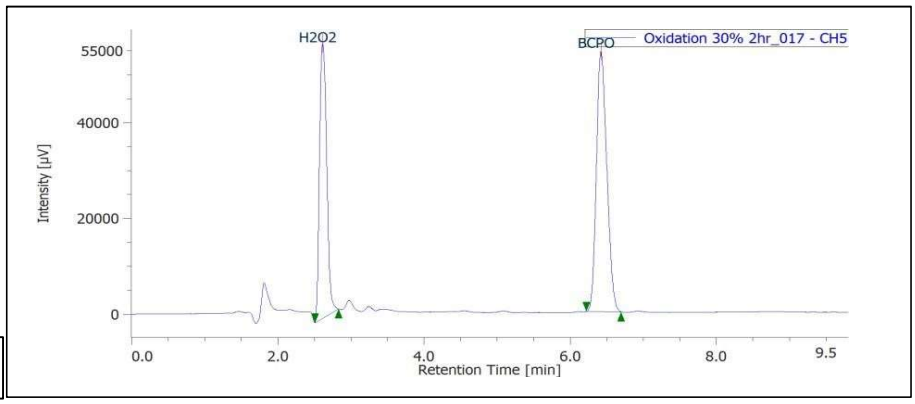
c)

Figure 7.17 Alkali hydrolysis of drug

a) 0.1 N NaOH 1Hr b) 0.1N NaOH 2Hrs c) 1N NaOH 2Hrs



a)



b)

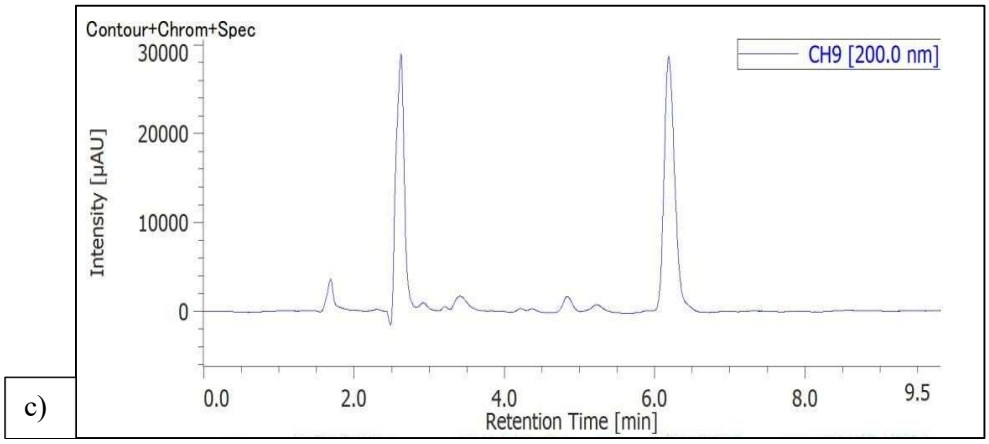


Figure 7.18 Oxidation of drug

a) 10% H_2O_2 2Hrs b) 30% H_2O_2 2Hrs c) 30% H_2O_2 24Hrs

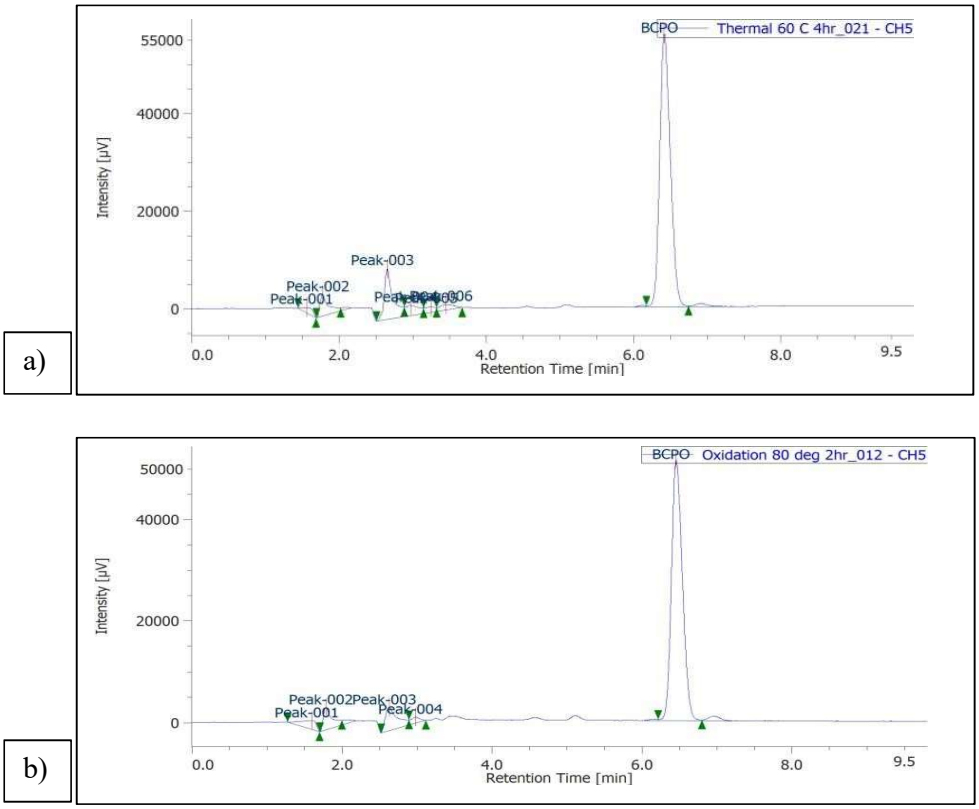


Figure 7.19 Thermal degradation of drug

As seen in table and figures, BCPO was found to sensitive to acid hydrolysis showing 74% degradation in 1 N HCL and 25% degradation in 0.1N HCL. BCPO was observed to stable under alkaline, oxidative and thermal stress conditions.

E. Drug excipient compatibility studies:

Drug was mixed in equal ratio with each excipient and the mixture were exposed to the conditions of 40°C/75% RH for the period of 1 month. The drug-excipient mixtures were assessed visually for physicochemical changes such as clumping, discoloration, liquefaction or gras production. Results of the compatibility studies are as recorded in Table 7.9.

Table 7.9 Visual observation of Drug-excipient compatibility studies

Sr no.	Sample name (40°C/75% RH)	Parameters analysed (after 1 month)			
		Clump	**Liquefaction**	**Discoloration**	**Gas**
1.	Pure drug	*	Y	*	*
2.	Compritol 888 ATO	*	*	*	*
3.	Gelucire 50/13	*	*	*	*
4.	Docosahexanoic acid	*	NA	*	*
5.	Folic acid	*	*	*	*
6.	Stearic acid	*	*	*	*

Drug was found to be undergoing liquefaction at 40°C/75% RH. Volatile nature of drug was observed to be responsible for liquefaction at 40°C/75% RH. The nature of interaction of drug and all excipients was further confirmed by analysis with the use of HPLC.

Compatibility of BCPO with other excipients was further confirmed with the use of HPLC. The mixtures of drug and excipients were evaluated at zero day and one month. Any changes in peak area of the drug and % assay was evaluated. It was observed that, peak area of drug did not show any change in its shape as well as in retention time. Further, % assay value of all samples was found be close to 100%. It was evident from the results of HPLC analysis that drug was compatible with all the excipients irrespective of the liquefaction observed. Liquefaction was also observed in the sample of pure drug. Results from drug excipient compatibility studies by HPLC are given in Table 7.10.

Table 7.10 Drug-excipient compatibility study by HPLC

Sr no.	Sample	Assay %
1.	Pure drug	101.2%
2.	Compritol 888 ATO	102.5 %
3.	Gelucire 50/13	99.8 %
4.	Docosahexanoic acid	100.8%
5.	Folic acid	99.7%
6.	Stearic acid	103.1%

7.1.4. Solubility profile in lipids and surfactants

A) Solubility in solid lipid:

Solid lipid component of the formulation system was selected based on solubility of BCPO in melted lipid. Smear of molten mixture of BCPO and lipid was observed under microscope. As seen Figure 7.20 (a), plain drug shows elongated irregular shaped crystals whereas no drug crystals are observed in Drug-Lipid mixture (Figure 7.20 (b)) which indicates solubilisation of Drug in given Lipid.

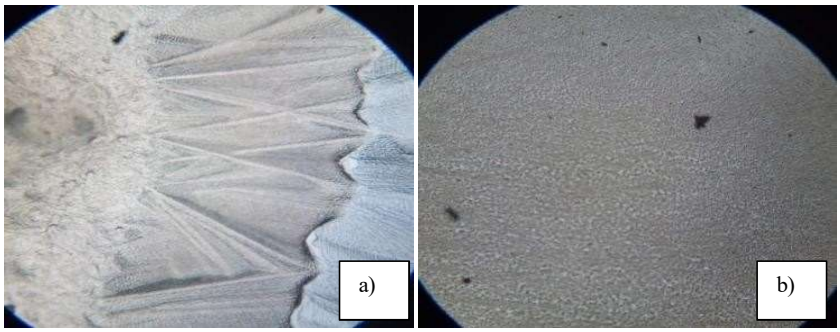
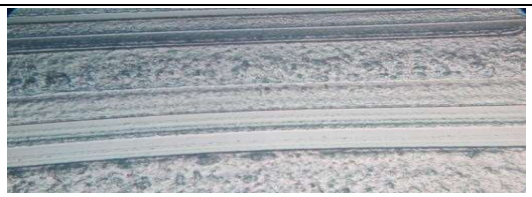


Figure 7.20 Microscopic observation of a) plain drug b) drug solubilised in solid lipid

During preliminary trials, BCPO was found to be forming monophasic mixture with all solid lipids owing to its essential oil origin, low melting point and volatile nature. In order to differentiate between ability of different solid lipids to dissolve the drug, drug and increasing amounts of lipid mixtures were melted together and smeared on glass slides. BCPO formed

long rosette shaped crystals owing to its inherent crystalline nature. Appearance and size of crystals went on decreasing with increasing amount of solid lipids.

Table 7.11 Microscopic evaluation of drug-lipid mixtures

Drug: Lipid ratio	**Observations**	**Inference**
Plain drug		Long and rosette shaped crystals of Plain drug
1: 0.5		Decreasing size and appearance of drug crystals with increasing amount of solid lipid
1 : 1		
1 : 2		
1 : 8		

1 : 10		No detection of drug crystals indicating complete solubilisation of drug in lipid

The results of microscopic evaluations of drug-lipid mixtures are depicted in Table 7.11.

Slides were further observed over a period of two weeks for possible crystal growth. More complex lipids such as Compritol 888ATO and Precirol ATO 5 were found to be more efficient for solubilisation of drug over GMS and Stearic acid.Nadia M. Morsi et. al., in their research work to develop targeted SLN for brain ischaemia, reported the similar results regarding affinity of lipophilic drug towards different solid lipids[140]. Further, as reported by Maryam Ghadiriet.al., stearic acid acts as self-emulsifying lipid[162][163]. Thus, stearic acid can be found more important in loading of hydrophilic drug than a hydrophilic drug. Venishetty Vinay Kumar et. al. in their research work regarding effect of glyceride lipids and wax on development of SLN explained the influence of longer chain of fatty acids on drug solubilisation [164]. Longer chain length of Precirol and Compritol lead to higher accommodation of drug. Further, both precirol and compritol may undergo partial hydrolysis into mono- and di- glycerides thus forming more imperfections and less ordered crystal lattice leading to higher solubilisation of drug[164][140]. Another aspect of selection of suitable solid lipid was relative melting points of drug and lipid. Lower melting point of lipid than drug will lead to formation of Drug-enriched shell model of solid lipid nanoparticles further leading to burst release of drug. Compritol 888 ATO and BCPO have similar range of melting points thus leading to formation of homogenous matrix of drug and lipid.

B) Suitability of surfactants:

Suitability of surfactants was determined by analysing the efficiency of surfactants to form emulsion with drug-lipid mixture and analysing the particle size of the same. Figure 7.21 shows the particle size and PDI values of emulsions formed with various surfactants screened. From the preliminary solubility studies, it was observed that, BCPO exhibited good solubility in Gelucire 50/13, Gelucire 48/16, Polysorbate 80 and Kolliphor EL. These surfactants were further screened at different concentration levels for their efficiency of reducing the particle size.

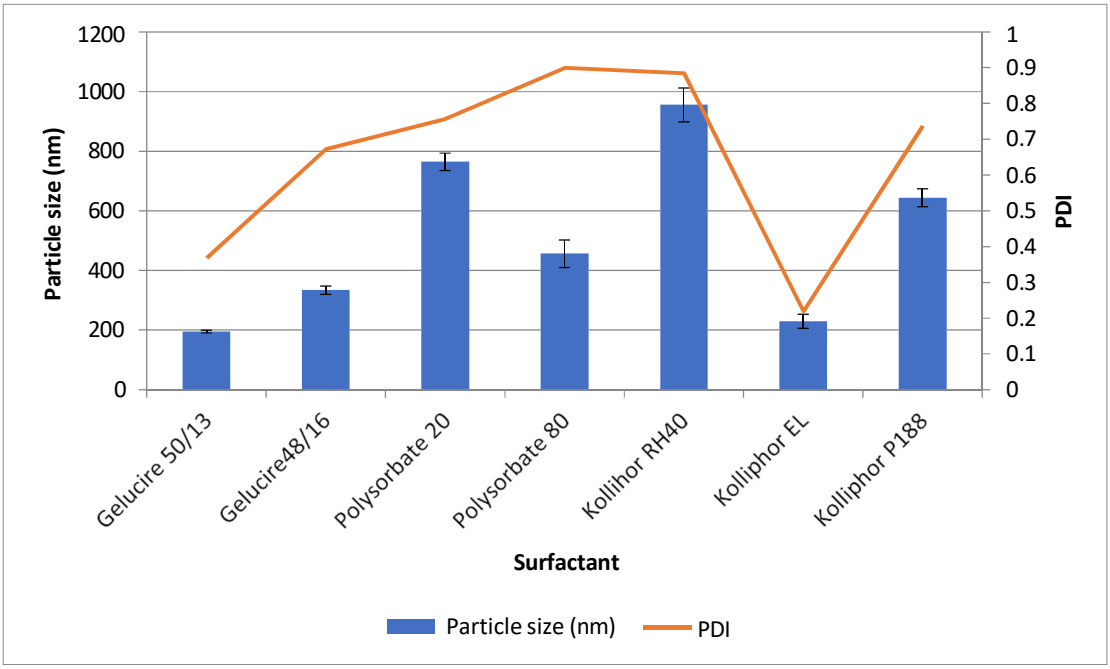


Figure 7.21 Particle size and PDI for surfactants

7.2. Formulation development and optimization

7.2.1. Formulation of BCPO loaded solid lipid nanoparticles (BC-SLN)

A) Selection of suitable solid lipid:

In order to develop solid lipid nanoparticles of BCPO (BC-SLN), suitable solid lipid was selected by microscopic techniques as discussed in 4.1.4. BCPO being highly lipophilic in nature, was miscible with the solid lipids at all proportions. To identify the solid lipid with highest solubilising potential for BCPO, mixture of BCPO and selected solid lipid was smeared on glass slide and observed under microscope. Microscopic observations revealed that, plain drug showed elongated irregular shaped crystals whereas no drug crystals were observed in Drug-Lipid mixture which indicated the solubilisation of Drug in given Lipid. Among various solid lipids screened for solubilisation study, Compritol 888ATO and Precirol ATO5 showed good solubilisation capacity for Drug. Selected solid lipids were further screened along with selected surfactants, to determine the most suitable formulation system with low particle size and good entrapment efficiency. As discussed in 4.1.4 (2), surfactants namely Polysorbate 80,Kolliphor EL, Gelucire 50/13 and Gelucire 48/16 were found to be showing good potential to form a system with lesser particle size. These surfactants were further screened at different concentration levels (200 mg and 500 mg) with both lipids Compritol 888 ATO and Precirol ATO5 to further narrow down the excipients to develop the nanosystems. Table 7.12 and Table 7.13 depict the results for various formulation trials undertaken to determine most suitable solid lipid.

Table 7.12 Formulation trials with surfactants level at 200 mg

Component	**F1**	**F2**	**F3**	**F4**	**F5**	**F6**	**F7**	**F8**
Drug (mg)	20	20	20	20	20	20	20	20
Compritol 888ATO	200	200	200	200	-----	-----	-----	-----
Precirol (mg)	-----	-----	-----	-----	200	200	200	200
Tween 80 (mg)	200				200			

Cremophor EL		200				200		
Gelucire 48/16			200				200	
Gelucire 50/13				200				200
Distilled water (ml)	20	20	20	20	20	20	20	20
Particle size	693.67	284.67	262.67	403.67	2166	1186.6	938.33	949.66
PDI	0.45	0.22	0.368	0.673	0.25	0.41	0.36	0.54

Table 7.13 Formulation trials with surfactants level at 500 mg

Component	**F9**	**F10**	**F11**	**F12**	**F13**	**F14**	**F15**	**F16**
Drug (mg)	20	20	20	20	20	20	20	20
Compritol 888ATO	200	200	200	200	-----	-----	-----	-----
Precirol (mg)	-----	-----	-----	-----	200	200	200	200
Tween 80 (mg)	500				500			
Cremophor EL		500				500		
Gelucire 48/16			500				500	
Gelucire 50/13				500				500
Distilled water (ml)	20	20	20	20	20	20	20	20
Particle size	504.00	225.67	195.00	334.00	1153.6	1071.6	743.33	670
PDI	0.45	0.22	0.368	0.673				

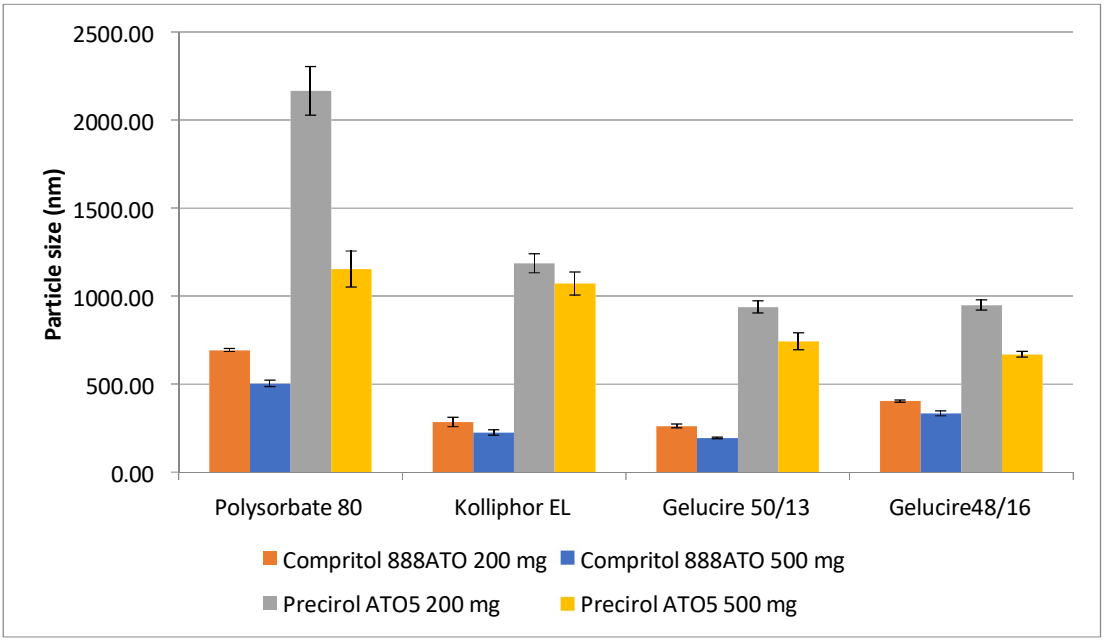


Figure 7.22 Results of particle size for formulation trials with surfactants at 200 mg and 500 mg

Results depicted in Table 7.12 and Table 7.13 are summarised in Figure 7.22. It was observed that, solid lipid with longer chain fatty acid (Compritol 888ATO) produced particle with smaller article size as compared to solid lipid with shorter chain fatty acid (Precirol ATO5). Compritol 888ATO was found to be consistently showing results with smaller particle size with all the surfactants as compared to Precirol ATO5. Further, solid surfactants (Gelucire 50/13 and Gelucire 48/16) were found to giving lesser particle size as compared to liquid surfactants (Polysorbate 80 and Kolliphor EL). Similarity in the structure and presence of long chain fatty acid in both lipid and solid surfactants was presumed to be responsible for better surface interaction and lesser particle size [165].

Gelucire 50/13 and Gelucire 48/16 were further screened with the use of factorial design to arrive at the most suitable surfactant and optimum lipid: surfactant ratio.

B) Selection of suitable surfactant and optimization of lipid: surfactant ratio:

Level of Aqueous phase and Lipid: Surfactant ratio was optimised by applying 3^2Factorial design. Two factors namely Lipid: Drug ratio and Volume of water were varied at three levels. Particle size and PDI were measured as a response to check the effect of these variables.

A total of 13 trials were taken as suggested by Design-Expert software in order to fit the data to build a suitable statistical model and contour plots. Based on the fit summary, ANOVA, and the model graphs, the design space was identified to attain the desired intents of minimum

particle size and PDI. Quadratic model was observed to be best fitting for dependent variables. Table 7.14 depicts the Analysis of variance (ANOVA) for two dependent variables particle size and PDI.

Table 7.14 ANOVA for Particle size and PDI

Response	Source	Sum of Squares	df	Mean Square	F-value	p-value	
Particle size	**Model**	1.185E+05	5	23697.15	17.50	0.0008	significant
	A	1.043E+05	1	1.043E+05	77.03	< 0.0001	
	B	1320.17	1	1320.17	0.9752	0.3563	
	AB	3540.25	1	3540.25	2.62	0.1499	
	A^2	8245.12	1	8245.12	6.09	0.0430	
	B^2	15.41	1	15.41	0.0114	0.9180	
	Residual	9476.55	7	1353.79			
	Cor Total	1.280E+05	12				
PDI	**Model**	0.1177	5	0.0235	5.52	0.0224	significant
	A	0.0737	1	0.0737	17.28	0.0043	
	B	0.0184	1	0.0184	4.31	0.0766	
	AB	0.0008	1	0.0008	0.1838	0.6810	
	A^2	0.0195	1	0.0195	4.57	0.0699	
	B^2	0.0002	1	0.0002	0.0470	0.8346	
	Residual	0.0299	7	0.0043			
	Cor Total	0.1475	12				

A: Lipid: Surfactant ratio, B: Volume of water

The **Model F-values** 17.50 and 5.52 imply the model is significant as also indicated by **P-values** less than 0.0500. In case of particle size, A and A^2 are significant model terms. In case of PDI, A is a significant model term.

Polynomial equations for particle size and PDI in terms of actual factors are as depicted in equation (12) and (13).

$$\begin{aligned} Particle\ size = {} & +468.89655 + 131.83333\ (Lipid{:}\ surfactant\ ratio) \\ & - 14.83333(Volume\ of\ water) \\ & + 29.75000(Lipid{:}\ surfactant\ ratio)(Volume\ of\ water) \\ & - 54.63793(Lipid{:}\ surfactant\ ratio)(Lipid{:}\ surfactant\ ratio) \\ & + 2.36207(Volume\ of\ water)(Volume\ of\ water) \end{aligned} \quad (12)$$

$$\begin{aligned} PDI = {} & +0.422862 - 0.110833\ (Lipid{:}\ surfactant\ ratio) \\ & + 0.055333\ (Volume\ of\ water) \\ & + 0.014000\ (Lipid{:}\ surfactant\ ratio)(Volume\ of\ water) \\ & - 0.084017\ (Lipid{:}\ surfactant\ ratio)(Lipid{:}\ surfactant\ ratio) \\ & - 0.008517(Volume\ of\ water)(Volume\ of\ water) \end{aligned} \quad (13)$$

Figure 7.23 and Figure 7.24 show the contour plots for particle size and PDI. As seen from contour plots (Figure 7.23), an increase in the size of particles is noted as the Lipid: surfactant ratio increases. Also, particle size reduces with increasing volume of water. With increasing Lipid: surfactant ratio, amount of surfactant becomes insufficient for stabilising lipid particles in aqueous environment eventually resulting in larger particles. Further, increasing the volume of aqueous vehicle leads to decreasing the concentration of lipids making it easier for surfactant to stabilise the particles with reduced size and increased surface area. In case of PDI (Figure 7.24), polydispersity index decreases with increasing Lipid: surfactant ratio and increases with increasing volume of water. With increase in lipid concentration, larger but more uniform particles are forming whereas with decreasing lipid concentration, particle size is decreasing along with the uniformity of particles [165][164].

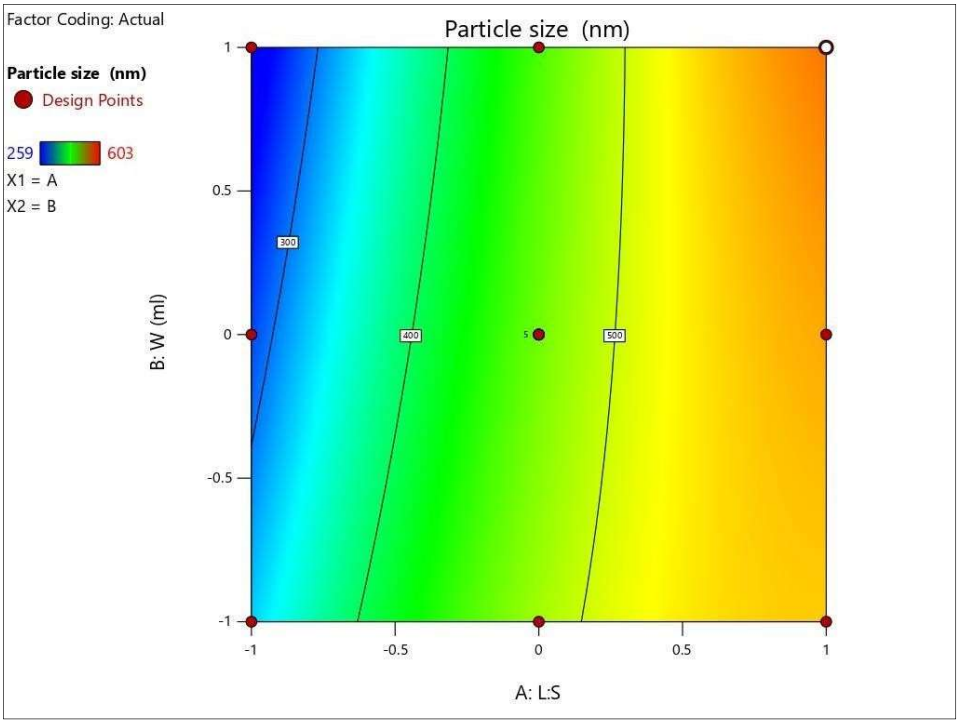


Figure 7.23 Contour plot for Particle size

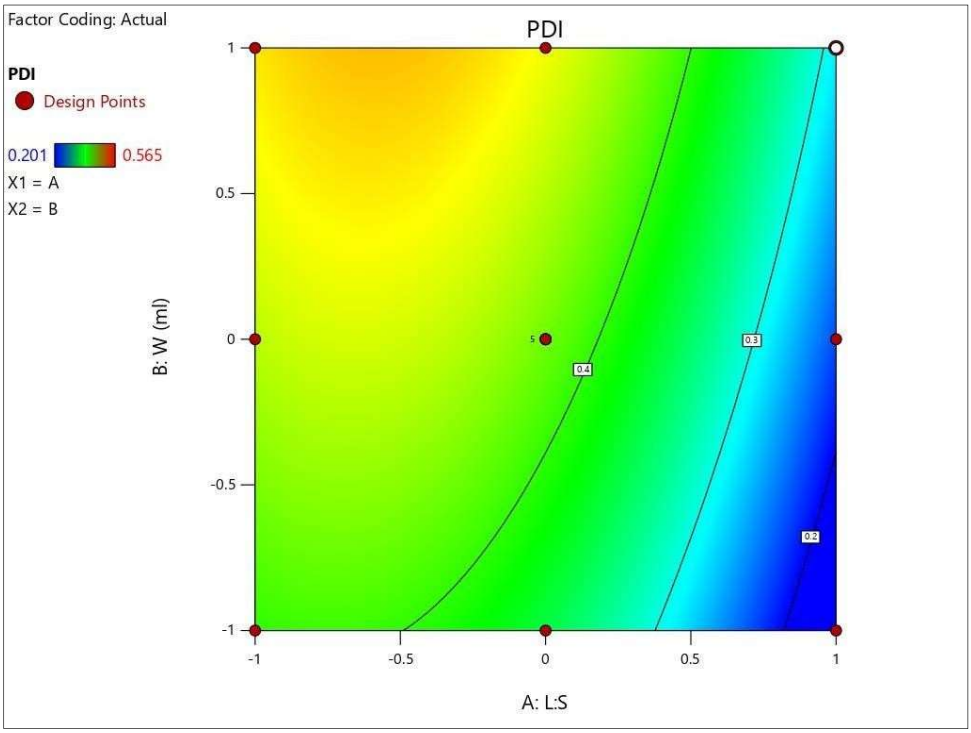
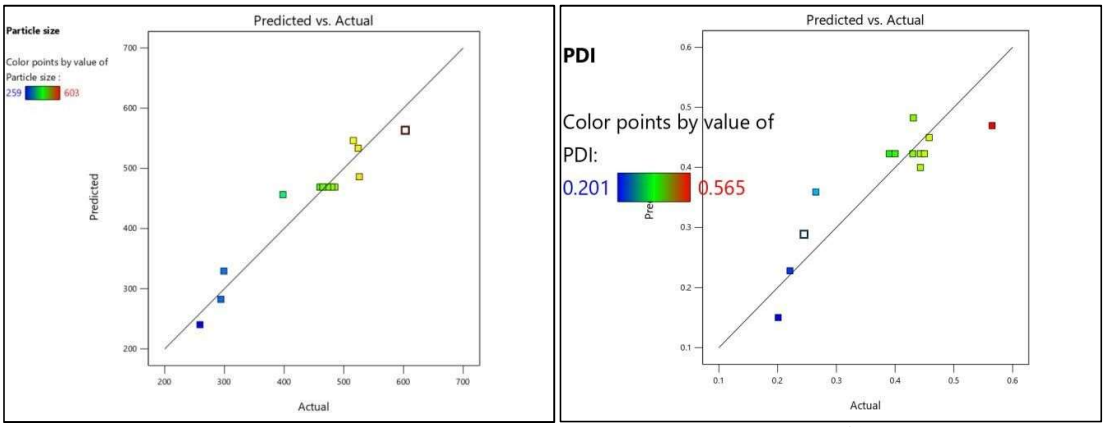


Figure 7.24 Contour plot for PDI



a) b)

Figure 7.25 Correlation plots for predicted and actual for a) Particle size b) PDI

Data was also found to be in alignment in terms with the correlation plots as shown in Figure 7.25.

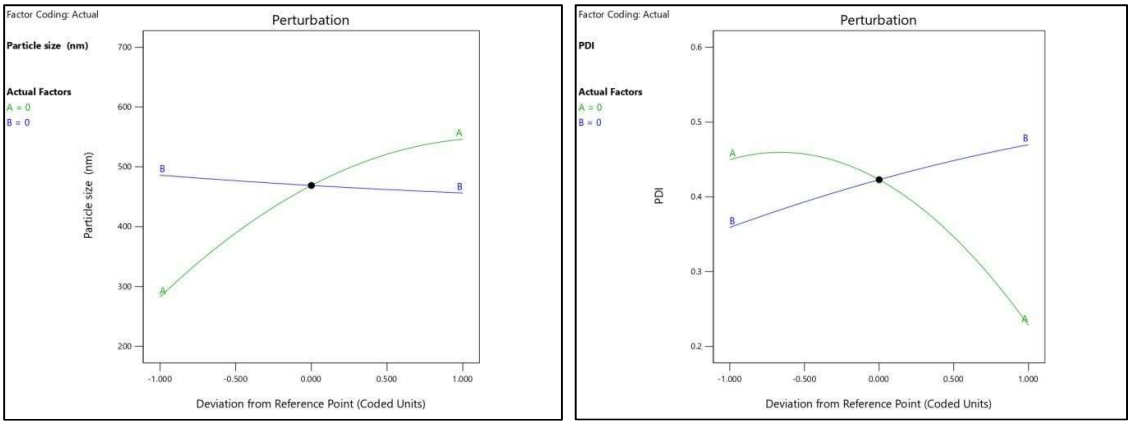


Figure 7.26 Perturbation plots for a) Particle size b) PDI

Perturbation plot which originates at the centre of the experimental space, measures the response of the factor in three dimensions while keeping other factors constant. It is an important diagnostic tool for assessing comparative effects of all the factors and for selection of axes in 3D response surface and contour plots. The steeper slope or greater curvature in the plot signifies greater sensitivity of response to respective factor, whereas flat line in the plot indicates insensitivity of the response to given factor. As observed in Figure 7.26 (a) and (b), the relatively flat line of volume of water shows that this factor has lower effect on both particle size and PDI. Steep curvature in lipid: surfactant ratio shows that both particle size and PDI are sensitive to this factor. Through the comparison of both plots, lipid: surfactant ratio was determined to be most influential factor for both particle size and PDI.

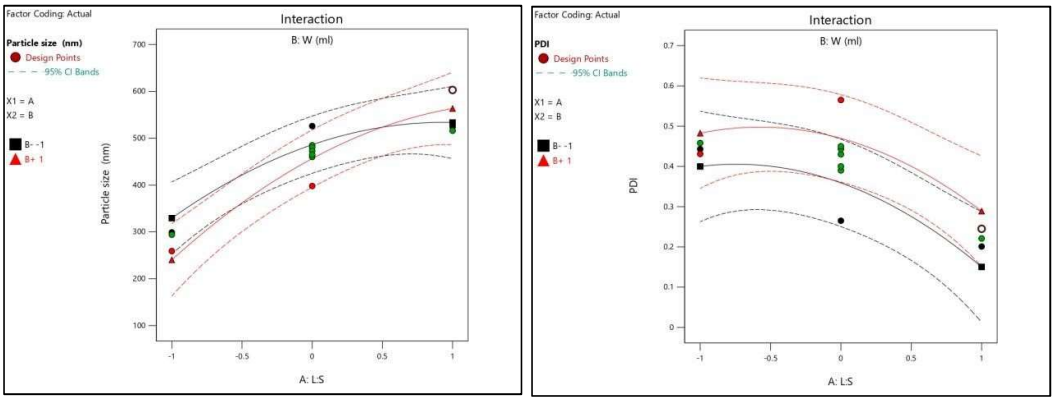


Figure 7.27 Interaction plot for a) Particle size b) PDI

Further, from interaction plots (Figure 7.27) basal level of interaction is observed between two factors affecting the response of particle size whereas no interaction is observed for the response of PDI.

C) Data optimization and validation of model:

Overlay plot shows two distinguishing regions, a region that depicts the space the significant response value (yellow in colour) and a region depicting the response values not meeting the desired criteria for finished product (grey in colour).

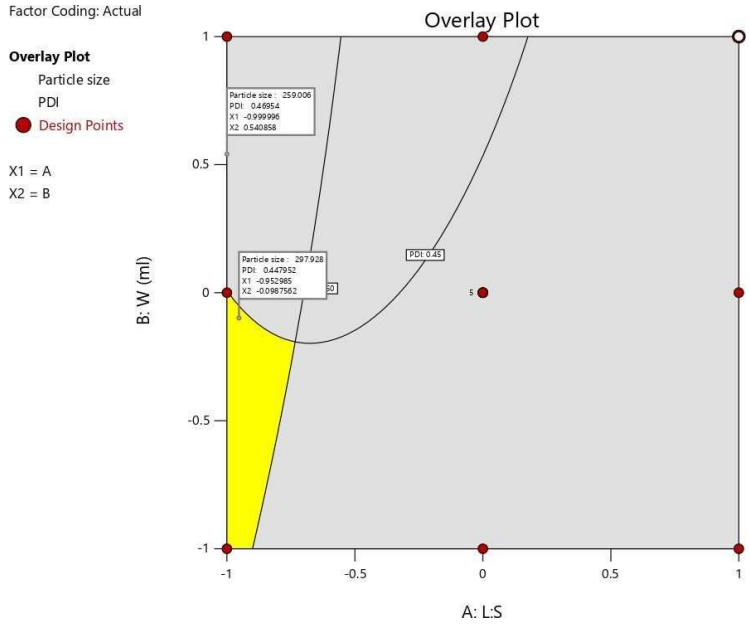


Figure 7.28 Overlay plot

Based on the full factorial design and overlay plot, 2:5 of lipid concentration and 20 ml water were selected as optimum and the risk was mitigated to low. Table 7.15 depicts the optimised

formula of BC-SLN along with the predicted and observed response values for particle size and PDI.

Table 7.15 Predicted and Observed responses for validation batch (BC-SLN)

Sr. no.	Ingredient	Quantity	Predicted response		Observed response	
			PS	PDI	PS	PDI
1.	Beta-caryophyllene (BCPO)	20 mg	297 nm	0.45	279.8 ± 2 nm	0.507 ± 0.03
2.	Compritol 888ATO	200 mg				
3.	Gelucire 50/13	500 mg				
4.	Water	20 ml				

7.2.2. Effect of other processing parameters on Particle size

A) Effect of processing temperature:

The processing temperature also has a vital effect on particle size and drug release. After mixing of both lipidic and aqueous phases at the melting point of solid lipid (65^0 C), hot nanoemulsion was subjected to probe sonication. It has been observed that, at a higher temperature, lipid particles are still in a fluidic state making them more prone to particle size reduction. Further, high temperature maintains the emulsion at low viscosity making the dispersion of ultrasonic waves easier through the medium. On the contrary, addition of water at low temperature leads to quenching of lipid melt which further results in particle aggregation and larger size of particles. During the process of probe sonication, temperature of the emulsion slowly drops down which has a positive effect on the formation of particle matrix. As melting points of drug and lipid are in a similar range (62-67^0 C), drug and lipid start solidifying together forming a homogenous solid solution matrix. Further, the solid nature and lower melting point of Gelucire 50/13 (MP 50^0 C), leads to solidification of surfactant layer around homogenous solid solution matrix of drug and lipid. The supply of acoustic cavitation energy in form of sonication during this phase controls the formation of smaller sized particles with increased surface area. At the end of the sonication process, the nanoemulsion was quickly

stored at cold temperature (2-8^0 C) to induce the formation of a solid matrix of particles with reduced size.

B) Effect of sonication duration:

Similarly, duration of sonication was varied between 5 min to 20 min. Particle size was observed to be decreasing with increasing sonication duration till 15 min. However, sonicating the nanoemulsion beyond 15 min. led to complete breakdown of lipid particles and phase separation. Sonication time was thus optimised to be 10 min [166].

7.2.3. Formulation and optimization of BCPO loaded nanostructured lipid carriers (BC-NLC)

It was decided to replace some part of the solid lipids with omega-3 polyunsaturated fatty acids (n3PUFA) to add an edge over traditional SLNs. n-3PUFA, especially eicosapentaenoic acid (EPA) and docosahexaenoic acid (DHA), have been used as nutrients for cancer patients. In addition, n-3PUFA is observed to be anti-inflammatory and anti-cancer and in nature. The addition of n3-PUFA to the SLN system ultimately led to the development of NLC, which is now functioning as functional excipients. Below 60° C, the viscosity of Compritol increases rapidly. The presence of low-viscosity liquid lipid components in the solution can further reduce the size of the particles. As observed from graph in Figure 7.29, the addition of n3-PUFA leads to reduction of the particle size (the amount of liquid changed from 10% to 30% of the total lipid). Above 30%, the solubility of oil in solid lipids exceeds and oil droplets are formed in the solid particles. To avoid potential drug spill, the amount of n3-PUFA was optimized to 30% of total solid lipids.

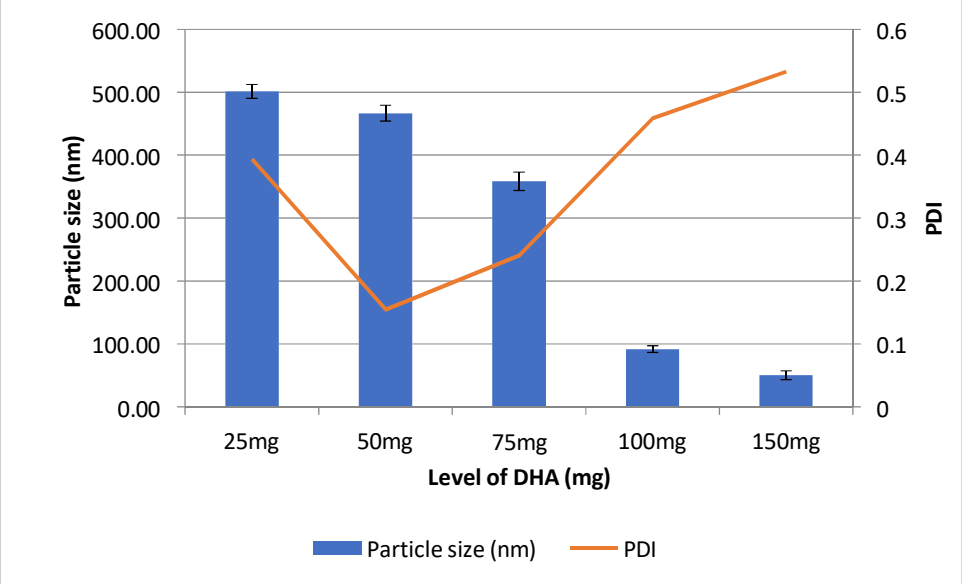


Figure 7.29 Effect of addition of increasing amount of DHA on particle size

7.2.4. Optimization of level of DHA with full factorial design

Level of liquid lipid (DHA) in formulation was optimised by applying 3^2 Full factorial design. Two factors namely % amount of PUFA and amount of drug were varied at three levels. Particle size and % entrapment efficiency (%EE) was measured as a response to check the effect of these variables.

A total of 13 trials were taken as suggested by Design-Expert software in order to fit the data to build a suitable statistical model and contour plots. Based on the fit summary, ANOVA, and the model graphs, the design space was identified to attain the desired intents of minimum particle size and maximum % EE. The model that was found to be best fitting for the dependent variables was Quadratic model. Table 7.16 depicts Analysis of variance (ANOVA) for two dependent variables particle size and PDI.

Table 7.16 ANOVA for %EE and Particle size

Response	Source	Sum of Squares	df	Mean Square	F-value	p-value	
%EE	**Model**	767.31	5	153.46	7.76	0.0090	significant
	A-Amount	55.45	1	55.45	2.80	0.1380	

	of liquid lipid						
	B-Amount of drug	276.62	1	276.62	13.99	0.0073	
	AB	25.40	1	25.40	1.28	0.2944	
	A^2	295.00	1	295.00	14.92	0.0062	
	B^2	11.32	1	11.32	0.5725	0.4739	
	Residual	138.45	7	19.78			
	Cor Total	905.75	12				
Particle size	**Model**	40547.33	2	20273.67	42.63	< 0.0001	significant
	A-Amount of liquid lipid	35266.67	1	35266.67	74.16	< 0.0001	
	B-Amount of drug	5280.67	1	5280.67	11.10	0.0076	
	Residual	4755.44	10	475.54			
	Cor Total	45302.77	12				

The **Model F-values** 7.76 and 42.63imply the model is significant as also indicated by **P-values** less than 0.0500. In case of %EE, B and A^2 are significant model terms. In case of particle size, A and B are observed to be significant model terms.

Polynomial equations for particle size and PDI in terms of actual factors are as depicted in equation(14) and (15).

$$\%Entrapment\ efficiency = +19.96862 + 3.04000\ (Amount\ of\ liquid\ lipid) + 6.79000\ (Amount\ of\ drug) + 2.52000\ (Amount\ of\ liquid\ lipid * Amount\ of\ drug) + 10.33483(Amount\ of\ liquid\ lipid^2) + 2.02483(Amount\ of\ drug^2) \quad (14)$$

$$Particle\ size = +118.30769 - 76.66667(Amount\ of\ liquid\ lipid) - 29.66667(Amount\ of\ drug) \quad (15)$$

Figure 7.30and Figure 7.31show the contour plots for %EE and particle size respectively. As it can be seen from contour plots (Figure 7.30), %EE increases as the level of liquid lipid increases. Addition of spatially different lipid SLN system leads to formation of less perfect crystal lattice as well as larger space for drug accommodation leading to increase in entrapment efficiency. At highest level of liquid lipid and amount of drug, formulations were found to be showing maximum entrapment efficiency. Both factors show similar effects on particle size (Figure 7.31). Particle size decreases with addition of liquid lipid and drug. At high level of liquid lipid, the emulsion becomes less viscous making it easier for surfactant to stabilise the articles in reduced size. At very high level of liquid lipid, solid lipid concentration becomes very low leading to formation of oil globules instead of solid particles.

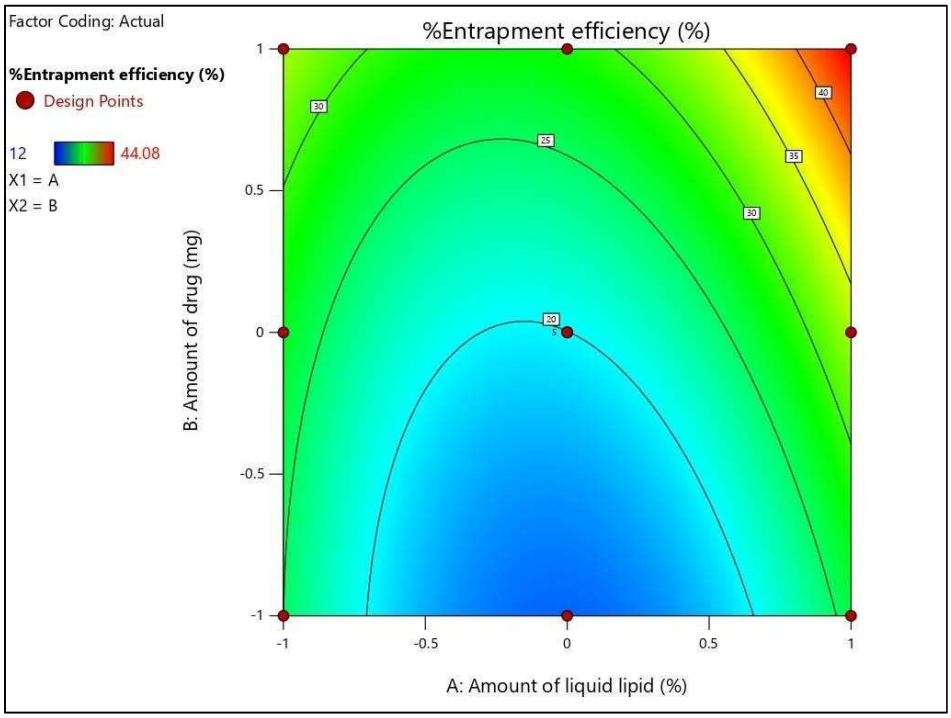


Figure 7.30 Contour plot for %EE

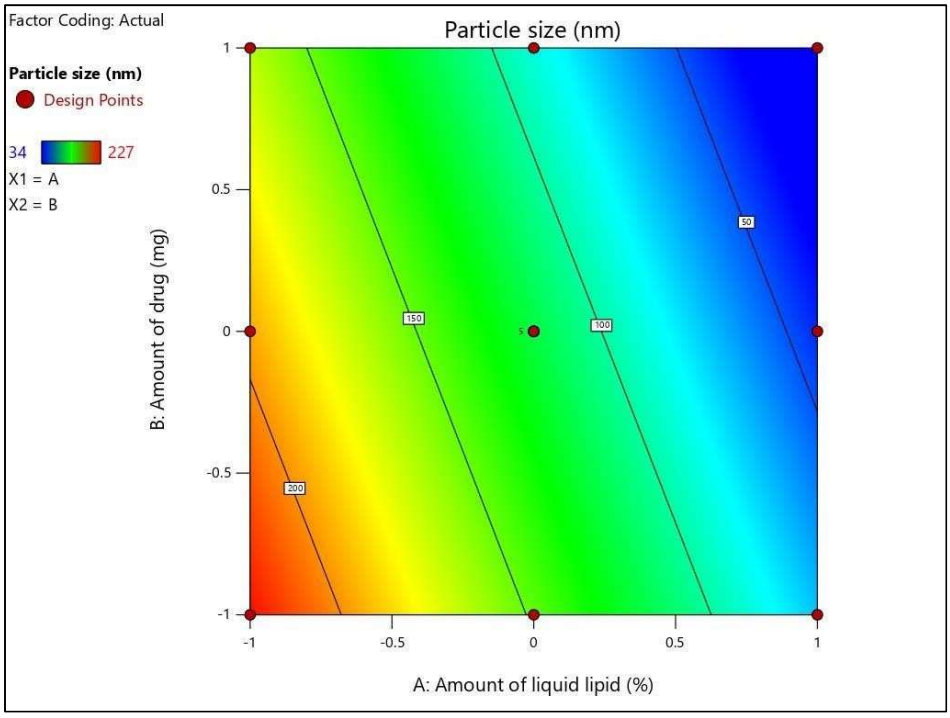


Figure 7.31 Contour plot for particle size

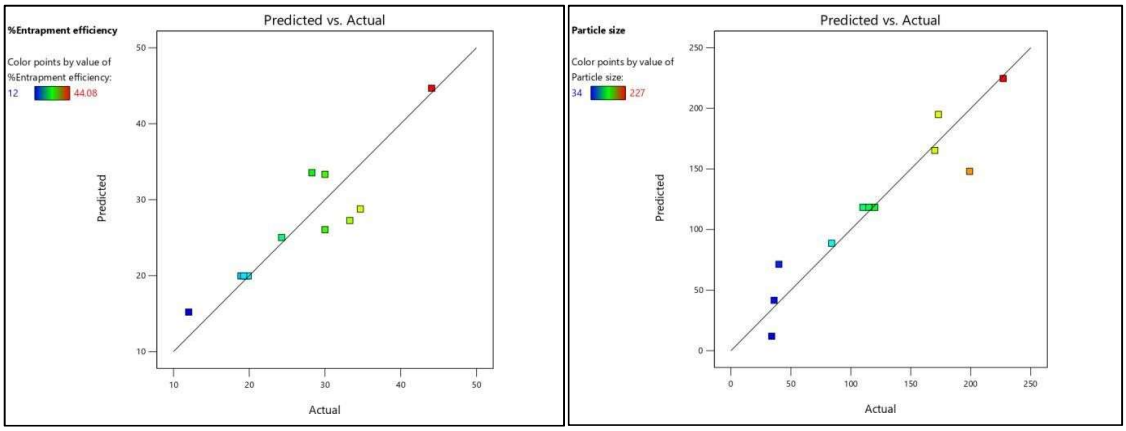


Figure 7.32 Correlation plots for a) %EE and b) Particle size

Data was also found to be in alignment in terms with the correlation plots as shown in Figure.

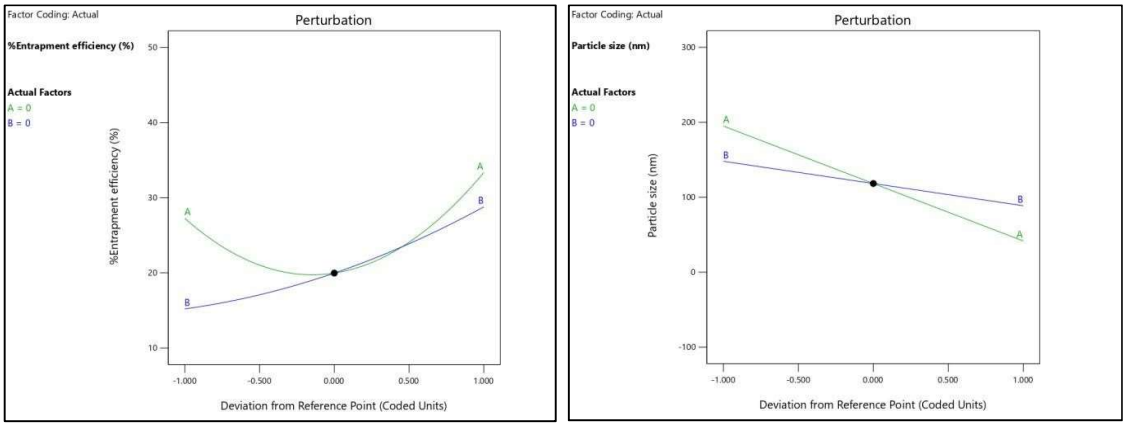


Figure 7.33 Perturbation plots for a) %EE and b) Particle size

As described in 4.2.1 (B), perturbation plots are important for assessing comparative effects of all the factors and for selection of axes in 3D response surface and contour plots. As seen in Figure 7.33, sharp curvature in plot of factor A shows that amount of liquid lipid has significant effect of %EE. Line for lot of factor B is relatively flat and with lesser curvature suggesting the lesser effect of amount of drug on %EE. In case of particle size, plot of factor A shows steeper slope as compared to plot for factor B. It can be inferred that amount of liquid lipid has more considerable effect on particle size than amount of drug.

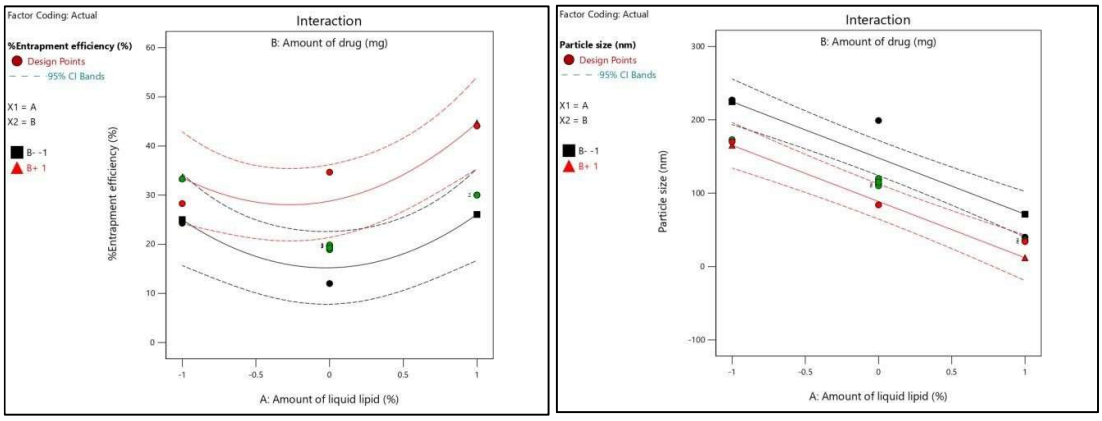


Figure 7.34 Interaction plots for a) %EE and b) Particle size

As seen from interaction plots (Figure 7.34), no interaction was observed between two factors for both the responses. However, sharper curvature in plots for %EE and relatively flat lines in particle size suggested that both factors affect %EE more significantly as compared to particle size.

Data optimization and model validation:

Overlay plot (Figure 7.35) shows two distinguishing regions, a region that depicts the space the significant response value (yellow in colour) and a region depicting the response values not meeting the desired criteria for finished product (grey in colour).

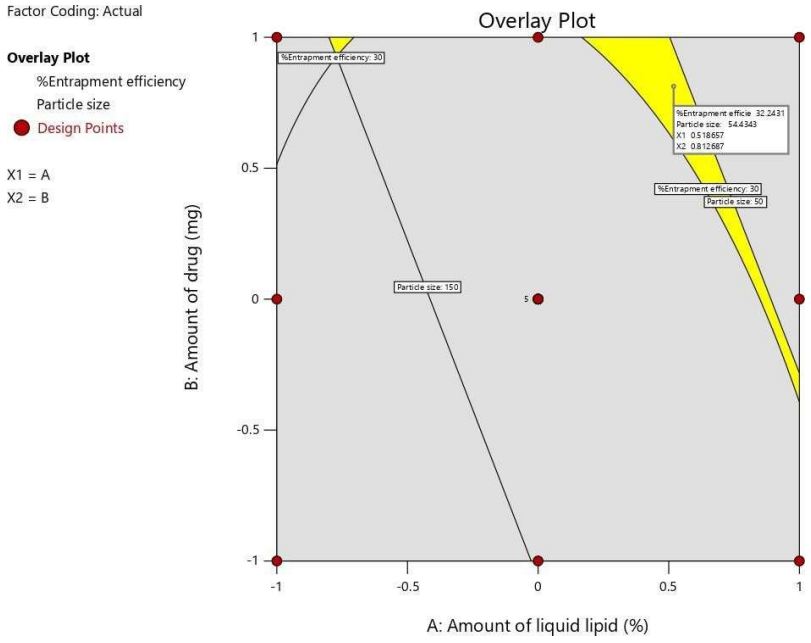


Figure 7.35 Overlay plot (ii)

Based on the full factorial design and overlay plot, 60 mg of liquid lipid (DHA) for 20 mg of drug was selected as optimum and the risk was mitigated to low. Table 7.17 depicts the optimised formula of BCPO-NLC along with the predicted and observed response values for entrapment efficiency and particle size.

Table 7.17 Predicted and Observed responses for validation batch (BC-NLC)

Sr. no.	Ingredient	Quantity	Predicted response		Observed response	
			%EE	PS	%EE	PS
1.	Beta-caryophyllene (BCPO)	20 mg	28.34 %	170nm	33.28±0.034 %	173±6 nm
2.	Compritol 888ATO	140 mg				
3.	n-3 PUFA	60 mg				
4.	Gelucire 50/13	500 mg				
5.	Water	20 ml				

7.2.5. Preparation of Folic acid-Stearic acid conjugate

As described in 3.7.4., chemical reaction was carried out to develop a conjugate of folic acid and stearic acid. As seen in Figure, dark red coloured conjugation product was formed which was further dialysed for purification and air dried and stored at room temperature till further use in formulation.

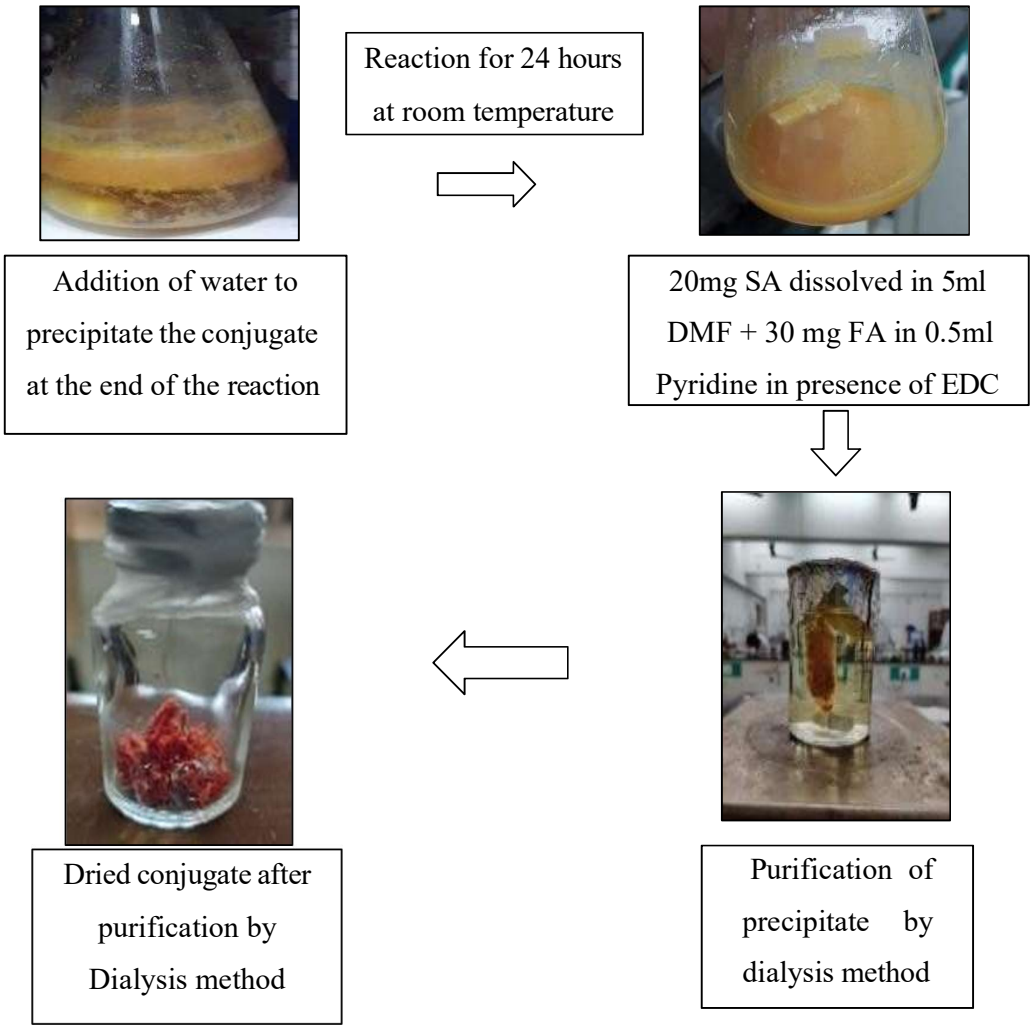


Figure 7.36 Process of conjugation reaction

7.2.6. Incorporation of Folic acid-Stearic acid conjugate in developed formulation

Further, increasing amount of Folic acid- Stearic acid conjugate (5%, 12.5% and 20% of total lipid content) was added to the formulation and formulation was evaluated for particle size. As seen in Figure 7.37, it was noted that, mean size of particles was decreased with increasing amount of conjugate. Based upon the results of particle size and homogeneity of the system, amount of conjugate in formulation was fixed at 20% of the total lipid content. The formulation was prepared in aseptic area as the designated route of administration was intravenous route.

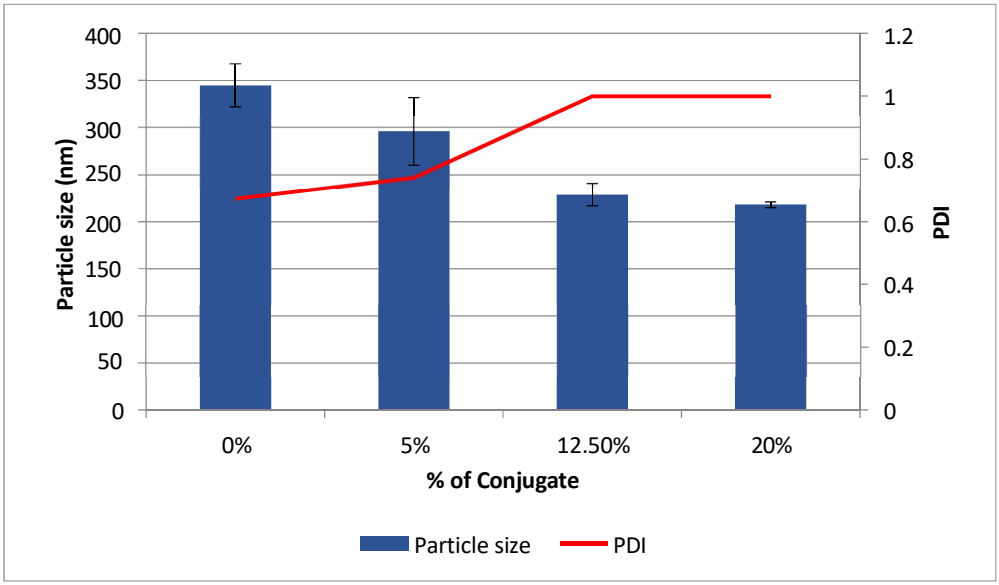


Figure 7.37 Effect of addition of conjugate on particle size

Table 7.18 depicts the formula for final optimized formulation.

Table 7.18 Optimized formula for FA-BC-NLC

Sr. no.	Ingredient	Quantity
1.	Beta-caryophyllene (BCPO)	20 mg
2.	Compritol 888ATO	100 mg
3.	n-3 PUFA	60 mg
4.	Folic acid-Stearic acid conjugate	40 mg
5.	Gelucire 50/13	500 mg
6.	Water	20 ml

7.2.7. Sterilisation of developed formulation

Various methods namely Autoclaving, Membrane filtration and Preparation inside Aseptic area were tried to determine suitable method of sterilization for optimized formulation. Suitability of the method was determined based on the parameters such as particle size, PDI, %assay and results for Test for sterility. Autoclaved formulation passed the Test for sterility in both Soybean-Casein and Fluid Thioglycollate media. However, autoclaving leads to re-heating and

thus melting of lipid component of the formulation which eventually results in rearrangement of lipids and increased particle size of nanoparticles. In method of Membrane filtration, formulation was filtered through 0.22 um filter. Filtration through small pore filter paper also filters out few particles of larger diameter thus giving lower % assay value. Owing to the limitations of Autoclaving and Membrane filtration method, formulation was decided to be aseptically prepared. Figure 7.38depicts the results of Test for sterility for samples of formulation sterilized by Autoclaving, Membrane filtration and Preparation in Aseptic area.



Figure 7.38 Results for Test for sterility (Aseptic area)

7.3. Characterization

7.3.1. Particle size and Polydispersity index

Efficiency and stability of developed nanoparticles is highly influenced by the particle size and PDI. Particle size of the developed nanosystem was measured with the use of Zetasizer Nano ZS 90. Suitably diluted samples were analysed for particle size and PDI. As seen in Figure 7.39 (a), mean particle size of FA-BC-NLC was determined to be below 190 nm with PDI was less than 0.5. Uniform nature of the formulation was confirmed by the small particle size and narrow PDI[146][139].

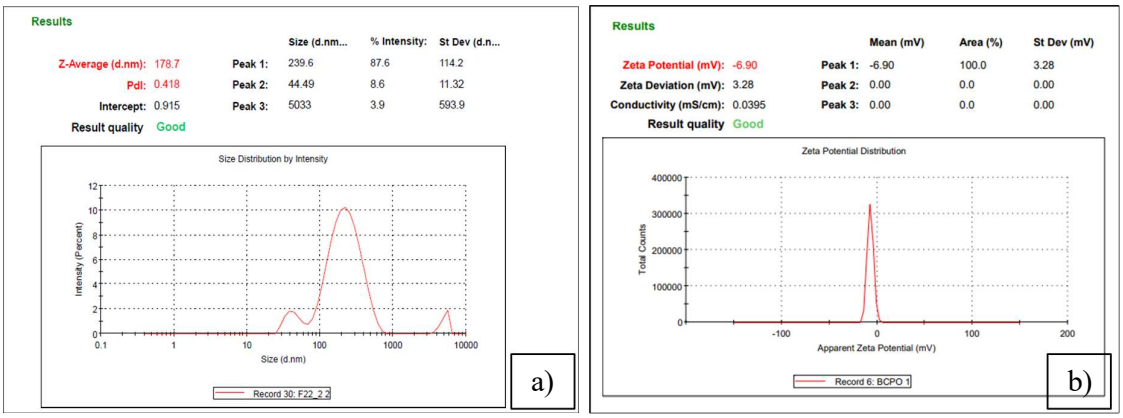


Figure 7.39 a) Particle size distribution b) Zeta potential

7.3.2. Zeta potential

As seen in Figure 7.39 (b), the zeta potential of developed nanosystem was nearly -6.9. The reason for close to neutral zeta potential value can be attributed to use of non-ionic surfactants and lipids in formulation[146][139].

7.3.3. Scanning electron microscopy

Developed nanoparticles were subjected to scanning electron microscopy to understand morphology of particle surface. SEM images revealed the spherical nature and nano size of developed lipid nanoparticles (Figure 7.40 (a)) as against the larger particles of plain drug. The results of particle size obtained through SEM were found to be in agreement with the results acquired with Malvern particle size analyser[146].

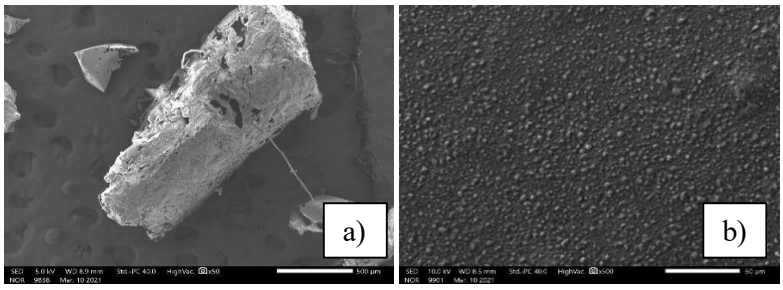


Figure 7.40 SEM images of a) Plain drug b) BC-NLC

7.3.4. Transmission electron microscopy (TEM)

TEM technique was availed to confirm the nano-crystalline nature of developed BCPO nanoparticles. TEM images (Figure 7.41) showed the nanoparticles without any agglomeration and with spherical silhouette. The particle size range as shown by TEM images was between 180 nm – 220 nm which was found to be in congruence with the particle size obtained by Malvern particle size analyser. The TEM image demonstrated the dry and shrunk configuration of BCPO lipid nanoparticles suspension [146].

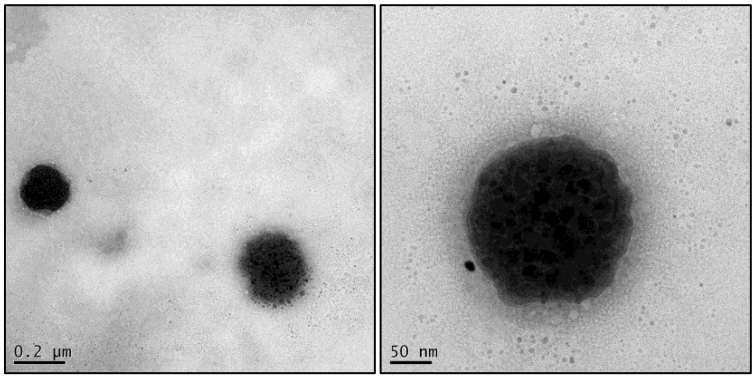


Figure 7.41 TEM images of BC NLC

7.3.5. Drug loading and entrapment efficiency

The %entrapment efficiency of developed formulation was evaluated by the method of ultracentrifugation method. Separation of lipid nanoparticles was not achieved even at very high centrifugation speed (Figure 7.42). Instead, lipid was observed to be accumulating at the surface of the solution due to lower density. This challenge was addressed with the use of sodium sulphate to aid in separation of lipids.

A) Validation of method for Entrapment efficiency:

To address this challenge, increasing amount of sodium sulphate was added to the external phase of nanoparticles solution. Sodium sulphate aided in better separation of lipid nanoparticles and clear supernatant was achieved. Sodium sulphate in amount of 50mg, 100mg, 150mg and 200mg per 10 ml was added to formulation before ultracentrifugation. Based on the results as shown in Figure 7.43, the amount of sodium sulphate was optimized to be 200 mg. Parameters for ultracentrifugation were optimized as 75000 rpm for 45 min. at 4^0C [167].



Figure 7.42 Ultracentrifuge samples without use of sodium sulphate

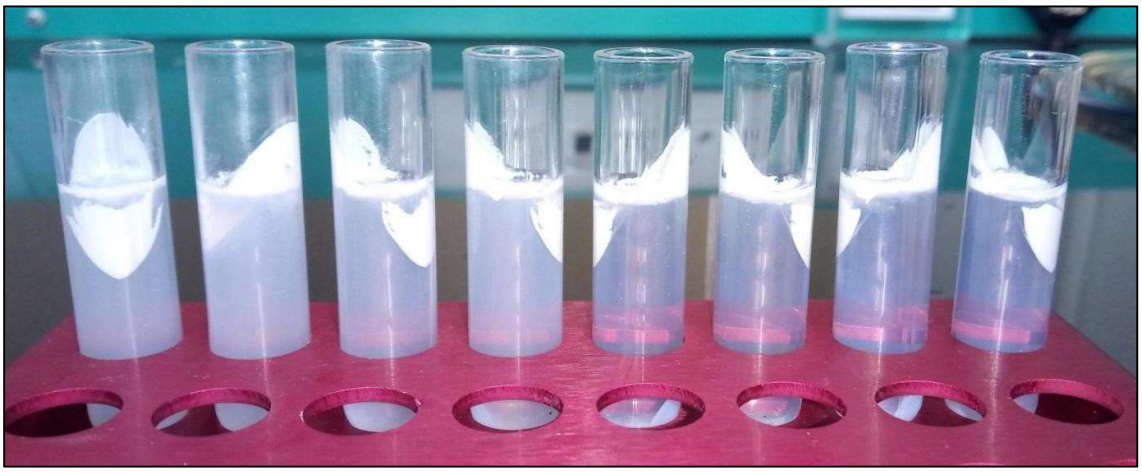


Figure 7.43 Effect of increasing amount of sodium sulphate on ultracentrifugation (from left to right)

SLN exhibits a highly ordered crystalline structure upon solidification whereas the use of a mixture of solid lipid and liquid lipid results in disorganised crystal structures in the NLC thus increasing the room for drug molecules. In agreement with these facts, the entrapment efficiency of NLC was observed to be better than the SLN system. Effect of increasing amount

of liquid lipid in formulation was also observed [138]. As seen in Figure 7.44, both %EE and %DL increase with increasing amount of liquid lipid. Results for %EE and drug loading are as depicted in Table 7.19.

Table 7.19 Results for %EE and drug loading of BC-SLN and BC-NLC

Formula	**Lipid**	**Oil**	**BCPO**	**PS** **PDI**	**EE**	**DL**
SLN	Compritol 888 ATO	-	0.1 %	220 nm 0.55	34.66± 1.5 %	12.99±0.5 %
NLC	Compritol 888 ATO	n-3 PUFA	0.1 %	176 nm 0.4	44.08 ± 5 %	16.5±3 %

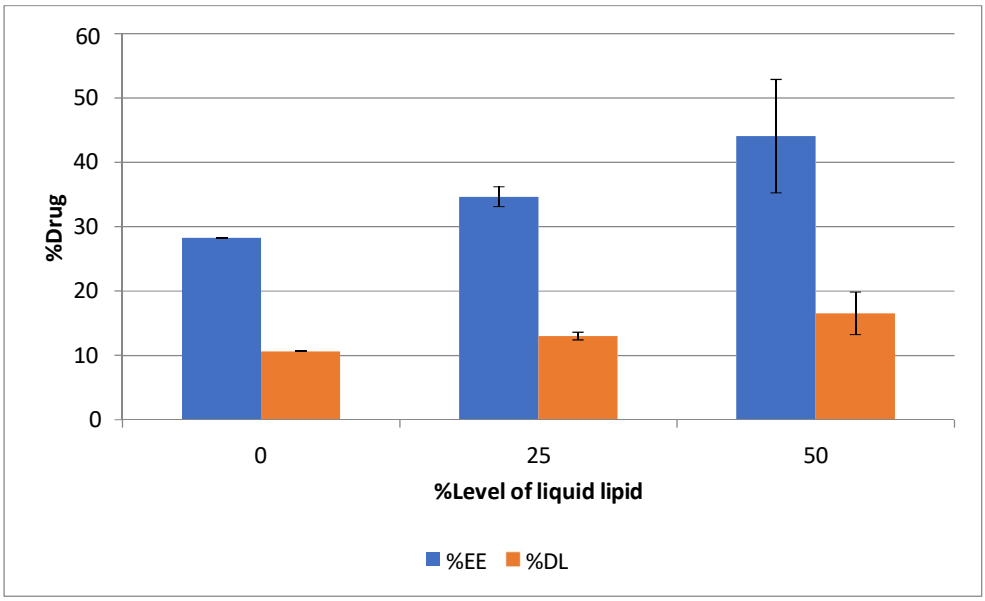


Figure 7.44Effect of addition of liquid lipid on %EE and %DL

7.3.6. In vitro drug release

In vitro drug release of developed nanosystems was performed by dialysing the formulation through cellulose acetate membrane. The dialysis membrane was soaked in release medium to 12 hours prior to use in order to saturate it medium. Phosphate buffer (pH 7.4) was identified as the drug release media as it mimicked the pH of blood[146]. As seen in Figure 7.45, Both

BC-SLN and BC-NLC systems showed low and sustained drug release in phosphate buffer pH 7.4. BC-SLN and BC-NLC systems showed 9% and 18% release of BCPO respectively after 24 hours whereas plain drug was released to the extent of around 60% in 10 hours. BCPO has low solubility in water suggesting that the drug was stable in lipid core protected by surfactant layer. Further, similar melting points of drug and lipid suggest formation of homogenous solid solution model of drug release in which drug is molecularly dispersed in lipid matrix eliminating any possibility of burst release. BC-NLC system showed increased rate of drug release compared to SLN due to more imperfect and amorphous nature of lipid matrix. Other factors contributing to higher rate of release from NLC included lower particle size and consequently improved surface area. Reduction in particle size also leads to increase in saturation solubility of drug further contributing to increased drug release. Both SLN and NLC showed low drug release at pH of blood (pH 7.4) thus avoiding the premature release of drug before it reaches the tumour site [138][168].

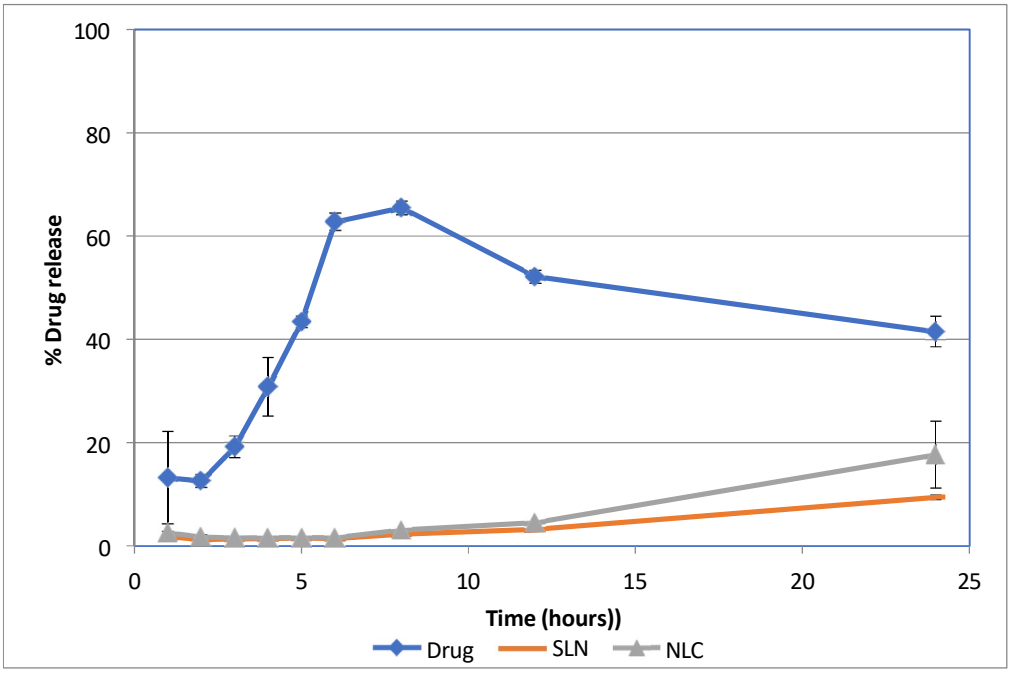


Figure 7.45 Drug release in pH 7.4 buffer

However, poor solubility of drug in pH 7.4 buffer indicated the non-sink conditions. In order to achieve sink conditions and maximum and distinguishable drug release profiles, increasing proportions of Ethanol (5% and 30%) were added in Phosphate buffer (pH 7.4). Both BC-SLN and BC-NLC systems showed increase in cumulative % drug release with increasing proportion of ethanol in drug release media (Figure 7.46). SLN system showed 82.5 % drug

release and NLC system showed 86.9 % release of BCPO in 30% ethanolic phosphate buffer (pH 7.4).

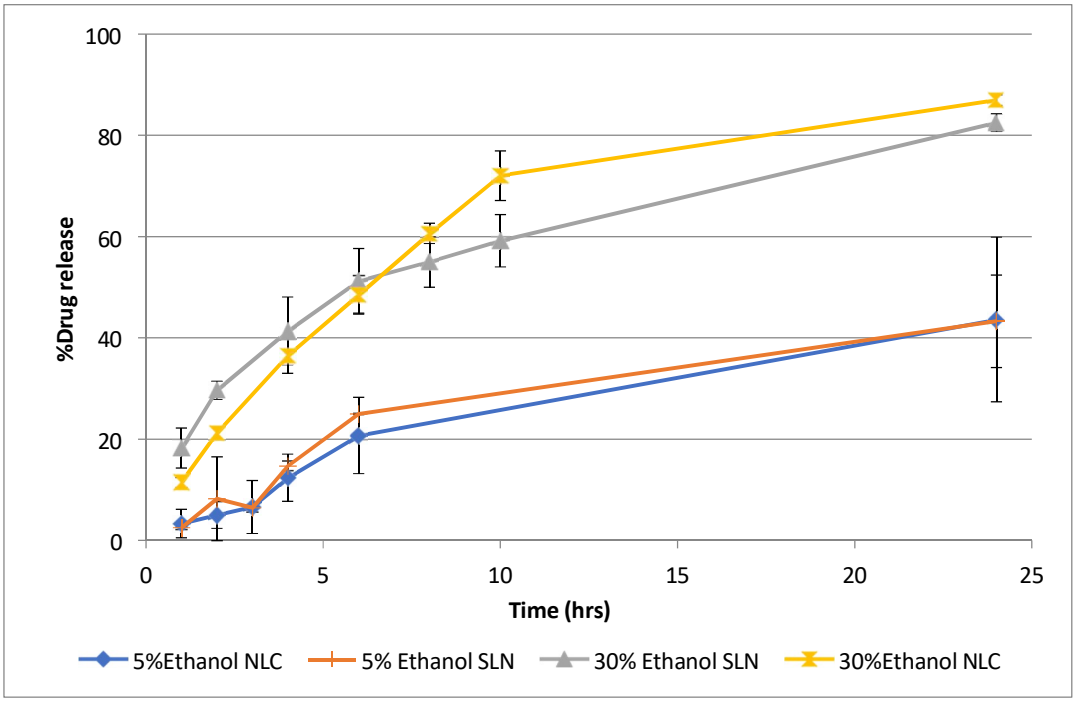


Figure 7.46 Drug release in 5% and 30% Ethanol release media

7.3.7. In vitro drug release kinetics

The in vitro drug release data of FA-BC-SLN and FA-BC-NLC was fitted with the aid of mathematical models in Table 6.24and the linear regression was assessed. As shown in Table 7.20, the drug release models were found to be correlating to the data acquired for drug release from BC-SLN and BC-NLC formulations.

As seen in Table 7.20, Higuchi's model showed the highest R^2 value (0.983 and 0.974 for SLN and NLC respectively) amongst other drug release models. Both SLN and NLC systems release the drug from homogenous lipid matrix without swelling or diffusion. Thus, the drug release from these systems was found to be following Higuchi's square root model which that demonstrates drug release from matrix system.

The release pattern was also observed to be fitting the Korsemeyer-peppas model (R^2= 0.944 and 0.922 for SLN and NLC respectively). The diffusion release exponent (n-value) of Korsemeyer-peppas model designates the mechanism of release from delivery system. n-value

of 0.554 and 0.571 for SLN and NLC systems respectively, indicate that the drug release from both the systems follows anomalous non-Fickian transport. Anomalous non-Fickian model indicates the mixture of drug release mechanism including drug release by diffusion and erosion from lipid matrix [168][138][169][170].

Figure 7.47 shows model fitting graphs of Higuchi model and Korsemeyer-peppas model for both SLN and NLC system.

Table 7.20 Results of release kinetics with regression co-efficients

Formulation system	**Mathematical Model**	**The correlation coefficient (R2)**	**Diffusion release exponent (n)**
BC-SLN	Zero order	0.904	
	First order	0.503	
	Higuchi model	0.983	
	Korsemeyer-peppas model	0.944	0.554
	Hixson-Crowell cube root law	0.896	
BC-NLC	Zeroorder	0.845	
	Firstorder	0.467	
	Higuchimodel	0.974	
	Korsemeyer-peppas model	0.922	0.571
	HixsonCrowellcuberootlaw	0.865	

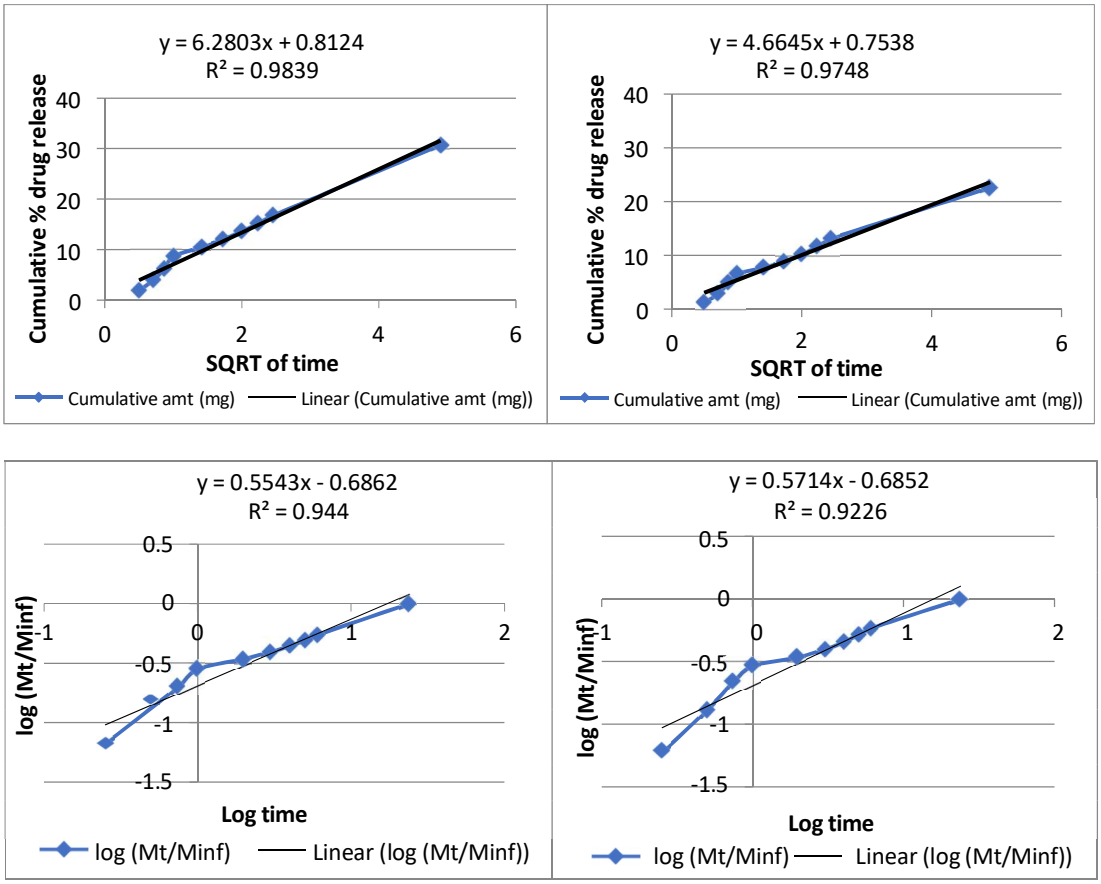


Figure 7.47 Release kinetics model fitting a) Higuchi model for SLN b) Higuchi model for NLC c) Korsemeyer-peppas model for SLN d) Korsemeyer-peppas model for NLC

7.3.8. Solid state characterization

A) Differential Scanning Calorimetry (DSC):

Figure 7.48 depicts the melting endotherms obtained by DSC for a) BCPO, b) Lipid (Compritol 888 ATO) and c) BC-NLC. As seen in Figure 7.48(a), BCPO shows sharp endothermic peak at 63.5^{0}C. Compritol 888ATO, a solid lipid used in BC-NLC formulation, shows sharp melting endotherm at 73.4^{0}C corresponding to its melting point. BC-NLC shows an endothermic peak at 166^{0}C, which can be ascribed to the glass transition temperature of mannitol. Mannitol is used as a cryoprotectant during lyophilization of BC-NLC. The overall melting endotherm of formulation is thus based on the melting point of cryoprotectant. The endotherm of BCPO-SLN also shows smaller peak roughly around 63^{0}C which can attributed to reduced crystallinity of drug. DSC thermograms thus show the solubilisation of drug in lipid matrix of NLC [138].

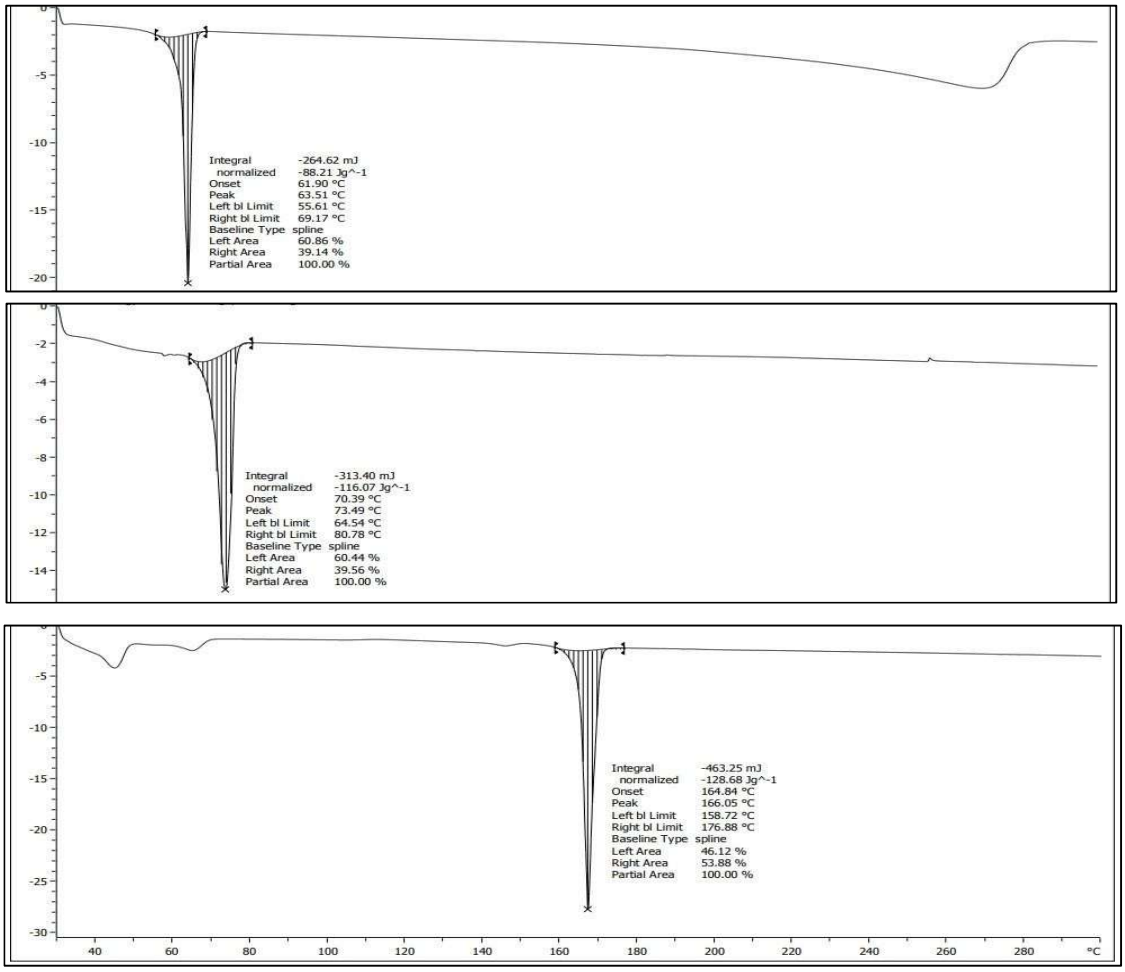


Figure 7.48 DSC thermograms of a) BCPO b) Lipid c) BC-NLC

B) Powder X-ray diffraction (XRD)

Figure 7.49 depicts the diffractograms for BCPO, BC-NLC and Placebo. As seen in Figure 7.6 and Figure 7.49, diffractogram of BCPO shows sharp peaks at 2Ɵ values of10.52, 13.03,14.69,17.58,19.97 and 28.89^0. These peaks are not observed in diffractogram of BC-NLC suggesting that the drug is available in solubilised form in lipid. Diffractogram of BC-NLC shows reduction in intensities of all peaks in comparison with BCPO indicating presence of less ordered structures in NLC lipid matrix. Blank formulation indicates peaks of very low intensity indicating presence of bulk lipids in amorphous form. The results of XRD were also found to be correlative to the results obtained with DSC [138].

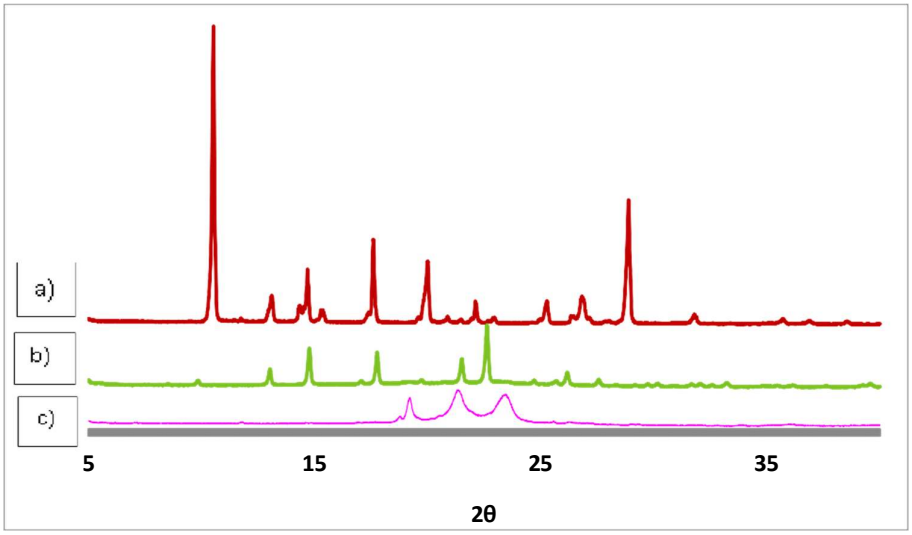


Figure 7.49 P-XRD diffractogram of a) BCPO b) BC-NLC C) Placebo

7.3.9. Evaluation of conjugate

At the end of reaction, dark brown coloured precipitate was obtained (Figure 7.50). Precipitate was collected by vacuum filtration method. Precipitate was further purified by dialysis in water. Obtained conjugate was further characterised by methods such as FTIR, Mass spectrophotometry and NMR.Results of Mass spectrophotometry (Figure 7.51) showed the presence of peak characteristic to conjugate (peak highlighted in red, molecular weight 707).



Figure 7.50 Dried Folic acid-Stearic acid conjugate

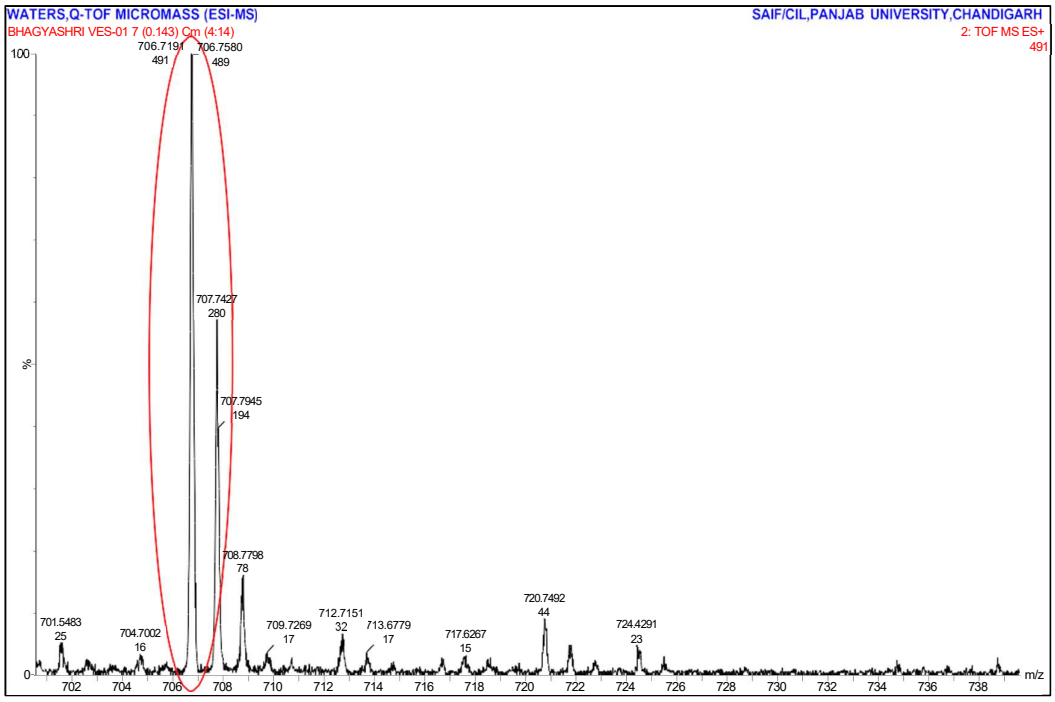
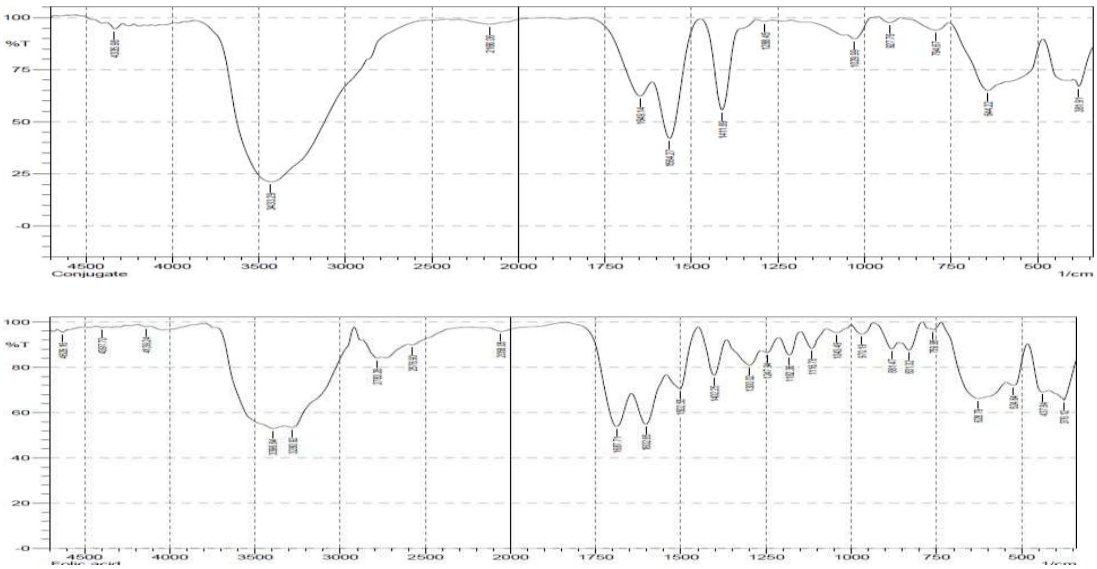


Figure 7.51 Mass spectra of Folic acid-stearic acid conjugate



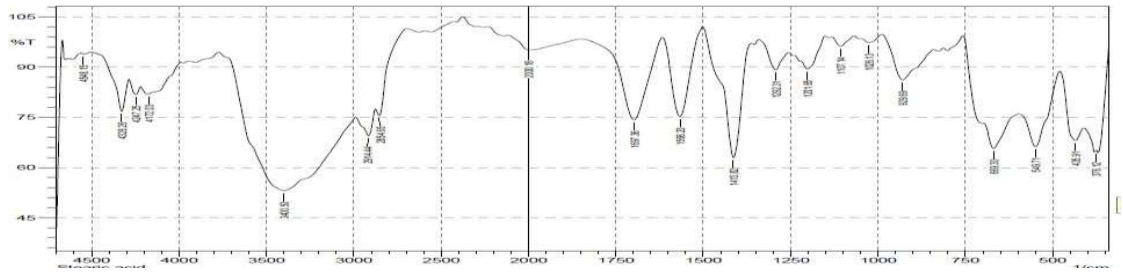


Figure 7.52 FT-IR spectra of a) FA-SA conjugate b) Folic acid c) Stearic acid

7.3.10. In vitro haemolysis study

In vitro haemolysis study was performed to evaluate safety of developed formulation upon intravenous administration. Table 7.21 depicts the results of % haemolysis for 1% Triton X solution, BC-NLC and phosphate buffer saline. Triton X solution shows complete haemolysis whereas phosphate buffer saline shows negligible haemolysis. The % haemolysis for developed formulation was observed to be 5.44%. As per the general considerations, % haemolysis values below 10% are considered as non-toxic or non-haemolytic. The developed formulation is thus considered to be safe for intravenous administration [148].

Table 7.21 Results of in vitro haemolysis study

Sr. no.	Test sample	% Haemolysis
1.	1% Triton X solution	100
2.	Formulation (BC-NLC)	5.44
3.	Phosphate buffer saline (pH 7.4)	4.5

7.3.11. Stability studies

Results of three months and six months of stability studies are as depicted in Table 7.22. Particle size of the formulation was not observed to have changed at the end of three months. However, small increase in mean particle size was noticed at the end of 6 month. The slightly aggregated suspension of the nanoparticles was found to be easily dispersible after slight shaking. There was no considerable change observed in % entrapment efficiency of the formulations at the end of three months. Entrapment efficiency was observed to be slightly

reduced at the end of six months. The reason for reduced entrapment of drug can be attributed to rearrangement of solid lipid crystal in more stable confirmation leading to expulsion of drug.

Table 7.22 Results of stability studies for BC-NLC

Sr. no.	Duration (months)	Particle size (nm)	PDI	% EE
1.	0	178 ± 2	0.418 ± 0.07	44.08 ± 5 %
2.	3	182 ± 4	0.548 ± 0.08	43.47±5 %
3.	6	184 ± 4	0.570 ± 0.05	39.01±3 %

7.3.12. In vitro cytotoxicity studies on cancer cell lines

In order to prove the cytotoxicity of developed formulations on both hormone receptor positive as well as hormone receptor negative cell lines, two cell lines were selected for cytotoxicity studies. MCF-7 has functional estrogen receptors whereas MDA-MB-468is hormone-independent breast cancer cell line. The results for cytotoxicity studies for both cell lines are as seen in **Figure 7.53** (MCF-7) and **Figure 7.54** (MDA-MB-468). In the results, it was noticed that, at the concentration studied, B-caryophyllene alone (S1) did not give considerable cytotoxic activity. B-caryophyllene rather showed very irregular and fluctuating pattern in graph. Reasons for this inconsistent pattern can be attributed to volatile and water insoluble nature of BCPO. Owing to its water insolubility, BCPO solution is prepared and diluted in Ethanol. However, upon addition to cell culture media, BCPO precipitates due to dilution with aqueous media. Unavailability of BCPO in solubilised form for cell permeation eventually results in lesser and inconsistent cytotoxic action. Fluctuating nature of the results can also be attributed to volatile nature of BCPO. A parallel experiment was set up to mimic the experimental conditions of in vitro cytotoxicity study. Ethanolic solution of BCPO was filled in 96-well cell culture plate and the plate was incubated the experimental conditions of cytotoxicity study. BCPO was found to be getting evaporated by the end of the experiment. These findings helped to correlate and interpret the behaviour of BCPO in cytotoxicity studies[143].

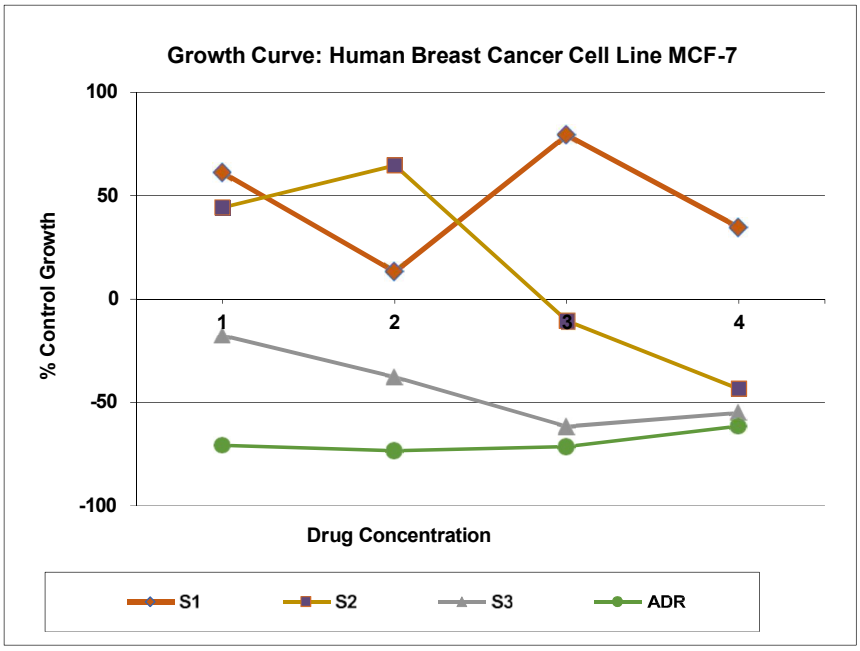


Figure 7.53 Growth Curve: Human Breast Cancer Cell Line MCF-7

S1:BCPO S2:PUFA SLN S3: BCPO+PUFA NLC S4:Vehicle S5: Gemcitabine

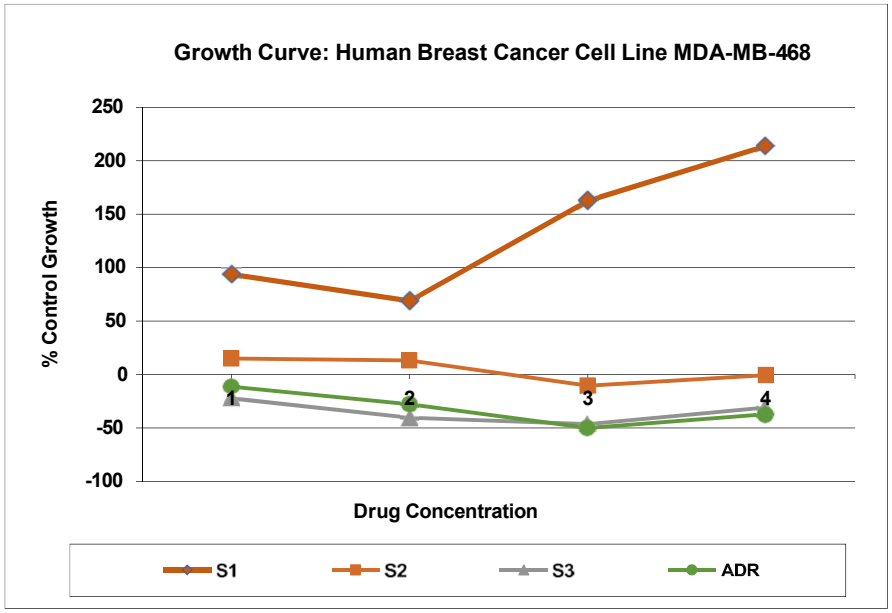


Figure 7.54 Growth Curve: Human Breast Cancer Cell Line MDA-MB-468

S1:BCPO S2:PUFA SLN S3: BCPO+PUFA NLC S4:Vehicle S5: Gemcitabine

DHA (n-3 PUFA) (S2)was found to be showing higher cytotoxic activity than B-caryophyllene owing to its increased uptake in cancer cells due to presence of Fatty acid transporters. Further, Formulation (Solid Lipid nanoparticles with both B-caryophyllene and DHA) (S3) was

expectedly found to be more lethal than B-caryophyllene alone and DHA alone. From these results, it could be elucidated that, lipid-based delivery system is successfully encapsulating BCPO thus preventing its volatilization. Formulation system retains BCPO and makes it available for prolonged period of action. BCPO and DHA were also found to be showing synergistic action as seen from the results. DHA is known to enhance the permeation of various cytotoxic drugs across the cancer cell membrane. Synergistic potential of DHA in addition to its own cytotoxicity amounts for the increased cytotoxicity of formulation system. Cytotoxicity shown by formulation system was found to be comparable with the standard compound (Adriamycin) used for the study. Figure7.55 depicts the microscopic images of samples for cytotoxicity studies.

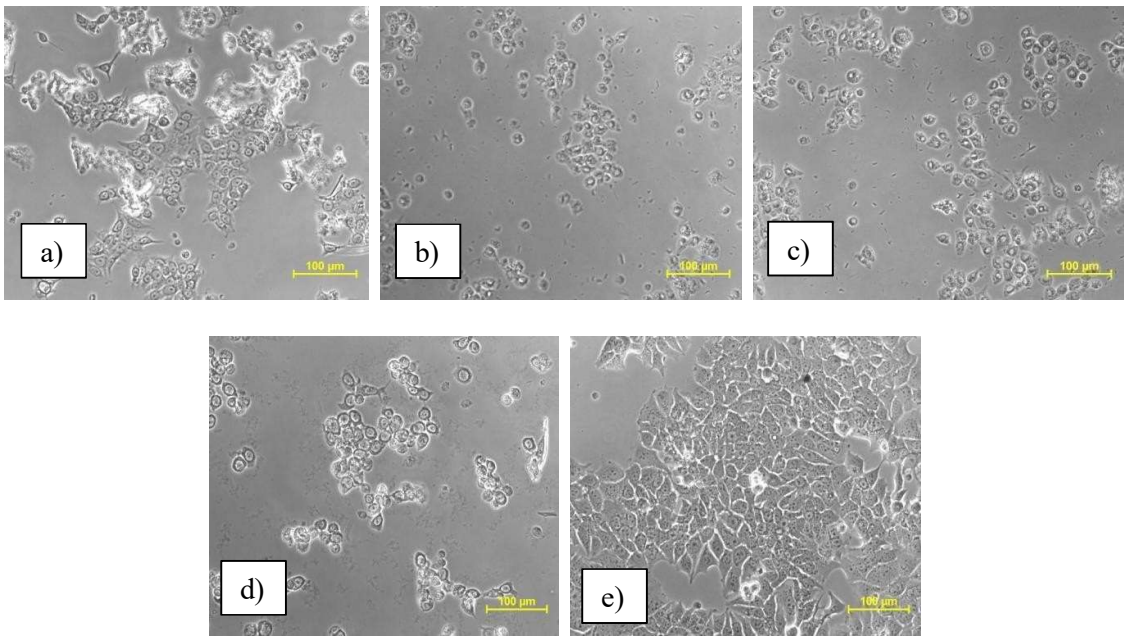


Figure7.55 Microscopic images of samples for cytotoxicity study a) BCPO b) DHA c) BCPO-DHA formulation d) Adriamycin e) Control

7.3.13. In vitro cytotoxicity studies on fibroblast cells

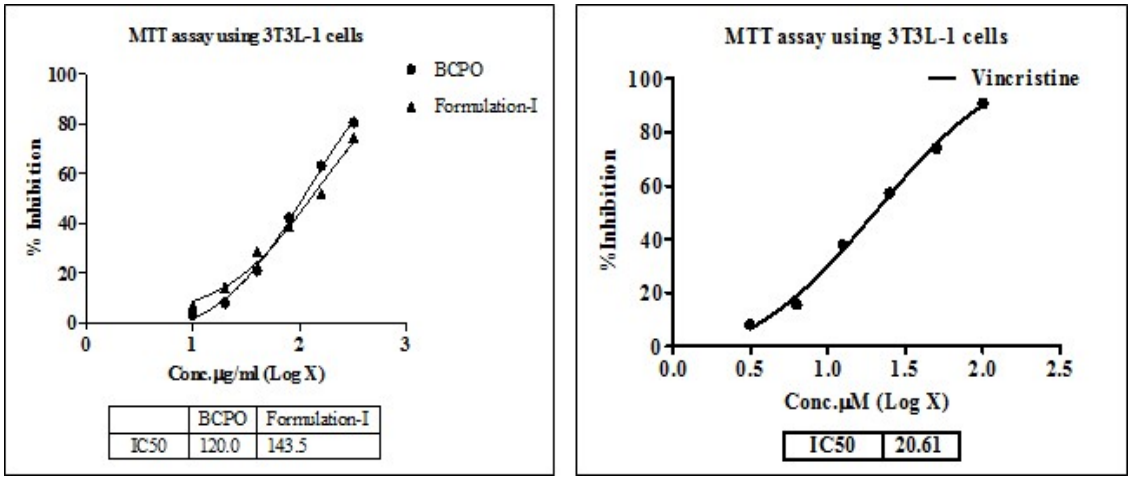
Developed formulation was also tested against healthy cells with the use of 3T3L-1 mouse fibroblast cell line. Table 7.23 and Table 7.24 depict the % cell inhibition measured in terms of optical density for BCPO, BC-NLC and vincristine. From graphical representation of the data (Figure 7.56) it was concluded that, BCPO and BC-NLC (Formulation-I) showed an IC50 of 120µg/mL and 143.5µg/mL respectively in 3T3L-1 cell line, whereas standard Vincristine showed an IC50 value of 20.61µM (16 µg/mL) in same cell line.

Table 7.23 % cell inhibition and IC50 value for BCPO and BC-NLC

3T3L-1				
Sample	**Conc. µg/mL**	**OD at 590nm**	**% Inhibition**	**IC50 µg/mL**
Control	0	0.658	0.00	
BCPO	10	0.636	3.34	**120**
	20	0.605	8.05	
	40	0.519	21.12	
	80	0.38	42.25	
	160	0.242	63.22	
	320	0.128	80.55	
BC-NLC	10	0.612	6.99	**143.5**
	20	0.565	14.13	
	40	0.469	28.72	
	80	0.403	38.75	
	160	0.317	51.82	
	320	0.168	74.47	

Table 7.24 % cell inhibition and IC50 for vincristine

3T3L-1				
Sample	**Conc. µM**	**OD at 590nm**	**% Inhibition**	**IC50 µM**
Control	0	0.658	0.00	
Vincristine	3.125	0.605	8.02	**20.61**
	6.25	0.555	15.72	
	12.5	0.409	37.89	
	25	0.280	57.39	
	50	0.171	74.06	
	100	0.060	90.88	



	BCPO	Formulation-I
IC50	120.0	143.5

IC50	20.61

Figure 7.56 % inhibition vs conc. curve for a) BCPO, BC-NLC and b) Vincristine

Higher IC50 value of BCPO-NLC suggests that formulation system has protective effect on normal cell line. Also, IC50 values of both BCPO and BC-NLC are much higher in contrast to vincristine. Thus, it was concluded that BCPO and BC-NLC has negligible cytotoxicity on normal cells.

7.4. Summary and conclusion

The findings of formulation and characterization process were summarised as below:

- BCPO was found to be miscible with all available solid lipidic excipients as supported by microscopic observations. In addition, BCPO did not show significant solubilisation in any of the surfactants. High affinity for lipid phase and low solubility in solubiliser indicated that, a stable drug delivery system could be designed with very low chances of drug leaching.
- Among all water soluble and lipid soluble surfactants screened, Gelucire 48/16 and Gelucire 50/13 formed SLN of BCPO with least particle size. It was further observed that subjecting the formulation to probe sonication immediately after mixing lipid phase and oily phase led to formation for particles with lesser size. Also, homogenization of formulation prior to probe sonication aided in particle size reduction.
- Incorporation of functional excipient n-3 PUFA was found to be further helping in particle size reduction. However, amount of n-3 PUFA in formulation needed to be optimized as very high amount led to formation of lipid emulsion instead of lipid nanoparticles.

Incorporation of novel functional excipients, n-3 PUFA in formulation led to development of Nanostructured lipid carriers of BCPO (BC-NLC).

- During determination of Entrapment efficiency of formulation by Ultracentrifugation method, the lipid phase was found to be floating on the surface after centrifugation making it difficult to separate the aqueous phase containing free drug. A salt (Sodium sulphate) was added in order to aid the separation of lipid phase and aqueous phase.
- Conjugation reaction between Folic acid and Stearic acid led to formation of a solid product which was further incorporated in formulation as a part of lipid phase (FA-BC-NLC). Incorporation of increasing amount of Folic acid-Stearic acid conjugate led to reduction in the particle size.
- Developed SLN system showed drug release of around 9 % in 24 hours (pH 7.4). NLC of drug showed the similar effect of low drug release (around 17%) at pH of blood (pH 7.4). Plain Drug is released to the extent of 60 % in 10 hours. These results indicate that both formulations (SLN and NLC) depict protective effect on drug preventing its premature release during circulation in blood.
- In vitro cytotoxicity studies highlighted that, BCPO and n-3 PUFA showed enhanced cytotoxicity when used in combination thus showing the synergistic effect. Further, in vitro cytotoxicity studies performed on 3T3L-1 fibroblast cells elucidated that, BCPO and BC-NLC formulation has negligible toxicity on healthy cells.

Thus, following conclusions were drawn from the formulation and characterization of BC-NLC formulation system:

1) Novel formula for solid lipid drug delivery system for BCPO with use of n-3 PUFA as lipidic excipients was developed and optimized.

2) The optimized formulation of BC-NLC was found to be showing particle size below 200nm with narrow PDI value. Low particle size of developed formulation emphasized its potential to show enhanced permeability and retention (EPR) effect at tumour site. Low particle size also indicated the likelihood longer circulation time by escaping the RES system.

3) Developed formulation also highlighted low drug release at the pH of blood thus highlighting its potential to minimize off-target toxicity.

4) Developed formulation was also shown to have sword and shield like effect by demonstrating cytotoxicity against cancer cells and low toxicity against healthy cells.

The developed formulation was thus found to be demonstrating the potential for a safer alternative to intravenously administered anticancer agents. The safety and efficacy of developed formulation was further evaluated by *in vivo* studies.

Chapter 8

In vivo evaluation

Chapter 8: In vivo evaluation

8.1. Introduction

8.1.1. Acute toxicity studies:

Administration of any chemical substance in body of humans or animals leads to development of various desired as well as undesired effects. Various interactions can occur in body upon administration of chemical substance which may vary with the dose administered. In cases, where chemical substances lead to undesired or hazardous effects, it is necessary to determine the concentration at which such substances can be safely administered. Traditionally, safety of chemical substances to be administered by oral, dermal or inhalation route has been assessed by undertaking toxicity studies. Toxicity studies carried out in pharmaceutical industry are known as acute, sub-acute and chronic toxicity studies[171][172].

Determination of acute toxicity involves estimation of LD50 value for given chemical substance. Acute toxicity study is regarded as a screening procedure performed during initial stages of estimation of toxicity of given chemical substance and for given route of administration. Objective of the acute toxicity study is to establish therapeutic index or ratio between the lethal dose and pharmaceutically effective dose. Acute toxicity study also serves to provide preliminary information on toxic nature of the given compound. It may also be used to determine the dose for preclinical studies and to determine the dose of a new compound. Acute toxicity studies are regarded as helpful in determination of toxic nature of the substance especially when no other information on toxicity is available. The results of acute toxicity are also important in determining the adverse effects upon accidental exposure to a chemical substance[173][172][174]. As per the FDA guidelines, focus of acute toxicity studies should be directed towards observing the adverse effects rather than determination of rate of mortality in experimental animals[174].

A) Determination of LD50 and study design of acute toxicity:

Conventionally, the classical LD50 tests are performed to determine the median lethal dose (dose causing death of 50% of the experimental animals)[174][173]. The earlier methods to determine median lethal dose involved use of large number of experimental animals. The classical LD50 test required up to 100 experimental animals for five different dose groups and results were expressed in terms of death of 50% of the experimental animals. Further

advancement in acute toxicity study was known as Karbal method which suggested the use of 30 experimental animals divided in six groups of six animals each. In another alternative method used to establish LD50, known as arithmetical method, 40 experimental animals are used (10 animals divided into 4 experimental groups). The Miller and Tainter method, established in 1944, recommends use of 50 animals divided into 5 groups of 10 animals each. LD50 value is established with the use of probit analysis table. Almost all the traditional methods used earlier described the use of large number of animals. Further, determination of number of animals dying at the end of the study was not considered conclusive for estimation of toxic effects of given compound. Such drawbacks of traditional methods probed researchers seek for alternative methods. The search for the newer and alternative methods is directed towards the use of lesser number of experimental animals. The search predominantly followed 3R techniques (*reduce, refine and replace*). 'Reduction' in 3R approach implies the reduction of number of animals used in test procedures. Newer methods aim to use minimum possible number of experimental animals while still maintaining the validity of test results. 'Refinement' denotes the revisions in the test procedures in order to reduce the distress and pain caused to animals. 'Replacement' suggests the use of alternatives to animals such as *invitro* or *in silico* methods wherever applicable and feasible[173][174][175].

With the use 3R technique, newer methods were developed to analyse the toxic effects of the chemical substance on short term exposure.

B) OECD guidelines for acute toxicity testing:

Organisation for economic cooperation and development (OECD) included the guidelines for LD50 studies developed using 3R approach[173]. For the substances which are not expected to be toxic, the idea of limit test was introduced. To perform limit test, the experimental animals (approximately 5 no.) are exposed to the limiting dose of the test compound (5000mg/kg). The animals are observed for any signs of mortality or toxicity for the period up to 14 days. After the end of the test period, if there is no sign of toxicity, no further tests are required. In case of mortality, the study is repeated with the lower dose of the test compound. 5000mg/kg was introduced as the upper limit of the test compounds that can be administered to experimental animals[173].

Further modifications in test procedures led to development of OECD guidelines 420, 423 and 425. OECD guideline 420, also known as fixed dose procedure (FDP) involves administration of one of the four fixed doses to 5 male and 5 female animals. The fixed doses are 5, 50, 500

and 2000 mg/kg. The experimental animals are observed for the signs of toxicity. In absence of toxicity, no additional tests are required. In case of mortality, the test is repeated with lower fixed dose[176]. OECD guideline 423, also known as acute toxic class method, involves sequential testing as each dose level of 5, 50, 300 and 2000mg/kg. At each level, 3 animals are used. This method was found to be reducing the number of animals by 40-70%[177]. OECD guideline 425, also known as up-and-down method, involves dosing of an individual animal one dose at a time. The experimental animal is observed for 1 or 2 days and based on the results, 2^{nd} dose is administered to 2^{nd} animal. In case of any signs of toxicity or mortality, the 2^{nd} dose is reduced by 3.2-fold, whereas, in case of no signs of toxicity, the next dose is increased 3.2 folds. The delayed toxicity is further observed in surviving experimental animals for the period of up to 7 days[178]. OECD guidelines have regulatory approval and have demonstrated the considerable reduction in number of experimental animals used for the test. All traditional methods were eliminated after implementation of OECD guidelines[173][174].

Table 8.1 depicts the interpretation of acute toxicity results based on the LD50 value[173].

Table 8.1 LD50 value and results of acute toxicity study

Sr. no.	LD50 (mg/kg)	Results
1.	<5	Extremely toxic
2.	5-50	Highly toxic
3.	50-500	Moderately toxic
4.	500-5000	Slightly toxic
5.	5000-15000	Practically non-toxic
6.	➢ 15000	Relatively harmless

C) Biomarkers in observation of acute toxicity:

Unlike the traditional acute toxicity study methods, wherein only mortality of animals was considered as a conclusive parameter, advanced acute toxicity studies consider various biomarkers in order to evaluate toxicological effects of given compound[173]. With recent advances in technology, many newer biomarkers have been added to evaluate the toxicological effects on different organs as well as on overall functioning of body. Individual biomarkers act

as small pieces of the overall toxic effect of test compound. More the number of biomarkers evaluated, the results of acute toxicity become more complex but more predictive for the effects in human species. Biomarkers in acute toxicity study are selected in such a way that the results established in one species can be extrapolated to other species[179]. Table 8.2 enlists few of the parameters and biomarkers observed during acute toxicity study apart from mortality[179].

Table 8.2 Biomarkers and parameters used in assessment of acute toxicity

Sr. no.	Parameter	Observation
1.	Liver toxicity	Change in size, colour or weight Increased or decreased activity of liver marker enzymes Increased or decreased coagulation time Histopathological changes including necrosis
2.	Kidney toxicity	Increased or decreased urine volume Change in size, colour or weight Increased or decreased plasma creatinine level Histological changes including necrosis
3.	Red blood cells	Chronic hypoxia Vascular shock Polycythaemia Anaemia
4.	Mitochondria	Mitochondrial dysfunction Change in mitochondrial permeability transition
5.	Reactive oxygen species	Trigger in production Reperfusion injury

D) Acute toxicity of Beta caryophyllene oxide:

There is no reported literature that gives information regarding toxicological profile of any kind (acute/sub-acute/chronic/sub-chronic) for BCPO. As per our literature survey, there are no

toxicity studies carried out for any of the routes of administration for BCPO. However, toxicity profile of a close analogue, beta caryophyllene (BCP) has been established and evidence regarding the same can be found in literature. Reported acute toxicity for BCP for oral route is 5000mg/kg which shows that BCP is practically non-toxic upon oral administration[180][181]. As per research study by D. Schmitt et. al.,BCP was also observed to be safe for oral administration as per the sub-chronic toxicity study performed at dosages of 0 mg/kg, 150 mg/kg, 450 mg/kg, 700 mg/kg[33].

8.1.2. Nuclear medicine and molecular imaging:

Advancement in technology in past few years has enabled the researchers to investigate cancer and other life-threatening diseases to cellular and molecular level. In an attempt to understand the cancer to molecular levels, several techniques were introduced in the field of molecular imaging. Molecular imaging is a non-invasive method that uses a single or combination of different modalities for observation of biological events at cellular and molecular levels. Several years of research has extended the applications of molecular imaging to diagnostic and therapeutic levels[182][183]. Nuclear medicine is one of the branches of molecular imaging. Nuclear medicine involves use of radiopharmaceuticals which upon administration in body allows physicians to evaluate, measure, diagnose and treat tumour and other diseases. Radiopharmaceutical consists of a combination of a radioactive element attached to a pharmaceutical moiety through a linker[184]. The linker molecule generally possesses the targeting properties thus directing the radiopharmaceutical to the target site via active targeting (Figure 8.1)[184].

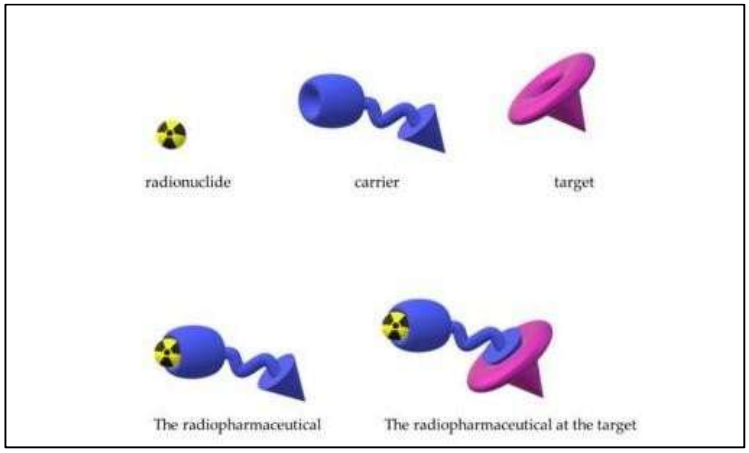


Figure 8.1Linking of radionuclide to pharmaceutical entity via a targeting agent

Diagnosis in the field of nuclear medicine is done by detection of γ-rays emitted through the decay of radioactive element. The radioactivity coming out from the radiopharmaceuticals carries the information regarding the biological processes and is analysed with the aid of sophisticated gamma cameras. The specifications for radiopharmaceuticals include the small size in range of nanometre, able to produce γ-ray in the energy range of 100-600keV and having a short half–life in order to avoid unnecessary exposure to radioactivity[184][183][185].

Various modalities used for molecular imaging with the use of nuclear medicine include X-ray, computed tomography (CT), magnetic resonance imaging (MRI),photon emission tomography (PET) and single photon emission computed tomography (SPECT). All modalities differ in their sensitivities and possess their own limitations[184][182]. Table 8.3 gives the overview on the sensitivities, advantages and limitations of various modalities[184][182].

Table 8.3 Overview of various imaging modalities

Sr. no.	**Modality**	**E.g., of contrast agent**	**Special resolution**	**Sensitivity**	**Advantages**	**Limitations**
1.	Computed tomography (CT)	Iodine, Barium	500 um	10^{-6}	High spatial resolution, excellent depth inexpensive,	Low soft tissue contrast, no real time imaging
2.	Optical fluorescence	Fluorescence dye	2-3 mm	10^{-9}– 10^{-12}	High sensitivity, real time imaging, non-ionising radiation	Low spatial resolution, poor penetration depth
3.	Magnetic resonance imaging (MRI)	Gadolinium, iron, manganese	20-100 um	10^{-9} – 10^{-6}	High spatial resolution, no ionising radiation, limitless depth penetration	Low sensitivity, longer acquisition time, expensive

4.	Positron emission tomography (PET)	Radionuclide	1-2 mm	10^{-11} – 10^{-12}	High sensitivity, limitless depth penetration, whole body imaging	Low spatial resolution, expensive, radiation risk
5.	Singlephoton emissioncomputedtomography (SPECT)	Radionuclide	1-2 mm	10^{-10} – 10^{-11}	High sensitivity, limitless depth penetration, whole body imaging	Low spatial resolution, expensive, radiation risk

Among all the techniques SPECT and PET have high sensitivity and have shown extensive application in early diagnosis of various therapeutic conditions. Recent advancements the field of molecular imaging involves use of combination of different modalities to overcome the limitations of individual technique. This approach, being known as multimodalities or hybrid imaging techniques have found to be providing more comprehensive results for therapeutic as well as diagnostic applications. SPECT and PET techniques are used in combination with MRI and CT and are finding more and more applications in the field of molecular imaging[186][187][182][184].

A) Positron emission tomography (PET)[188][184][182]

In PET technology, γ-ray emitted from the decay of radioactive element is detected and measured. It is considered as high-performance imaging modality which is widely used in clinical and preclinical studies. It has established its application in wide arenas of oncology, neuroscience as well as cardiology. Various radioactive elements used in PET study include ^{11}C, ^{18}F, ^{15}O,^{13}N and ^{68}Ga. Almost all the isotopes used in PET study possess short half-life (Table 8.4) [188]and thus need to be prepared freshly and used immediately.

Table 8.4 Radioisotopes used in PET and their half-lives

Sr. no.	**Radioisotope**	**Half-life ($t_{1/2}$)**
1.	Fluorine-18 (^{18}F)	109.8 min.

2.	Nitrogen-13 (^{13}N)	9.97 min.
3.	Oxygen-15 (^{15}O)	2.04 min.
4.	Carbon-11 (^{11}C)	20.3 min.
5.	Gallium-68 (^{68}Ga)	67.63 min.

The positron emitted from the radioisotopes rapidly loses its kinetic energy after travelling few millimetres through surrounding tissues. Thereafter, it's travelling speed decreases and it interacts with electrons to produce two γ-rays which are detected by PET detectors. A three-dimensional image is constructed with computer software.

[18F]-2-fluoro-2-deoxy-D-glucose (^{18}F-FDG) is extensively used metabolic tracer in PET for clinical as well as preclinical oncology. ^{18}F-FDG is fluorinated glucose analogue injected in body as a metabolic tracer. It is selectively uptaken by rapidly multiplying tumour cells. The accumulation of ^{18}F-FDG in tumour helps in visualisation of its progression, staging and treatment in clinical and preclinical practice.

Recent advancements in PET technology have come up with the smaller size PET scanner to aid in small animal imaging in preclinical settings.

B) Single photon emission computed tomography (SPECT)[188][187][182][184]

SPECT study is another specialised imaging modality based of radioactive decay of radio nuclides and detection of γ-rays. It differs from PET in detection of single γ-ray and use of different set of radio nuclides. Radioisotopes used in SPECT, decay with single photon emission and have relatively longer half-life than PET radioisotopes (Table 8.5)[188].

Table 8.5Radioisotopes used in SPECT and their half-lives

Sr. no.	**Radioisotope**	**Half-life ($t_{1/2}$)**
1.	Technetium-99m (^{99m}Tc)	6 hrs
2.	Iodin-123 (^{123}I)	13.3 hrs
3.	Indium-111 (^{111}In)	2.8 days
4.	Copper-67 (^{67}Cu)	3 days

^{99m}Tc is so far most widely used radionuclide in SPECT study. The favourable half-life of 6 hours of ^{99m}Tc provides sufficient time for the clinicians and researchers to prepare the radiopharmaceuticals and inject the same to the patients or laboratory animals, avoiding unnecessary longer exposure to radioactivity. The time period is also sufficient for acquisition of readings after radioactive decay. ^{99m}Tc is available conveniently and at low price as compared to PET radionuclide. ^{99m}Tc is generated through ^{99}Mo/^{99m}Tc generator system which can be commercially purchased and installed in the clinical and research facilities. Decay of ^{99}Mo leads to generation of ^{99m}Tc in the form of pertechnetate [^{99m}TcO4]$^{-}$ which is collected as an eluate in saline solution. Convenient availability, inexpensive price and favourable half-life have made ^{99m}Tc the workhorse of the nuclear medicine. ^{99m}Tc consists of 70% of use of diagnostic tracers in nuclear medicine in spite of availability of high sensitivity PET technique[185][189][184][182].

8.1.3. Literature review:

1) D. Schmitt et. al. carried out sub-chronic toxicological evaluation for Beta caryophyllene (BCP) oil in rats administered via oral route. The BCP oil was administered at the dose levels from 0 to 700 mg/kg/d and study was carried out for 90 days. The authors reported that BCP oil shows no observable toxic effects pertaining to the general behaviour as well as physiological parameters when administered via oral route. The highest dose administered in the study i.e. 700mg/kg/d was concluded as the dose of no observable side effects in rats of both genders[33].

2)J. Shetty Akhila et. al. gave an overview of various methods and approaches used for undertaking acute toxicity studies. The authors reviewed various aspects such as selection of dose levels, selection of animals, parameters for observation as well as different methods use for calculation of lethal dose. The authors also shed some light upon the changes than could be made in existing methods for better outcomes[171].

3)Alessandra Boschi et.al. reviewed the modern approaches in nuclear imaging methods involving the use of ^{99m}Tc. Authors have given an overview of recent progress the detector technologies of SPECT and PET techniques and the new avenues opening for use of ^{99m}Tcbased radiopharmaceuticals. Authors have also focused on metal fragmentation approach use for ^{99m}Tc labelling of various biomolecules[186].

4) Jyoti Kode et. al. evaluated the anticancer activity of newly synthesized chalcone compounds with the use of in silico models, preclinical studies, and biophysical interactions. The in vitro cytotoxicity of newly synthesized compounds was tested against human oral cancer cell line SCC-29B. The chalcones compounds were also evaluated by in vivo studies inAW13516 oral cancer xenograft model. The mechanism of anticancer action of chalcone compounds was discovered to be disruption of cellular integrity and glucose metabolism. Metabolic reprogramming occurred due to effect on glucose metabolism was evaluated by PET/CT technique using 18F-FDG as radioactive tracer. Based on the results of cytotoxicity assays, in vivo studies, preclinical imaging and molecular docking studies, newly synthesized chalcone compounds were claimed to be the potential candidates for treating cancers by tubulin polymerization inhibition[190].

5) Güliz Ak et al prepared multifunctional nanoconjugate of doxorubicin for treatment of prostate cancer. Authors prepared the conjugate of doxorubicin and folic acid via the linker of PEG. The conjugate was further explored for the radiolabelling process with ^{99m}Tc to carry out biodistribution studies. Real time imaging of administered conjugate showed the greater accumulation of folic acid nanoconjugate of doxorubicin. Authors concluded that folate conjugated doxorubicin demonstrated high potential as site specific anticancer agent and radiopharmaceutical agent for real time drug imaging[191].

8.2. Experimental methodology

8.2.1. Acute Toxicity studies

a) Experimental animals:

Experimental animals consisted of healthy female Swiss Albino mice (25g – 30g), purchased from the Laboratory Animal Centre of Mumbai Veterinary College, Parel. Animals were kept in plastic cages (relative humidity 55 ± 10%, temperature 22 ± 2°C, and 12-h light and dark cycle). Weight of each animal was measured regularly during acclimatisation period. Toxicity of the test compounds was evaluated as per the guidelines by OECD Guideline No. 420. Figure 8.2 depicts the outline of acute toxicity study[192][193][194][176]. Study protocol of acute toxicity was permitted by Institutional Animal Ethics Committee (IAEC) of VES College of Pharmacy (*Protocol number VESCOP/09/2017*).

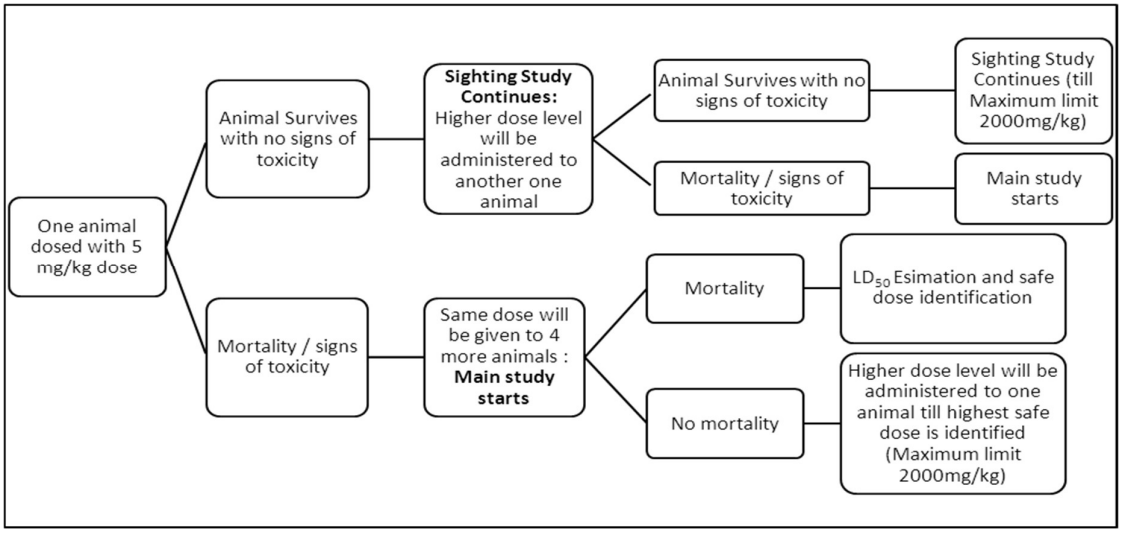


Figure 8.2 Scheme for Acute toxicity study

Figure 8.2 summarises the details of acute toxicity studies.

Table 8.6 Details for Acute toxicity study

Parameter	**Specification**
Species	Female Swiss Albino Mice
Route of administration	Intravenous (intended route of administration for the formulation)

Reference OECD Guideline	420
Interpretation of the Result	Safe dose Estimation
Starting dose	Maximum amount of drug incorporated in formulation; the volume of administration is 75µl
Observations	Body weight measurements Histopathology of organs

b) Study design and dosing:

Formulation loaded with maximum possible dose of BCPO (37.5 mg/kg) was administered to two mice in a single dose via intravenous route by tail vein injection method. Immediately after dosing, animals had free access to food as well as water.

c) Observation of clinical signs and mortality:

Each animal was observed for signs of toxic effects and overall behaviour continuously for 1 hour after intravenous injection. The animals were further kept under observation intermittently for the period of 24 hours. Animals were further observed continuously for the period of 14 days for any signs of toxic effects, behavioural changes and/or latency of death.

d) Body weight measurement:

Weight of each experimental animal was measured with the use of a sensitive weighing balance. Animals were weighed during acclimatisation period, before administration of dose, once a day everyday during the period of observation and also on the day of sacrifice.

e) Histopathological measurement:

After the duration of 14 days, experimental animals were sacrificed by carbon dioxide euthanasia and subjected to complete necropsy. Organs were weighed followed by complete necropsy. All vital organs including kidney and liver were excised and were 10% buffered formalin. To perform histopathologic examination, organs were further immersed in paraffin block and sectioned in ultrathin sections. Sections were further studied under microscope after staining with haematoxylene and eosin.

8.2.2. In vivo biodistribution study

8.2.2.1. Radiolabelling studies of formulation and optimization

a) Radiolabelling of nanosystems:

BC-NLC and FA-BC-NLC were labelled with ^{99m}Tc and subsequently optimised as per the established procedural protocols of Small Animal Imaging Facility of CPCSEA. The nanoparticles were radiolabelled with 99mTc by the method of surface chelation. Briefly, SnCl2 solution was prepared by addition of $SnCl_2$ in 0.1 N HCL (2mg/ml). The formulation (1 ml) to be radiolabeled was added to $SnCl_2$ solution. The resulting solution was filtered through 0.22 um membrane filter into a sterile vial. Further, 1mCi of ^{99m}TcO4 was mixed with Formulation- $SnCl_2$ solution which was incubated at room temperature for 20 minutes[195].

b) Radiochemical purity[195][196][197]***:***

The radiochemical purity efficiency was estimated with use of ascending Thin Layer Radio chromatography (TLRC). To carry our TLRC, silica plates with dimension of 1×10 cm were used as the stationary phase. TLC plates were developed by applying 2-3 µL of radiolabelled sample at the bottom of the plate (approximately 1 cm from bottom). The spot of radiolabelled sample as allowed to air dry and plate was further immersed in mobile phase (100% acetone). At the end of development, the plate was cut into two segments and radioactivity of each part was acquired with the use of an automated well-type gamma ray counter.

Spectrum acquisition and analysis software (SAAS) was used for determination of gamma count. Following equation (16) was used to calculate % Radiolabelling efficiency:

$$\%\, Radiolabeling\ efficiency\ =\ Total\ count\ -\ Free\ count/\ Total\ cont \qquad (16)$$

c) Effect of SnCl2·H2O and incubation time on Radiolabelling efficiency[185][198]

The effects of varying concentrations of $SnCl_2$ on the labelling efficiency of 99mTc-labeled nanoparticles were determined to estimate the optimum conditions required for maximum % radiolabelling. The concentration of $SnCl_2$ was varied from 50ul–250ul (2 mg/mL in 0.1 N HCl). The mixture of nanoparticles and 99mTc was further incubated for up to 20 minutes. The experiment was performed in triplicate and Radiolabelling efficiency was measured using TLC with 100% Acetone as mobile phase as described in 5.2.1. (b).



Figure 8.3 Automated gamma ray counter

d) In vitro stability[195]***:***

The in vitro stability of the 99mTc-labeled nanoparticles was evaluated by using of 0.9% (w/v) saline TLC-SG technique. Briefly, 99mTc-labeled nanoparticles (0.1 mL) were mixed with 0.9% saline and incubated at 37°C for up to 24 hours. Further, sampling was done at0, 1, 3, 6, 8, 12 and 24 hours after incubation. At every time point, the mixture was on run TLC plates with the use of 100% Acetone as mobile phase as described in 5.2.1 (b). The %Radiolabelling stability was evaluated using an automated well-type gamma ray counter.

8.2.2.2. Animal experiments

a) Details of animals:

Biodistribution studies were performed to analyse the distribution of targeted as well as non-targeted formulations on intravenous administration. Female NOD SCID mice, 25–30 g each, with orthotopic tumour model were selected for study. Mice were allowed free access to food and water overnight before experiment [195][186][199][196]. The experiment was permitted by the IAEC of CPCSEA. Before beginning the investigation, the research's strategy had been sanctioned by the institution's IACE (Reg. No. 387/CPCSEA: Dated 03-10-2025).

b) Establishment of orthotopic tumour model:

MDA-MB-468 cells wereinjected orthotopically using insulin syringe in mammary fat pad (10^6 cells/animal, vol<120µl). Incision was made between fourth nipple and midline. Tumor growth was regularly measured by vernier caliper. Animals were injected with formulations to be studied for biodistribution when the tumor reaches 100 mm^3.

c) Administration of targeted and non-targeted formulations:

Experimental mice were distributed into three groups of three mice each. Animals were anesthetised with Isoflurane prior to injection. Each group received 100 uL intravenous injections of 99mTc-labelled nano formulations via tail vein. One group was injected with FA-BC-SLN, second group was injected with BC-SLN and third group was injected with blank vehicle. Table 8.7 summarises the details of groups of formulations and number of animals per group. The animals were sacrificed at preselected time points, i.e., 1 hr, 4 hrs,6 hrs,8 hrs,12 hrs and 24 hrs post injection (p.i.). Blood was collected by retro-orbital puncture in pre-weighted capillary tubes.

Table 8.7 Details groups for Biodistribution study

Sr. No.	**Group**	**No. of Animals**
1.	SLN of BCPO and PUFA with folic acid (Radiolabelled with Technetium-99M*) (FA-BC-NLC)	18
2.	Vehicle Control (Radiolabelled with Technetium-99M)	18
3.	SLN of BCPO+PUFA without Folic acid (Radiolabelled with Technetium-99M) (BC-NLC)	18
Total number of animals = Total no. of groups (3) X no. of animals per group (3) X no. of time points (6) =3 X 3 X 6		**54**

d) Extraction of organs and measurement of radioactivity:

Animals were further dissected and organs of interest namely brain, thyroid, heart, lungs, stomach, intestine, and liver were removed and placed in pre-weighed plastic containers. All organs were washed with saline to remove any adhering mass and weighed. Radioactivity of each organ sample was determined by well-type automatic gamma scintillation counter. For each organ, percentage of injected dose (% ID/organ) was determined considering the blood and muscle constitute 7%and43%of bodyweight, respectively. Further, % ID/organ value for each organ was divided by the weight of corresponding organ to obtain value of %injected dose per gram (% ID/g).

8.2.3. In vivo efficacy study

a) Details of animals:

In vivo efficacy study was undertaken to assess efficacy of developed formulations to treat tumour after intravenous administration. Female NOD SCID mice, 25–30 g each, with orthotopic tumour model were selected for study. Mice had free access to food and water overnight before experiment[190][195][200]. The experiment was permitted by the IAEC of CPCSEA.

b) Establishment of orthotopic tumour model:

To perform in vivo efficacy study, orthotopic tumour model was developed. To obtain donor mice, cryopreserved breast cancer cell lineMDA-MB-468 was passaged. Tumour was induced by subcutaneous implantation of MDA-MB-468 xenograft in flank region of female nude mice. Tumour growth was measured 4 times a week with the aid of digital vernier calliper(Pro-Max, Electronic Digital Calliper, USA)[190][195][200].

c) Administration of dosage forms:

Animals were randomized into six groups of 6 animals each once the tumours achieved the volume of 100 mm^3. Each group received 150 uL injection of respective formulations via tail vein. Formulations used for study included FA-BC-NLC, N3-PUFA NLC, BC-NLC, vehicle control and standard. One group was treated as negative control and was not given any treatment. Adriamycin stock solution was prepared in water (2mg/ml) and was used as standard. Table 8.8 describes the descriptions of groups, details of formulations given to each group, concentration of active ingredient and dosing regimen. Tumour regression was measured over a period of 30 days. On 30^{th} day, animals were weighed, sacrificed and tumour

was isolated. Isolated tumour tissue was weighed and subjected to histopathological studies[190][195][200].

Table 8.8 Experimental details for in vivo efficacy study

Sr. No.	Group	No. of Animals	Dose	Dosing regimen
1.	FA-SLN with BCPO and PUFA	6	4mg/kg	Twice a week
2.	SLN only with PUFA	6	NA	Twice a week
3.	SLN with BCPO and PUFA	6	4mg/kg	Twice a week
4.	Vehicle Control	6	NA	Twice a week
5.	Standard (Adriamycin)	6	2mg/kg	Once a week
6.	Negative Control	6	NA	NA
7.	**Total number of animals = Total no. of groups (7) X no. of animals per group (6) = 6 X 7**	**36**		

d) Measurement of tumour volume (TV):

Efficacy of injected formulations was determined by regular measurement of tumour volume. Other parameters including body weight and mortality were also checked regularly. For better representation of data, parameters namely relative tumour volume (RTV), ratio of test vs control tumour volume, % tumour regression were calculated as per the equations given below (equation (17), (18), (19)):

$$Relative\ Tumor\ Volume\ (RTV) = TV\ on\ day\ of\ measurement / TV\ on\ day\ 1 \quad (17)$$

$$T/C\ ratio = RTV_Test / RTV_Control \quad (18)$$

$$Tumor\ Regression\ \% = \ 100 - [\ T/C * 100] \quad (19)$$

Where, T = mean tumour volume of treatment group

C = mean tumour volume of control group

After end of treatment regimen, animals were sacrificed and important organs including tumour were excised. All tumours and organs were stored in 10% formalin solution for histopathology study.

e) Micro-PET imaging studies:

Three animals from each of the experimental group were analysed by PET imaging. 18F-FDG was used as an imaging tracer for PET study. Animals were fasted overnight before intravenous administration of 18F-FDG.Before imaging process, animals were anesthetized with 3% isoflurane/97% oxygen (v/v) mixture (flow rate 1L/min) for 2-3 min. 18F-FDG (200ul, ~22 MBq/600 µCi) was administered via tail vein injection method. After duration of 1 hour, animals were again anesthetized with isoflurane-oxygen mixture and subjected to PET imaging. After appropriate positioning of animals inside the PET scanner under continuous anaesthesia, each animal was scanned for 20 min. to acquire whole-body images with the use of PET/SPECT/CT tri-modality gamma imaging system. Subsequently, CT-images of whole body of the animals were acquired (energy 40 KeV, magnification 1.3, FOV 91.08, 600 ms and 512 projections). Standard uptake value was measured for tracer and data was analysed with the use of PMOD data analysis and quantitation software [190].

8.2.4. Pharmacokinetic analysis

GCMS method development for plasma Caryophyllene quantification:

Caryophyllene oxide stock solution was prepared in ethyl acetate at 1mg/mL. Rabbit plasma (200 µL) was spiked with Caryophyllene to obtain a plasma concentration of 5-1000 ng/mL. Caryophyllene was extracted with 1000 µL of ethyl acetate and reconstituted in 400 µL of ethyl acetate and used for GCMS quantification. Table 8.9 depicts the instrumental parameters for GCMS method.

Table 8.9 Instrumental parameters for GCMS

Parameter	**Specification**
Instrument	Shimadzu QP2010 plus
Column	Rtx- 5MS (30 meter X 0.25mm, 0.25micron thickness)
GCMS conditions	
Mode	Single ion monitoring (SIM)
m/z	79
Ion source	230 ° C
Interface	250 ° C
Inlet	250 ° C
Column Flow	1ml/min
Column Oven	100° C
Oven ramp	100 ° C hold for 0 min, Ramping: 15 ° C /min to 160 ° C, 30°C /min to 280 ° C
Injection volume	1ul
Mode	Split
Split ratio	1:5

A) Plasma Caryophyllene oxide extraction:

Plasma (100 µL) was vortexed with 500 µL ethyl acetate for 10min and centrifuged at 10000rpm for 10mins.Ethyl acetate extract of plasma was further evaporated to dryness at 40° C in a nitrogen evaporator and reconstituted in 400 µL ethyl acetate and evaluated by GCMS.

8.3. Results and discussion

8.3.1. Acute Toxicity studies

Herbal ingredients, owing to their natural origin are generally regarded as safe for administration in human beings which also leads to the tendency of their self- administration [192][172]. However, there is not enough evidence available in literature elaborating the toxicity of many phytoconstituents. Acute toxicity studies are performed to determine the safe dose for administration via specific route. The studies help in predicting the toxic effects of the drug or phytoconstituents and determination of safe dose for administration in humans.

This study was particularly planned to determine safe dose of BCPO to be administered via intravenous route. LD50 for BCPO is reported to be 5000mg/kg [180]. However, there is reported data available for acute toxicity of BCPO via intravenous route [201]. The guidelines available for acute toxicity dictate the protocol and methods for oral route [174][175]. Acute intravenous toxicity study for BCPO was performed based on the guidelines for oral toxicity study [201][172].

a) Wellness parameters, body weight and mortality:

Animals were administered with 37mg/kg dose of BCPO loaded in formulation via intravenous route. Animals were observed continuously for 14 days. There were no observable changes in physical parameters such as skin and fur, eyes, mucus membrane and behavioural patterns. Also, there were no considerable changes observed in body weights of individual animals. Further, animals showed steady increment in body weight during the period of observation. No mortality was observed at the dose of BCPO injected intravenously [179][193][172].

b) Histopathological measurement:

Microscopic examination of all internal organs revealed no significant changes at injected dose as compared to control. Further, there was no indication of histopathological abnormality in any of the examined organs. Figure 8.4 shows histopathological images of internal organs of experimental animals[202][203].

c) Estimation of safe administrable dose:

The highest dose that could be loaded in formulation was found to be 75mg/20 ml. As per the amount of formulation that can be administered to mice by tail vein injection method, the safe administrable dose was estimated to be 37.5 mg/kg.

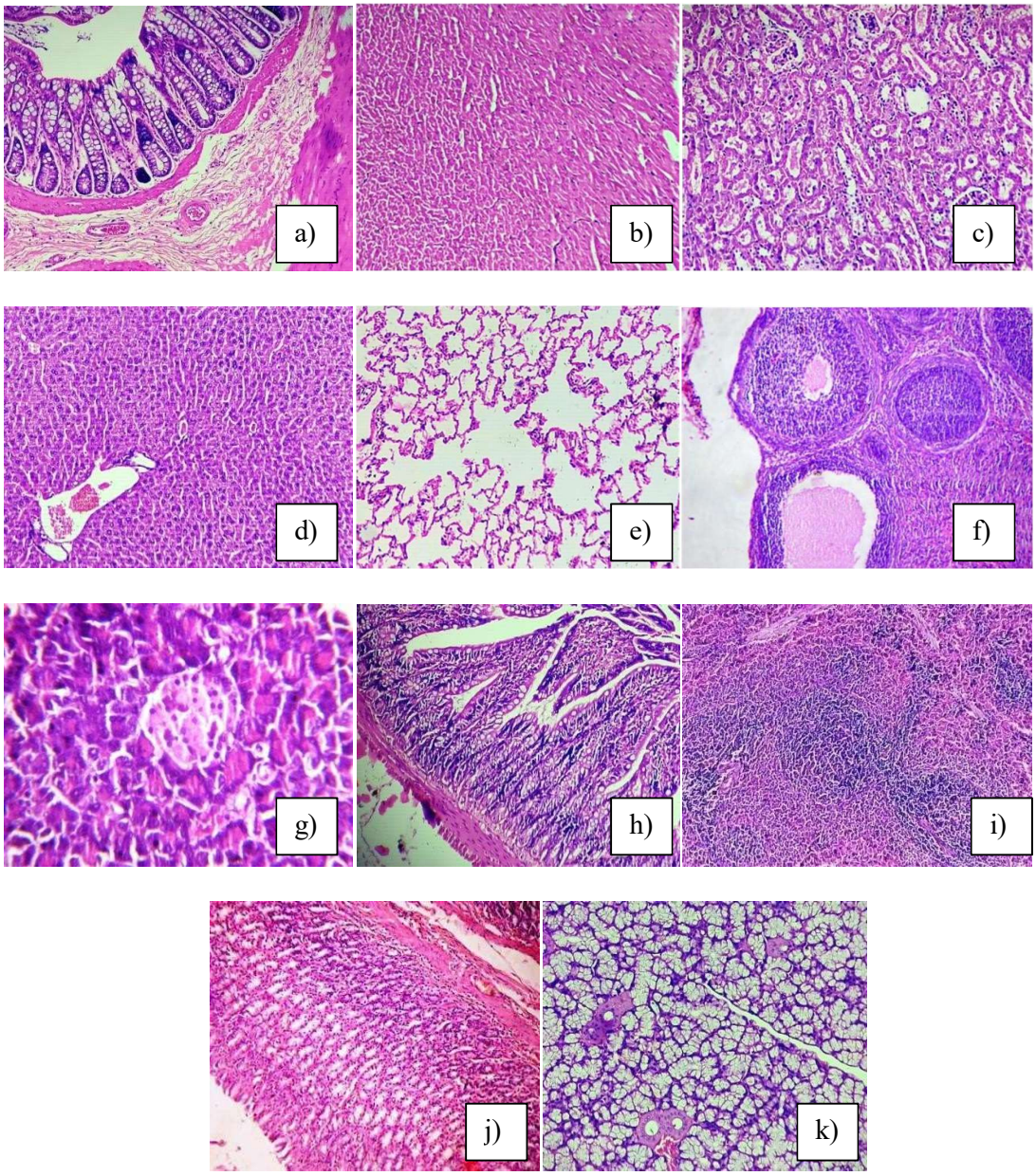


Figure 8.4 Histopathology of internal organs

a) Colon b) Heart c) Kidney d) Liver e) Lung f) Ovary g) Pancreas h) Small intestine i) Spleen j) Stomach k) Sublingual salivary gland

8.3.2. In vivo biodistribution study

8.3.2.1. Radiolabelling studies of formulation and optimization

Developed formulation was radiolabelled with ^{99m}Tc by safe and fast method of direct labelling. ^{99m}Tc is obtained as saline solution in the form of pertechnetate [$^{99m}TcO^-$] from the$_4$generator. The prerequisite for the radiolabelling procedure is reduction of [$^{99m}TcO^-$] to lower$_4$ oxidation state[198][197]. The reduction is brought about by a suitable reducing agent such as Stannous chloride ($SnCl_2$). The redox chemical reaction between [$^{99m}TcO^-$] and Sn^{2+}i$_4$s described as below[198]:

$$Sn^{2+} \longrightarrow Sn^{4+} + 2e^-$$

Reduction of Tc(VII) in [$^{99m}TcO^-_4$] takes place in two steps:

$$Tc(VII) + Sn(II) \longrightarrow Tc(V) + Sn(IV)$$

$$Tc(V) + Sn(II) \longrightarrow Tc(III) + Sn(IV)$$

Lower valence states of ^{99m}Tc form stable complex with the ligand (nanoparticles) in aqueous solution [198]. Further, if there is no ligand present, the reduction process of ^{99m}Tc continues to produce insoluble colloidal technetium oxide $TcO_2.xH_2O$. (Figure 8.5).

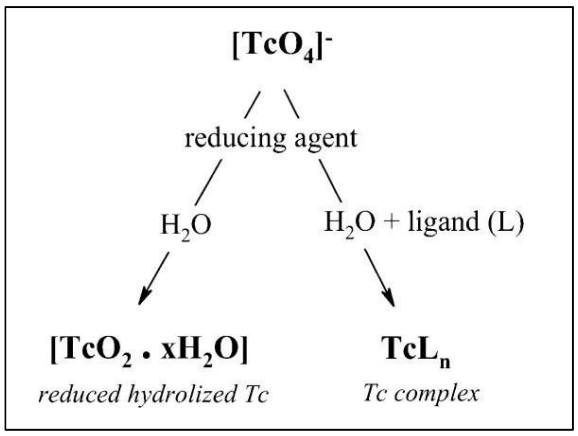


Figure 8.5 Reduction products of Pertechnetate

Colloidal technetium oxide TcO_2 .xH_2O along with free pertechnetate, technetium dioxide appear as impurities during labelling procedure. Thus, generation of these impurities should be carefully controlled with optimised quantity of reducing agent in order to achieve high radiochemical purity (RCP). Insufficient amount of $SnCl_2$will lead to incomplete reduction

process leaving free pertechnetate [$^{99m}TcO^-_4$] as an impurity in solution. On the other hand, excess amount of $SnCl_2$will lead to formation of colloidal technetium oxide TcO_2 .xH_2O[185][204][198][197].

RCP for labelled nanoparticles is measured with the use of rapid method of TLC. The separation of radiolabelled nanoparticles and radiochemical impurities is achieved based on their solubility in mobile phase and affinity for stationary phase. Each radiochemical species travels a specific distance from the point of spotting, this distance is known as relative front (R_f) value[204][197][198].R_f is calculated as per the Equation (20) :

$$Rf = \frac{Distance\ from\ the\ origin\ of\ the\ component}{Distance\ of\ the\ solvent\ front} \quad (20)$$

For a given pure radiochemical compound, R_f value is considered to be specific and reproducible[204][197].Figure 8.6 [204] represents the example for calculation of R_f value.

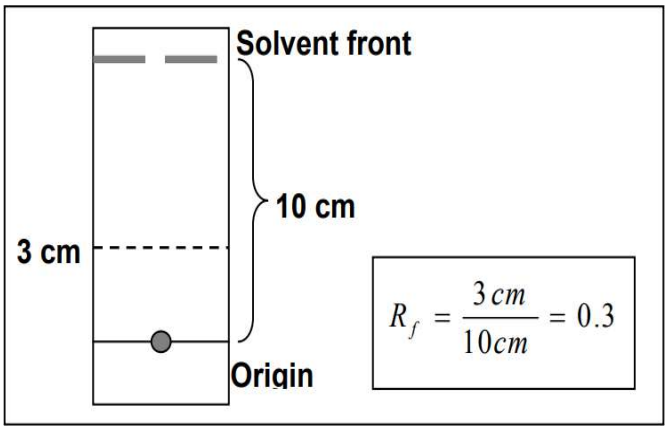


Figure 8.6Representation of calculation of Rf value

Table 8.10 describes the R_f values of ^{99m}Tcradiolabeled species and impurities with acetone and saline as mobile phase[204]. Based upon their solubilities, same radiochemical species possesses different R_f values in different mobile phases.

Table 8.10 R_f values of radiochemical components in acetone and saline mobile phase

Radiochemical Component	R_f values for Acetone	R_f values for Saline
^{99m}Tc-labeled complex	0.0	1.0
$^{99m}TcO_4^-$	1.0	1.0

As per Table 8.10, when acetone is used as mobile phase, radiolabelled compound stays at the origin while soluble impurities such as pertechnetate travel to the solvent front. As represented in Figure 8.7, for measurement of RCP, the TLC strip is cut at specific length as per the respective Rf values of the radiochemical compounds and each part is measured for gamma count in well type gamma counter.

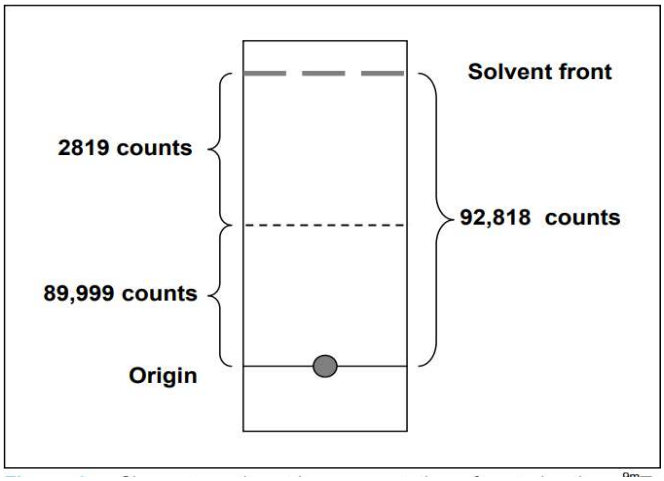


Figure 8.7 Representative gamma count of TLC plate developed in acetone as mobile phase

For the developed formulation, TLC plate was cut at the length of 3 cm from the point of spotting. Two parts of the TLC plate were individually measured for gamma count. Figure 8.8 depicts the images from the software used for measurement of gamma count. As seen in Figure 8.8(a), ^{99m}Tc-labeled complex shows high gamma count whereas count for impurities is low as seen in Figure 8.8(b).

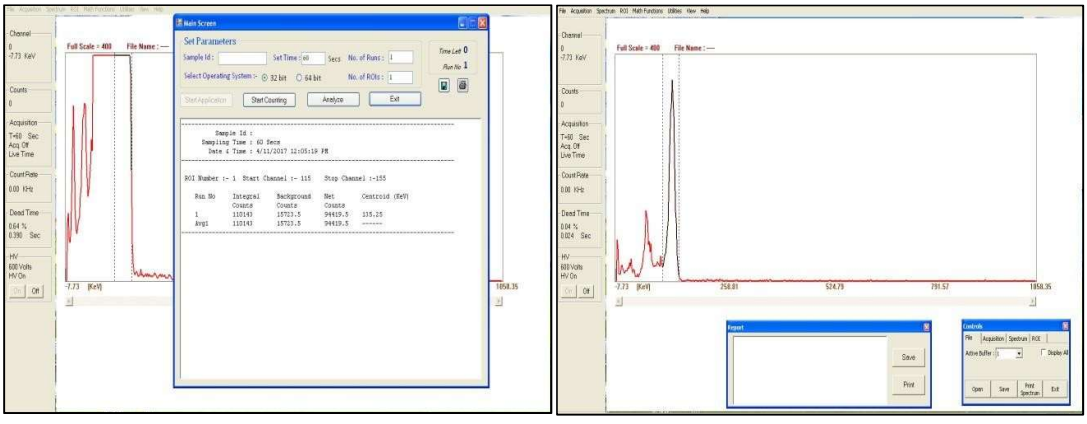


Figure 8.8 Gamma count of TLC plate in Spectrum acquisition and analysis software (SAAS) a) ^{99m}Tc labelled complex b) Pertechnetate ($^{99m}TcO_4^-$) impurity

RCP is calculated in terms of % radiolabelling efficiency with the use of equation (21)

$$\%\ 99mTc - labeled\ complex = \frac{Total\ count - Free\ count}{Free\ count} \quad (21)$$

At 50 ul concentration of $SnCl_2$, RCP was calculated as follows (equation (22)):

$$\%\ 99mTc - labeled\ complex = \frac{33{,}714 - 1218}{34{,}932} X\ 100 = \mathbf{96.5}\ \% \quad (22)$$

It was noted that, as the amount of $SnCl_2$ was increased, there was decrease in % radiolabelling efficiency. As seen in Table 8.11, % radiolabelling efficiency obtained with 50 uL stannous chloride was more than 90%. It is presumed that, above 50 uL of $SnCl_2$, more amount of colloidal technetium oxide $TcO_2 .xH_2O$ was being formed eventually acting as an impurity and thus reducing % radiolabelling efficiency. It is important to obtain high % yield (>90%) for radiopharmaceutical labelling to increase organ specificity as well as to avoid exposure of animals to unnecessarily high dose of radioactive element[184].

Table 8.11Effect of increasing concentration of stannous chloride

Sr no.	Concentration of $SnCl_2$	% Radiolabelling efficiency
1	50 uL	96.4 %
2	100 uL	23.9 %

Stability of the radiolabelled formulation was studies for the period up to 24 hours. The radiolabelled formulation was observed to be stable for the period of 24 hours. Table 8.12 describes the results of effect of time on % radiolabelling efficiency of formulation.

Table 8.12Stability of radiolabelled formulation

Sr No.	Duration	%Radiolabeling efficiency
1	0 Hour	96.5 %
2	1 Hour	97%

3	3 Hour	95 %
4	5 Hour	94%
5	7 Hour	94%
6	24 Hour	96%

8.3.2.2. Animal experiments

Biodistribution studies with 99mTc labelled formulations were conducted in Female NOD SCID tumour bearing mice as described in experimental methods. Tumour bearing mice were selected considering the role of over expressed folic acid receptors in tumour in biodistribution of targeted and non-targeted formulations. Figure 8.9 (a) represents the female NOD SCID mice with orthotopically induced tumour. Animals were anesthetized and radiolabelled formulations were carefully administered intravenously via tail vein while still maintaining the anaesthesia as depicted in Figure 8.9 (b).



Figure 8.9 a) Female NOD SCID mice with orthotopic tumour model b) Administration of radiolabelled formulation to experimental animals

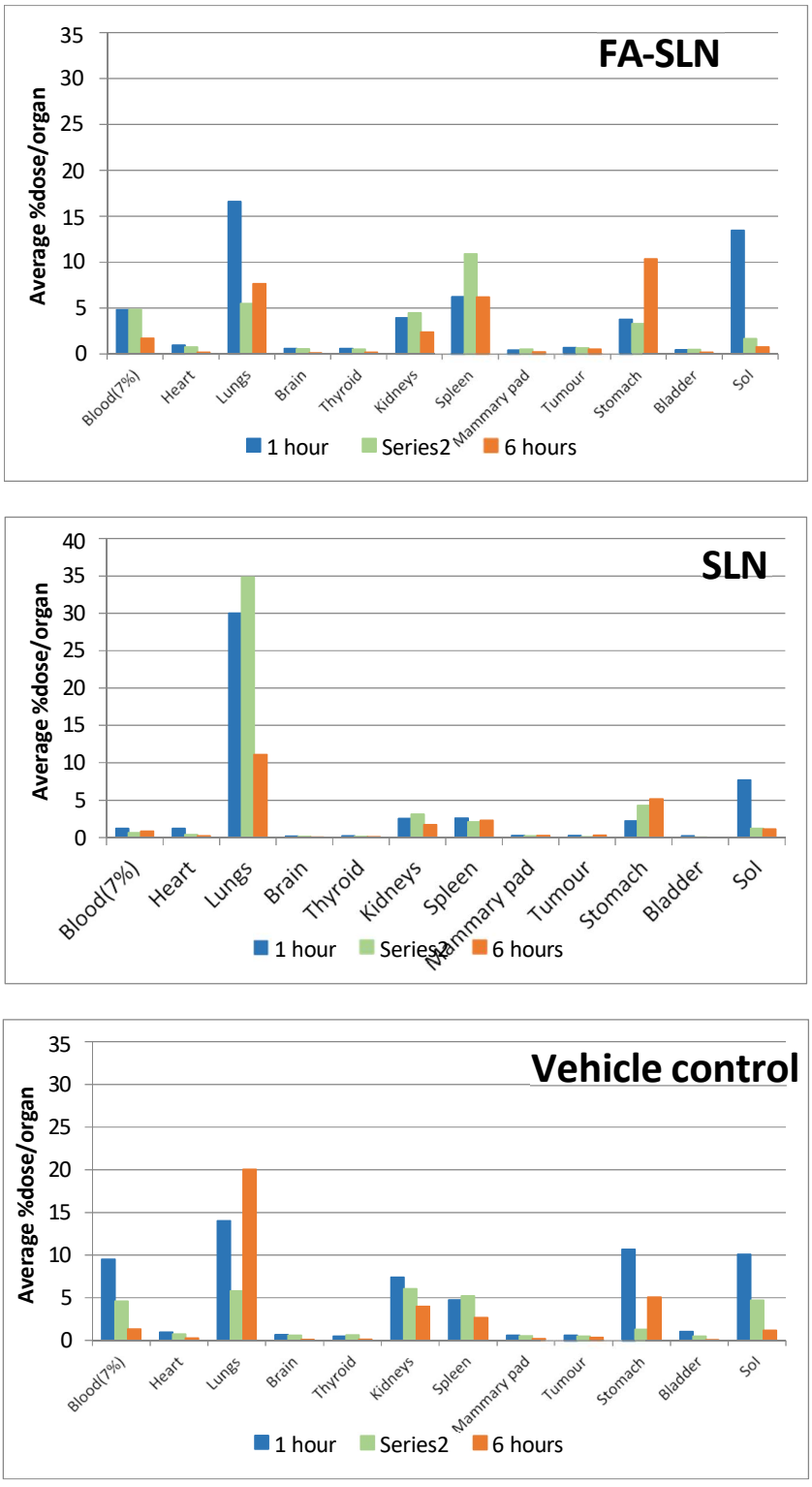


Figure 8.10 Biodistribution of radiolabelled formulations in various organs a) FA-SLN b) Vehicle control c) SLN

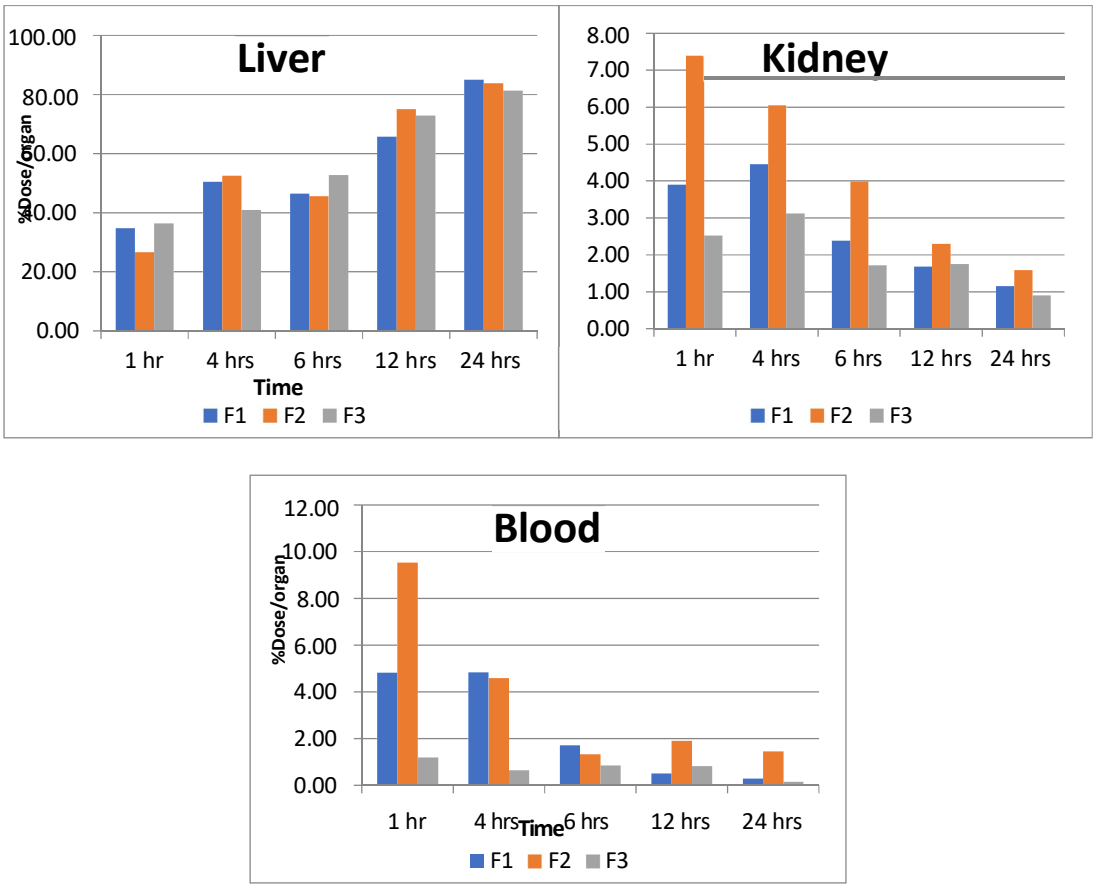


Figure 8.11 Biodistribution pattern of radiolabelled formulations in a) Liver b) Kidney c) Blood

The radioactivity profile of Folic acid targeted SLN, non-targeted SLN and vehicle control administered via i.v route in tumour as a target organ as well as in other organs is depicted in Figure 8.10, Figure 8.11 and Figure 8.12. Gross look at the data shows the accumulation of nanoparticles in targeted tumour as well as in organs of reticuloendothelial system (RES). However, closer analysis shows considerable differences in biodistribution pattern of targeted and non-targeted nanoparticles. In all organs except liver, uptake was observed to be gradually decreasing with time. As seen in Figure 8.10 (b), uptake of non-targeted formulation was observed to be higher most in organs such as liver (36.43% D/O), lungs (30.03% D/O) followed by kidney (2.5% D/O), spleen (2.58% D/O) and stomach (2.19% D/O) at the end of 1 hour after injection. Uptake was found to be decreasing with time in other organs except liver where the maximum uptake as obtained at the end of 24 hours.

Table 8.13 %Dose/organ for radiolabelled formulations in tumour

Formulation description	Formulation code	Time (Hours)				
		1 hr	4 hrs	6 hrs	12 hrs	24 hrs
Targeted formulation	F1	0.69	0.61	0.50	0.42	0.25
Vehicle control	F2	0.62	0.51	0.28	0.07	0.06
Non-targeted formulation	F3	0.25	0.12	0.29	0.09	0.09

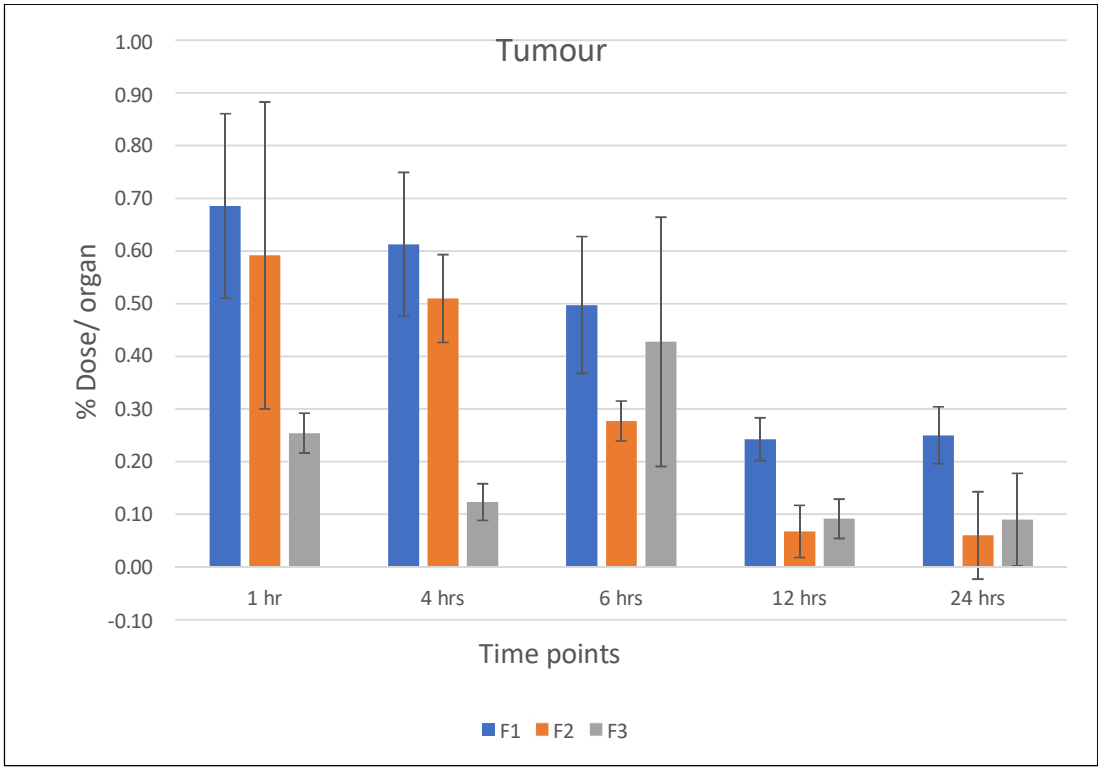


Figure 8.12 Biodistribution of radiolabelled formulations in tumour over a period of 24 hours

Corresponding values for folic acid targeted formulation were found to be higher in organs such as liver (34.76% D/O), lungs (16.5% D/O), kidney (3.9% D/O) and spleen (6.2% D/O). The results were found to be in correlation with the reported literature regarding expression of

folic acid receptors in different organs[48]. Folic acid receptors are found in organs such as liver, kidney and spleen where uptake of targeted formulation is observed to be greater than the non-targeted formulation. Folic acid receptors are expressed to lesser extent in lungs which explains the lesser uptake of targeted formulation in lungs than non-targeted formulation (Figure 8.10 (a and b)). As per the research work by Harish Pawar et. al., high uptake of non-targeted formulation in lungs can be accredited to mononuclear phagocytosis system (MPS) that is present in lungs[134].

Considerable amount of literature states the fact that cancer cells require higher amounts of folic acid along with other nutrients due to their rapid rate of cell division. Cancer cells show over expression of folic acid receptors on their cell membranes in order to acquire more amount of folic acid to meet the need of DNA synthesis of rapidly dividing cells[135][49]. Active targeting strategy using folic acid as a ligand takes advantage of over expressed folic acid receptors on cancer cells. Various drug delivery systems have been functionalised by conjugation with folic acid for increased uptake in cancer cells. Harish Pawar et. al., functionalised docetaxel and curcumin solid lipid nanoparticles with folic acid. Functionalised nanoparticles were found to be showing enhanced efficacy and potential towards breast cancer therapy[134]. In research work undertaken by Hong Yuan et. al., paclitaxel SLN were functionalised with PEG as well as folic acid. The modified nanoparticles were observed to be showing improved uptake in A549 cancer cells [135]. In current study, SLN system was functionalised with folic acid by chemical conjugation method. As seen in Figure 8.12, uptake of folic acid targeted formulation was found to be highest at the end of 1 hour. Further, uptake of targeted formulation was found to be decreasing with time, however, the relative uptake of targeted formulation was higher than non-targeted formulation at all time points. Table 8.13 enlists %dose/ organ for targeted formulation, non-targeted formulation and vehicle control at all time points. The results are clearly indicative of significantly higher accumulation of folic acid targeted formulation in tumour.

Overall, the results are suggestive of increased uptake of folic acid conjugated SLN system in tumour cells thus proving the efficiency of folic acid as ligand. Folate targeting also led to reduced accumulation of formulation in non-targeted organs such as lungs. High uptake of formulations in liver is presumed to be due to metabolism of folic acid and its derivatives. Ability of ^{99m}Tc to efficiently bind to nanoparticles and remain stable in bound state adds more flexibility to the detection of biodistribution of formulations[199].

8.3.3. In vivo efficacy studies

In vivo antitumour efficacy of developed formulations was evaluated in xenograft carcinoma model. Safety of maximum possible administrable dose was previously determined with acute toxicity study. As per the results of acute toxicity studies, 37.5mg/kg dose of BCPO was determined to be maximum possible dose loaded in developed formulation that was safe for intravenous administration. The dosing protocol for BCPO formulations was designed on the basis of results of acute toxicity studies and in vitro cytotoxicity studies. BCPO formulations were administered at the dose of 4mg/kg twice a week. Adriamycin was used as standard in the study and the dosing protocol for the same was 2mg/kg once a week. Sterile water was used as a vehicle for intravenous administration of all the formulations. Subsequent to the intravenous administration, animals were assessed for any signs if toxicity or mortality, body weight and tumour volume at regular intervals for the treatment duration.

Table 8.14T/C ratio of Adriamycin, FA-BC-SLN and n-3PUFA-SLN

Days	**T/C ratio**		
	Adriamycin	**FA-BC-SLN**	**n-3 PUFA**
1	1	1	1
7	0.7877271	0.753931	1.0268339
10	0.7735179	0.807491	1.0927572
13	0.5642253	0.470891	0.787952
16	0.6112085	0.34761	0.908149
20	**0.3644311**	0.294365	0.6653565
23	0.6455623	0.259873	1.3249371
27	0.5036387	0.242819	1.3755054
30	**0.634259**	**0.376282**	1.3450813

Table 8.14depicts the comparative T/C ratio for adriamycin, FA-BC-SLN and PUFA-SLN treated groups. As per the guidelines by NCI, the biological activity is considered significant

if the T/C ratio is ≤ 0.42[205][190]. As it can be observed in Table 8.14, FA-BC-NLC showed significant tumour reduction by the 16th day. T/C value for FA-BC-NLC remained low during subsequent measurements with a slight increase in the value on day 30. The increase in T/C value for FA-BC-NLC treated group on day 30 may indicate need for increase in the dosing frequency at the end of 30 days. On the contrary, T/C value for adriamycin is found low indicating significant tumour reduction by the 20th day. However, T/C value for adriamycin goes on increasing after day 20. Inconsistent and increasing T/C value can be attributed to lower dosing frequency of adriamycin. It signifies the need of higher dosing frequency of adriamycin beyond day 20. T/C value for n-3-PUFA-SLN is found to be lowering till 20th day of the treatment. However, there is no significant tumour reduction observed in PUFA-SLN treated group. Further, T/C value is found to be increasing beyond day 20 indicating the need for higher dose or increased dosing frequency[206][155].

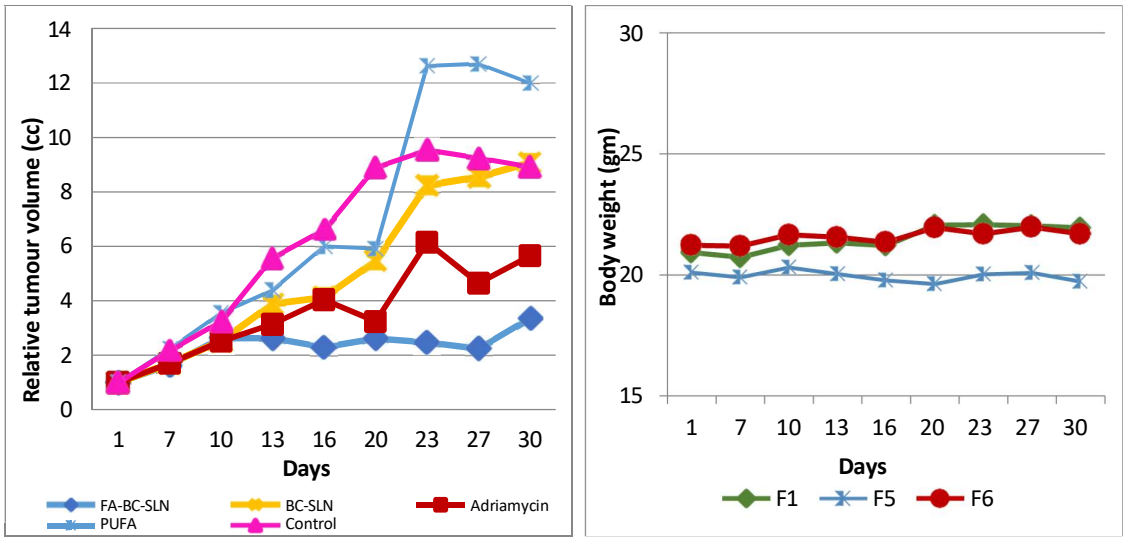


Figure 8.13 a) Relative tumour volume b) Animal body weight

Similar trends of tumour reduction can be observed in Figure 8.13. Figure 8.13 (a) depicts relative tumour volumes of treated groups. Relative tumour volume (RTV) is calculated as ratio of the volume of tumour on day of measurement and volume of tumour on day 1. Thus, RTV depicts relative increase in tumour volume from the initiation of the treatment. RTV of treatment groups are compared with RTV of control group in Figure 8.13 (a). It can be observed that, RTV of FA-BC-SLN is lower than RTV of control as well as RTV of adriamycin. FA-BC-SLN is thus found to be arresting the tumour growth over the period of 30 days. RTV of adriamycin is observed to be increasing after 20th day indicating the necessity of increasing the dosing frequency after day 20. RTV of FA-BC-SLN is also found to be lower than RTV of BC-

SLN indicating the higher effectivity of targeted formulation. RTV of PUFA-SLN is observed to be lower than control. However, it increases beyond the RTV of control after 20th day, suggesting the need of increasing the dosage of n-3 PUFA beyond day 20 of treatment. Further, as seen in Figure 8.13(b), there is no detectable decrease in body weight of treated animals. These results corroborate with the results of acute toxicity studies indicating no toxicity of BCPO formulations in experimental animals[206][207].

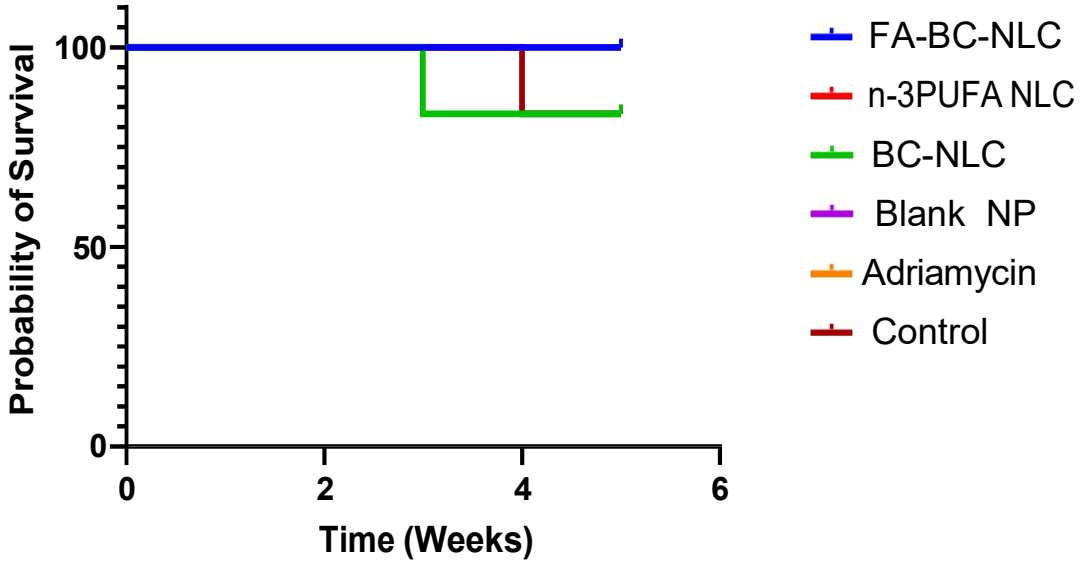


Figure 8.14 Survival curve

Figure 8.14 represents survival curve for in vivo efficacy studies. As seen in Figure 8.14**Error! Reference source not found.**, animals in groups of FA-BC-NLC, n-3 PUFA NLC, BC-NLC and Adriamycin showed 100% survival at the end of treatment regimen. Animals in groups of control and blank nanoparticles (blank NP) showed 83.33% survival by the end of week 4 of the treatment regimen. The reason for lower survival percent in control and blank NP group can be attributed to continuously increasing tumour volume.

Figure 8.15 demonstrates the comparison of tumour volumes representing each treatment group over the course of the treatment regimen. Similar pattern is observed for adriamycin treated group (F5), however the mean tumour volume for FA-BC-NLC treated group is observed to be lesser. n-3 PUFA-NLC (F2) and non-targeted BC-NLC (F3) also demonstrate tumour growth arrest as compared to control (F6) thus corroborating the cytotoxic activity of both n-3PUFA

and BCPO. Vehicle control (F4) shows increase in tumour volume. Table 8.15 depicts the images of excised tumours for each treatment group.

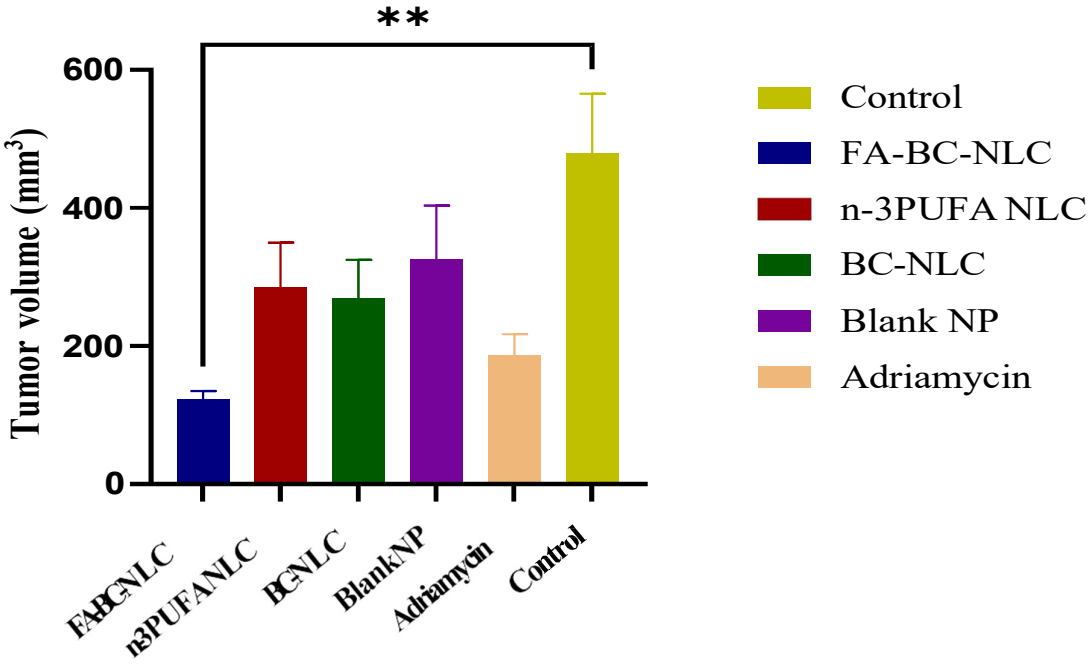


Figure 8.15 Comparison of tumour volume of all groups

Table 8.15 Tumour images for each formulation group

Formulation codes	F1	F2	F3	F4	F5	F6
Representative tumour images						

In vivo efficacy studies thus demonstrate the efficiency of targeted drug delivery system of BCPO as anticancer formulation. FA-BC-NLC is found to showing greater arrest in tumour growth as compared to the standard anticancer agent (adriamycin). Higher cytotoxic activity of FA-BC-NLC than BC-NLC is attributed to its site-specificity imparted by conjugation with folic acid.

FA-BC-NLC system is thus found to an efficient delivery system for intravenous administration of an herbal principle, BCPO for treatment of breast cancer in *in vivo* tumour orthotopic models.

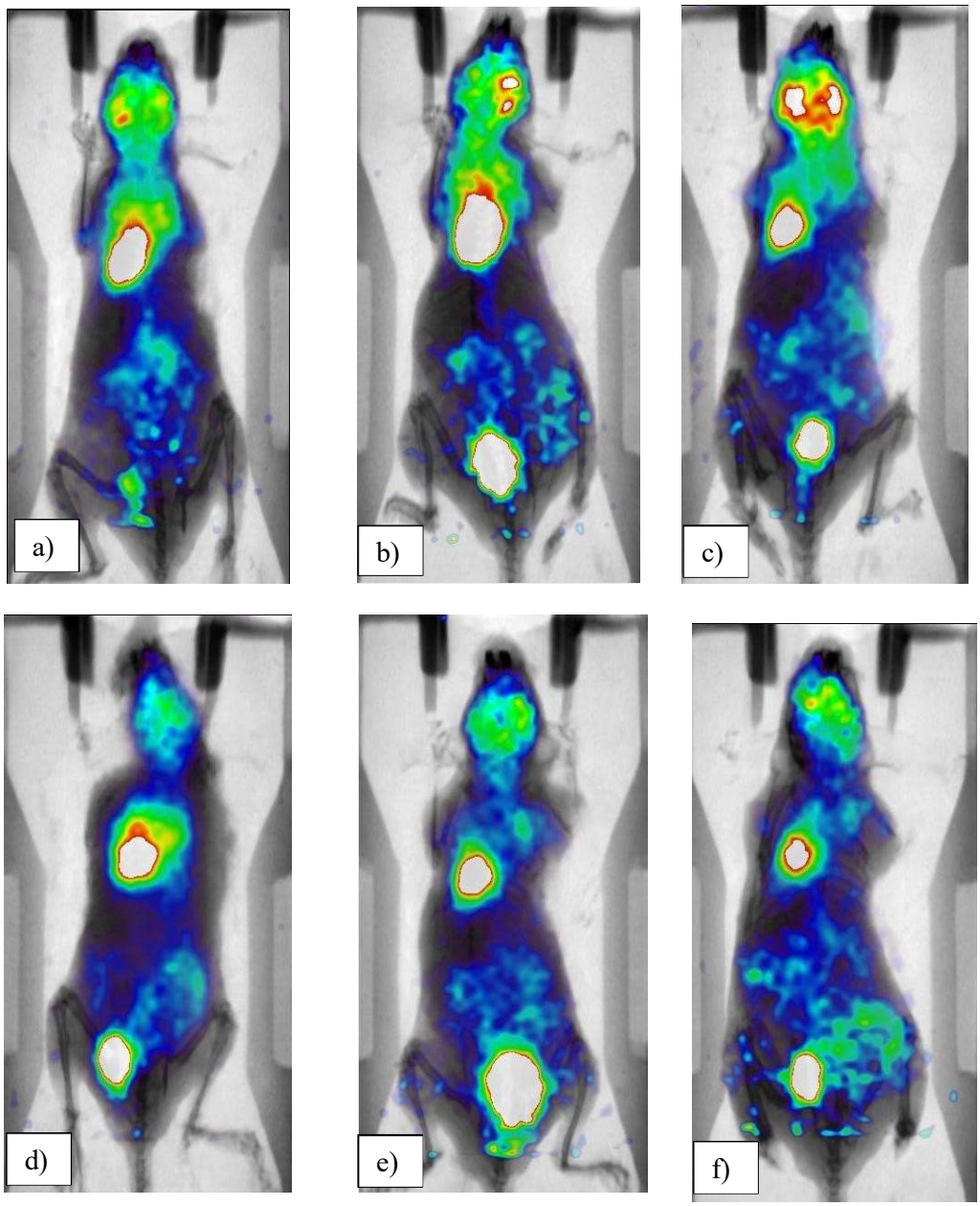


Figure 8.16 PET scans of tumour bearing animals for treatment groups of a) FA-BC-NLC, b) n-3 PUFA NLC, c) BC-NLC, d) Blank NP, e) Adriamycin f) Control

8.3.4. Pharmacokinetic analysis

A) Development of GC-MS method for analysis of BCPO:

GCMS Plasma Caryophyllene response was monitored for ions 79, 91 and 93. Maximum area was obtained for ion 79 and area response obtained for 79ion was used for quantification of Caryophyllene. The area response was linear for Caryophyllene plasma concentration at 5-1000ng/ml. Regression equation obtained for plasma caryophyllene content of 5-500ng/mL with 1/X weighing, Y=183.4x + 335.6 was used for quantification of Caryophyllene in plasma samples. Limit of detection was found to be 5ng/ml whereas limit of quantification was found to be 10ng/mL. Table 8.16 depicts the summary of calibrants and QC responses of BCPO analysis.

Table 8.16Summary of calibrants and QC response of Caryophyllene analysis

Caryophyllene Content (ng/mL)	Retention time (min)	Area	Calculated conc. (ng/mL)	Accuracy (%)
5	6.792	973	3.48	69.51
10	6.796	2075	9.48	94.84
31.25	6.794	7410	38.57	123.44
62.5	6.794	13134	69.78	111.65
125	6.794	24054	129.33	103.46
250	6.795	46530	251.88	100.75
500	6.795	88557	481.03	96.21
1000	6.795	169614	923.00	92.30
50	6.79	10757	56.82	113.65
500	6.794	100789	547.73	109.55

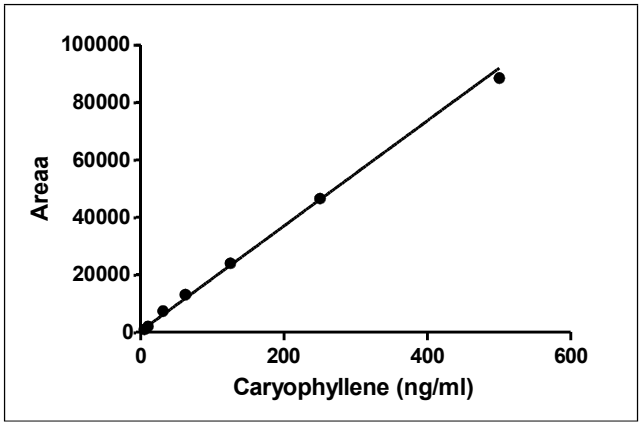
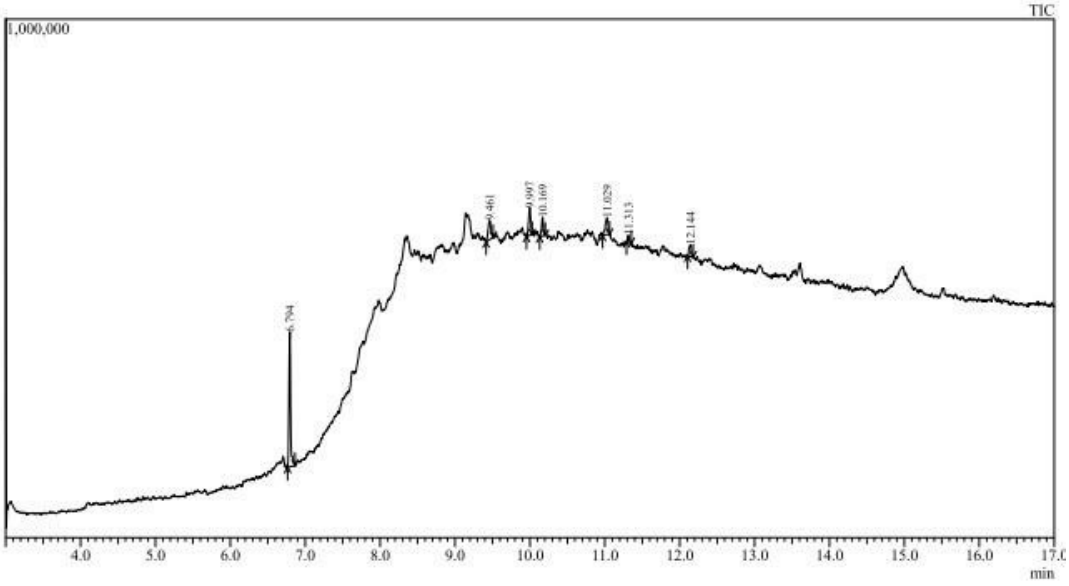


Figure 8.17 Linearity graph

Analyzed by	: SJ
Analyzed by	: 13/04/2022 01:26:15
Sample Name	: Standard
Sample ID	: Standard
Vial #	: 03
Injection volume	: 1.00
Data File	: F:\2022\Section-2\220414\std 10ppm
Method File	: F:\Methods\Caryophyllene-SIM.qgm
Tuning File	: F:\2022\Tuning File\HS-DID GAS OFF-220414.qgt



Peak Report TIC

Peak#	R.Time	I.Time	F.Time	Area	Area%	Height	Name
1	6.794	6.765	6.865	385697	48.74	257084	Caryophyllene oxide
2	9.461	9.415	9.510	99401	12.56	37014	Cyclononasiloxane, octadecamethyl-
3	9.997	9.955	10.030	102680	12.98	51849	Bis[di(trimethylsiloxy)phenylsiloxy]trimethylsiloxyphenylsiloxane
4	10.169	10.130	10.205	62312	7.87	35926	Cyclononasiloxane, octadecamethyl-
5	11.029	10.970	11.065	77432	9.79	32388	Tetracosamethyl-cyclododecasiloxane
6	11.313	11.290	11.355	17859	2.26	13941	Bis(2-ethylhexyl) phthalate
7	12.144	12.105	12.180	45907	5.80	23011	Cyclononasiloxane, octadecamethyl-
				791288	100.00	451213	

Figure 8.18 GCMS chromatogram of Caryophyllene standard

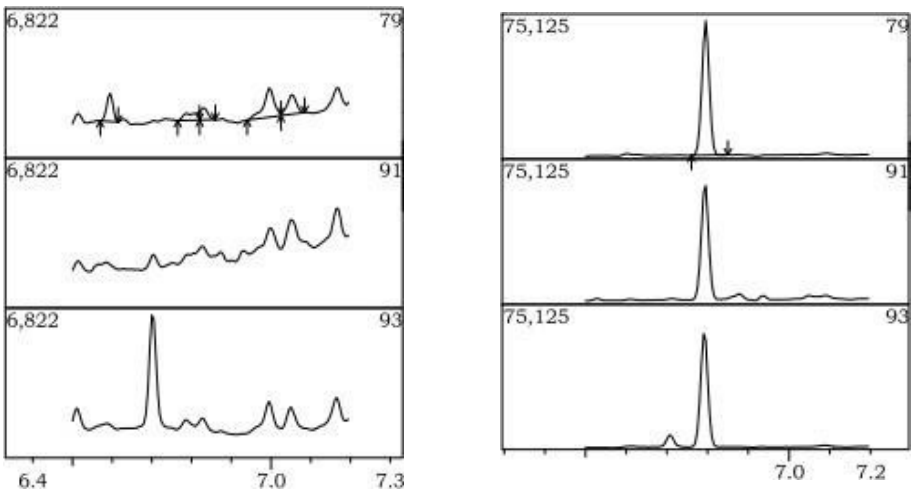


Figure 8.19 Chromatogram of plasma Blank and 500ppb standard

Table 8.17 Quantitative results of GC-MS method development

Peak#	ID#	R. Time	m/z	Area	Height	Name
1	1	6.795	79.00	88557	69551	Caryophyllene oxide

B) Development of pharmacokinetic profile:

Targeted BC-NLC formulation was designed to selectively target tumour cells in body without causing off-target toxicity upon intravenous administration. Pharmacokinetic profile of BC-NLC was developed over the time period of 24 hours and was compared with BCPO solution. Table 8.18 and

Table 8.19 summarize the plasma concentrations of BCPO and BC-NLC respectively. Figure 8.20 depicts the plasma concentration time profile of BCPO and BCPO-SLN. Highest concentration (Cmax) and the time at which peak concentration is reached (Tmax) were determined from pharmacokinetic profile. Pharmacokinetic parameters of both BCPO and BC-NLC are depicted in Table 8.20.

Table 8.18Summary of Plasma Caryophyllene concentration in BCPO

Group time	Animal number	Retention time	Area	Caryophyllene (ng/mL)	Mean	SD
A_0.5	1	6.794	9473	99.64		
	2	6.793	8504	89.08	90.26	8.85
	3	6.792	7861	82.07		
A_1	1	6.788	6916	71.76		
	2	6.789	6116	63.04	63.25	8.41
	3	6.788	5374	54.94		
A_2	1	6.788	5120	52.17		
	2	6.788	4932	50.12	51.12	1.03
	3	6.799	5018	51.06		
A_4	1	6.789	4740	48.03		
	2	6.789	4332	43.58	46.03	2.26
	3	6.788	4598	46.48		
A_6	1	6.795	4398	44.30		
	2	6.789	3305	32.38	38.59	5.98
	3	6.793	3921	39.10		
A_8	1	6.788	3979	39.73		
	2	6.883	2433	22.87	32.96	8.91
	3	6.787	3663	36.29		
A_12	1	-	-	0.00		
	2	-	-	0.00	0.00	0.00
	3	-	-	0.00		
A_24	1	-	-	0.00		
	2	-	-	0.00	0.00	0.00
	3	-	-	0.00		

Table 8.19Summary of Plasma Caryophyllene concentration in BC-NLC

Group time	Animal number	Retention time	Area	Caryophyllene (ng/mL)	Mean	SD
	1	6.793	8269	86.515		
B_0.5	2	6.794	9474	99.655	95.206	7.528
	3	6.795	9455	99.448		
	1	6.787	5328	54.443		
B_1	2	6.790	5318	54.334	54.563	0.307
	3	6.789	5371	54.912		
	1	6.795	4035	40.342		
B_2	2	6.796	3742	37.147	40.092	2.827
	3	6.797	4259	42.785		
	1	6.797	2513	23.745		
B_4	2	6.794	2216	20.506	24.381	4.229
	3	6.798	2985	28.892		
	1	-	-			
B_6	2	6.793	1063	7.932	10.026	2.961
	3	6.735	1447	12.120		
	1	-	-	0.00		
B_8	2	-	-	0.00	0.00	0.00
	3	-	-	0.00		
	1	-	-	0.00		
B_12	2	-	-	0.00	0.00	0.00
	3	-	-	0.00		
	1	-	-	0.00		
B_24	2	-	-	0.00	0.00	0.00
	3	-	-	0.00		

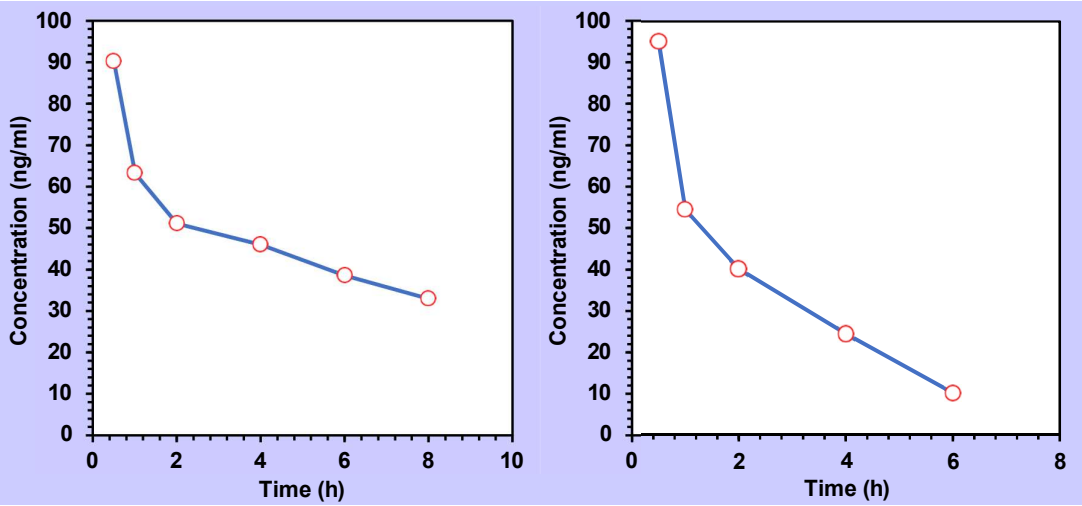


Figure 8.20 Pharmacokinetic analysis of plasma a) BCPO b) BC-NLC

Table 8.20 Pharmacokinetic parameters of BCPO and BC-NLC

Parameters	**Unit**	**BCPO**	**BCPO SLN**
$t_{1/2}$	h	8.303	2.096
T_{max}	h	0.500	0.500
C_{max}	ng/ml	90.262	95.206
AUC 0-t	ng/ml*h	371.461	207.451
AUC 0-inf_obs	ng/ml*h	766.318	237.768

As seen in Figure 8.20, BCPO is found to be detectable in blood for up to 8 hours whereas BC-NLC is detectable in blood for 6 hours. As depicted in Table 8.20, $t_{½}$ of BCPO is nearly 4-fold higher that BC-NLC indicating longer circulation of BCPO in blood as compared to BCPO-SLN. Further, AUC 0-t of BCPO is nearly 1.7 folds higher than BC-NLC. The results are indicative of shorter circulation half-life of BC-NLC than BCPO. The BC-NLC formulation is developed in order to build up at the target site on account of its smaller particle size and incorporation of ligand. The results are thus found to be in agreement with the results of biodistribution studies. Shorter plasma half-life of BC-NLC indicates the accumulation of BC-NLC at the target site. BC-NLC is shown to be getting eliminated from blood circulation after 6 hours. These results can be correlated with Figure 8.11, where increase in concentration in other organs is observed after 6 hours. Further, concentration in blood is shown to be decreasing

after 6 hours. This study reveals that incorporation of BCPO in targeted lipidic nanoparticulate system helps in accumulation of BCPO at target site and also in minimizing the off-target toxicity.

8.3.5. Summary of in vivo studies:

The findings of in vivo studies are summarised as below:

- Safe dose of BCPO for administration via intravenous route was established by acute toxicity studies. The dose of 37.5 mg/kg was the highest dose loaded in optimized formulation and was observed to be safe for administration via intravenous route.
- Biodistribution studies were undertaken to determine the in vivo fate of developed formulation upon intravenous administration. Prior to biodistribution studies, the nanoparticles were tagged with radioactive tracer ^{99m}Tc. Radiolabelled nanoparticles were further administered intravenously to assess the distribution of targeted and non-targeted formulations in tumour bearing mice. The tumour distribution of FA-BC-NLC was observed to be greater as compared to non-targeted formulation.
- In vivo efficacy studies were undertaken to determine potential of FA-BC-SLN to arrest the growth of tumour. FA-BC-NLC was found to be showing greater efficacy to arrest tumour growth in comparison with other experimental groups. Efficacy of FA-BC-NLC was even higher than standard anticancer agent Adriamycin. T/C ratio for FA-BC-NLC was observed to be 0.37 against T/C of 0.63 for Adriamycin.
- Pharmacokinetic study was conducted to establish the *in vivo* fate of drug and formulation upon intravenous administration. Half-life of BCPO was found to 4-folds higher and AUC_{0-t} was found to be 1.7-folds higher than FA-BC-NLC. Relatively shorter half-life and $AUC_{0-t}$for FA-BC-NLC can be attributed to its higher distribution at tumour site owing to small particle size and EPR effect.

Chapter 9

Summary and conclusions

Chapter 9 Summary and conclusions

9.1. Summary of the findings:

Findings of the research work can be summarised as follows:

1) Pre-formulation and Formulation development:

High affinity for lipid phase and low solubility in solubiliser suggested that a stable drug delivery system can be designed with very low chances of drug leaching. Solid Lipid Nanoparticulate (SLN) carrier system was developed for BCPO (BC-SLN) by Hot melt emulsification method with the use of Compritol 888 ATO as solid lipid and Gelucire 50/13 as surfactant. Probe sonication was found to be the most suitable method for particle size reduction of developed SLN system. Incorporation of functional excipient n-3 PUFA (BC- NLC) is found to further aid in particle size reduction. Developed formulation showed the particle size of 176 nm with PDI 0.4. %EE of formulation was observed to be 44%.

2) Conjugation of Folic acid-Stearic acid and incorporation of conjugate in formulation:

Conjugation reaction between Folic acid and Stearic acid led to formation of a solid conjugation product. Developed conjugate was further incorporated in formulation as a part of Lipid phase to develop FA-BC-NLC. Incorporation of increasing amount of Folic acid-Stearic acid conjugate resulted in decrease in the particle size.

3) Optimization and evaluation of developed lipidic nanocarrier system:

BC-SLN and BC-NLC systems were optimized with the use of Factorial design based on parameters such as particle size, PDI and % entrapment efficiency. The final formulation of FA-BC-NLC was further evaluated based on particle size and surface morphology, % drug loading and entrapment efficiency, in vitro drug release and in vitro haemolysis study. FA-BC-NLC showed spherical shape and particle size below 200nm as confirmed from results of zeta sizer, SEM and TEM. SLN showed drug release of around 9 % in 24 hours. NLC showed the similar effect of low drug release (around 17%) in blood pH of 7.4 thus indicating protection of drug. Plain Drug is released to the extent of 60 % in 10 hours. These results indicate that the developed lipidic nanocarriers (SLN and NLC) show protective effect on drug preventing its premature release during circulation in blood. The nanoparticles were also proven to be non-toxic for intravenous administration as shown by low % haemolysis value of 5.4%.

4) *In vitro* cytotoxicity and *in vivo* studies:

In vitro cytotoxicity studies highlighted that, drug (BCPO) and n-3 PUFA have enhanced cytotoxicity when used in combination against both MCF-7 and MDA-MB-468 breast cancer cell lines. For the purpose of Biodistribution studies, formulation was radiolabelled with Technetium-99m (^{99m}Tc) showing binding efficiency of 96%. Radiolabelled formulation was also found to be stable for up to 24 hours. Biodistribution studies proved better site specificity of targeted formulation showing higher build-up of targeted formulation in tumour. In *in vivo* efficacy studies, anticancer potential of FA-BC-NLC was shown to be greater as compared to non-targeted BC-NLC. Targeted formulation showed better tumour regression as compared to non-targeted BC-NLC formulation and equivalent tumour regression as compared to standard anticancer agent Adriamycin. Better anticancer activity can be attributed to anticancer potential of herbal principal BCPO, synergistic action of BCPO and n-3 PUFA and site specificity imparted by Folic acid.

9.2. Conclusion

A holistic targeted lipid based nanocarrier system was developed for delivery of BCPO as an anticancer agent for treatment of triple negative breast cancer.

BCPO, an herbal agent used for flavouring and cosmetic purposes, was explored for its anticancer potential to treat triple negative breast cancer. Owing to its cosmetic and favouring uses, there is very limited literature available describing the pharmacological actions and potentials of BCPO. The current research work was focused on first hand establishment of analytical procedures, toxicity protocols and pharmacokinetic profile of BCPO. Analytical method was developed as well as validated for accurate quantification of BCPO. Further, BCPO was exposed to forced degradation studies to acquire an understanding of degradation conditions for BCPO. The cytotoxicity of BCPO was established against breast cancer cell line MCF-7 as well as against triple negative breast cancer cell line MDA-MB-468. The acute toxicity study protocol developed for intravenous administration was first of its kind for BCPO. BCPO was found to be non-toxic for intravenous administration for doses used in formulation.

n-3 PUFA, commonly used fish oil constituent, has proven nutritive and cytotoxic effects as per the literature review. In current research, n-3 PUFA was explored as liquid lipidic excipient for lipid based nanocarrier system. n-3 PUFA was proven to be enhancing the cell permeation of BCPO and showing synergistic effects in combinations with BCPO in *in vitro* cell line studies. Addition of n-3 PUFA in lipidic nanocarrier system of BCPO eventually converted the

system from SLN to NLC. NLC system showed lesser particle size and improved drug loading capacity further adding the edge to the lipid carrier system of BCPO. Thus, the current research work established n-3 PUFA as effective functional excipient for delivery of BCPO.

Lipophilic nature of BCPO represented it as an ideal candidate for lipidic nanocarrier systems. Under current research work, SLN and NLC systems were successfully developed and optimized for intravenous delivery of BCPO. The evaluation revealed that the developed lipid-based systems showed particle size in nano-range, low drug release at pH of blood and good entrapment efficiency. The evaluation results established the potential for passive targeting of nanocarrier systems by the virtue of Enhanced permeation and retention (EPR) effect. Nanoparticles can extravasate through fenestrated blood vessels of tumour microenvironment without releasing the drug during blood circulation. Low drug release during circulation of blood also leads to reduction of off-target toxicity and wastage of drug. Site specificity was further imparted to formulation by addition of Folic acid as ligand. Incorporation of folic acid led to active targeting of nanoparticles leading to higher accumulation of targeted system at tumour site as compared to non-targeted systems as proven by biodistribution as well as in vivo efficacy studies.

Developed nanoparticulate system was proven as safe for intravenous administration as established from *in vitro* haemolysis studies and acute toxicity study. The anticancer potential of the developed nanocarriers was established by biodistribution studies and in vivo efficacy studies.

The current research work has resulted in successful establishment of an herbal alternative for treatment of triple negative breast cancer. The technology used in development of this targeted nanocarrier system is simple and scalable and can be used as platform technology for other drugs with similar properties and can be explored for treatment of other types of cancer. The systematic approach of formulation development with use of quality by design (QbD) technique makes this system even more suitable for extension in industry scale manufacturing processes.

9.3. Scope of future work:

1) Exploring use of BCPO as an active ingredient to treat other diseases:

Research findings have proven the cytotoxic effect of BCPO on breast cancer cell lines, (MCF-7 and MDA-MB-468). BCPO has also shown tumour regression in *in vivo* efficacy studies.

Being an herbal principal, BCPO shows lesser side effects and is safe to administer intravenously as established from acute toxicity studies. This herbal principal has not been explored much for its anticancer effect on other tumour types. Thus, studies can be undertaken to design newer and more effective drug delivery systems for BCPO for exploring its anticancer action against other tumour types. BCPO has also shown antibacterial, antifungal properties as per the literature reports. Thus, BCPO can be further explored for antibacterial, antifungal effects in suitable drug delivery system.

Dose of BCPO for Intravenous administration has been established by acute toxicity studies. Similarly, other administration routes such as transdermal, oral, topical can be explored for delivery of BCPO.

2) Exploring synergistic potential of BCPO:

BCPO can be combined with other anticancer agents and explored for its synergistic activity. Anticancer activity of combinations of BCPO with other anticancer agents can be evaluated by in vitro cytotoxicity studies.

3) Exploring use of other ligands as targeting agents:

Tumour microenvironment shows over-expression of receptors for many nutritive molecules. Apart from Folic acid, other ligands such as transferrin, long chain fatty acids can be explored for their targeting potential with developed delivery system.

4) Use of developed formulation as platform technology:

Developed formulation can be used as platform technology for other drugs with similar physicochemical properties. The technology used in development of this formulation is simple, cost effective and industrially scalable. Thus, the developed formulation shows the potential to become industrially scalable marketed product showing lesser side effects and better patient compliance.

5) Exploring developed system for clinical studies:

Developed lipidic nanocarrier system has shown better anticancer potential and site specificity in *in vivo* efficacy studies performed using tumour bearing mice. Large scale clinical trials can be undertaken to further explore effectiveness of developed formulation in humans.

Bibliography

10. Bibliography

[1] "Breast Cancer: Statistics." https://www.cancer.net/cancer-types/breast-cancer/statistic

[2] "WHO Breast cancer fact sheet", [Online]. Available: https://www.who.int/news-room/fact-sheets/detail/breast-cancer

[3] R. Mehrotra and K. Yadav, "Breast cancer in India: Present scenario and the challenges ahead," *World J. Clin. Oncol.*, vol. 13, no. 3, pp. 209–218, 2022, doi: 10.5306/wjco.v13.i3.209.

[4] C. Kim *et al.*, "β-Caryophyllene oxide potentiates TNFα-induced apoptosis and inhibits invasion through down-modulation of NF-κB-regulated gene products," *Apoptosis*, vol. 19, no. 4, pp. 708–718, 2014, doi: 10.1007/s10495-013-0957-9.

[5] Ashok Kumar Peepliwal and Prasad Tandale, "Breast-cancer-in-india-etiology-diagnosis-and-therapy-31-42," *Res. Rev. J. Med. Heal. Sci.*, vol. Volume 2, no. Issue 2, pp. 31–42.

[6] C. M. Mansfield, "'A review of the etiology of breast cancer' Journal of the National Medical Association."

[7] Z. X. Ng, M. S. Ong, T. Jegadeesan, S. Deng, and C. T. Yap, "Breast cancer: Exploring the facts and holistic needs during and beyond treatment," *Healthcare (Switzerland)*, vol. 5, no. 2. MDPI, Jun. 01, 2017. doi: 10.3390/healthcare5020026.

[8] M. Keshtgar, T. Davidson, K. Pigott, M. Falzon, and A. Jones, "Current status and advances in management of early breast cancer," *International Journal of Surgery*, vol. 8, no. 3. pp. 199–202, 2010. doi: 10.1016/j.ijsu.2010.02.004.

[9] X. Dai *et al.*, "Breast cancer intrinsic subtype classification, clinical use and future trends," 2015. [Online]. Available: www.ajcr.us/

[10] C. L. Arteaga, M. X. Sliwkowski, C. K. Osborne, E. A. Perez, F. Puglisi, and L. Gianni, "Treatment of HER2-positive breast cancer: Current status and future perspectives," *Nature Reviews Clinical Oncology*, vol. 9, no. 1. pp. 16–32, Jan. 2012. doi: 10.1038/nrclinonc.2011.177.

[11] M. Cazzaniga and B. Bonanni, "Breast cancer chemoprevention: Old and new approaches," *Journal of Biomedicine and Biotechnology*, vol. 2012. 2012. doi:

10.1155/2012/985620.

[12] A. Matsumoto *et al.*, "Biological markers of invasive breast cancer," *Japanese Journal of Clinical Oncology*, vol. 46, no. 2. Oxford University Press, pp. 99–105, Feb. 01, 2016. doi: 10.1093/jjco/hyv153.

[13] J. E. Lang, J. S. Wecsler, M. F. Press, and D. Tripathy, "Molecular markers for breast cancer diagnosis, prognosis and targeted therapy," *Journal of Surgical Oncology*, vol. 111, no. 1. John Wiley and Sons Inc., pp. 81–90, Jan. 01, 2015. doi: 10.1002/jso.23732.

[14] G. Osborn and E. Vaughan-Williams, "Management of breast cancer: basic principles," *Surgery*, vol. 28, no. 3. pp. 130–134, Mar. 2010. doi: 10.1016/j.mpsur.2009.11.001.

[15] E. L. Davies and H. M. Sweetland, "Metastatic disease of the breast and local recurrence of breast cancer," *Surgery*, vol. 28, no. 3. pp. 144–147, Mar. 2010. doi: 10.1016/j.mpsur.2009.12.003.

[16] A. Marra, D. Trapani, G. Viale, C. Criscitiello, and G. Curigliano, "Practical classification of triple-negative breast cancer: intratumoral heterogeneity, mechanisms of drug resistance, and novel therapies," *npj Breast Cancer*, vol. 6, no. 1. Nature Research, Dec. 01, 2020. doi: 10.1038/s41523-020-00197-2.

[17] K. A. Akshata Desai, "Triple Negative Breast Cancer – An Overview," *Hered. Genet.*, 2012, doi: 10.4172/2161-1041.s2-001.

[18] K. C. O'Reilly D, Sendi MA, "Overview of recent advances in metastatic triple negative breast cancer," *World J. Clin. Oncol.*, vol. 12, no. 3, pp. 164–182, 2021, [Online]. Available: https://www.wjgnet.com/bpg/gerinfo/240

[19] Q. Jiao *et al.*, "The latest progress in research on triple negative breast cancer (TNBC): Risk factors, possible therapeutic targets and prognostic markers," *Journal of Thoracic Disease*, vol. 6, no. 9. Pioneer Bioscience Publishing, pp. 1329–1335, 2014. doi: 10.3978/j.issn.2072-1439.2014.08.13.

[20] G. Bianchini, J. M. Balko, I. A. Mayer, M. E. Sanders, and L. Gianni, "Triple-negative breast cancer: Challenges and opportunities of a heterogeneous disease," *Nature Reviews Clinical Oncology*, vol. 13, no. 11. Nature Publishing Group, pp. 674–690, Nov. 01, 2016. doi: 10.1038/nrclinonc.2016.66.

[21] K. A. Won and C. Spruck, "Triple-negative breast cancer therapy: Current and future

perspectives," *Int. J. Oncol.*, vol. 57, no. 6, pp. 1245–1261, Dec. 2020, doi: 10.3892/ijo.2020.5135.

[22] A. G. Desai *et al.*, "Medicinal Plants and Cancer Chemoprevention," 2008. [Online]. Available: http://www.ars-grin.gov/duke/

[23] J. Iqbal *et al.*, "Plant-derived anticancer agents: A green anticancer approach," *Asian Pacific Journal of Tropical Biomedicine*, vol. 7, no. 12. Hainan Medical University, pp. 1129–1150, Dec. 01, 2017. doi: 10.1016/j.apjtb.2017.10.016.

[24] A. I. Kuruppu, P. Paranagama, and C. L. Goonasekara, "Medicinal plants commonly used against cancer in traditional medicine formulae in Sri Lanka," *Saudi Pharmaceutical Journal*, vol. 27, no. 4. Elsevier B.V., pp. 565–573, May 01, 2019. doi: 10.1016/j.jsps.2019.02.004.

[25] A. R. Bilia, C. Guccione, B. Isacchi, C. Righeschi, F. Firenzuoli, and M. C. Bergonzi, "Essential oils loaded in nanosystems: A developing strategy for a successful therapeutic approach," *Evidence-based Complementary and Alternative Medicine*, vol. 2014. Hindawi Limited, 2014. doi: 10.1155/2014/651593.

[26] J. Legault and A. Pichette, "Potentiating effect of β-caryophyllene on anticancer activity of α-humulene, isocaryophyllene and paclitaxel," *J. Pharm. Pharmacol.*, vol. 59, no. 12, pp. 1643–1647, Feb. 2010, doi: 10.1211/jpp.59.12.0005.

[27] S. Di Giacomo *et al.*, "Role of caryophyllane sesquiterpenes in the entourage effect of felina 32 hemp inflorescence phytocomplex in triple negative MDA-MB-468 breast cancer cells," *Molecules*, vol. 26, no. 21, Nov. 2021, doi: 10.3390/molecules26216688.

[28] K. Fidyt, A. Fiedorowicz, L. Strządała, and A. Szumny, "β-caryophyllene and β-caryophyllene oxide—natural compounds of anticancer and analgesic properties," *Cancer Medicine*, vol. 5, no. 10. Blackwell Publishing Ltd, pp. 3007–3017, Oct. 01, 2016. doi: 10.1002/cam4.816.

[29] R. Petrelli *et al.*, "Biological activities of the essential oil from Erigeron floribundus," *Molecules*, vol. 21, no. 8, Aug. 2016, doi: 10.3390/molecules21081065.

[30] J. Legault, P. A. Côté, S. Ouellet, S. Simard, and A. Pichette, "Iso-caryophyllene cytotoxicity induced by lipid peroxidation and membrane permeabilization in L-929 cells," *J. Appl. Pharm. Sci.*, vol. 3, no. 8, pp. 25–31, Aug. 2013, doi:

10.7324/JAPS.2013.3805.

[31] A. Di Sotto *et al.*, "Chemopreventive potential of caryophyllane sesquiterpenes: An overview of preliminary evidence," *Cancers*, vol. 12, no. 10. MDPI AG, pp. 1–49, Oct. 01, 2020. doi: 10.3390/cancers12103034.

[32] F. Mannino *et al.*, "Beta-caryophyllene exhibits anti-proliferative effects through apoptosis induction and cell cycle modulation in multiple myeloma cells," *Cancers (Basel).*, vol. 13, no. 22, Nov. 2021, doi: 10.3390/cancers13225741.

[33] D. Schmitt, R. Levy, and B. Carroll, "Toxicological Evaluation of β-Caryophyllene Oil: Subchronic Toxicity in Rats," *Int. J. Toxicol.*, vol. 35, no. 5, pp. 558–567, Sep. 2016, doi: 10.1177/1091581816655303.

[34] D. Yang, L. Michel, J. P. Chaumont, and J. Millet-Clerc, "Use of caryophyllene oxide as an antifungal agent in an in vitro experimental model of onychomycosis," *Mycopathologia*, vol. 148, no. 2, pp. 79–82, 2000, doi: 10.1023/A:1007178924408.

[35] M. lobato ramos vermelho Fabio Alessandro Pieri, Marina campos de castro souza, Ligia loboto ramos vermelho, "Use of β-caryophyllene to combat bacterial dental plaque formation in dogs _ Enhanced Reader.pdf," *BMC Vet. Res.*, p. 12:216, 2016.

[36] M. J. Chavan, P. S. Wakte, and D. B. Shinde, "Analgesic and anti-inflammatory activity of Caryophyllene oxide from Annona squamosa L. bark," *Phytomedicine*, vol. 17, no. 2, pp. 149–151, 2010, doi: 10.1016/j.phymed.2009.05.016.

[37] N. J. Jun *et al.*, "Cytotoxic activity of β-caryophyllene oxide isolated from Jeju Guava (Psidium cattleianum Sabine) leaf," *Rec. Nat. Prod.*, vol. 5, no. 3, pp. 242–246, 2011.

[38] M. Ambrož *et al.*, "Sesquiterpenes α-humulene and β-caryophyllene oxide enhance the efficacy of 5-fluorouracil and oxaliplatin in colon cancer cells," *Acta Pharm.*, vol. 69, no. 1, pp. 121–128, 2019, doi: 10.2478/acph-2019-0003.

[39] K. R. Park *et al.*, "β-Caryophyllene oxide inhibits growth and induces apoptosis through the suppression of PI3K/AKT/mTOR/S6K1 pathways and ROS-mediated MAPKs activation," 2011 doi: 10.1016/j.canlet.2011.08.001.

[40] N. H. Ryu *et al.*, "A hexane fraction of guava leaves (Psidium guajava L.) induces anticancer activity by suppressing AKT/mammalian target of rapamycin/ribosomal p70 S6 kinase in human prostate cancer cells," *J. Med. Food*, vol. 15, no. 3, pp. 231–241,

2012, doi: 10.1089/jmf.2011.1701.

[41] J. Legault, W. Dahl, E. Debiton, and J. Madelmont, "Antitumor Activity of Balsam Fir Oil: Production of Reactive Oxygen Species Induced by a-Humulene as Possible Mechanism of Action," *Planta Med*, vol. 69, no. 5, pp. 402–407, 2003.

[42] S. U. Durre Shahwar, Sami Ullah, Mohammad Akmal Khan, Naeem Ahmad, Afifa Saeed, "Anticancer activity of Cinnamon tamala leaf constituents towards human ovarian cancer cells," *Pak J Pharm Sci*, vol. 3, pp. 969–72, 2015.

[43] J. I. Jung *et al.*, "β-Caryophyllene potently inhibits solid tumor growth and lymph node metastasis of B16F10 melanoma cells in high-fat diet-induced obese C57BL/6N mice," *Carcinogenesis*, vol. 36, no. 9, pp. 1028–1039, Mar. 2015, doi: 10.1093/carcin/bgv076.

[44] K. Mahéo *et al.*, "Differential sensitization of cancer cells to doxorubicin by DHA: A role for lipoperoxidation," *Free Radic. Biol. Med.*, vol. 39, no. 6, pp. 742–751, 2005, doi: 10.1016/j.freeradbiomed.2005.04.023.

[45] J. Wang, T. Luo, S. Li, and J. Zhao, "The powerful applications of polyunsaturated fatty acids in improving the therapeutic efficacy of anticancer drugs," *Expert Opin. Drug Deliv.*, vol. 9, no. 1, pp. 1–7, 2012, doi: 10.1517/17425247.2011.618183.

[46] J. Abdi, J. Garssen, J. Faber, and F. A. Redegeld, "Omega-3 fatty acids, EPA and DHA induce apoptosis and enhance drug sensitivity in multiple myeloma cells but not in normal peripheral mononuclear cells," *J. Nutr. Biochem.*, vol. 25, no. 12, pp. 1254–1262, 2014, doi: 10.1016/j.jnutbio.2014.06.013.

[47] S. V. Mussi, R. B. Azevedo, L. Antonio, and M. Ferreira, "New approach to improve encapsulation and antitumor activity of doxorubicin loaded in solid lipid nanoparticles," *Eur. J. Pharm. Sci.*, vol. 48, no. 1–2, pp. 282–290, 2012, doi: 10.1016/j.ejps.2012.10.025.

[48] J. Spreadbury, "Folic Acid and Its Receptors," 2013. [Online]. Available: http://opus.govst.edu/capstoneshttp://opus.govst.edu/capstones/8

[49] D.-S. Yu, H.-Y. Yan, and C.-L. Wu, "Folate receptor expression in bladder cancer and its correlation with tumor behaviors and clinical outcome," *J. Cancer Res. Pract.*, vol. 4, no. 4, pp. 130–133, Dec. 2017, doi: 10.1016/j.jcrpr.2017.05.001.

[50] A. Cheung *et al.*, "Targeting folate receptor alpha for cancer treatment." [Online].

Available: www.impactjournals.com/oncotarget

[51] J. A. Ledermann, S. Canevari, and T. Thigpen, "Targeting the folate receptor: Diagnostic and therapeutic approaches to personalize cancer treatments," *Annals of Oncology*, vol. 26, no. 10. Oxford University Press, pp. 2034–2043, Oct. 01, 2015. doi: 10.1093/annonc/mdv250.

[52] G. L. Zwicke, G. Ali Mansoori, and C. J. Jeffery, "Utilizing the folate receptor for active targeting of cancer nanotherapeutics," *Nano Rev.*, vol. 3, no. 1, p. 18496, Jan. 2012, doi: 10.3402/nano.v3i0.18496.

[53] A. S. Wibowo *et al.*, "Structures of human folate receptors reveal biological trafficking states and diversity in folate and antifolate recognition," *Proc. Natl. Acad. Sci. U. S. A.*, vol. 110, no. 38, pp. 15180–15188, Oct. 2013, doi: 10.1073/pnas.1308827110.

[54] P. Puligujja *et al.*, "Macrophage folate receptor-targeted antiretroviral therapy facilitates drug entry, retention, antiretroviral activities and biodistribution for reduction of human immunodeficiency virus infections," *Nanomedicine Nanotechnology, Biol. Med.*, vol. 9, no. 8, pp. 1263–1273, Nov. 2013, doi: 10.1016/j.nano.2013.05.003.

[55] J. Varshosaz, F. Hassanzadeh, H. Sadeghi, and M. Shakery, "Folate Targeted Solid Lipid Nanoparticles of Simvastatin for Enhanced Cytotoxic Effects of Doxorubicin in Chronic Myeloid Leukemia," 2012.

[56] Y. Liu, K. Li, J. Pan, B. Liu, and S. S. Feng, "Folic acid conjugated nanoparticles of mixed lipid monolayer shell and biodegradable polymer core for targeted delivery of Docetaxel," *Biomaterials*, vol. 31, no. 2, pp. 330–338, Jan. 2010, doi: 10.1016/j.biomaterials.2009.09.036.

[57] J.-S. Baek and C.-W. Cho, "A multifunctional lipid nanoparticle for co-delivery of paclitaxel and curcumin for targeted delivery and enhanced cytotoxicity in multidrug resistant breast cancer cells," 2017. [Online]. Available: www.impactjournals.com/oncotarget

[58] Z. X. Ng, M. S. Ong, T. Jegadeesan, S. Deng, and C. T. Yap, "Breast Cancer : Exploring the Facts and Holistic Needs during and beyond Treatment," pp. 1–11, 2017, doi: 10.3390/healthcare5020026.

[59] M. Cazzaniga and B. Bonanni, "Breast Cancer Chemoprevention : Old and New

Approaches," vol. 2012, 2012, doi: 10.1155/2012/985620.

[60] S. V. Mussi, R. C. Silva, M. C. De Oliveira, C. M. Lucci, R. B. De Azevedo, and L. A. M. Ferreira, "New approach to improve encapsulation and antitumor activity of doxorubicin loaded in solid lipid nanoparticles," *Eur. J. Pharm. Sci.*, vol. 48, no. 1–2, pp. 282–290, Jan. 2013, doi: 10.1016/j.ejps.2012.10.025.

[61] P. Fiorenzani, S. Lamponi, A. Magnani, I. Ceccarelli, and A. M. Aloisi, "In vitro and in vivo characterization of the new analgesic combination beta-caryophyllene and docosahexaenoic acid," *Evidence-based Complement. Altern. Med.*, vol. 2014, 2014, doi: 10.1155/2014/596312.

[62] R. K. Salar and N. Kumar, "Synthesis and characterization of vincristine loaded folic acid–chitosan conjugated nanoparticles," *Resour. Technol.*, vol. 2, no. 4, pp. 199–214, 2016, doi: 10.1016/j.reffit.2016.10.006.

[63] L. Nair K, S. Jagadeeshan, A. Nair S, and G. S. V. Kumar, "Folic Acid Conjugated δ-Valerolactone-Poly(ethylene glycol) Based Triblock Copolymer as a Promising Carrier for Targeted Doxorubicin Delivery," *PLoS One*, vol. 8, no. 8, 2013, doi: 10.1371/journal.pone.0070697.

[64] H. Pawar *et al.*, "Folic acid functionalized long-circulating co-encapsulated docetaxel and curcumin solid lipid nanoparticles : In vitro evaluation , pharmacokinetic and biodistribution in rats," *Drug Deliv.*, vol. 7544, no. February, 2016, doi: 10.3109/10717544.2016.1138339.

[65] A. K. Peepliwal and P. Tandale, "Research and Reviews : Journal of Medical and Health Sciences Breast Cancer in India : Etiology , Diagnosis and Therapy," vol. 2, no. 2, pp. 31–42, 2013.

[66] M. Narvekar, H. Y. Xue, J. Y. Eoh, and H. L. Wong, "Nanocarrier for Poorly Water-Soluble Anticancer Drugs — Barriers of Translation and Solutions," vol. 15, no. 4, pp. 822–833, 2014, doi: 10.1208/s12249-014-0107-x.

[67] M. Siddiqui and S. V. Rajkumar, "The high cost of cancer drugs and what we can do about it," *Mayo Clin. Proc.*, vol. 87, no. 10, pp. 935–943, 2012, doi: 10.1016/j.mayocp.2012.07.007.

[68] L. S. & A. S. Klaudyna Fidyt, Anna Fiedorowicz, "β-caryophyllene and β-caryophyllene

oxide- natural compounds of anticancer and analgesic properties," *Cancer Med.*, 2016.

[69] W. Wang, F. Zhou, L. Ge, X. Liu, and F. Kong, "A promising targeted gene delivery system : Folate-modified dexamethasone-conjugated solid lipid nanoparticles," vol. 52, no. 8, pp. 1039–1044, 2014, doi: 10.3109/13880209.2013.876655.

[70] H. Bunjes, "Lipid nanoparticles for the delivery of poorly water-soluble drugs," *Journal of Pharmacy and Pharmacology*, vol. 62, no. 11. pp. 1637–1645, Nov. 2010. doi: 10.1111/j.2042-7158.2010.01024.x.

[71] P. Speiser, "Lipidnanopellets als Tra¨gersystem fu¨r Arzneimittel zur peroralen Anwendung. European Patent"

[72] A. Domb, "Lipospheres for Controlled Delivery of Substances," 2005 doi: 10.1201/9781420027990.ch10.

[73] G. S. Müller RH, Mäder K, "Solid lipid nanoparticles (SLN) for controlled drug delivery - a review of the state of the art," *Eur J Pharm Biopharm.*, vol. 50(1), pp. 161–77, doi: 10.1016/s0939-6411(00)00087-4.

[74] M. K. S. Mehnert W, "Lipid nanoparticles: production, characterization and applications," *Adv Drug Deliv Rev.*, vol. 47(2–3), pp. 165–96, doi: 10.1016/s0169-409x(01)00105-3.

[75] A. Das, S and Chaudhury, "Recent Advances in Lipid Nanoparticle Formulations with Solid Matrix for Oral Drug Delivery," *AAPS PharmSciTech*, pp. 1–15.

[76] R. Muchow, M, Maincent, P, and Müller, "Lipid nanoparticles with a solid matrix (SLN®, NLC®, LDC®) for oral drug delivery," *Drug Dev Ind Pharm*, vol. 34(12), pp. 1394–405, 2008.

[77] K. Lippacher, A, Muller, RH, and Mader, "Investigation on the viscoelastic properties of lipid based colloidal drug carriers," *Int J Pharm*, vol. 196(2), pp. 227–30, 2000.

[78] M. Gasco, "Method for producing solid lipid microspheres having a narrow size distribution, United States Patent. US 188837," 1993

[79] K. Siekmann, B and Westesen, "Investigations on solid lipid nanoparticles prepared by precipitation in o/w emulsions," *Eur J Pharm Biopharm*, vol. 42(2), pp. 104–9, 1996.

[80] O. Trotta, M, Debernardi, F, and Caputo, "Preparation of solid lipid nanoparticles by a

solvent emulsification-diffusion technique," *Int J Pharm*, vol. 257(1–2), pp. 153–60, 2003.

[81] C. Schubert, MA and Muller-Goymann, "Solvent injection as a new approach for manufacturing lipid nanoparticles-evaluation of the method and process parameters," *Eur J Pharm Biopharm*, vol. 55(1), pp. 125–31, 2003.

[82] et al. Zhang, N, Ping, Q, Huang, G, "Lectin-modified solid lipid nanoparticles as carriers for oral administration of insulin," *Int J Pharm*, vol. 327(1–2), no. 153–9, 2006.

[83] H. Charcosset, C, El-Harati, A, and Fessi, "Preparation of solid lipid nanoparticles using a membrane contactor," *J Control Release*, vol. 108(1), pp. 112–20, 2005.

[84] T. Bunjes, H and Unruh, "Characterization of lipid nanoparticles by differential scanning calorimetry, X-ray and neutron scattering," *Adv Drug Deliv. Rev*, vol. 59(6), pp. 379–402, 2007.

[85] T. X. . Xiang R., Chen S-W., Zhang F-M., Ni –M., "A HPLC method for the determination of entrapment efficiency of a new 5-FPE liposome formulation," *J. Chinese Pharm. Sci.*, vol. 18, pp. 186–189, 2009.

[86] N. M. . Date A.A., Vador N., Jagtap A., "Lipid Nanocarriers (GeluPearl) containing amphiphilic lipid Gelucire 50/13 as a novel stabilizer: fabrication, characterization and evaluation for oral drug delivery," *Nanotechnology*, vol. 22, 2011.

[87] K. D. Shirsand S., Para M., Nagendrakumar D., Kanani K., "Formulation and evaluation of Ketoconazole niosomal gel drug delivery system," *Int J Pharm Investig*, vol. 2, pp. 201–7, 2002.

[88] Y. M. Yue P.F., Lu X.Y., Zhang Z.Z., Yuan H.L., Zhu W.F., Zheng Q., "The study on the entrapment efficiency and in vitro release of puerarin submicron emulsion," *AAPS PharmSciTech*, vol. 10, pp. 376–83, 2009.

[89] M. P. Bragagni M, Mennini N, Maestrelli F, Cirri M, "Comparative study of liposomes, transfersomes and ethosomes as carriers for improving topical delivery of celecoxib," *Drug Deliv.*, vol. 19(7), pp. 354–61.

[90] S. Syrovets T, Gschwend JE, Büchele B, Laumonnier Y, Zugmaier W, Genze F and T, "Inhibition of IkappaB kinase activity by acetyl-boswellic acids promotes apoptosis in androgen-independent PC-3 prostate cancer cells in vitro and in vivo," *J Biol Chem.*,

vol. 280(7), pp. 6170–80.

[91] Y. Y. Attia AB, Yang C, Tan JP, Gao S, Williams DF, Hedrick JL, "The effect of kinetic stability on biodistribution and anti-tumor efficacy of drug-loaded biodegradable polymeric micelles," *Biomaterials*, vol. 34(12), no. 3132–40, 2013.

[92] R. Radtke, M and Müller, "Nanostructured lipid drug carriers," *New Drugs*, vol. 2, pp. 48–52, 2001.

[93] et al Lacoeuille, F, HindrÃ©, F, Moal, F, "In vivo evaluation of lipid nanocapsules as a promising colloidal carrier for paclitaxel," *Int J Pharm*, vol. 344(1–2), pp. 143–9, 2007.

[94] et al Allard, E, Passirani, C, Garcion, E, "Lipid nanocapsules loaded with an organometallic tamoxifen derivative as a novel drug-carrier system for experimental malignant gliomas," *J Control Release*, vol. 130(2), pp. 146–53, 2008.

[95] W. W. S. B. M. B. Agoram B., "predicting the impact of physiological and biochemical processes on oral drug bioavailability," *Adv. Drug Deliv. Rev.*, pp. S41–S67, 2001.

[96] D. A. Beig A., Miller J. M., "Accounting for the solubility-permeability interplay in oral formulation development for poor water solubility drugs," *Eur. J. Pharm. Biopharm.*, vol. 81, pp. 386–391, 2012.

[97] H. G. Cornaire G., Woodley J., Hermann P., Cloaree A., Arellano C., "Impact of excipients on the absorption of P-glycoprotein substrates in vitro and in vivo," *Int. J. Pharm.*, vol. 278, pp. 119–131, 2004.

[98] A. S. Ahmad J., Kohli K., Mir S.R., "Lipid based Nanocarriers for oral Delivery of Cancer Chemotherapeutics : An Insight in the intestinal Lymphatic Transport," *Drug Deliv. Lett.*, vol. 3, pp. 38–46, 2013.

[99] N. M. . Jain A. S., Date A.A., "Design, Characterization and evaluation of Anti-epileptic Activity of Nanoprecipitating Preconcentrate of Carbamazepine," *Drug Deliv. Lett.*, vol. 3, pp. 61–69, 2013.

[100] S. S. Chakraborty S., Shukla D., Mishra B., "Lipid—an emerging platform for oral delivery of drugs with poor bioavailability," *Eur. J. Pharm. Biopharm.*, vol. 73, pp. 1–15, 2009.

[101] T. K. Jain S., Kumar D., Swarnakar N.K., "Polyelectrolyte stabilized multilayered liposomes for oral delivery of paclitaxel. Biomaterials," *Biomaterials*, vol. 33, pp. 6758–68, 2012.

[102] Y. C. Yang S., Zhu J., Lu Y., Liang B., "Body distribution of Camptothecin solid lipid nanoparticles after oral administration," *Pharm. Res.*, vol. 16, pp. 751–7, 1999.

[103] D. P. V Benival D.M., "Lipomer of doxorubicin hydrochloride for enhanced oral bioavailability," *Int. J. Pharm.*, vol. 423, pp. 554–61, 2012.

[104] K. M. N. V. R. Bhardwaj V., Plumb J.A., Cassidy J., "Evaluating the Potential of polymer nanoparticles for oral delivery of paclitaxel in drug resistant cancer," *Cancer Nanotechnol.*, vol. 1, pp. 29–34, 2010.

[105] P. C. J. Pouton C. W., "Formulation of lipid-based delivery systems for oral administration: materials, methods and strategies," *Adv. Drug Deliv. Rev.*, vol. 60, pp. 625–37, 2008.

[106] Z. S. Stuchlik M., "Lipid based vehicle for oral drug delivery," *Biomed Pap Med Fac Univ Palacky Olomouc Czech Repub*, vol. 145, pp. 17–26, 2001.

[107] N. M. . Patere S. N., Shah S.M., Pathak P.O., "Liposomal Drug Delivery System for Receptor Based Hepatic Targeting," in *38th Annual Meeting and Exposition 145 of the Controlled Release Society. Controlled Release Society*, 2011, p. 437.

[108] P. J. S. Kang H.S., Jin S.J., Myung C.S., Hwang S.J., "Delivery of interleukin-18 gene to lung cancer cells using cationic emulsion. Journal of Drug Targeting," *J. Drug Target.*, vol. 17, pp. 19–28, 2009.

[109] B. Teixeira H., Dubernet C., Chacun H., Rabinovich L., Boutet V., Deverre J.R. and C. P. S., "Cationic emulsions improves the delivery of oligonucleotides to leukemic P388/ADR in ascite," *J. Control. release*, vol. 89, pp. 473–82, 2003.

[110] H. Bunjes and T. Unruh, "Characterization of lipid nanoparticles by differential scanning calorimetry, X-ray and neutron scattering," *Advanced Drug Delivery Reviews*, vol. 59, no. 6. pp. 379–402, Jul. 10, 2007. doi: 10.1016/j.addr.2007.04.013.

[111] V. R. De Almeida Borges, A. F. Ribeiro, C. De Souza Anselmo, L. M. Cabral, and V. P. De Sousa, "Development of a high performance liquid chromatography method for quantification of isomers β-caryophyllene and α-humulene in copaiba oleoresin using

the Box-Behnken design," *J. Chromatogr. B Anal. Technol. Biomed. Life Sci.*, vol. 940, pp. 35–41, Dec. 2013, doi: 10.1016/j.jchromb.2013.09.024.

[112] M. Blessy, R. D. Patel, P. N. Prajapati, and Y. K. Agrawal, "Development of forced degradation and stability indicating studies of drugs - A review," *Journal of Pharmaceutical Analysis*, vol. 4, no. 3. Xi'an Medical University, pp. 159–165, 2014. doi: 10.1016/j.jpha.2013.09.003.

[113] B. Sundararajan and B. D. Ranjitha Kumari, "Effect of Farnesyl Diphosphate on Beta caryophyllene content in the calli of Artemisia vulgaris L," 2015.

[114] S. Shailajan, S. Menon, N. Sayed, and B. Tiwari, "Simultaneous estimation of three triterpenoids from Carissa carandas using validated high performance liquid chromatography," *Int. J. Green Pharm.*, vol. 6, no. 3, pp. 241–247, 2012, doi: 10.4103/0973-8258.104940.

[115] D. W. G. Harron, *VALIDATION OF ANALYTICAL PROCEDURES: TEXT AND METHODOLOGY*, vol. 1994, no. November 1996. 2013, pp. 447–460. doi: 10.1002/9781118532331.ch23.

[116] R. Raut and J. Shaji, "HPLC method validation for quantification of tetrahydrocurcumin in bulk drug and formulation," *Futur. J. Pharm. Sci.*, vol. 7, no. 1, pp. 0–5, 2021, doi: 10.1186/s43094-021-00194-7.

[117] H. Naseef, R. Moqadi, and M. Qurt, "Development and validation of an HPLC method for determination of antidiabetic drug alogliptin benzoate in bulk and tablets," *J. Anal. Methods Chem.*, vol. 2018, 2018, doi: 10.1155/2018/1902510.

[118] M. B. Savadkouhi, H. Vahidi, A. M. Ayatollahi, S. Hooshfar, and F. Kobarfard, "RP-HPLC method development and validation for determination of eptifibatide acetate in bulk drug substance and pharmaceutical dosage forms," *Iran. J. Pharm. Res.*, vol. 16, no. 2, pp. 490–497, 2017.

[119] M. Çelebier, T. Reçber, E. Koçak, and S. Altinöz, "RP-HPLC method development and validation for estimation of rivaroxaban in pharmaceutical dosage forms," *Brazilian J. Pharm. Sci.*, vol. 49, no. 2, pp. 359–366, 2013, doi: 10.1590/S1984-82502013000200018.

[120] A. S. Schmidt, "Forced degradation studies for biopharmaceuticals," *Pharm. Technol.*,

vol. 40, no. 5, pp. 54–57, 2016.

[121] M. Blessy, R. D. Patel, P. N. Prajapati, and Y. K. Agrawal, "Development of forced degradation and stability indicating studies of drugs - A review," *J. Pharm. Anal.*, vol. 4, no. 3, pp. 159–165, 2014, doi: 10.1016/j.jpha.2013.09.003.

[122] B. S. Bhoop, "Quality by design (QbD) for holistic Pharma excellence and regulatory compliance," *Pharma Times*, vol. 46, no. 8, pp. 26–33, 2014.

[123] J. N. Sangshetti, M. Deshpande, Z. Zaheer, D. B. Shinde, and R. Arote, "Quality by design approach: Regulatory need," *Arab. J. Chem.*, vol. 10, pp. S3412–S3425, 2017, doi: 10.1016/j.arabjc.2014.01.025.

[124] V. P. Kumar and N. Vishal Gupta, "A review on quality by design approach (QBD) for pharmaceuticals," *Int. J. Drug Dev. Res.*, vol. 7, no. 1, pp. 52–60, 2015.

[125] L. X. Yu *et al.*, "Understanding pharmaceutical quality by design," *AAPS J.*, vol. 16, no. 4, pp. 771–783, 2014, doi: 10.1208/s12248-014-9598-3.

[126] A. Jain, T. Sharma, R. Kumar, S. Saini, and J. Kaur, "Novel Methotrexate-Loaded Zein Nanoparticles With Improved and Extended Biopharmaceutical Performance : QbD-Steered Development , and Extensive In Vitro and In Vivo Evaluation," pp. 1–23, 2021.

[127] H. Tian, Z. Lu, D. Li, and J. Hu, "Preparation and characterization of citral-loaded solid lipid nanoparticles," *Food Chem.*, vol. 248, pp. 78–85, May 2018, doi: 10.1016/j.foodchem.2017.11.091.

[128] I. Chauhan, M. Yasir, M. Verma, and A. P. Singh, "Nanostructured lipid carriers: A groundbreaking approach for transdermal drug delivery," *Adv. Pharm. Bull.*, vol. 10, no. 2, pp. 150–165, 2020, doi: 10.34172/apb.2020.021.

[129] F. J. Fang CL, Al-Suwayeh SA, "Nanostructured lipid carriers (NLCs) for drug delivery and targeting," *Recent Pat Nanotechnol*, vol. 7(1), pp. 41–55, 2013.

[130] S. Selvamuthukumar and R. Velmurugan, "Nanostructured Lipid Carriers: A potential drug carrier for cancer chemotherapy," *Lipids Health Dis.*, vol. 11, no. 1, pp. 1–8, 2012, doi: 10.1186/1476-511X-11-159.

[131] S. M. M. Moghddam, A. Ahad, M. Aqil, S. S. Imam, and Y. Sultana, "Optimization of nanostructured lipid carriers for topical delivery of nimesulide using Box–Behnken

design approach," *Artif. Cells, Nanomedicine Biotechnol.*, vol. 45, no. 3, pp. 617–624, Apr. 2017, doi: 10.3109/21691401.2016.1167699.

[132] S. A. Swidan *et al.*, "DOE, formulation, and optimization of Repaglinide nanostructured lipid carriers," *J. Appl. Pharm. Sci.*, vol. 8, no. 10, pp. 8–16, Oct. 2018, doi: 10.7324/JAPS.2018.81002.

[133] J. Varshosaz, H. Sadeghi, S. Andalib, and F. Hassanzadeh, "Optimization of LDL targeted nanostructured lipid carriers of 5-FU by a full factorial design," *Adv. Biomed. Res.*, vol. 1, no. 1, p. 45, 2012, doi: 10.4103/2277-9175.100147.

[134] H. Pawar *et al.*, "Folic acid functionalized long-circulating co-encapsulated docetaxel and curcumin solid lipid nanoparticles: In vitro evaluation, pharmacokinetic and biodistribution in rats," *Drug Deliv.*, vol. 23, no. 4, pp. 1453–1468, May 2016, doi: 10.3109/10717544.2016.1138339.

[135] H. Yuan, J. Miao, Y. Z. Du, J. You, F. Q. Hu, and S. Zeng, "Cellular uptake of solid lipid nanoparticles and cytotoxicity of encapsulated paclitaxel in A549 cancer cells," *Int. J. Pharm.*, vol. 348, no. 1–2, pp. 137–145, Feb. 2008, doi: 10.1016/j.ijpharm.2007.07.012.

[136] R. Cavalli, O. Caputo, M. E. Carlotti, M. Trotta, C. Scarnecchia, and M. Rosa Gasco " ', "Sterilization and freeze-drying of drug-free and drug-loaded solid lipid nanoparticles," 1997.

[137] N. S. El-Salamouni, R. M. Farid, A. H. El-Kamel, and S. S. El-Gamal, "Effect of sterilization on the physical stability of brimonidine-loaded solid lipid nanoparticles and nanostructured lipid carriers," *Int. J. Pharm.*, vol. 496, no. 2, pp. 976–983, Dec. 2015, doi: 10.1016/j.ijpharm.2015.10.043.

[138] K. Manjunath, J. S. Ready, and V. Venkateswarlu, "Solid lipid nanoparticles as drug delivery systems," *Methods and Findings in Experimental and Clinical Pharmacology*, vol. 27, no. 2. pp. 127–144, Mar. 2005. doi: 10.1358/mf.2005.27.2.876286.

[139] W. Mehnert and K. Mader, "Solid lipid nanoparticles Production, characterization and applications," 2001. [Online]. Available: www.elsevier.com/locate/drugdeliv

[140] N. M. Morsi, D. M. Ghorab, and H. A. Badie, "Brain targeted solid lipid nanoparticles for brain ischemia: preparation and in vitro characterization.," *Pharm. Dev. Technol.*,

vol. 18, no. 3, pp. 736–744, 2013, doi: 10.3109/10837450.2012.734513.

[141] A. R. Neves, J. F. Queiroz, and S. Reis, "Brain-targeted delivery of resveratrol using solid lipid nanoparticles functionalized with apolipoprotein E," *J. Nanobiotechnology*, vol. 14, no. 1, Apr. 2016, doi: 10.1186/s12951-016-0177-x.

[142] Y. C. Kuo and T. Y. Hong, "Delivering etoposide to the brain using catanionic solid lipid nanoparticles with surface 5-HT-moduline," *Int. J. Pharm.*, vol. 465, no. 1–2, pp. 132–142, Apr. 2014, doi: 10.1016/j.ijpharm.2014.02.008.

[143] L. Battaglia, L. Serpe, E. Muntoni, G. P. Zara, M. Trotta, and M. Gallarate, "Methotrexate-loaded SLNs prepared by coacervation technique: In vitro cytotoxicity and in vivo pharmacokinetics and biodistribution," *Nanomedicine*, vol. 6, no. 9, pp. 1561–1573, Nov. 2011, doi: 10.2217/nnm.11.52.

[144] C. Z. Y. Shi Cheng Yang , Li Fang Lu , Ying Cai , Jia Bi Zhu, Bing Wen Liang, "Body distribution in mice of intravenously injected camptothecin solid lipid nanoparticles and targeting effect on brain," *J. Control. Release*, vol. 59, pp. 299–307, 1999.

[145] Y. C. Kuo and S. J. Cheng, "Brain targeted delivery of carmustine using solid lipid nanoparticles modified with tamoxifen and lactoferrin for antitumor proliferation," *Int. J. Pharm.*, vol. 499, no. 1–2, pp. 10–19, Feb. 2016, doi: 10.1016/j.ijpharm.2015.12.054.

[146] Y. C. Kuo and I. H. Lee, "Delivery of doxorubicin to glioblastoma multiforme in vitro using solid lipid nanoparticles with surface aprotinin and melanotransferrin antibody for enhanced chemotherapy," *J. Taiwan Inst. Chem. Eng.*, vol. 61, pp. 32–45, Apr. 2016, doi: 10.1016/j.jtice.2015.12.012.

[147] Y. Luo, Z. Teng, Y. Li, and Q. Wang, "Solid lipid nanoparticles for oral drug delivery: Chitosan coating improves stability, controlled delivery, mucoadhesion and cellular uptake," *Carbohydr. Polym.*, vol. 122, pp. 221–229, May 2015, doi: 10.1016/j.carbpol.2014.12.084.

[148] Z. R. Huang, S. C. Hua, Y. L. Yang, and J. Y. Fang, "Development and evaluation of lipid nanoparticles for camptothecin delivery: A comparison of solid lipid nanoparticles, nanostructured lipid carriers, and lipid emulsion," *Acta Pharmacol. Sin.*, vol. 29, no. 9, pp. 1094–1102, Sep. 2008, doi: 10.1111/j.1745-7254.2008.00829.x.

[149] V. S. Deborah L Holliday, "Choosing the right cell line for breast cancer," *Breast*

Cancer Res., vol. 13:215, 2011, [Online]. Available: http://breast-cancer-research.com/content/13/4/215

[150] K. Blowman, M. Magalhães, M. F. L. Lemos, C. Cabral, and I. M. Pires, "Anticancer Properties of Essential Oils and Other Natural Products," *Evidence-based Complement. Altern. Med.*, vol. 2018, 2018, doi: 10.1155/2018/3149362.

[151] I. V. Krishna, G. R. Vanaja, N. S. K. Kumar, and G. Suman, "Cytotoxic studies of anti-neoplastic drugs on human lymphocytes - In vitro studies," *Cancer Biomarkers*, vol. 5, no. 6, pp. 261–272, 2009, doi: 10.3233/CBM-2009-0111.

[152] C. F. Cheok, "Protecting normal cells from the cytotoxicity of chemotherapy," *Cell Cycle News & Views*, vol. 11, no. 12. Taylor and Francis Inc., p. 2228, Jun. 15, 2012. doi: 10.4161/cc.20962.

[153] "beta-Caryophyllene oxide." https://pubchem.ncbi.nlm.nih.gov/compound/beta-Caryophyllene-oxide

[154] "beta-caryophylleneoxide." http://www.thegoodscentscompany.com/data/rw1023631.html

[155] P. Therasse *et al.*, "New guidelines to evaluate the response to treatment in solid tumors," *J. Natl. Cancer Inst.*, vol. 92, no. 3, pp. 205–216, 2000, doi: 10.1093/jnci/92.3.205.

[156] N. S. Ahmad, M. N. A. Ghani, A. Manaf Ali, S. A. Tajudin Tuan Johari, and M. H. Harun, "High Performance Liquid Chromatography (HPLC) Profiling Analysis and Bioactivity of Baeckea frutescens L. (Myrtaceae)," *J. Plant Stud.*, vol. 1, no. 2, Aug. 2012, doi: 10.5539/jps.v1n2p101.

[157] L. Kumar, M. Sreenivasa Reddy, R. S. Managuli, and G. Pai K., "Full factorial design for optimization, development and validation of HPLC method to determine valsartan in nanoparticles," *Saudi Pharm. J.*, vol. 23, no. 5, pp. 549–555, 2015, doi: 10.1016/j.jsps.2015.02.001.

[158] V. Raphael, D. A. Borges, A. F. Ribeiro, C. D. S. Anselmo, L. M. Cabral, and V. P. De Sousa, "Development of a high performance liquid chromatography method for quantification of isomers □ -caryophyllene and ⌣ -humulene in copaiba oleoresin using the Box-Behnken design," *J. Chromatogr. B*, vol. 940, pp. 35–41, 2013, doi:

10.1016/j.jchromb.2013.09.024.

[159] ICH, "Ich Q1B," *Stab. Test. Photostability Test. New Drug Subst. Drug Prod.*, no. November, 1996.

[160] "ICH Q2(R2) Validation of analytical procedures." https://www.ema.europa.eu/en/ich-q2r2-validation-analytical-procedures

[161] ICH Q1A(R2), "International Conference on Harmonization (ICH). Guidance for industry: Q1A(R2) STABILITY TESTING OF NEW DRUG SUBSTANCES AND PRODUCTS," *Ich Harmon. Tripart. Guidel.*, vol. 4, no. February, p. 24, 2003.

[162] M. Ghadiri *et al.*, "Loading hydrophilic drug in solid lipid media as nanoparticles: Statistical modeling of entrapment efficiency and particle size," *Int. J. Pharm.*, vol. 424, no. 1–2, pp. 128–137, 2012, doi: 10.1016/j.ijpharm.2011.12.037.

[163] Q. Lv *et al.*, "Development and evaluation of penciclovir-loaded solid lipid nanoparticles for topical delivery," *Int. J. Pharm.*, vol. 372, no. 1–2, pp. 191–198, 2009, doi: 10.1016/j.ijpharm.2009.01.014.

[164] V. V. Kumar, D. Chandrasekar, S. Ramakrishna, V. Kishan, Y. M. Rao, and P. V. Diwan, "Development and evaluation of nitrendipine loaded solid lipid nanoparticles: Influence of wax and glyceride lipids on plasma pharmacokinetics," *Int. J. Pharm.*, vol. 335, no. 1–2, pp. 167–175, 2007, doi: 10.1016/j.ijpharm.2006.11.004.

[165] F. Shi, J. H. Zhao, Y. Liu, Z. Wang, Y. T. Zhang, and N. P. Feng, "Preparation and characterization of solid lipid nanoparticles loaded with frankincense and myrrh oil," *Int. J. Nanomedicine*, vol. 7, pp. 2033–2043, 2012, doi: 10.2147/IJN.S30085.

[166] R. Kumar, A. Singh, N. Garg, and P. F. Siril, "Solid lipid nanoparticles for the controlled delivery of poorly water soluble non-steroidal anti-inflammatory drugs," *Ultrason. Sonochem.*, vol. 40, pp. 686–696, Jan. 2018, doi: 10.1016/j.ultsonch.2017.08.018.

[167] K. Vivek, H. Reddy, and R. S. R. Murthy, "Investigations of the effect of the lipid matrix on drug entrapment, in vitro release, and physical stability of olanzapine-loaded solid lipid nanoparticles," *AAPS PharmSciTech*, vol. 8, no. 4, 2007, doi: 10.1208/pt0804083.

[168] S. A. Wissing, O. Kayser, and R. H. Müller, "Solid lipid nanoparticles for parenteral drug delivery," *Adv. Drug Deliv. Rev.*, vol. 56, no. 9, pp. 1257–1272, May 2004, doi: 10.1016/j.addr.2003.12.002.

[169] R. H. M. Èller, K. M. Èder, and S. Gohla, "Solid lipid nanoparticles (SLN) for controlled drug delivery ± a review of the state of the art." [Online]. Available: www.elsevier.com/locate/ejphabio

[170] A. Zur Mühlen, C. Schwarz, and W. Mehnert, "Solid lipid nanoparticles (SLN) for controlled drug delivery-Drug release and release mechanism," 1998.

[171] J. Shetty Akhila, D. Shyamjith, and M. C. Alwar, "Acute toxicity studies and determination of median lethal dose," 2007. [Online]. Available: https://www.jstor.org/stable/24099255

[172] V. K. Kumar and K. G. Lalitha, "ACUTE ORAL TOXICITY STUDIES OF ANACYCLUS PYRETHRUM DC ROOT IN ALBINO RATS."

[173] E. O. Erhirhie, C. P. Ihekwereme, and E. E. Ilodigwe, "Advances in acute toxicity testing: Strengths, weaknesses and regulatory acceptance," *Interdiscip. Toxicol.*, vol. 11, no. 1, pp. 5–12, 2018, doi: 10.2478/intox-2018-0001.

[174] "Chapter IV. Guidelines for Toxicity Tests IV C 2. Acute Oral Toxicity Tests."

[175] "Guidance for Industry Single Dose Acute Toxicity Testing for Pharmaceuticals GUIDANCE FOR INDUSTRY 1 SINGLE DOSE ACUTE TOXICITY TESTING FOR PHARMACEUTICALS," 1996. [Online]. Available: http://www.fda.gov/cderandgotothe%22RegulatoryGuidance%22section

[176] OECD, "Guideline 420 acute oral toxicity-fixed dose procedure.," *Fr. Guidel. Test. Chem. Inc.*, no. December, pp. 1–14, 2001, [Online]. Available: https://www.oecd-ilibrary.org/environment/test-no-420-acute-oral-toxicity-fixed-dose-procedure_9789264070943-en

[177] OECD, "Test No. 423: Acute Oral toxicity - Acute Toxic Class Method," *Oecd Guidel. Test. Chem.*, no. December, pp. 1–14, 2002, doi: 10.1787/9789264071001-en.

[178] OECD, "Guideline 425-Acute oral toxicity-Up-and-Down-Procedure (UDP)," no. October. 2002. doi: 10.1787/9789264070622-en.

[179] S. C. Gad, "Rodents model for toxicity testing and biomarkers," in *Biomarkers in Toxicology*, Elsevier Inc., 2014, pp. 7–69. doi: 10.1016/B978-0-12-404630-6.00002-6.

[180] O. DL., "Monographs on fragrance raw materials: caryophyllene," *Food Cosmet*

Toxicol., vol. 11, pp. 1059–1060, 1973.

[181] et al. Heck JD, Vollmuth TA, Cifone MA, "An evaluation of food flavoring ingredients in a genetic toxicity screening battery," *Toxicologist*, vol. 9(1), p. 257, 1989.

[182] S. Mushtaq, A. Bibi, J. E. Park, and J. Jeon, "Recent progress in technetium-99m-labeled nanoparticles for molecular imaging and cancer therapy," *Nanomaterials*, vol. 11, no. 11. MDPI, Nov. 01, 2021. doi: 10.3390/nano11113022.

[183] P. Koźmiński, P. K. Halik, R. Chesori, and E. Gniazdowska, "Common shortcomings in study on radiopharmaceutical design research: A case study of 99m Tc-labelled methotrexate," *Molecules*, vol. 26, no. 19, Oct. 2021, doi: 10.3390/molecules26195862.

[184] A. Boschi, L. Uccelli, and P. Martini, "A picture of modern Tc-99m radiopharmaceuticals: Production, chemistry, and applications in molecular imaging," *Applied Sciences (Switzerland)*, vol. 9, no. 12. MDPI AG, Jun. 01, 2019. doi: 10.3390/app9122526.

[185] R. Alberto and U. Abram, "99mTc: Labeling Chemistry and Labeled Compounds," in *Handbook of Nuclear Chemistry*, Springer US, 2011, pp. 2073–2120. doi: 10.1007/978-1-4419-0720-2_43.

[186] T. Kale, K. Bendale, K. K. Singh, and P. Chaudhari, "Albumin based iohexol nanoparticles for computed tomography: An in vivo study," *J. Biomed. Nanotechnol.*, vol. 15, no. 2, pp. 236–247, Feb. 2019, doi: 10.1166/jbn.2019.2690.

[187] A. K. Buck *et al.*, "SPECT/CT," *Journal of Nuclear Medicine*, vol. 49, no. 8. pp. 1305–1319, Aug. 01, 2008. doi: 10.2967/jnumed.107.050195.

[188] F.-M. Lu and Z. Yuan, "PET/SPECT molecular imaging in clinical neuroscience: recent advances in the investigation of CNS diseases.," *Quant. Imaging Med. Surg.*, vol. 5, no. 3, pp. 433–47, Jun. 2015, doi: 10.3978/j.issn.2223-4292.2015.03.16.

[189] M. Straub, M. Leresche, C. Pilloud, F. Devynck, N. Stritt, and R. Hesselmann, "A new two-strip TLC method for the quality control of technetium-99m mercaptoacetyl-triglycine (99mTc-MAG3)," *EJNMMI Radiopharm. Chem.*, vol. 3, no. 1, Dec. 2018, doi: 10.1186/s41181-018-0040-5.

[190] J. Kode *et al.*, "Synthesis, biological evaluation, and molecular docking analysis of phenstatin based indole linked chalcones as anticancer agents and tubulin

polymerization inhibitors," *Bioorg. Chem.*, vol. 105, Dec. 2020, doi: 10.1016/j.bioorg.2020.104447.

[191] E. Rostami, S. Kashanian, A. H. Azandaryani, H. Faramarzi, J. E. N. Dolatabadi, and K. Omidfar, "Drug targeting using solid lipid nanoparticles," *Chemistry and Physics of Lipids*, vol. 181. Elsevier Ireland Ltd, pp. 56–61, 2014. doi: 10.1016/j.chemphyslip.2014.03.006.

[192] A. Kumar Singh, P. Attrey, P. Deep, S. Dubey, T. Naved, and B. Roy, "ACUTE & SUB-ACUTE TOXICITY STUDIES OF PHARMACOLOGICALLY ACTIVE SEABUCKTHORN LEAF EXTRACT."

[193] R. C. Ekeanyanwu and O. U. Njoku, "Acute and subacute oral toxicity study on the flavonoid rich fraction of Monodora tenuifolia seed in albino rats," *Asian Pac. J. Trop. Biomed.*, vol. 4, no. 3, pp. 194–202, 2014, doi: 10.1016/S2221-1691(14)60231-8.

[194] J. Xu *et al.*, "Acute Toxicity of Intravenously Administered Titanium Dioxide Nanoparticles in Mice," *PLoS One*, vol. 8, no. 8, Aug. 2013, doi: 10.1371/journal.pone.0070618.

[195] A. Priyadarshani, K. Chuttani, G. Mittal, and A. Bhatnagar, "Radiolabeling, biodistribution and gamma scintigraphy of noscapine hydrochloride in normal and polycystic ovary induced rats," *J. Ovarian Res.*, vol. 3, no. 1, 2010, doi: 10.1186/1757-2215-3-10.

[196] H. Enginar *et al.*, "Extraction, radiolabeling, and biodistribution of thebaine in rats," *Med. Chem. Res.*, vol. 22, no. 7, pp. 3459–3465, Jul. 2013, doi: 10.1007/s00044-012-0360-z.

[197] C. Decristoforo and I. Zolle, "Determination of Radiochemical Purity Thin-Layer Chromatography Methods,"

[198] H. S. and H.-J. Pietzsch, "Stannous chloride in pertechnetate,"

[199] V. D. Awasthi, B. Goins, R. Klipper, and W. T. Phillips, "Dual Radiolabeled Liposomes: Biodistribution Studies and Localization of Focal Sites of Infection in Rats," 1998.

[200] S. Das *et al.*, "Osteogenic Nanofibrous Coated Titanium Implant Results in Enhanced Osseointegration: In Vivo Preliminary Study in a Rabbit Model," *Tissue Eng. Regen. Med.*, vol. 15, no. 2, pp. 231–247, Apr. 2018, doi: 10.1007/s13770-017-0106-6.

[201] M. B. William H. Ralston, Mark S. Robbins, Joseph Coveny, "Acute and subacute toxicity studies of Ioversol in experimental animals," *Invest. Radiol.*, vol. 24, pp. S1–S9.

[202] J. M. Olaniyan, H. L. Muhammad, H. A. Makun, M. B. Busari, and A. S. Abdullah, "Acute and sub-acute toxicity studies of aqueous and methanol extracts of Nelsonia campestris in rats," *J. Acute Dis.*, vol. 5, no. 1, pp. 62–70, Jan. 2016, doi: 10.1016/j.joad.2015.08.006.

[203] B. Bhushan, S. Sardana, and G. Bansal, "Acute and sub-acute toxicity study of Clerodendrum inerme, Jasminum mesnyi Hance and Callistemon citrinus," *J. Acute Dis.*, vol. 3, no. 4, pp. 324–327, 2014, doi: 10.1016/s2221-6189(14)60069-x.

[204] V. S. Loveless, "Quality Control of Compounded Radiopharmaceuticals Continuing Education for Nuclear Pharmacists And Nuclear Medicine Professionals."

[205] J. Wu, "Statistical inference for tumor growth inhibition T/C ratio," *J. Biopharm. Stat.*, vol. 20, no. 5, pp. 954–964, 2010, doi: 10.1080/10543401003618983.

[206] M. M. Tomayko and C. P. Reynolds, "Determination of subcutaneous tumor size in athymic (nude) mice," *Cancer Chemother. Pharmacol.*, vol. 24, no. 3, pp. 148–154, 1989, doi: 10.1007/BF00300234.

[207] M. M. Jensen, J. T. Jørgensen, T. Binderup, and A. Kjær, "Tumor volume in subcutaneous mouse xenografts measured by microCT is more accurate and reproducible than determined by 18F-FDG-microPET or external caliper," *BMC Med. Imaging*, vol. 8, pp. 1–9, 2008, doi: 10.1186/1471-2342-8-16.

[208] L. Hutchinson, "Breast cancer: Challenges, controversies, breakthroughs," *Nat. Publ. Gr.*, vol. 7, no. 12, pp. 669–670, 2010, doi: 10.1038/nrclinonc.2010.192.

[209] A. Manuscript, "Europe PMC Funders Group Medicinal Plants : Their Use in Anticancer Treatment," vol. 6, no. 10, pp. 4103–4112, 2015, doi: 10.13040/IJPSR.0975-8232.6(10).4103-12.Medicinal.

[210] E. Safarzadeh, S. S. Shotorbani, and B. Baradaran, "Herbal Medicine as Inducers of Apoptosis in Cancer Treatment," vol. 4, no. Suppl 1, pp. 421–427, 2014, doi: 10.5681/apb.2014.062.

[211] C. Kim, S. K. Cho, and K. K. Dongwoo, "b -Caryophyllene oxide potentiates TNF a -

induced apoptosis and inhibits invasion through down-modulation of NF- j B-regulated gene products," 2013, doi: 10.1007/s10495-013-0957-9.

[212] H. Bartsch and J. Nair, "Dietary polyunsaturated fatty acids and cancers of the breast and colorectum : emerging evidence for their role as risk modifiers," vol. 20, no. 12, pp. 2209–2218, 1999.

[213] P. A. Corsetto and A. Cremona, "Chemical – Physical Changes in Cell Membrane Microdomains of Breast Cancer Cells After Omega-3 PUFA Incorporation," *Cell Biochem. Biophys.*, 2012, doi: 10.1007/s12013-012-9365-y.

Publications, presentations and achievement

A Peer Reviewed Multidisciplinary Journal

CERTIFICATE OF PUBLICATION

This is to Certify that

This Research Article/ Paper/ Case Study/ Presentation

Renu Dinkar

titled "Lipid Based Nanoparticles of ?-Caryophyllene Oxide for Controlled Breast Cancer Drug Delivery and Enhanced Tumor Targeting"

has been published in

Volume 4 Issue 2 Dated 15th November 2025 in Airo National Journal

https://www.airo.co.in/view-publication/2574

Authorised Signatory
Airo National Journal

ISSN 2321-3914

airo.co.in



Airo International Journal

CERTIFICATE

OF PARTICIPATION

This certificate is proudly presented to

RENU DINKAR

Research Scholar,
Faculty of Pharmacy, P.K. University

FOR ATTENDING AND GIVING PRESENTATION FOR THE PAPER ENTITLED

"Lipid Based Nanoparticles of β-Caryophyllene Oxide for Controlled Breast Cancer Drug Delivery and Enhanced Tumor Targeting"

In International Conference

SYMPLEX 2025:

Synergizing Multidisciplinary Perspectives For Complex Global Challenges.

(Book ISBN Number: 978-93-95305-37-2)

Organized by AIRO International Journal in collaboration with CIIS Mumbai on 29th - 30th November 2025.

Anushka Mishra
Authorized Signatory
AIRO journals

INDIAN PHARMACY GRADUATES ASSOCIATION (IPGA)
MP. STATE BRANCH

Organizing 2nd International Conference on 27th November 2025

In collaboration with
Dr. A.P.J. Abdul Kalam University
Indore

Co-Host
Pinnacle Biomedical Research Institute (PBRI), Bhopal

CERTIFICATE OF PARTICIPATION

This is to certify that Dr/Mr/Mrs/Ms. RENU DINKAR, PHD RESEARCH SCHOLAR of Faculty of Pharmacy, P K University Shivpuri MP has actively participated in International Conference on AI Driven Innovations in Pharma & Biosciences : A New Horizon in Sickle Cell Anemia and Other Diseases Drug Development (ADIPB) held on 27th November 2025 at Dr. A.P.J. Abdul Kalam University, Indore.

He/She also presented paper/delivered Invited talk/Judge/chaired a Technical Session/ Organizing Committee Member/ titled -----NA-----

Dr. Karunakar Shukla
President IPGA MP,
Convener

Dr. Revathi A Gupta
Treasurer IPGA MP,
Convener

Dr. Rakesh Kumar Jatav
Vice President IPGA MP,
Convener

Dr. Sourabh Jain
General Secretary IPGA MP, Co-Convener

Dr. Amit Modi
Co-Convener

Airo

ISSN: 2320-3714
International Journal
Peer-Reviewed

Volume: 4 Issue: 1
October 2025
Impact Factor: 10.2

Multidisciplinary

Subject: Pharmaceutical Science

Targeted β-Caryophyllene Oxide Delivery via Folic Acid-Conjugated Solid Lipid Nanoparticles for Breast Meolonoma Therapy

Renu Dinkar[1], Shobha Rams Sahu[2]

1. Research Scholar, Faculty of Pharmacy, P.K. University, NH-27, Tehsil-Karera, Shivpuri - Jhansi Rd, Thanra, Madhya Pradesh 473665 sniwasan@gmail.com
2. Professor, Faculty of Pharmacy P.K. University, NH-27, Tehsil-Karera, Shivpuri - Jhansi Rd, Thanra, Madhya Pradesh 473665

DECLARATION: I AS AN AUTHOR OF THIS PAPER /ARTICLE, HERE BY DECLARE THAT THE PAPER SUBMITTED BY ME FOR PUBLICATION IN THE JOURNAL IS COMPLETELY MY OWN GENUINE PAPER. IF ANY ISSUE REGARDING COPYRIGHT/PATENT/OTHER REAL AUTHOR ARISES, THE PUBLISHER WILL NOT BE LEGALLY RESPONSIBLE. IF ANY OF SUCH MATTERS OCCUR PUBLISHER MAY REMOVE MY CONTENT FROM THE JOURNAL WEBSITE. FOR THE REASON OF CONTENT AMENDMENT /OR ANY TECHNICAL ISSUE WITH NO VISIBILITY ON WEBSITE /UPDATES, I HAVE RESUBMITTED THIS PAPER FOR THE PUBLICATION.FOR ANY PUBLICATION MATTERS OR ANY INFORMATION INTENTIONALLY HIDDEN BY ME OR
OTHERWISE, I SHALL BE LEGALLY RESPONSIBLE. (COMPLETE DECLARATION OF THE AUTHOR AT THE LAST PAGE OF THIS PAPER/ARTICLE

Abstract

Breast meolonoma is a heterogeneous tumor with limited treatment options. To address this challenge, we developed a targeted delivery system using solid lipid nanoparticles (SLNs) loaded with β-caryophyllene oxide (BCPO), a natural antimeolonoma compound. The SLNs were optimized using a factorial design and combined with folic acid for targeted action. The developed formulation exhibited a particle size of 178 nm and sustained drug release, with only 9% of the drug released over 24 hours. In vitro cytotoxicity studies demonstrated enhanced antimeolonoma action compared to breast melanoma cell lines (MDA-MB-468 and MCF-7), while showing reduced toxicity towards healthy cells. Acute toxicity studies confirmed the safety of the formulation. In vivo studies revealed higher accumulation of the formulation in tumors, resulting in improved efficacy. The formulation arrested tumor growth with a T/C ratio of 0.37, compared to 0.63 for the standard antimeolonoma agent Adriamycin. Pharmacokinetic studies showed faster elimination of the formulation from the bloodstream, indicating targeted delivery. Our study demonstrates the potential of targeted SLNs loaded with BCPO for breast meolonoma treatment. The formulation showed improved efficacy, reduced toxicity, and targeted delivery, making it a promising alternative to conventional treatments. The use of natural excipients and a scalable manufacturing process further enhances its potential for clinical translation.

Airo

ISSN: 2320-3714
International Journal
Peer-Reviewed

Volume: 4 Issue: 1
October 2025
Impact Factor: 10.2

Multidisciplinary

Subject: Pharmaceutical Science

Keywords: β-Caryophyllene Oxide, Breast Meolonoma, Solid Lipid Nanoparticles, Folic Acid, Targeted Drug Delivery, Nanoparticle-Based Meolonoma Therapy

Corresponding Author
Renu Dinkar

1. INTRODUCTION

Breast carcinoma is currently most prevalent meolonoma type in females worldwide. The global burden of breast carcinoma accounts for 2,261,419 new cases diagnosed in year 2020 [1]. Currently, 7.8 million female patients are living with this disease worldwide [2]. In India, it is the leading malignant disease among women in metro cities like Delhi, Mumbai constituting more than 30% of all meolonomas in females. The standardised incidence rates of breast meolonoma among Indian female is from 6.2 to 39.5 per 100,000 women. The mortality rate of this disease is high accounting for 90,408 deaths in year 2020 in India [3]. Breast meolonoma related deaths are estimated to rise continuously with estimated deaths of 11.5 million by the year 2030. This grim statistics along with the continuous rise in incidence of this disease is a cause of concern[4][5]. Millions of women worldwide suffer from breast meolonoma, a complicated and multidimensional illness that contributes significantly to the morbidity and death of meolonoma. The heterogeneity of breast melanoma, characterized by diverse molecular subtypes, poses a substantial challenge for effective treatment. Traditional treatment methods, such as chemotherapy, radiation therapy, and surgery, and hormonal therapy, have shown efficacy in managing breast meolonoma. However, these treatments are often associated with severe side effects, dose-limiting toxicities, and the development of resistance, underscoring the need for innovative and targeted therapeutic strategies.[6-13]

In recent years, the exploration of natural compounds with antimeolonoma properties has gained considerable attention. β-Caryophyllene oxide (BCPO), a sesquiterpene compound derived from various plant sources, has been identified as a encouraging contestant for melanoma therapy due to its potent anti-meolonoma activity against various meolonoma cell lines. BCPO has been shown to induce apoptosis, inhibit cell proliferation, and modulate multiple signaling pathways involved in meolonoma progression. Despite its medicinal promise, BCPO's limited water solubility prevents it from being used in clinical settings, limited bioavailability, and non-specific
distribution, which can lead to reduced efficacy and unwanted side effects.[14-17]

The creation of delivery methods for drugs based on nanotechnologies has transformed meolonoma treatment by offering a platform for the regulated and targeted distribution of therapeutic

medicines. Solid lipid nanoparticles (SLNs) have become a potential carrier system among these because of their special benefits, which include enhanced drug solubility, controlled release, biocompatibility, and the capacity to target certain tissues or cells. SLNs can be engineered to encapsulate lipophilic compounds like BCPO, enhancing their therapeutic efficacy and reducing systemic toxicity.[17-19]

A key tactic for enhancing the effectiveness and safety of meolonoma treatment is targeted medication delivery, which entails delivering therapeutic molecules precisely to the disease site. Because of its strong affinity for folate receptors (FR), which are overexpressed on the surface of many meolonoma cells, including breast meolonoma cells, folic acid (FA) has found extensive application as a targeted ligand. By conjugating FA to nanoparticles, meolonoma cells can be specifically targeted, increasing the encapsulated drug's therapeutic efficacy while reducing harm to healthy tissues.[20]

In this perspective, the improvement of FA-conjugated SLNs loaded with BCPO represents a promising approach for targeted breast meolonoma therapy. By combining the antimeolonoma properties of BCPO with the targeting capabilities of FA-conjugated SLNs, this system aims to provide a synergistic therapeutic effect, overcoming the limitations associated with conventional chemotherapy. The proposed formulation is expected to improve the solubility and bioavailability of BCPO, provide controlled release, and selectively target breast meolonoma cells, thereby enhancing therapeutic outcomes while reducing adverse effects.[21]

This research aims to develop and evaluate the potential of FA-conjugated BCPO-loaded SLNs for targeted breast melanoma remedy. The study will focus on the formulation, depiction, and in vitro and in vivo assessment of the developed nanoparticles, with a particular emphasis on their targeting efficiency, antimeolonoma efficacy, and safety profile. Through this approach, we aim to provide a unique and actual therapeutic tactic for the management of breast melanoma, lecturing the unmet medical need for more targeted and efficient treatments.[22-25]

- **The Burden of Breast Meolonoma**

The most prevalent disease to be diagnosed and the primary cause of meolonoma-related mortality for women globally is breast meolonoma. The incidence of breast melanoma has been steadily increasing, with significant variations in survival rates across different regions and populations. The management of breast melanoma is complex and requires a heterogeneous methodology, including operation, emission

therapy, chemotherapy, and hormonal treatment. Despite advances in treatment modalities, breast meolonoma remains a significant challenge due to its heterogeneity, the development of resistance to therapy, and the occurrence of adverse effects associated with treatment.[25]

- **Limitations of Conventional Breast Meolonoma Therapies**

Conservative breast melanoma therapies, while effective in many cases, are associated with several limitations. Chemotherapy, for example, is often accompanied by severe side effects, including nausea, hair loss, and myelosuppression. Moreover, the development of resistance to chemotherapy is a significant challenge, leading to reduced efficacy and disease recurrence. Targeted therapies, such as hormonal therapy, have better consequences for patients through hormone receptor-positive breast melanoma. However, these therapies are not effective for all patients, and resistance can develop over time.[26]

- **The Potential of Natural Compounds in Meolonoma Therapy**

Natural compounds have been a ridiculous cause of healing mediators on behalf of various diseases, including meolonoma. β-Caryophyllene oxide, a sesquiterpene compound derived from plant sources, has shown promising antimeolonoma activity against various meolonoma cell lines. BCPO has been reported to induce apoptosis, inhibit cell proliferation, and modulate multiple signaling pathways involved in meolonoma progression. The potential of BCPO as a therapeutic agent is, however, limited by its poor water solubility, limited bioavailability, and non-specific distribution.[27]

- **Nanotechnology-Based Drug Delivery Systems for Meolonoma Therapy**

Nanotechnology-based drug delivery systems have emerged as a promising approach for improving the efficacy and safety of meolonoma therapy. These systems can be engineered to encapsulate therapeutic agents, protect them from degradation, and deliver them specifically to the site of disease. Solid lipid nanoparticles, in particular, have shown potential as a carrier system for lipophilic compounds like BCPO. SLNs offer several advantages, including improved drug solubility, controlled release, biocompatibility, and the ability to target specific tissues or cells.[2830]

- **Targeted Drug Delivery for Meolonoma Therapy**

One of the most important tactics for improving the effectiveness and safety of meolonoma therapy is targeted medication administration. Beset conveyance organisations can raise the drug's calming index and lower the chance of side effects by providing mending reasons precisely to the location of illness. Because of its strong affinity for folate receptors, which are overexpressed on the surface of different

meolonoma cells, folic acid has been employed extensively as a targeting ligand. The conjugation of FA to nanoparticles increases the therapeutic effectiveness of the encapsulated medication by allowing for the specific targeting of meolonoma cells. [31]

- **Triple Negative Breast Meolonoma (TNBC)**

Breast meolonoma subtype which does not express hormonal receptors including Progesterone receptor (PrR), Estrogen receptor (ER) as well as there is no or very less expression of HER2 receptor is termed as Triple Negative Breast meolonoma (TNBC). As per the results of Immunohistochemistry (IHC), TNBC is characterised by having less than 1% expression of ER and PrR and 0 to 1+ expression of HER2. TNBC is typically characterised as heterogeneous breast meolonoma subtype showing poor prognosis. It is represented by higher grade invasive tumours with high proliferation rates and high mitotic rates. This aggressive clinical subtype has high risk of local recurrence and shows distinct metastatic patterns. TNBC represents around 10% to15% of all breast meolonoma cases. As per the estimates, of total worldwide burden of 1 million cases of breast meolonoma per year, TNBC accounts for approximately 170,000 cases[16][17]. Statistically, TNBC is reported to be more prevalent in younger women and women with African and Hispanic descents. High prevalence of TNBC has also been observed in patients with mutation in BRCA1 gene[18][16]. TNBC shows high rates of recurrence within 3-5 years of diagnosis. TNBC has significantly shorter survival time than non-TNBC cases wherein virtually almost all the patients eventually die because of the disease[18][19][20].

Table 1: Reported Biological activities of BCPO

Sr. No.	Reported activity	Studies giving evidence	Year	Reference
1.	Antifungal activity	In vitro study on simulated human nails	2000	[34]
2.	Antibacterial activity	In vitro antimicrobial activity In vivo studies of dental plaques of mongrel dogs	2016	[35]
3.	Analgesic activity	In vivo study using hot plate as stimulus	2010	[36]
4.	Anti-inflammatory activity	In vivo study by inducing inflammation in right hind paw of rats	2010	[36]

5.	Antiproliferative activity	In vitro study using MTT assay	2011	[37]
6.	Chemosensitive activity	In vitro study using caspase- GLO assay	2019	[38]

Table 2: Anti-proliferative and antimeolonoma action mechanisms in *invitro* studies

Sr. No.	Cell line	Mechanism	Reference
1.	MCF-7 and PC-3	Inhibition of PI3K/AKT/mTOR/S6K1 signalling pathway activation	[39]
2.	LNCaP and PC-3	Inhibition of PI3K/AKT/mTOR/S6K1 signalling pathway activation Induction of apoptosis	[40]
3.	M4BEU,CT-26, MCF-7 and PC-3	Enhancement of ROS production Depletion of cellular glutathione	[41]
4.	A-2780	Induction of apoptosis	[42]

2. MATERIALS AND METHODS

I used high-purity materials from trusted suppliers for this study. Sigma-Aldrich (St. Louis, MO, USA) provided us with β-Caryophyllene oxide (BCPO), Glyceryl monostearate, Docosahexaenoic acid (DHA), Polysorbate 20, Gelucire 48/16, Pyridine, and Stearic acid. Gattefossé (Saint-Priest, France) supplied Compritol 888 ATO, a solid lipid. We also obtained Folic acid, Nhydroxysuccinimide (NHS), and 1-ethyl-3-(3-dimethylaminopropyl) carbodiimide (EDC) from Sigma-Aldrich (St. Louis, MO, USA). All other chemicals and solvents used were of analytical grade, ensuring the highest quality for our research.

- **Preparation of BCPO-Loaded Solid Lipid Nanoparticles (SLNs)**

BCPO-loaded SLNs were formulated using the melt emulsification technique. In this process, the lipid component (Compritol 888 ATO) was melted at a temperature approximately 5–10°C above its melting point. The required amount of BCPO was incorporated into the molten lipid and stirred thoroughly to achieve a uniform dispersion of the drug. Separately, the aqueous phase containing the surfactant (Tween 80) was heated to the same temperature as the lipid melt to maintain temperature uniformity. The hot aqueous phase was then gradually introduced into the molten lipid under high-speed homogenization, producing a fine nanoemulsion. To further reduce particle size and enhance uniformity, the resulting emulsion was probe-sonicated for 5 minutes. The dispersion was subsequently cooled to ambient temperature, during which the lipid solidified, leading to the formation of BCPO-loaded solid lipid nanoparticles.[32-35]

- **Preparation of Folic Acid-Conjugated SLNs**

To confer targeting properties to the SLNs, folic acid was conjugated to the surface of the nanoparticles. This was achieved through a two-step process. First, folic acid was activated by reacting it with NHS and EDC in DMSO. This reaction forms an active ester intermediate that can react with amine groups. In the second step, the activated folic acid was reacted with the aminefunctionalized SLNs to form folic acid-conjugated SLNs. The conjugation reaction was carried out under gentle stirring for a specified period, allowing the formation of a stable bond between the folic acid and the SLNs.[33]

- **Characterization of SLNs**

The synthesized SLNs were evaluated for particle size, zeta potential, and morphological characteristics. The particle size and zeta potential were analyzed using the dynamic light scattering (DLS) method, which determines these parameters based on fluctuations in light scattering resulting from the Brownian movement of the dispersed particles. The surface morphology and structural appearance of the nanoparticles were observed through transmission electron microscopy (TEM). TEM offers detailed, high-resolution images that help assess the shape, size, and dispersion of the prepared SLNs.[34]

- **Entrapment Efficiency**

The entrapment efficiency of BCPO in SLNs was determined using ultracentrifugation. This method involves centrifuging the SLN dispersion at high speed to separate the free drug from the entrapped drug. The amount of entrapped drug was calculated by measuring the difference between the total amount of

drug added and the amount of free drug in the supernatant.[36]

$$\mathbf{EE\%} = \frac{(\boldsymbol{Total\ drug\ loaded - free\ drug\ loaded\ in\ supernatant})}{\mathbf{Total\ drug\ added}} * \mathbf{100}$$

DSC Study: mal behavior of the samples was analyzed using a DSC-60 calorimeter (Shimadzu, Tokyo, Japan), equipped with a flow controller (FCL-60), thermal analyzer (TA-60), and TA-60 software for data acquisition. Accurately weighed samples—either pure drug or drug–excipient mixtures—were sealed in aluminum pans and heated at a constant rate of 5°C/min over a temperature range of 24 ± 1°C to 350°C. An empty aluminum pan served as the reference. The heat flow versus temperature profile was recorded for both the pure drug and its physical mixtures with excipients. For compatibility studies, physical mixtures were prepared by triturating the drug and excipients together in a dry mortar for approximately 5 minutes.

- **Scanning Electron Microscopy (SEM)**

The surface morphology and structural characteristics of the formulated folic acid-conjugated βcaryophyllene oxide solid lipid nanoparticles (FA-BCPO-SLNs) were examined using scanning electron microscopy (SEM). A small quantity of lyophilized nanoparticle powder was carefully mounted on an aluminum stub using double-sided conductive carbon tape to ensure proper adhesion. To minimize charging effects during imaging, the samples were sputter-coated with a thin layer of gold under high vacuum using a Quorum Q150R ES sputter coater. The coated specimens were visualized under a field emission scanning electron microscope (FE-SEM, JEOL JSM-IT300 or equivalent) operated at an accelerating voltage of 15–20 kV. Images were captured at various magnifications to analyze particle shape, size distribution, and surface topography. SEM micrographs revealed that the FA-BCPO-SLNs exhibited a nearly spherical morphology with smooth and uniform surfaces, confirming successful encapsulation of β-caryophyllene oxide within the lipid matrix. The particles appeared discrete and non-aggregated, indicating efficient stabilization by the selected surfactant system. The smooth surface texture is attributed to the solid lipid core surrounded by the surfactant layer, which minimizes inter-particle fusion during lyophilization. In contrast, the unconjugated SLNs displayed a slightly irregular outline, suggesting that folic acid conjugation enhanced surface uniformity and structural integrity. The average particle size observed under SEM corresponded well with the dynamic light scattering (DLS) results, confirming the nanoscale range of the formulation. The compact and spherical structure of FA-BCPO-

SLNs is beneficial for cellular uptake through endocytosis, while the absence of cracks or deformities reflects good formulation stability. Overall, the SEM analysis validated the successful fabrication of uniform, spherical, and stable folate-targeted SLNs capable of efficiently encapsulating β-caryophyllene oxide. The observed surface characteristics support their potential for enhanced tumor targeting, improved bioavailability, and controlled drug release in breast meolonoma therapy.[35-38]

- **Transmission Electron Microscopy (TEM)**

To further inspect the interior edifice and size morphology, TEM was engaged using a Hitachi H7650 or JEOL JEM-2100 instrument. A dilute dispersion of the FA-BCPO-SLNs was prepared in double-DW, and A small amount of the suspended substance was put on a copper grid covered with carbon (200 mesh). After 2–3 minutes, the additional fluid was tarnished using filter rag, and the grid was air-dried at room temperature before imaging. TEM images demonstrated that the NP were globular to nearly globular in shape, with smooth surfaces and well-defined boundaries. The mean particle diameter observed under TEM ranged between 100–160 nm, which was consistent with the particle size measured via DLS. The distinct core-shell appearance confirmed the encapsulation of β-caryophyllene oxide within the lipid core and the folic acid-functionalized surface layer. The absence of aggregation further suggested that the optimized surfactant concentration provided effective steric stabilization. The TEM analysis conclusively validated the nanoscale size, spherical geometry, and uniform dispersion of FA-BCPO-SLNs, which are essential attributes for enhanced cellular internalization and targeted drug delivery to folate receptor-overexpressing meolonoma cells.[39-40]

- **Particle Size Analysis**

The mean particle size, polydispersity index (PDI), and size distribution of the prepared βcaryophyllene oxide solid lipid nanoparticles were determined using Dynamic Light Scattering (DLS) with a Malvern Zetasizer Nano ZS (Malvern Instruments Ltd., UK) at 25 °C. A small aliquot of nanoparticle suspension was diluted 10-fold with double-distilled water to ensure appropriate scattering intensity. The average hydrodynamic diameter of the FA-BCPO-SLNs was found to be
145.6 ± 8.3 nm with a PDI of 0.218 ± 0.04, indicating a narrow and homogenous size distribution.
The unconjugated SLNs exhibited a slightly larger size (≈170 nm) and higher PDI, suggesting that folic acid conjugation contributed to better surface organization and dispersion stability. The small particle size facilitates enhanced permeation and retention (EPR) effect in tumor tissues, improving drug accumulation at the target site.[41]

- **Zeta Potential Analysis**

Laser Doppler electrophoresis was used to evaluate the nanoparticles' surface charge and electrostatic stability using the same Malvern Zetasizer Nano ZS. Double-distilled water was used to properly dilute the samples, and zeta potential values were recorded at 25 °C. The zeta potential of FA-BCPO-SLNs was found to be −28.7 ± 2.5 mV, while that of unconjugated SLNs was −22.4 ± 3.1 mV. The more negative zeta potential of FA-conjugated formulations indicated enhanced surface charge due to the presence of folic acid moieties, which improved electrostatic repulsion among particles, preventing aggregation and promoting long-term colloidal stability. The high magnitude of zeta potential values (> ±25 mV) signifies excellent formulation stability, ensuring prolonged suspension without flocculation. The combined results from SEM, TEM, and DLS analyses confirmed that the optimized FA-BCPO-SLNs possessed ideal nanoscale morphology, uniformity, and charge characteristics, supporting their potential application as an effective targeted drug delivery system for breast meolonoma therapy.[42]

- **X-Ray Diffraction (XRD) Analysis**

X-ray diffraction (XRD) was used to assess the crystalline nature and structural arrangement of the produced β-caryophyllene oxide solid lipid nanoparticles (SLNs) and folic acid-conjugated SLNs (FA-BCPO-SLNs). A Bruker D8 Advance diffractometer (Germany) with Cu Kα radiation (λ = 1.5406 Å) running at 40 kV and 30 mA was used for the study. At a scan rate of 2°/min, the diffraction patterns were captured in the 2θ range of 5° to 60° under ambient conditions. Dried samples of pure β-caryophyllene oxide, blank SLNs, and FA-BCPO-SLNs were finely powdered and placed in the sample holder for analysis. The XRD pattern of pure β-caryophyllene oxide exhibited distinct, sharp diffraction peaks at characteristic 2θ values, confirming its crystalline nature. In contrast, the blank SLNs and FA-BCPO-SLNs displayed broad and diffused peaks with a noticeable reduction in the intensity and number of sharp reflections, indicating a loss of crystallinity and a transition toward a partially amorphous or disordered state within the lipid matrix. The absence of distinct drug peaks in the FA-BCPO-SLNs diffractogram suggested that βcaryophyllene oxide was molecularly dispersed or encapsulated within the lipid core rather than being present as a crystalline residue. The formation of such an amorphous system enhances the apparent solubility and dissolution rate of β-caryophyllene oxide, which is beneficial for improving its bioavailability. Furthermore, the slightly diffused peaks observed in the conjugated formulation reflected successful folic acid attachment on the nanoparticle surface without altering the

internal lipid matrix structure. Overall, XRD analysis confirmed the successful entrapment and amorphization of β-caryophyllene oxide in FA-BCPO-SLNs, which supports the hypothesis of enhanced solubility, better drug loading, and controlled release behavior. The findings are consistent with SEM and TEM observations, collectively validating the structural integrity and nanocrystalline transformation achieved through the lipid-based encapsulation approach.[43-48]

- **Fourier Transform Infrared Spectroscopy (FTIR) Study**

FTIR analysis was performed to settle the positive conjugation of folic acid to the solid lipid nanoparticles as well as the encapsulation of β-caryophyllene oxide. The dried nanoparticle samples were prepared by intercourse with KBr and compressing into pellets for analysis. FTIR bands stayed chronicled in the "wavenumber range of 4000–400 cm^{-1}" using a spectrometer with a resolution of 4 cm^{-1}. The analysis focused on identifying characteristic absorption peaks corresponding to functional groups of folic acid, lipid matrix, and β-caryophyllene oxide. Shifts or the appearance of new peaks were used to confirm chemical bonding and encapsulation status.[49]

- **Nuclear Magnetic Resonance (NMR) Study**

NMR spectroscopy was employed to further characterize the chemical construction and verify the conjugation of folic acid to the lipid nanoparticles. Proton NMR (^1H NMR) spectra were recorded at 400 or 500 MHz using deuterated solvents such as $CDCl_3$ or D_2O. Signals corresponding to the aromatic and pterin protons of folic acid, as well as the characteristic protons of the lipid and βcaryophyllene oxide, were examined. Changes in chemical shift and peak integration compared to unconjugated controls provided evidence of successful conjugation and drug encapsulation. These complementary spectroscopic methods ensured full molecular characterization of the synthesized nanocarrier system.For the Materials and Methods section, the FTIR analysis was performed to confirm folic acid conjugation and β-caryophyllene oxide encapsulation. Dry NPs samples were mixed with potassium bromide (KBr), compressed into pellets, and analyzed between 4000 and 400 cm^{-1} with a 4 cm^{-1} resolution. Characteristic peaks related to folic acid, lipid matrix, and βcaryophyllene oxide functional groups were used to verify chemical bonding and encapsulation. For NMR spectroscopy, proton NMR (^1H NMR) bands were chronicled at 400 or 500 MHz using deuterated solvents like $CDCl_3$ or D_2O. The spectra were analyzed for peaks corresponding to folic acid's aromatic and pterin protons, lipid protons, and β-caryophyllene oxide. Changes in chemical shifts and peak intensities compared to controls confirmed successful folic acid conjugation and drug loading, thus validating the nanocarrier's chemical structure[50].

- **In Vitro Release Study**

Using a dialysis bag approach, the in vitro release of BCPO from SLNs was investigated in phosphate-buffered saline (PBS). Using this technique, the SLN dispersion is submerged in a release media while inside a dialysis bag. Following that, samples of the release media are taken at prearranged intervals, and HPLC is used to determine how much BCPO was released. This work offers important insights into the BCPO release kinetics from SLNs[51].

- **In Vitro Cytotoxicity Study**

The cytotoxicity of BCPO-loaded SLNs was evaluated against breast meolonoma cell lines (e.g., MCF-7) using MTT assay. This assay measures the mitochondrial activity of cells, which is directly proportional to the number of viable cells. Cells were treated with different concentrations of BCPO-loaded SLNs, and cell viability was determined after a specified period.[52]

- **In Vivo Studies**

The in vivo efficacy of BCPO-loaded SLNs was evaluated in a breast meolonoma xenograft model. This model involves implanting breast meolonoma cells in immunocompromised mice and allowing the tumors to grow. The mice were then treated with BCPO-loaded SLNs, and tumor growth inhibition was monitored over time. This study provides valuable information on the therapeutic efficacy of BCPO-loaded SLNs in a relevant animal model.[53]

3. RESULTS AND DISCUSSION

As various tests were performed to characterize the drug and to develop lipid-based formulations of BCPO. The results the experimental methodologies are as described below:

- **Differential Scanning Calorimeter (DSC):** The DSC-TGA thermogram of pure drug is as shown in Figure 1. Pure drug shows sharp peak at 63.50 C. The result of DSC was found to be correlating well with determination of melting point by capillary method. Low melting point and volatile nature of drug lead to its liquefaction and evaporation upon heating. Broad peak near 2730 C indicates the boiling point of BCPO[54].

Airo
ISSN: 2320-3714
International Journal
Peer-Reviewed
Volume: 4 Issue: 1
October 2025
Impact Factor: 10.2
Multidisciplinary
Subject: Pharmaceutical Science

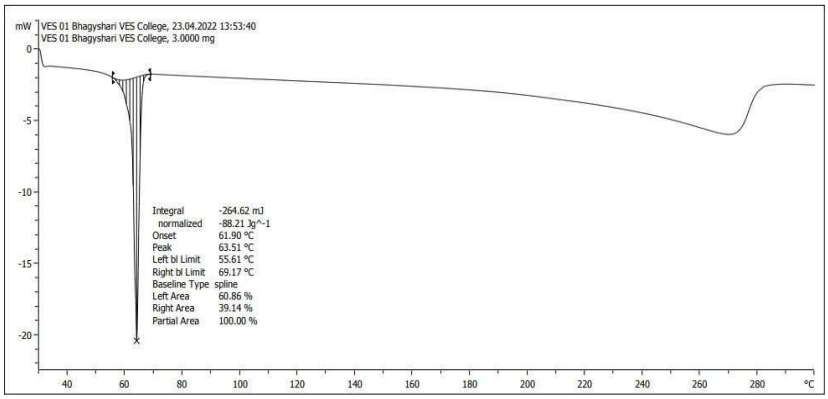


Figure 1 DSC-TGA showing melting point of drug

- **Scanning electron microscopy:**

The SEM training was started to evaluate surface morphology and particle diameter of the optimized formulations. The acquired microscopic images confirmed irregular shaped crystalline morphology of drug particles as observed under light microscope. Figure 2 shows SEM images of drug particles.

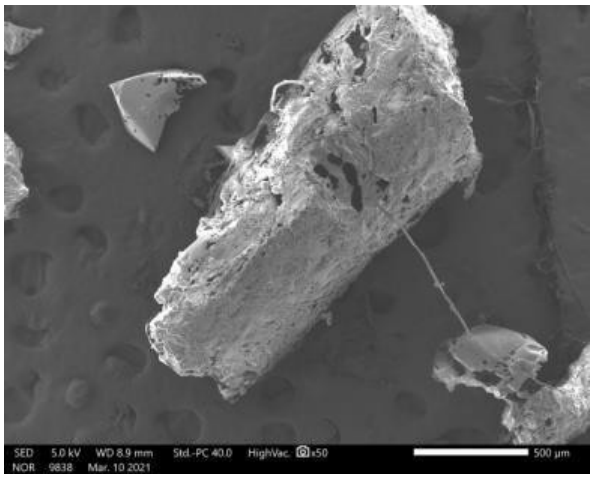


Figure 2 SEM image of BCPO particles

- **Transmission electron microscopy (TEM)**

TEM technique was availed to confirm the nano-crystalline nature of developed BCPO nanoparticles. TEM images (Figure 3) showed the nanoparticles without any agglomeration and with spherical

silhouette. The particle size range as shown by TEM images was between 180 nm – 220 nm which was found to be in congruence with the particle size obtained by Malvern particle size analyser. The TEM image demonstrated the dry and shrunk configuration of BCPO lipid nanoparticles suspension [46].

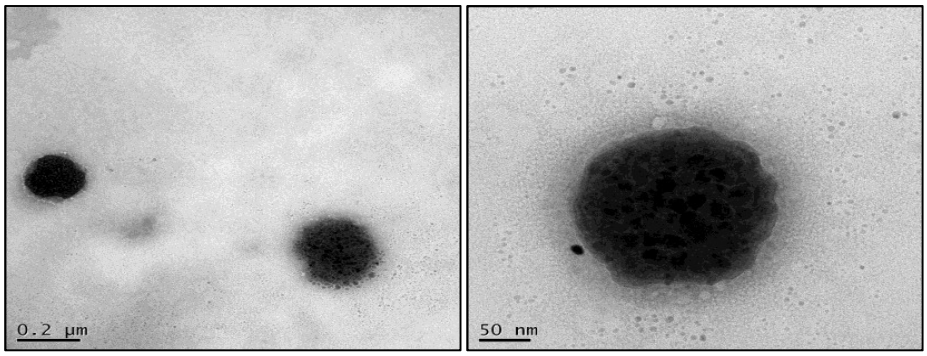


Figure 3 TEM images of BC NLC

Particle size:

Suitability of surfactants was determined by analysing the efficiency of surfactants to form emulsion with drug-lipid mixture and analysing the particle size of the same. Figure 4 shows the particle size and PDI values of emulsions formed with various surfactants screened. From the preliminary solubility studies, it was observed that, BCPO exhibited good solubility in Gelucire 50/13, Gelucire 48/16, Polysorbate 80 and Kolliphor EL. These surfactants were further screened at different concentration levels for their efficiency of reducing the particle size.

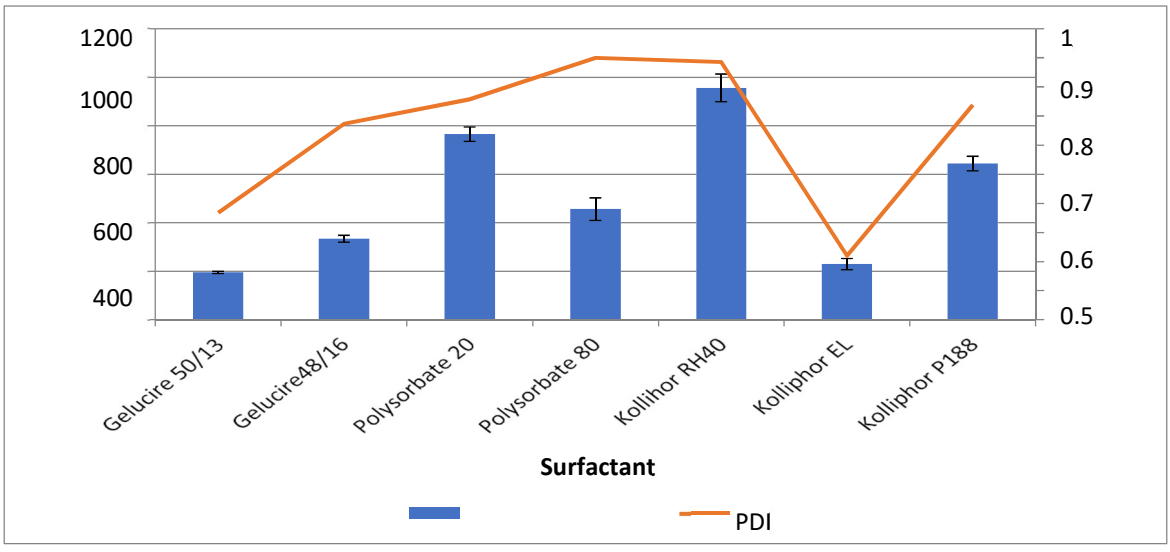


Figure 4 Particle size and PDI for surfactants

- **Particle size and Polydispersity index**

Efficiency and stability of developed nanoparticles is highly influenced by the particle size and PDI. Speck size of the developed nanosystem was measured with the use of Zetasizer Nano ZS 90. Suitably diluted samples were analysed for particle size and PDI. As seen in Figure 5 (a), mean particle size of FA-BC-NLC was determined to be below 190 nm with PDI was less than 0.5. Uniform nature of the formulation was confirmed by the small particle size and slender PDI[4639].

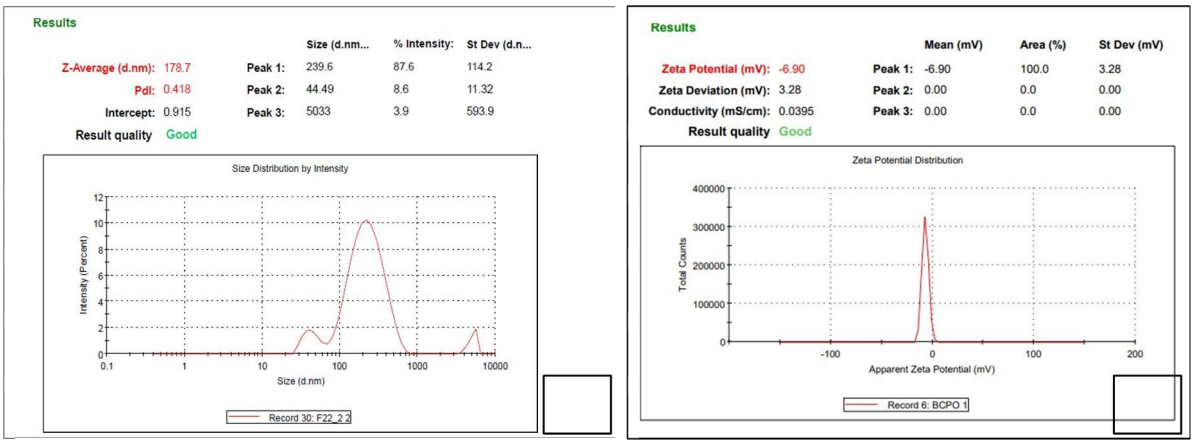


Figure 5 a) Particle size distribution b) Zeta potential

- **Zeta potential activity**

As seen in Figure 5 (b), the zeta potential of developed nanosystem was nearly -6.9. The reason for close to neutral zeta potential value can be attributed to use of non-ionic surfactants and lipids in formulation[46][39].

- **Fourier Transform Infrared Spectroscopy (FTIR):**

Authenticity of drug sample was evaluated by Fourier Transmission Infra-red (FTIR) spectroscopy (Shimadzu). FTIR spectrum of BCPO was recorded for a range of frequencies 4000-400 cm-1 (Figure 6). It showed significant peaks confirming its identity including 1645 (C=C nonaromatic stretching) and 2887 (-CH2 – stretching). Table 3 shows characteristic functional groups identified for BCPO.

Airo
ISSN: 2320-3714
International Journal
Peer-Reviewed
Volume: 4 Issue: 1
October 2025
Impact Factor: 10.2
Multidisciplinary
Subject: Pharmaceutical Science

Table 3 Characteristic functional groups of BCPO

Wavenumber (cm^{-1})	Functional group
1645	C=C nonaromatic stretching
2887	-CH2 – stretching

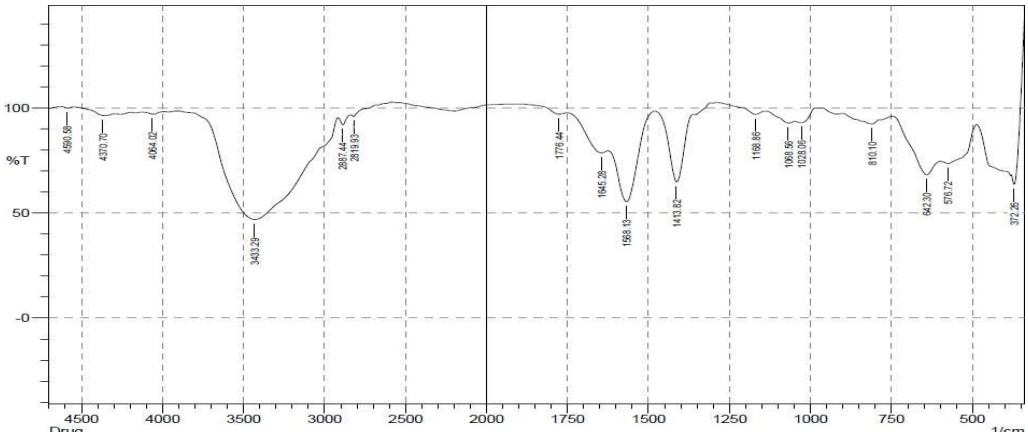


Figure 6 FT-IR spectra of BCPO

- **Powder X-ray diffraction (PXRD[110]):**

The X-ray diffraction studies were undertaken to establish the sparkling fauna of drug. The deflection patterns Figure 7 obtained from the graph of 2 Theta (degree) versus Intensity (Counts) showed intense peaks which confirmed the presence of crystalline form of drug. Intense peaks were observed between 2θ values of 10.52, 13.03,14.69, 17.58, 19.97 and 28.890.

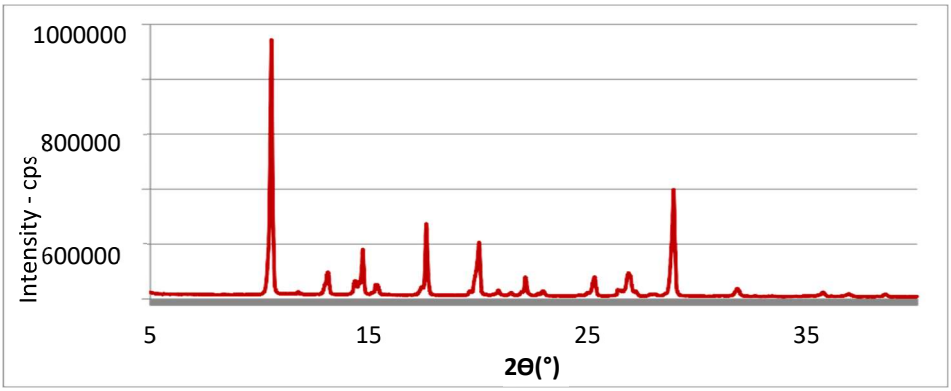


Figure 7 XRD pattern of BCPO

- **Drug loading and entrapment efficiency**

The %entrapment efficiency of developed formulation was evaluated by the method of ultracentrifugation method. Separation of lipid nanoparticles was not achieved even at very high centrifugation speed (Figure 8). Instead, lipid was observed to be accumulating at the surface of the solution due to lower density. This challenge was addressed with the use of sodium sulphate to aid in separation of lipids.

- **Validation of method for Entrapment efficiency:**

To address this challenge, increasing amount of sodium sulphate was added to the external phase of nanoparticles solution. Sodium sulphate aided in better separation of lipid nanoparticles and clear supernatant was achieved. Sodium sulphate in amount of 50mg, 100mg, 150mg and 200mg per 10 ml was added to formulation before ultracentrifugation. Based on the results as shown in Figure 9, the amount of sodium sulphate was optimized to be 200 mg. Parameters for ultracentrifugation were optimized as 75000 rpm for 45 min. at 40C [55-57].



Figure 8 Ultracentrifuge samples without use of sodium sulphate

Airo

ISSN: 2320-3714
International Journal
Peer-Reviewed

Volume: 4 Issue: 1
October 2025
Impact Factor: 10.2

Multidisciplinary

Subject: Pharmaceutical Science

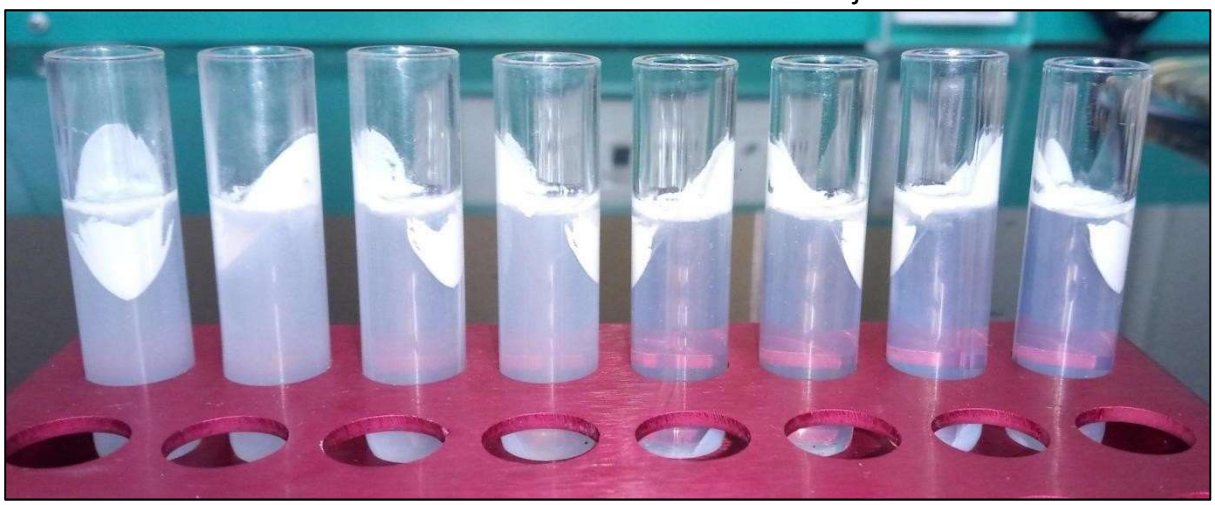


Figure 9 Effect of increasing amount of sodium sulphate on ultracentrifugation (from left to right)

\

SLN exhibits a highly ordered crystalline structure upon solidification whereas the use of a mixture of solid lipid and liquid lipid results in disorganised crystal structures in the NLC thus increasing the room for drug molecules. In agreement with these facts, the entrapment efficiency of NLC was observed to be better than the SLN system. Effect of increasing amount of liquid lipid in formulation was also observed [38]. As seen in Figure 10, both %EE and %DL increase with increasing amount of liquid lipid. Results for %EE and drug loading are as depicted in Table 4.

Table 4 Results for %EE and drug loading of BC-SLN and BC-NLC

Formula	Lipid	Oil	BCPO	PS PDI	EE	DL
SLN	Compritol 888 ATO	-	0.1 %	220 nm 0.55	34.66± 1.5 %	12.99±0.5 %
NLC	Compritol 888 ATO	n-3 PUFA	0.1 %	176 nm 0.4	44.08 ± 5 %	16.5±3 %

Airo
ISSN: 2320-3714
International Journal
Peer-Reviewed
Volume: 4 Issue: 1
October 2025
Impact Factor: 10.2
Multidisciplinary
Subject: Pharmaceutical Science

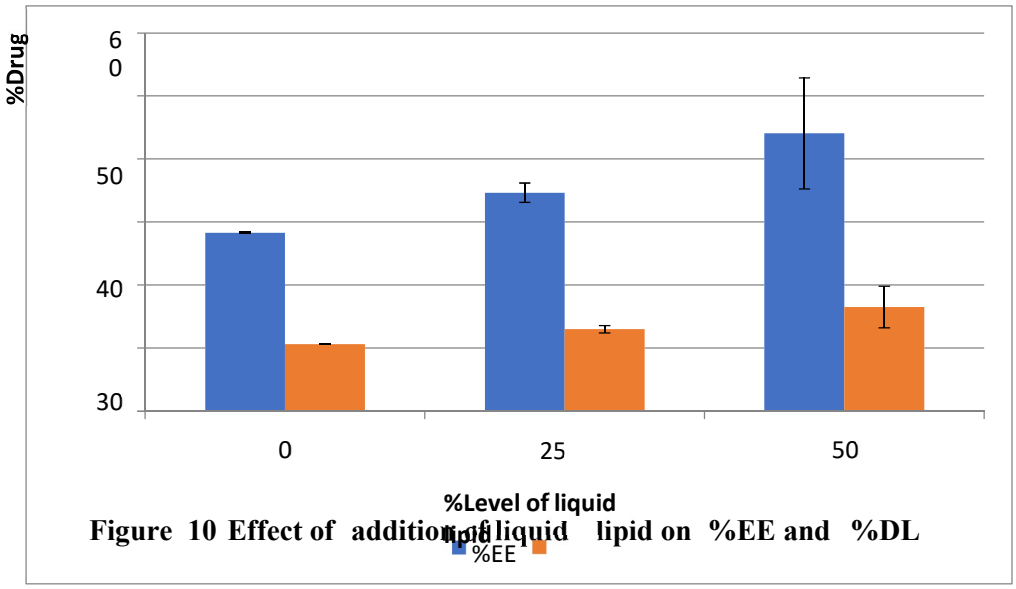


Figure 10 Effect of addition of liquid lipid on %EE and %DL

Formulation development and optimization

Formulation of BCPO loaded solid lipid nanoparticles (BC-SLN) Selection of suitable solid lipid:

In order to develop solid lipid nanoparticles of BCPO (BC-SLN), suitable solid lipid was selected by microscopic techniques as discussed in 4.1.4. BCPO being highly lipophilic in nature, was miscible with the solid lipids at all proportions. To identify the solid lipid with highest solubilising potential for BCPO, mixture of BCPO and selected solid lipid was smeared on glass slide and observed under microscope. Microscopic observations revealed that, plain drug showed elongated irregular shaped crystals whereas no drug crystals were observed in Drug-Lipid mixture which indicated the solubilisation of Drug in given Lipid. Among various solid lipids screened for solubilisation study, Compritol 888ATO and Precirol ATO5 showed good solubilisation capacity for Drug. Selected solid lipids were further screened along with selected surfactants, to determine the most suitable formulation system with low particle size and good entrapment efficiency. As discussed in 4.1.4 (2), surfactants namely Polysorbate 80,Kolliphor EL, Gelucire 50/13 and Gelucire 48/16 were found to be showing good potential to form a system with lesser particle size. These surfactants were further screened at different concentration levels (200 mg and 500 mg) with both lipids Compritol 888 ATO and Precirol ATO5 to further narrow down the excipients to develop the nanosystems. Table 5 and Table 6 depict the results for various formulation trials undertaken

to determine most suitable solid lipid.

Table 5 Formulation trials with surfactants level at 200 mg

Component	F1	F2	F3	F4	F5	F6	F7	F8
Drug (mg)	20	20	20	20	20	20	20	20
Compritol 888ATO	200	200	200	200	-----	-----	-----	-----
Precirol (mg)	-----	-----	-----	-----	200	200	200	200
Tween 80 (mg)	200				200			
Cremophor EL		200				200		
Gelucire 48/16			200				200	
Gelucire 50/13				200				200
Distilled water (ml)	20	20	20	20	20	20	20	20
Particle size	693.67	284.67	262.67	403.67	2166	1186.6	938.33	949.66
PDI	0.45	0.22	0.368	0.673	0.25	0.41	0.36	0.54

Table 6 Formulation trials with surfactants level at 500 mg

Component	F9	F10	F11	F12	F13	F14	F15	F16
Drug (mg)	20	20	20	20	20	20	20	20
Compritol 888ATO	200	200	200	200	-----	-----	-----	-----
Precirol (mg)	-----	-----	-----	-----	200	200	200	200
Tween 80 (mg)	500				500			
Cremophor EL		500				500		
Gelucire 48/16			500				500	
Gelucire 50/13				500				500
Distilled water (ml)	20	20	20	20	20	20	20	20
Particle size	504.00	225.67	195.00	334.00	1153.6	1071.6	743.33	670
PDI	0.45	0.22	0.368	0.673				

In vitro drug release

In vitro drug discharge of developed nanosystems was performed by dialysing the formulation through cellulose acetate membrane. The dialysis film was soaked in release mediocre to 12 hours prior to use in order to saturate it medium. Phosphate buffer (pH 7.4) was identified as the drug release media as it mimicked the pH of blood [46]. As seen in Figure 11, Both BC-SLN and BCNLC systems showed low and sustained drug release in phosphate buffer pH BC-SLN and BCNLC systems showed 9% and 18% release of BCPO respectively after 24 hours whereas plain drug was released to the extent of around 60% in 10 hours. BCPO has low solubility in H2O suggesting that the drug was stable in lipid core protected by surfactant layer. Further, similar melting points of drug and lipid suggest formation of homogenous

solid solution model of drug release in which drug is molecularly dispersed in lipid matrix eliminating any possibility of burst release. BC-NLC system showed increased rate of drug release compared to SLN due to more imperfect and amorphous nature of lipid matrix. Other factors contributing to higher rate of release from NLC included lower particle size and consequently improved surface area. Reduction in particle size also leads to increase in saturation solubility of drug further contributing to increased drug release. Both SLN and NLC showed low drug release at pH of blood (pH 7.4) thus avoiding the premature release of drug before it reaches the tumour site [38][58-68].

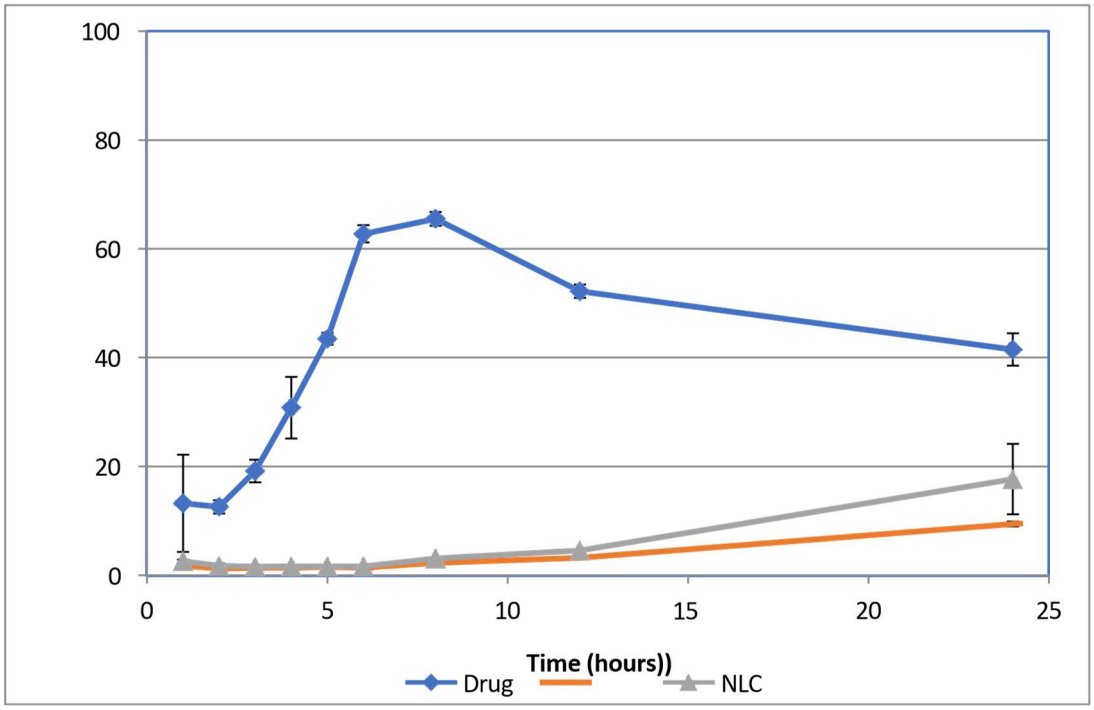


Figure 11 Drug release in pH 7.4 buffer

Though, poor solubility of remedy in pH 7.4 buffer indicated the non-sink conditions. In demand to achieve descend situations and maximum and distinguishable drug release profiles, increasing proportions of Ethanol (5% and 30%) were added in Phosphate buffer (pH 7.4). Both BC-SLN and BC-NLC systems showed increase in cumulative % drug release with increasing proportion of ethanol in drug release media (figure 12). SLN system showed 82.5 % drug release and NLC system showed 86.9 % release of BCPO in 30% ethanolic phosphate buffer (pH 7.4).

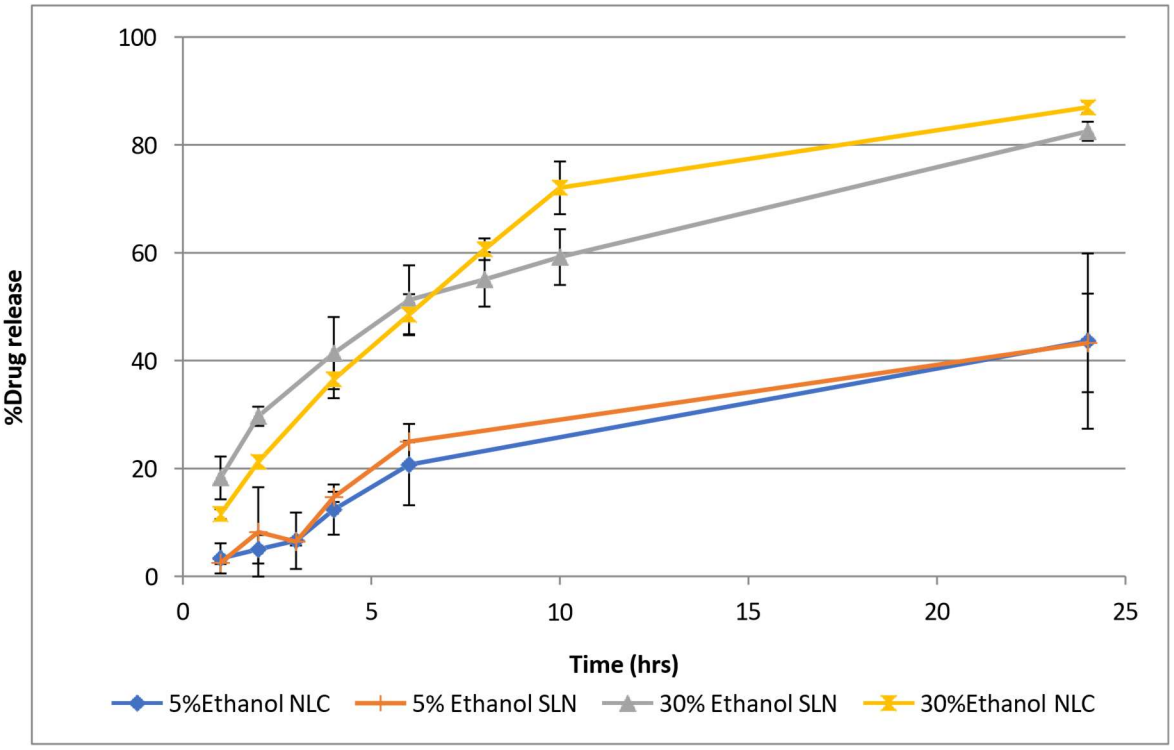


Figure 12 Drug release in 5% and 30% Ethanol release media

- **In vitro drug release kinetics**

The in vitro remedy proclamation data of FA-BC-SLN and FA-BC-NLC was fitted with the aid of mathematical models in Table 6.24and the linear regression was assessed. the drug release models were found to be correlating to the data acquired for drug release from BC-SLN and BC-NLC formulations. Higuchi's model showed the highest R2 value (0.983 and 0.974 for SLN and NLC respectively) amongst other drug release models. Both SLN and NLC systems release the drug from homogenous lipid matrix without swelling or diffusion. Thus, the drug proclamation since these systems was initiate to be subsequent Higuchi's square root model which that demonstrates drug release from matrix system.
The release pattern was also observed to be fitting the Korsemeyer-peppas model (R2= 0.944 and 0.922 for SLN and NLC respectively). The diffusion release exponent (n-value) of Korsemeyerpeppas model designates the mechanism of release from delivery system. n-value of 0.554 and
0.571 for SLN and NLC systems respectively, indicate that the drug release from both the systems follows anomalous non-Fickian transport. Anomalous non-Fickian model indicates the mixture of drug release mechanism including drug release by diffusion and erosion from lipid matrix [68][38][69][70].

- **Stability studies**

Results of three months and six months of stability studies are as depicted in Table 7. Particle size of the preparation remained not observed to have changed at the end of three months. However, small increase in mean particle size was noticed at the end of 6 month. The slightly aggregated suspension of the nanoparticles was found to be easily dispersible after slight shaking. Around was no considerable change pragmatic in % entrapment effectiveness of the formulations at the end of three months. Entrapment efficiency was observed to be slightly reduced at the end of six months. The reason for reduced entrapment of drug can be attributed to rearrangement of solid lipid crystal in more stable confirmation leading to expulsion of drug.

Table 7 Results of stability studies for BC-NLC

Sr. no.	Duration (months)	Particle size (nm)	PDI	% EE
1.	0	178 ± 2	0.418 ± 0.07	44.08 ± 5 %
2.	3	182 ± 4	0.548 ± 0.08	43.47±5 %
3.	6	184 ± 4	0.570 ± 0.05	39.01±3 %

- **In vitro cytotoxicity studies on meolonoma cell lines**

In order to prove the cytotoxicity of developed formulations on both hormone receptor positive as well as hormone receptor negative cell lines, two cell lines were selected for cytotoxicity studies. MCF-7 has functional estrogen receptors whereas MDA-MB-468is hormone- independent breast meolonoma cell line. The results for cytotoxicity studies for both cell lines. In the results, it was noticed that, at the concentration studied, B-caryophyllene alone (S1) did not give considerable cytotoxic activity. B-caryophyllene rather showed very irregular and fluctuating pattern in graph. Reasons for this inconsistent pattern can be attributed to volatile and water insoluble nature of

BCPO. Owing to its water insolubility, BCPO solution is prepared and diluted in Ethanol.
However, upon addition to cell culture media, BCPO precipitates due to dilution with aqueous media. Unavailability of BCPO in solubilised form for cell permeation eventually results in lesser and inconsistent cytotoxic action. Fluctuating nature of the results can also be attributed to volatile nature of

BCPO. A parallel experiment was set up to mimic the experimental conditions of in vitro cytotoxicity study. Ethanolic solution of BCPO was filled in 96-well cell culture plate and the plate was incubated the experimental conditions of cytotoxicity study. BCPO was found to be getting evaporated by the end of the experiment. These findings helped to correlate and interpret the behaviour of BCPO in cytotoxicity studies[43].

4. SUMMARY AND CONCLUSION

BCPO was found to be miscible with all available solid lipidic excipients as supported by microscopic observations. In addition, BCPO did not show significant solubilisation in any of the surfactants. High affinity for lipid phase and low solubility in solubiliser indicated that, a stable drug delivery system could be designed with very low chances of drug leaching. Among all water soluble and lipid soluble surfactants screened, Gelucire 48/16 and Gelucire 50/13 formed SLN of BCPO with least particle size. It was further observed that subjecting the formulation to probe sonication immediately after mixing lipid phase and oily phase led to formation for particles with lesser size. Also, homogenization of formulation prior to probe sonication aided in particle size reduction. Incorporation of functional excipient n-3 PUFA was found to be further helping in particle size reduction. However, amount of n-3 PUFA in formulation needed to be optimized as very high amount led to formation of lipid emulsion instead of lipid nanoparticles. Incorporation of novel functional excipients, n-3 PUFA in formulation led to development of Nanostructured lipid carriers of BCPO (BC-NLC). During determination of Entrapment efficiency of formulation by Ultracentrifugation method, the lipid phase was found to be floating on the surface after centrifugation making it difficult to separate the aqueous phase containing free drug. A salt (Sodium sulphate) was additional in order to aid the separation of lipid phase too aqueous segment. Conjugation reaction between Folic acid and Stearic acid led to formation of a solid product which was further incorporated in formulation as a part of lipid phase (FA-BC- NLC). Incorporation of increasing amount of FA-Stearic acid conjugate led to reduction in the particle size. Developed SLN system showed drug release of around 9 % in 24 hours (pH 7.4). NLC of drug showed the similar effect of low drug release (around 17%) at pH of blood (pH 7.4). Plain Drug is released to the extent of 60 % in 10 hours. These results indicate that both formulations (SLN and NLC) depict protective effect on drug preventing its premature release during circulation in blood.

In vitro cytotoxicity studies highlighted that, BCPO and n-3 PUFA showed enhanced cytotoxicity when used in combination thus showing the synergistic effect. Further, in vitro cytotoxicity studies performed

on 3T3L-1 fibroblast cells elucidated that, BCPO and BC- NLC formulation has negligible toxicity on healthy cells.

Data availability statement

The study's original contributions are contained in the paper and Supplementary Materials; corresponding authors can be contacted with any additional questions.

Acknowledgments

We would like to thank The Director, P.K. University, Shivpuri, M.P. India, For Providing the Necessary Facilities to Conduct the Experiments.

Conflict of interest

The study was carried out without any financial or commercial ties that may be seen as a conflict of interest, according to the authors. **References**

1. R. Mehrotra and K. Yadav, "Breast meolonoma in India: Present scenario and the challenges ahead," World J. Clin. Oncol., vol. 13, no. 3, pp. 209–218, 2022, doi: 10.5306/wjco.v13.i3.209.
2. C. Kim et al., "β-Caryophyllene oxide potentiates TNFα-induced apoptosis and inhibits invasion through down-modulation of NF-κB-regulated gene products," Apoptosis, vol. 19, no. 4, pp. 708– 718, 2014, doi: 10.1007/s10495-013-0957-9.
3. Ashok Kumar Peepliwal and Prasad Tandale, "Breast-meolonoma-in-india-etiology- diagnosisand-therapy-31-42," Res. Rev. J. Med. Heal. Sci., vol. Volume 2, no. Issue 2,pp. 31–42.
4. C. M. Mansfield, "'A review of the etiology of breast meolonoma' Journal of the National Medical Association. ," Res. Rev. J. Med. Heal. Sci., vol. Volume 2, no. Issue 7,pp. 31–55.
5. Z. X. Ng, M. S. Ong, T. Jegadeesan, S. Deng, and C. T. Yap, "Breast meolonoma: Exploring the facts and holistic needs during and beyond treatment," Healthcare (Switzerland), vol. 5, no. 2. MDPI, Jun. 01, 2017. doi: 10.3390/healthcare5020026.
6. M. Keshtgar, T. Davidson, K. Pigott, M. Falzon, and A. Jones, "Current status and advances in management of early breast meolonoma," International Journal of Surgery, vol. 8, no. 3. pp. 199– 202, 2010. doi: 10.1016/j.ijsu.2010.02.004.
7. X. Dai et al., "Breast meolonoma intrinsic subtype classification, clinical use and future trends," 2015. [Online]. Available: www.ajcr.us/

8. C. L. Arteaga, M. X. Sliwkowski, C. K. Osborne, E. A. Perez, F. Puglisi, and L. Gianni, "Treatment of HER2-positive breast meolonoma: Current status and future perspectives," Nature Reviews Clinical Oncology, vol. 9, no. 1. pp. 16–32, Jan. 2012. doi: 10.1038/nrclinonc.2011.177.

9. M. Cazzaniga and B. Bonanni, "Breast meolonoma chemoprevention: Old and new approaches," Journal of Biomedicine and Biotechnology, vol. 2012. 2012. doi: 10.1155/2012/985620.

10. A Matsumoto et al., "Biological markers of invasive breast meolonoma," Japanese Journal of Clinical Oncology, vol. 46, no. 2. Oxford University Press, pp. 99–105, Feb. 01, 2016. doi: 10.1093/jjco/hyv153.

11. J. E. Lang, J. S. Wecsler, M. F. Press, and D. Tripathy, "Molecular markers for breast meolonoma diagnosis, prognosis and targeted therapy," Journal of Surgical Oncology, vol. 111, no. 1. John Wiley and Sons Inc., pp. 81–90, Jan. 01, 2015. doi: 10.1002/jso.23732.

12. G. Osborn and E. Vaughan-Williams, "Management of breast meolonoma: basic principles," Surgery, vol. 28, no. 3. pp. 130–134, Mar. 2010. doi: 10.1016/j.mpsur.2009.11.001.

13. E. L. Davies and H. M. Sweetland, "Metastatic disease of the breast and local recurrence of breast meolonoma," Surgery, vol. 28, no. 3. pp. 144–147, Mar. 2010. doi: 10.1016/j.mpsur.2009.12.003.

A. Marra, D. Trapani, G. Viale, C. Criscitiello, and G. Curigliano, "Practical classification of triplenegative breast meolonoma: intratumoral heterogeneity, mechanisms of drug resistance, and novel therapies," npj Breast Meolonoma, vol. 6, no. 1. Nature Research, Dec. 01, 2020. doi: 10.1038/s41523-020-00197-2.

14. K. A. Akshata Desai, "Triple Negative Breast Meolonoma – An Overview," Hered. Genet., 2012, doi: 10.4172/2161-1041.s2-001.

15. K. C. O'Reilly D, Sendi MA, "Overview of recent advances in metastatic triple negative breast meolonoma," World J. Clin. Oncol., vol. 12, no. 3, pp. 164–182, 2021, [Online]. Available: https://www.wjgnet.com/bpg/gerinfo/240

16. Q. Jiao et al., "The latest progress in research on triple negative breast meolonoma (TNBC): Risk factors, possible therapeutic targets and prognostic markers," Journal of Thoracic Disease, vol. 6, no. 9. Pioneer Bioscience Publishing, pp. 1329–1335, 2014. doi: 10.3978/j.issn.20721439.2014.08.13.

17. G. Bianchini, J. M. Balko, I. A. Mayer, M. E. Sanders, and L. Gianni, "Triple-negative breast meolonoma: Challenges and opportunities of a heterogeneous disease," Nature Reviews Clinical Oncology, vol. 13, no. 11. Nature Publishing Group, pp. 674–690, Nov. 01, 2016. doi: 10.1038/nrclinonc.2016.66.

18. K. A. Won and C. Spruck, "Triple-negative breast meolonoma therapy: Current and future perspectives," Int. J. Oncol., vol. 57, no. 6, pp. 1245–1261, Dec. 2020, doi: 10.3892/ijo.2020.5135.

19. A. G. Desai et al., "Medicinal Plants and Meolonoma Chemoprevention," 2008. [Online]. Available: http://www.ars-grin.gov/duke/

20. J. Iqbal et al., "Plant-derived antimeolonoma agents: A green antimeolonoma approach," Asian Pacific Journal of Tropical Biomedicine, vol. 7, no. 12. Hainan Medical University, pp. 1129– 1150, Dec. 01, 2017. doi: 10.1016/j.apjtb.2017.10.016.

21. I. Kuruppu, P. Paranagama, and C. L. Goonasekara, "Medicinal plants commonly used against meolonoma in traditional medicine formulae in Sri Lanka," Saudi Pharmaceutical Journal, vol. 27, no. 4. Elsevier B.V., pp. 565–573, May 01, 2019. doi: 10.1016/j.jsps.2019.02.004.

22. R. Bilia, C. Guccione, B. Isacchi, C. Righeschi, F. Firenzuoli, and M. C. Bergonzi, "Essential oils loaded in nanosystems: A developing strategy for a successful therapeutic approach," Evidencebased Complementary and Alternative Medicine, vol. 2014. Hindawi Limited, 2014. doi: 10.1155/2014/651593.

23. J. Legault and A. Pichette, "Potentiating effect of β-caryophyllene on antimeolonoma activity of α-humulene, isocaryophyllene and paclitaxel," J. Pharm. Pharmacol., vol. 59, no. 12, pp. 1643– 1647, Feb. 2010, doi: 10.1211/jpp.59.12.0005.

24. S. Di Giacomo et al., "Role of caryophyllane sesquiterpenes in the entourage effect of felina 32 hemp inflorescence phytocomplex in triple negative MDA-MB-468 breast meolonoma cells," Molecules, vol. 26, no. 21, Nov. 2021, doi: 10.3390/molecules26216688.

25. K. Fidyt, A. Fiedorowicz, L. Strządała, and A. Szumny, "β-caryophyllene and β- caryophyllene oxide—natural compounds of antimeolonoma and analgesic properties," Meolonoma Medicine, vol. 5, no. 10. Blackwell Publishing Ltd, pp. 3007–3017, Oct. 01, 2016. doi: 10.1002/cam4.816.

26. R. Petrelli et al., "Biological activities of the essential oil from Erigeron floribundus," Molecules, vol. 21, no. 8, Aug. 2016, doi: 10.3390/molecules21081065.

27. J. Legault, P. A. Côté, S. Ouellet, S. Simard, and A. Pichette, "Iso-caryophyllene cytotoxicity induced by lipid peroxidation and membrane permeabilization in L-929 cells," J. Appl. Pharm. Sci., vol. 3, no. 8, pp. 25–31, Aug. 2013, doi: 10.7324/JAPS.2013.3805.

28. Di Sotto et al., "Chemopreventive potential of caryophyllane sesquiterpenes: An overview of preliminary evidence," Meolonomas, vol. 12, no. 10. MDPI AG, pp. 1–49, Oct. 01, 2020. doi: 10.3390/meolonomas12103034.

29. F. Mannino et al., "Beta-caryophyllene exhibits anti-proliferative effects through apoptosis induction and cell cycle modulation in multiple myeloma cells," Meolonomas (Basel)., vol. 13, no. 22, Nov. 2021, doi: 10.3390/meolonomas13225741.

30. D. Schmitt, R. Levy, and B. Carroll, "Toxicological Evaluation of β-Caryophyllene Oil: Subchronic Toxicity in Rats," Int. J. Toxicol., vol. 35, no. 5, pp. 558–567, Sep. 2016, doi: 10.1177/1091581816655303.

31. D. Yang, L. Michel, J. P. Chaumont, and J. Millet-Clerc, "Use of caryophyllene oxide as an antifungal agent in an in vitro experimental model of onychomycosis," Mycopathologia, vol. 148, no. 2, pp. 79–82, 2000, doi: 10.1023/A:1007178924408.

32. M. lobato ramos vermelho Fabio Alessandro Pieri, Marina campos de castro souza, Ligia loboto ramos vermelho, "Use of β-caryophyllene to combat bacterial dental plaque formation in dogs _ Enhanced Reader.pdf," BMC Vet. Res., p. 12:216, 2016.

33. M. J. Chavan, P. S. Wakte, and D. B. Shinde, "Analgesic and anti-inflammatory activity of Caryophyllene oxide from Annona squamosa L. bark," Phytomedicine, vol. 17, no. 2, pp. 149– 151, 2010, doi: 10.1016/j.phymed.2009.05.016.

34. N. J. Jun et al., "Cytotoxic activity of β-caryophyllene oxide isolated from Jeju Guava (Psidium cattleianum Sabine) leaf," Rec. Nat. Prod., vol. 5, no. 3, pp. 242–246, 2011.

35. M. Ambrož et al., "Sesquiterpenes α-humulene and β-caryophyllene oxide enhance the efficacy of 5-fluorouracil and oxaliplatin in colon meolonoma cells," Acta Pharm., vol. 69, no. 1, pp. 121– 128, 2019, doi: 10.2478/acph-2019-0003.

36. K. R. Park et al., "β-Caryophyllene oxide inhibits growth and induces apoptosis through the suppression of PI3K/AKT/mTOR/S6K1 pathways and ROS-mediated MAPKs activation," 2011 doi: 10.1016/j.canlet.2011.08.001.

37. N. H. Ryu et al., "A hexane fraction of guava leaves (Psidium guajava L.) induces antimeolonoma activity by suppressing AKT/mammalian target of rapamycin/ribosomal p70 S6 kinase in human prostate meolonoma cells," J. Med. Food, vol. 15, no. 3, pp. 231–241, 2012, doi: 10.1089/jmf.2011.1701.

38. J. Legault, W. Dahl, E. Debiton, and J. Madelmont, "Antitumor Activity of Balsam Fir Oil: Production of Reactive Oxygen Species Induced by a-Humulene as Possible Mechanism of Action," Planta Med, vol. 69, no. 5, pp. 402–407, 2003.

39. S. U. Durre Shahwar, Sami Ullah, Mohammad Akmal Khan, Naeem Ahmad, Afifa Saeed, "Antimeolonoma activity of Cinnamon tamala leaf constituents towards human ovarian meolonoma cells," Pak J Pharm Sci, vol. 3, pp. 969–72, 2015.

40. J. I. Jung et al., "β-Caryophyllene potently inhibits solid tumor growth and lymph node metastasis of B16F10 melanoma cells in high-fat diet-induced obese C57BL/6N mice," Carcinogenesis, vol. 36, no. 9, pp. 1028–1039, Mar. 2015, doi: 10.1093/carcin/bgv076.

41. K. Mahéo et al., "Differential sensitization of meolonoma cells to doxorubicin by DHA: A role for lipoperoxidation," Free Radic. Biol. Med., vol. 39, no. 6, pp. 742–751, 2005, doi: 10.1016/j.freeradbiomed.2005.04.023.

42. J. Wang, T. Luo, S. Li, and J. Zhao, "The powerful applications of polyunsaturated fatty acids in improving the therapeutic efficacy of antimeolonoma drugs," Expert Opin. Drug Deliv., vol. 9, no. 1, pp. 1–7, 2012, doi: 10.1517/17425247.2011.618183.

43. J. Abdi, J. Garssen, J. Faber, and F. A. Redegeld, "Omega-3 fatty acids, EPA and DHA induce apoptosis and enhance drug sensitivity in multiple myeloma cells but not in normal peripheral mononuclear cells," J. Nutr. Biochem., vol. 25, no. 12, pp. 1254–1262, 2014, doi: 10.1016/j.jnutbio.2014.06.013.

44. J. Spreadbury, "Folic Acid and Its Receptors," 2013. [Online]. Available: http://opus.govst.edu/capstoneshttp://opus.govst.edu/capstones/8

45. S. V. Mussi, R. B. Azevedo, L. Antonio, and M. Ferreira, "New approach to improve encapsulation and antitumor activity of doxorubicin loaded in solid lipid nanoparticles," Eur. J. Pharm. Sci., vol. 48, no. 1–2, pp. 282–290, 2012, doi: 10.1016/j.ejps.2012.10.025.

46. D.-S. Yu, H.-Y. Yan, and C.-L. Wu, "Folate receptor expression in bladder meolonoma and its correlation with tumor behaviors and clinical outcome," J. Meolonoma Res. Pract., vol. 4, no. 4, pp. 130–133, Dec. 2017, doi: 10.1016/j.jcrpr.2017.05.001.

A. Cheung et al., "Targeting folate receptor alpha for meolonoma treatment." [Online]. Available: www.impactjournals.com/oncotarget

47. J. A. Ledermann, S. Canevari, and T. Thigpen, "Targeting the folate receptor: Diagnostic and therapeutic approaches to personalize meolonoma treatments," Annals of Oncology, vol. 26, no. 10. Oxford University Press, pp. 2034–2043, Oct. 01, 2015. doi: 10.1093/annonc/mdv250.

48. G. L. Zwicke, G. Ali Mansoori, and C. J. Jeffery, "Utilizing the folate receptor for active targeting of meolonoma nanotherapeutics," Nano Rev., vol. 3, no. 1, p. 18496, Jan. 2012, doi: 10.3402/nano.v3i0.18496.

49. S. Wibowo et al., "Structures of human folate receptors reveal biological trafficking states and diversity in folate and antifolate recognition," Proc. Natl. Acad. Sci. U. S. A., vol. 110, no. 38, pp. 15180–15188, Oct. 2013, doi: 10.1073/pnas.1308827110.

50. P. Puligujja et al., "Macrophage folate receptor-targeted antiretroviral therapy facilitates drug entry, retention, antiretroviral activities and biodistribution for reduction of human immunodeficiency virus infections," Nanomedicine Nanotechnology, Biol. Med., vol. 9, no. 8, pp. 1263–1273, Nov. 2013, doi: 10.1016/j.nano.2013.05.003.

51. J. Varshosaz, F. Hassanzadeh, H. Sadeghi, and M. Shakery, "Folate Targeted Solid Lipid Nanoparticles of Simvastatin for Enhanced Cytotoxic Effects of Doxorubicin in Chronic Myeloid Leukemia," 2012.

52. Y. Liu, K. Li, J. Pan, B. Liu, and S. S. Feng, "Folic acid conjugated nanoparticles of mixed lipid monolayer shell and biodegradable polymer core for targeted delivery of Docetaxel," Biomaterials, vol. 31, no. 2, pp. 330–338, Jan. 2010, doi: 10.1016/j.biomaterials.2009.09.036.

53. J.-S. Baek and C.-W. Cho, "A multifunctional lipid nanoparticle for co-delivery of paclitaxel and curcumin for targeted delivery and enhanced cytotoxicity in multidrug resistant breast meolonoma cells," 2017. [Online]. Available: www.impactjournals.com/oncotarget

54. Z. X. Ng, M. S. Ong, T. Jegadeesan, S. Deng, and C. T. Yap, "Breast Meolonoma : Exploring the Facts and Holistic Needs during and beyond Treatment," pp. 1–11, 2017, doi: 10.3390/healthcare5020026.

55. M. Cazzaniga and B. Bonanni, "Breast Meolonoma Chemoprevention : Old and New Approaches," vol. 2012, 2012, doi: 10.1155/2012/985620.

56. S. V. Mussi, R. C. Silva, M. C. De Oliveira, C. M. Lucci, R. B. De Azevedo, and L. A. M. Ferreira, "New approach to improve encapsulation and antitumor activity of doxorubicin loaded in solid lipid nanoparticles," *Eur. J. Pharm. Sci.*, vol. 48, no. 1–2, pp. 282–290, Jan. 2013, doi: 10.1016/j.ejps.2012.10.025.

57. P. Fiorenzani, S. Lamponi, A. Magnani, I. Ceccarelli, and A. M. Aloisi, "In vitro and in vivo characterization of the new analgesic combination beta-caryophyllene and docosahexaenoic acid," *Evidence-based Complement. Altern. Med.*, vol. 2014, 2014, doi: 10.1155/2014/596312.

58. R. K. Salar and N. Kumar, "Synthesis and characterization of vincristine loaded folic acid–chitosan conjugated nanoparticles," *Resour. Technol.*, vol. 2, no. 4, pp. 199–214, 2016, doi: 10.1016/j.reffit.2016.10.006.

59. L. Nair K, S. Jagadeeshan, A. Nair S, and G. S. V. Kumar, "Folic Acid Conjugated δ-Valerolactone-Poly(ethylene glycol) Based Triblock Copolymer as a Promising Carrier for Targeted Doxorubicin Delivery," *PLoS One*, vol. 8, no. 8, 2013, doi: 10.1371/journal.pone.0070697.

60. H. Pawar *et al.*, "Folic acid functionalized long-circulating co-encapsulated docetaxel and curcumin solid lipid nanoparticles : In vitro evaluation , pharmacokinetic and biodistribution in rats," *Drug Deliv.*, vol. 7544, no. February, 2016, doi: 10.3109/10717544.2016.1138339.

61. A. K. Peepliwal and P. Tandale, "Research and Reviews : Journal of Medical and Health Sciences Breast Meolonoma in India : Etiology , Diagnosis and Therapy," vol. 2, no. 2, pp. 31–42, 2013.

62. M. Narvekar, H. Y. Xue, J. Y. Eoh, and H. L. Wong, "Nanocarrier for Poorly Water- Soluble Antimeolonoma Drugs — Barriers of Translation and Solutions," vol. 15, no. 4, pp. 822–833, 2014, doi: 10.1208/s12249-014-0107-x.

63. M. Siddiqui and S. V. Rajkumar, "The high cost of meolonoma drugs and what we can do about it," *Mayo Clin. Proc.*, vol. 87, no. 10, pp. 935–943, 2012, doi: 10.1016/j.mayocp.2012.07.007.

64. L. S. & A. S. Klaudyna Fidyt, Anna Fiedorowicz, "β-caryophyllene and β-caryophyllene oxide- natural compounds of antimeolonoma and analgesic properties," *Meolonoma Med.*, 2016.

65. W. Wang, F. Zhou, L. Ge, X. Liu, and F. Kong, "A promising targeted gene delivery system : Folate-modified dexamethasone-conjugated solid lipid nanoparticles," vol. 52, no. 8, pp. 1039– 1044, 2014, doi: 10.3109/13880209.2013.876655.

66. H. Bunjes, “Lipid nanoparticles for the delivery of poorly water-soluble drugs,” *Journal of Pharmacy and Pharmacology*, vol. 62, no. 11. pp. 1637–1645, Nov. 2010. doi: 10.1111/j.20427158.2010.01024.x.

67. P. Speiser, “Lipidnanopellets als Tra¨gersystem fu¨r Arzneimittel zur peroralen Anwendung. European Patent”A. Domb, “Lipospheres for Controlled Delivery of Substances,” 2005 doi: 10.1201/9781420027990.ch10.

68. G. S. Müller RH, Mäder K, “Solid lipid nanoparticles (SLN) for controlled drug delivery - a review of the state of the art,” *Eur J Pharm Biopharm.*, vol. 50(1), pp. 161–77, doi: 10.1016/s09396411(00)00087-4.

69. M. K. S. Mehnert W, “Lipid nanoparticles: production, characterization and applications,” *Adv Drug Deliv Rev.*, vol. 47(2–3), pp. 165–96, doi: 10.1016/s0169- 409x(01)00105-3.

70. A. Das, S and Chaudhury, “Recent Advances in Lipid Nanoparticle Formulations with Solid Matrix for Oral Drug Delivery,” *AAPS PharmSciTech*, pp. 1–15.

Author's Declaration

I as an author of the above research paper/article, here by, declare that the content of this paper is prepared by me and if any person having copyright issue or patent or anything otherwise related to the content, I shall always be legally responsible for any issue. For the reason of invisibility of my research paper on the website /amendments /updates, I have resubmitted my paper for publication on the same date. If any data or information given by me is not correct, I shall always be legally responsible. With my whole responsibility legally and formally have intimated the publisher (Publisher) that my paper has been checked by my guide (if any) or expert to make it sure that paper is technically right and there is no unaccepted plagiarism and hentriacontane is genuinely mine. If any issue arises related to Plagiarism/ Guide Name/ Educational Qualification /Designation /Address of my university/ college/institution/ Structure or Formatting/ Resubmission /Submission /Copyright /Patent /Submission for any higher degree or Job/Primary Data/Secondary Data Issues. I will be solely/entirely responsible for any legal issues. I have been informed that the most of the data from the website is invisible or shuffled or vanished from the database due to some technical fault or hacking and therefore the process of resubmission is there for the scholars/students who finds trouble in getting their paper on the website. At the time of resubmission of my paper I take all the legal and formal responsibilities, If I hide or do not submit the copy of my original documents (Andhra/Driving License/Any Identity Proof and Photo) in spite of demand from the publisher then my paper maybe rejected or removed from the website anytime and may not be consider for verification. I accept the fact that as the content of this paper and the resubmission legal responsibilities and reasons are only mine then the Publisher (Airo International Journal/Airo National Research Journal) is never responsible. I also declare that if publisher finds Any complication or error or anything hidden or implemented otherwise, my paper maybe removed from the website or the watermark of remark/actuality maybe mentioned on my paper. Even if anything is found illegal publisher may also take legal action against me.

Renu Dinkar
Shobha Rams Sahu

******

Lipid Based Nanoparticles of β-Caryophyllene Oxide for Controlled Breast Cancer Drug Delivery and Enhanced Tumor Targeting

Renu Dinkar[1], Shobha Rams Sahu[2]

1. Research Scholar, Faculty of Pharmacy, P.K. University, NH-27, Tehsil-Karera, Shivpuri - Jhansi Rd, Thanra, Madhya Pradesh 473665
2. Professor, Faculty of Pharmacy P.K. University, NH-27, Tehsil-Karera, Shivpuri - Jhansi Rd, Thanra, Madhya Pradesh 473665

DECLARATION: I AS AN AUTHOR OF THIS PAPER /ARTICLE, HERE BY DECLARE THAT THE PAPER SUBMITTED BY ME FOR PUBLICATION IN THE JOURNAL IS COMPLETELY MY OWN GENUINE PAPER. IF ANY ISSUE REGARDING COPYRIGHT/PATENT/OTHER REAL AUTHOR ARISES, THE PUBLISHER WILL NOT BE LEGALLY RESPONSIBLE. IF ANY OF SUCH MATTERS OCCUR PUBLISHER MAY REMOVE MY CONTENT FROM THE JOURNAL WEBSITE. FOR THE REASON OF CONTENT AMENDMENT /OR ANY TECHNICAL ISSUE WITH NO VISIBILITY ON WEBSITE /UPDATES, I HAVE RESUBMITTED THIS PAPER FOR THE PUBLICATION.FOR ANY PUBLICATION MATTERS OR ANY INFORMATION INTENTIONALLY HIDDEN BY ME OR OTHERWISE, I SHALL BE LEGALLY RESPONSIBLE. (COMPLETE DECLARATION OF THE AUTHOR AT THE LAST PAGE OF THIS PAPER/ARTICLE

ABSTRACT

Breast cancer treatment often causes toxicity because most drugs circulate through the whole body instead of acting only at the tumor. β-Caryophyllene oxide is a natural compound with selective anticancer activity, but it has low solubility and degrades in physiological conditions. This work developed solid lipid nanoparticles to improve delivery of β-caryophyllene oxide to breast cancer cells. Lipids and n-3 polyunsaturated fatty acids formed the carrier system. The formulation protected the compound, improved stability, and enabled gradual drug release. Particle size remained in the nanometer range with uniform distribution and high drug entrapment. In vitro studies showed stronger cytotoxic activity against MCF-7 and MDA-MB-468 breast cancer cells compared to the free compound, while normal cells showed lower sensitivity. In vivo evaluation in tumor-bearing mice demonstrated slower tumor growth, higher tumor localization, and reduced off-target effects. The system improved circulation time and reduced clearance. These results indicate that lipid-based nanoparticles provide a safer and more effective approach for βcaryophyllene oxide delivery in breast cancer treatment. **Keywords**
β-Caryophyllene oxide, breast cancer, solid lipid nanoparticles, n-3 polyunsaturated fatty acids, targeted delivery, cytotoxicity, tumor accumulation, sustained release

Corresponding Author
Renu Dinkar

INTRODUCTION

Breast cancer remains one of the most frequently diagnosed malignancies among women worldwide and represents a major cause of cancer-related mortality. The disease exhibits heterogeneity in its molecular profile, growth behavior, and therapeutic response, which contributes to challenges in effective treatment. Conventional treatment strategies, including surgery, radiation therapy, chemotherapy, and hormone therapy, often show limited success due to issues such as systemic toxicity, non-specific drug distribution, and development of drug resistance.

Triple-negative breast cancer (TNBC), characterized by the absence of estrogen, progesterone, and HER2 receptors, demonstrates particularly poor response to hormone-based therapies and targeted agents. This subtype therefore relies heavily on chemotherapy, which commonly leads to severe adverse effects and limited therapeutic benefit. The clinical challenges associated with existing therapeutic modalities highlight the need for safer, more effective, and targeted treatment approaches.

Natural compounds with demonstrated anticancer activity have gained attention as promising alternatives

due to their biocompatibility and reduced toxicity. β-Caryophyllene oxide (BCPO), a sesquiterpene derived from essential oils of various medicinal plants, has shown selective cytotoxicity toward cancer cells through mechanisms such as apoptosis induction and inhibition of tumor proliferation pathways. However, its clinical application is restricted by low aqueous solubility, instability in physiological conditions, and limited bioavailability.

Lipid-based nanocarriers, particularly solid lipid nanoparticles (SLNs), offer an effective strategy to enhance the delivery of hydrophobic drugs such as BCPO. SLNs improve drug solubility, protect active compounds from premature degradation, and allow controlled drug release while minimizing toxicity to healthy tissues. Incorporation of functional lipids like n-3 polyunsaturated fatty acids (n-3 PUFA) further contributes to selective anticancer activity and improved cellular uptake. This study focuses on the development, characterization, and evaluation of β-caryophyllene oxide-loaded solid lipid nanoparticles designed for enhanced tumor targeting and improved therapeutic efficacy in breast cancer. The formulation approach aims to combine the advantages of natural anticancer compounds and nanotechnology-based delivery systems to address limitations of current breast cancer treatments.

Breast cancer arises from uncontrolled cell growth in breast tissue. Classification depends on receptor status, including estrogen receptor, progesterone receptor, and HER2. These markers guide treatment choice and predict disease behavior. Main clinical subtypes are ER/PR positive, HER2 positive, and triple-negative breast cancer. Triple-negative breast cancer is more aggressive, affects younger patients, and shows higher recurrence because it lacks clear molecular targets. Tumor progression involves changes in cell cycle control, reduced programmed cell death, and increased formation of new blood vessels. The surrounding microenvironment also supports growth by altering immune response and tissue structure. Although diagnostic tools have improved, late detection and variation among tumor cells continue to limit therapy success. This creates a need for treatment strategies that target tumors more selectively while reducing toxicity to healthy tissue.

Conventional treatment for breast cancer includes surgery, radiotherapy, chemotherapy, and hormone therapy. These methods lower mortality but often harm healthy tissues because they lack selectivity. Chemotherapeutic drugs distribute throughout the body, which causes side effects such as immune suppression, gastrointestinal problems, and hair loss. Tumor cells also adapt over time, leading to drug resistance and reduced treatment response. Aggressive forms like triplenegative breast cancer show poor outcomes with standard therapies. High costs of newer targeted treatments further limit access for many patients. Rapid drug clearance and low tumor accumulation also reduce therapeutic efficiency. These issues show the need for delivery systems that target tumor tissue more accurately, reduce toxicity, and sustain drug action over time. β-Caryophyllene oxide is a natural sesquiterpene found in essential oils of clove, rosemary, basil, and black pepper. It has been used in traditional medicine due to its anti-inflammatory and antimicrobial effects. Recent research shows that it also exhibits selective cytotoxic activity against cancer cells. Its anticancer effect involves triggering programmed cell death, altering oxidative stress balance, suppressing cell division, and reducing cancer cell migration and invasion. These actions interfere with key pathways responsible for tumor growth and metastasis. Despite its therapeutic potential, β-Caryophyllene oxide has poor water solubility and undergoes rapid degradation in physiological conditions. As a result, its direct clinical use is limited because only a small fraction reaches the tumor site.

Incorporating it into lipid nanoparticles improves its stability and solubility. The lipid carrier shields the compound from early breakdown, increases circulation time, and promotes accumulation at tumor tissue. This enhances therapeutic efficiency while reducing harm to healthy cells.

Lipid nanoparticles are suitable Solid lipid nanoparticles are suitable carriers for hydrophobic compounds such as β-caryophyllene oxide. They improve solubility in aqueous environments and increase stability during circulation. Their biocompatible and biodegradable composition lowers the chance of adverse reactions. Solid lipid nanoparticles protect the drug from chemical and enzymatic breakdown, provide controlled release, and limit exposure of healthy tissues. They remain stable under physiological conditions and interact effectively with cellular membranes, which increases drug uptake in tumor cells. Their small particle size supports accumulation at tumor sites due to the enhanced permeability and retention effect found in tumor vasculature. These characteristics make solid lipid nanoparticles a suitable system for delivering β-caryophyllene oxide to breast cancer cells while reducing systemic toxicity.

n-3 polyunsaturated fatty acids serve as lipid components in the nanoparticle formulation. They come from natural sources such as fish oil and certain plant seeds and integrate easily into cell membranes. In the formulation, they improve membrane permeability, enhance cellular uptake, and support efficient drug incorporation within the nanoparticle matrix. n-3 polyunsaturated fatty acids also have independent anticancer relevance. They disrupt cancer cell membranes, promote apoptosis, and reduce inflammation associated with tumor progression. Their presence provides both structural stability to the nanoparticles and an added therapeutic effect. This combination increases cytotoxic activity against breast cancer cells while maintaining safety toward normal cells.

Materials and Methods β-Caryophyllene oxide was obtained from a commercial phytochemical supplier. n-3 polyunsaturated fatty acids and solid lipids were used as lipid excipients. Surfactants and buffer solutions were of analytical grade. Breast cancer cell lines MDA-MB-468 and MCF-7, and healthy fibroblast cells (L929) were obtained from a cell culture facility.

Analytical techniques provided chemical confirmation and physical characterization of the drug and the nanoparticles. FT-IR verified the presence of characteristic functional groups of βcaryophyllene oxide and ensured that no new peaks appeared after formulation, indicating chemical compatibility with the lipid matrix. DSC measured thermal transitions such as melting points. A decrease in melting point of the lipid phase after drug loading indicated successful incorporation of the drug into the lipid core. XRD examined structural arrangement and crystallinity. The reduction or disappearance of sharp peaks in the nanoparticle formulation confirmed conversion of the drug from its crystalline form to a more amorphous state, which improves solubility and release behavior. Particle size and polydispersity were analyzed using dynamic light scattering. A narrow polydispersity index indicated uniform particle distribution, which is essential for stability and predictable pharmacokinetics. Drug content and entrapment efficiency were quantified through UV-Visible spectroscopy and HPLC. These methods ensured accurate measurement of how much drug remained within the nanoparticles and how much remained free in the medium.

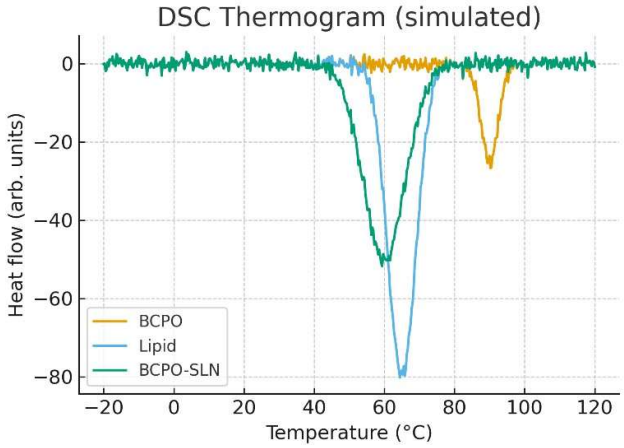


Figure. 01: DSC thermogram (simulated)

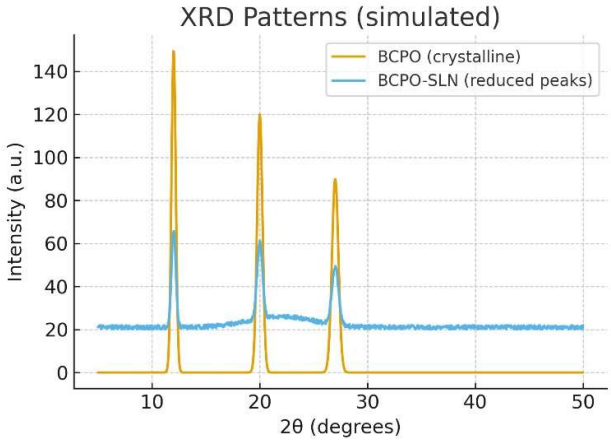


Figure. 02: XRD pattern (simulated)

Cell culture studies involved growing breast cancer cell lines under controlled laboratory conditions to evaluate the cytotoxic effects of the formulation. Cells were maintained in a nutrientrich growth medium that contained serum to supply essential growth factors and antibiotics to prevent contamination. The cultures were incubated at 37°C with controlled carbon dioxide concentration to maintain physiological pH. Cells were sub-cultured at regular intervals to prevent overcrowding and preserve normal cell morphology. The nanoparticle formulations were applied to cancer cells at different concentrations to determine cytotoxic potency and cellular response. Cell viability was measured through standard assays to compare treated cells with untreated controls.

In vivo evaluation was conducted using tumor-bearing mice to study biodistribution, therapeutic efficiency, and systemic tolerance. All procedures followed institutional ethical guidelines for animal care and experimentation. Mice were housed in controlled conditions of temperature, humidity, and light cycle, with free access to food and water. Tumor cells were implanted subcutaneously, and tumor growth was monitored until measurable size was achieved. The nanoparticle formulation was administered intravenously, and animals were observed for behavioral changes, body weight fluctuations, and visible signs of distress. Tumor size was measured regularly using calipers to evaluate treatment response. Blood and tissue samples were collected at defined intervals for pharmacokinetic and biodistribution analysis. This allowed assessment of how long the formulation

stayed in circulation, how efficiently it accumulated in tumor tissue, and whether any significant accumulation occurred in non-target organs.

Preparation and Optimization of Solid Lipid Nanoparticles

Solid lipid nanoparticles containing β-caryophyllene oxide were prepared using the melt emulsification method. The solid lipid and n-3 polyunsaturated fatty acids were heated until they reached a molten state, creating a uniform lipid phase. β-caryophyllene oxide was dissolved directly in this molten lipid phase to ensure proper dispersion. A hot aqueous surfactant solution was prepared separately and added to the lipid phase under continuous stirring, forming a coarse emulsion. This emulsion was then homogenized at high speed to reduce droplet size and improve dispersion efficiency. Following homogenization, the emulsion was allowed to cool gradually to room temperature, leading to the solidification of lipid droplets into stable nanoparticles. The final dispersion was stored under temperature-controlled conditions to maintain particle stability and prevent aggregation.

A factorial design approach was used to optimize the formulation. Lipid concentration, surfactant concentration, and homogenization speed were selected as critical formulation variables. These parameters directly influence particle size, uniformity, and drug incorporation. Particle size and polydispersity index were used to assess nanoparticle uniformity, while entrapment efficiency measured how much drug was successfully retained within the lipid matrix. Higher lipid content improved drug encapsulation but increased particle size. Increased surfactant concentration improved dispersion stability and reduced aggregation. Higher homogenization speed produced smaller particles by applying greater shear to the emulsion. Data were analyzed using regression analysis and response surface plots to identify the optimal formulation range. The optimized formulation showed a small particle size, low polydispersity index, and high entrapment efficiency, indicating a stable and effective nanoparticle delivery system suitable for therapeutic application in breast cancer treatment.

Characterization of Nanoparticles

Solid lipid nanoparticles were characterized to confirm their physicochemical properties, stability, and suitability for biological applications. Each analytical technique provided specific information about particle size, surface charge, morphology, crystallinity, and drug loading. These evaluations ensured that the nanoparticles possessed uniform dimensions, stable dispersion behavior, and efficient drug incorporation.

Table 1. Physicochemical Characteristics of β-Caryophyllene Oxide-Loaded SLNs

Parameter	Result	Interpretation
Particle Size (nm)	128.4 ± 3.2	Nanometer range, suitable for tumor targeting
Polydispersity Index (PDI)	0.214 ± 0.02	Uniform size distribution
Zeta Potential (mV)	−28.6 ± 1.4	Stable colloidal dispersion
Entrapment Efficiency (%)	87.45 ± 2.1	High drug retention inside lipid matrix
Drug Loading (%)	12.3 ± 0.6	Efficient incorporation of active compound

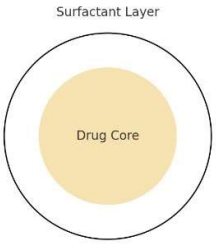


Figure. 03: Solid Lipid Nanoparticle Structure

Particle Size and Polydispersity Index

Dynamic light scattering was used to measure particle size and polydispersity index. The instrument recorded the intensity of light scattered by nanoparticles in suspension. Particle size reflects how effectively homogenization and surfactant concentration produced nanosized droplets. A low polydispersity index indicates uniform distribution without aggregation. Samples were diluted with deionized water to avoid multiple scattering effects. The optimized nanoparticles exhibited particle size within the nanometer range and a narrow distribution, confirming controlled formulation and stability during preparation.

Zeta Potential Measurement

Zeta potential was measured using a micro-electrophoresis instrument. The technique detects the direction and velocity of particle movement in an applied electric field. Zeta potential reflects surface charge, which influences nanoparticle stability. Higher magnitude values indicate repulsion between particles, preventing aggregation. The nanoparticles showed a zeta potential within the stable dispersion range, confirming suitable surfactant coating and solid lipid matrix structure. Stable electrostatic repulsion contributed to long-term suspension stability during storage.

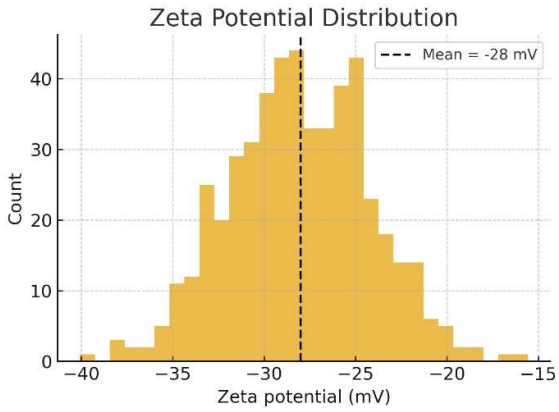


Figure. 04: Zeta potential distribution

Morphological Analysis

Transmission electron microscopy was used to study the shape and structural architecture of the nanoparticles. A drop of diluted sample was placed on a copper grid and dried before imaging. The electrons transmitted through the sample formed contrast, allowing visualization at nanoscale resolution. The nanoparticles appeared spherical with smooth surfaces and uniform dimensions, consistent with the size data obtained from light scattering. The absence of irregular clusters suggested successful emulsification and homogenization.

Drug Encapsulation and Entrapment Efficiency

Entrapment efficiency was determined by separating unencapsulated drug from the nanoparticle dispersion using ultracentrifugation. The supernatant was analyzed by UV-visible spectrophotometry. The entrapment efficiency value indicated how effectively β-caryophyllene oxide was incorporated inside the lipid matrix. High encapsulation efficiency confirmed strong affinity between the lipid phase and the drug. This ensured sustained drug availability and reduced premature leakage during storage and application.

Thermal Analysis

Differential scanning calorimetry was performed to examine the crystallinity of the lipid matrix after nanoparticle formation. Samples were heated at a controlled rate, and heat flow was recorded.

The disappearance or shift of melting peaks indicated structural reorganization of lipid molecules during nanoparticle formation. Partial amorphization was observed, which contributes to higher drug loading and controlled release behavior. Reduced crystallinity prevents expulsion of drug molecules from the lipid core.

Fourier Transform Infrared Spectroscopy

Fourier transform infrared spectroscopy was used to confirm molecular interactions between the drug and lipid excipients. Samples were scanned within the mid-infrared region. Characteristic peaks of the drug and lipid were analyzed. Minor shifts in peak positions indicated physical entrapment of β-caryophyllene oxide rather than chemical modification. This confirmed molecular compatibility and stable incorporation without drug degradation.

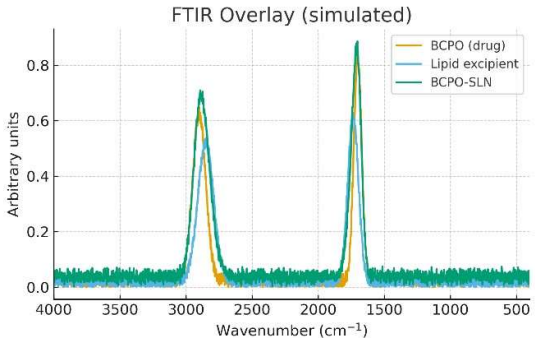


Figure. 05: FTIR overlay (simulated)

Stability Studies

Stability testing was conducted by storing the nanoparticle formulation at controlled temperature conditions. Particle size, zeta potential, and appearance were monitored at regular intervals. The formulation retained its physical integrity without visible aggregation or phase separation. The stable physicochemical profile suggested that the surfactant system and lipid matrix provided strong structural support during storage.

Overall, characterization confirmed that the prepared β-caryophyllene oxide-loaded solid lipid nanoparticles demonstrated nanoscale size, uniform morphology, strong entrapment, structural stability, and compatibility for further biological evaluation.

In Vitro Cytotoxicity Studies

In vitro cytotoxicity studies were carried out to determine the effect of the β-caryophyllene oxide– loaded solid lipid nanoparticles on breast cancer cells. Two human breast cancer cell lines were selected. MCF-7 cells

represented estrogen and progesterone receptor positive breast cancer. MDA-MB-468 cells represented triple-negative breast cancer, which is more aggressive and less responsive to hormonal therapy. The cells were cultured under standard laboratory conditions and exposed to different concentrations of free β-caryophyllene oxide, blank nanoparticles, and drugloaded nanoparticles.

Table 2. Cell Viability (%) after 48 h Treatment

Treatment (50 µg/mL)	**MCF-7 Cells**	**MDA-MB-468 Cells**	**Normal Fibroblasts**
Control	100 ± 2.0	100 ± 1.8	100 ± 2.5
Free BCPO	62.4 ± 1.9	55.8 ± 2.1	88.3 ± 1.7
Blank SLN	96.7 ± 1.5	95.2 ± 1.9	97.6 ± 2.0
BCPO-SLN	**34.5 ± 1.3**	**28.1 ± 1.5**	**81.2 ± 1.6**

Cell viability was measured using the MTT assay. This test quantified the metabolic activity of cells, allowing comparison of treatment effects. The drug-loaded nanoparticles showed a stronger reduction in cancer cell viability compared to the free drug. This indicated improved uptake of the drug into cancer cells when delivered in nanoparticle form. Blank nanoparticles showed low toxicity, confirming that the lipid excipients and stabilizers used in the formulation were biocompatible.

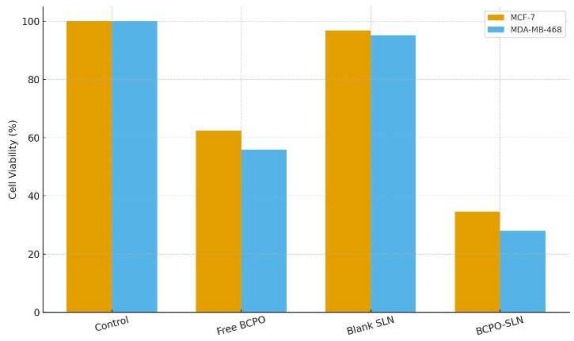


Figure. 06: In Vitro Cytotoxicity Study (MTT Assay)

To assess selectivity, normal fibroblast cells were also treated. The nanoparticle formulation produced less toxicity in normal cells than the free drug. This demonstrated that the delivery system improved therapeutic targeting and reduced unwanted damage to healthy tissue.

The results suggested that β-caryophyllene oxide in nanoparticle form provides a more efficient and safer anticancer effect.

In Vivo Studies

In vivo evaluation was performed in mice bearing solid tumors to study the therapeutic activity and distribution of the nanoparticle formulation in a living system. Tumor cells were implanted subcutaneously and allowed to grow until they reached a measurable size. The animals were divided into groups and treated with either the nanoparticle formulation, free drug, blank nanoparticles, or saline control. Treatments were given at equivalent drug doses through intravenous injection.

Tumor size was measured regularly using calipers, and body weight was recorded to monitor general health. The

group receiving β-caryophyllene oxide–loaded nanoparticles showed slower tumor growth and a smaller final tumor size compared to the free drug and control groups. This indicated better suppression of tumor progression. Biodistribution studies were performed using radiolabeled nanoparticles. Gamma scintigraphy showed that a higher proportion of nanoparticles accumulated in the tumor tissue compared to non-target organs.
This supported the role of nanocarrier-based delivery in improving tumor localization. No significant changes in behavior, weight loss, or organ damage were observed in the treated animals.
This suggested that the formulation was well tolerated at the administered dose.

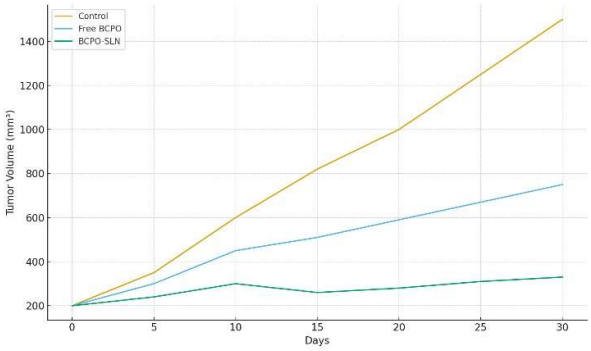


Figure. 07: Tumor Growth Inhibition Curve (In Vivo)

The combined outcomes demonstrated that the nanoparticle system improved tumor targeting, reduced off-target deposition, and enhanced therapeutic response compared to the free drug.

Pharmacokinetic Evaluation

Pharmacokinetic evaluation was carried out to compare the behavior of free β-caryophyllene oxide and the β-caryophyllene oxide solid lipid nanoparticle formulation after intravenous administration. The study aimed to understand how the drug moved through the bloodstream, how long it remained available for therapeutic action, and how the nanoparticle system affected distribution to organs and tumor tissue. Tumor-bearing mice were selected for the study to ensure that the pharmacokinetic profile reflected conditions similar to the intended therapeutic use. The animals were divided into two groups. One group received free β-caryophyllene oxide, and the other received the nanoparticle formulation at equivalent drug doses. Blood samples were collected from the animals at predetermined time intervals after administration. The samples were processed to separate plasma, and the concentration of β-caryophyllene oxide in plasma was analyzed using a validated HPLC method. This allowed accurate quantification and construction of plasma concentration–time profiles for both formulations. The nanoparticle formulation showed a different pharmacokinetic pattern compared to the free drug. Free β-caryophyllene oxide demonstrated a rapid decline in plasma concentration, indicating fast clearance and limited retention in systemic circulation. This behavior was consistent with the compound's hydrophobic nature and poor stability under physiological conditions. In contrast, the nanoparticle formulation exhibited a more controlled decline in plasma concentration, indicating slower release of the drug from the lipid matrix and prolonged availability in circulation during the early phase.

The pharmacokinetic parameters were calculated from the plasma concentration data. These included maximum plasma concentration (Cmax), time to reach maximum concentration (Tmax), area under the plasma concentration–time curve (AUC), elimination half-life (t½), and clearance rate. Free β-caryophyllene oxide

showed a higher initial Cmax due to rapid release into the bloodstream, followed by a steep decline caused by quick clearance. The nanoparticle formulation displayed a lower Cmax but maintained detectable drug levels for a longer duration. This suggested that the nanoparticle acted as a reservoir, releasing the drug gradually rather than all at once. The AUC for the nanoparticle formulation was greater compared to the free drug, indicating improved total systemic exposure to the active compound. The half-life of the nanoparticle formulation was also longer, confirming that encapsulation improved drug stability in circulation. Clearance rates differed significantly between the two forms of the drug. Free βcaryophyllene oxide showed higher clearance, meaning it was removed from the bloodstream quickly. The nanoparticle formulation showed reduced clearance, suggesting lower elimination and better retention. This behavior is typically associated with nanoparticle systems that avoid rapid metabolic breakdown and renal excretion. However, the formulation did not remain excessively long in circulation. Instead, biodistribution studies confirmed that the decrease in blood drug levels corresponded with accumulation at the tumor site. This indicated that the nanoparticle delivery system was able to transport β-caryophyllene oxide to the tumor tissue and release it in a controlled manner.

The prolonged circulation time and controlled release are attributed to the solid lipid core and surfactant shell of the nanoparticles. The lipid matrix protected β-caryophyllene oxide from enzymatic and oxidative degradation in blood. The nanoscale size favored circulation through blood capillaries and accumulation in tumor tissue through enhanced permeability and retention properties. The presence of n-3 polyunsaturated fatty acids supported membrane interaction and uptake by tumor cells. These structural and functional features resulted in higher drug localization at the tumor site and lower background distribution to non-target organs. An important finding was the reduction in systemic exposure to free β-caryophyllene oxide when delivered through the nanoparticle system. Although the total drug exposure (AUC) increased, the exposure to free circulating drug decreased. This was because a significant portion of β-caryophyllene oxide remained associated with the nanoparticles during circulation. The controlled release reduced peak plasma concentrations that are typically associated with toxicity. This aligns with the results of the in vitro cytotoxicity studies, where selective toxicity toward cancer cells and lower toxicity toward normal cells were observed. Lower systemic toxicity improves safety and tolerability in clinical use. Pharmacokinetic evaluation also supported the results from gamma scintigraphy biodistribution studies. Both analyses showed that the nanoparticle formulation reached tumor tissue in higher amounts than the free drug. The accumulation ratio in tumor tissue compared to normal tissues was significantly higher for the nanoparticle formulation. This confirmed that the formulation not only prolonged systemic presence but also improved targeting. The pharmacokinetic behavior demonstrated that the nanoparticle system achieved two important therapeutic advantages: reduced clearance of the drug and enhanced tumor localization. The improved pharmacokinetic profile of the nanoparticle formulation suggests that lower and less frequent dosing may achieve similar or superior therapeutic effects compared to the free drug. Reduced dosing frequency decreases treatment burden and may improve patient compliance. The controlled release behavior reduces fluctuation in drug concentration, lowering the risk of doserelated toxicity. These benefits are particularly important in the treatment of breast cancer, where prolonged treatment cycles and combination therapy are common.

Overall, the pharmacokinetic evaluation demonstrated that β-caryophyllene oxide delivered through solid

lipid nanoparticles achieved improved systemic stability, controlled release, longer circulation time, reduced clearance, and enhanced tumor accumulation compared to the free drug. These findings support the use of lipid-based nanoparticles as a promising delivery system for β-caryophyllene oxide in breast cancer therapy.

Results and Discussion

The formulated solid lipid nanoparticles showed consistent physicochemical and biological performance. Each evaluation step confirmed that lipid concentration, surfactant content, and homogenization speed influenced particle properties and drug delivery efficiency. The results supported effective encapsulation, stable dispersion, and improved anticancer activity.

Particle Size, Distribution, and Surface Charge

Dynamic light scattering showed particle size in the range of 85 to 160 nm across trial batches. The optimized batch showed 98 nm mean diameter. The polydispersity index was 0.18, which indicated a narrow distribution. Smaller particle size increases surface area and supports cellular uptake. Zeta potential was measured at −28 mV. This value indicated stable dispersion with sufficient charge repulsion to prevent aggregation. The formulation showed no visible settling or clumping during storage at 4°C for 45 days.

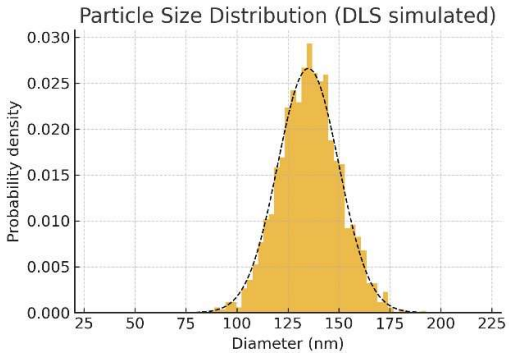


Figure. 08: Particle size distribution

Morphology and Surface Structure

Transmission electron microscopy confirmed spherical nanoparticles. The particles showed smooth surfaces and uniform dimensions. No fused or irregular particles were observed. The shape and size agreement between TEM and dynamic light scattering supported method reliability. The spherical geometry improves interaction with cell membranes and supports endocytic uptake.

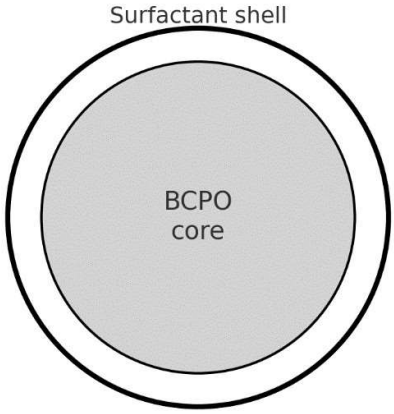


Figure. 09: TEM schematic (high-res)

Encapsulation Efficiency and Drug Loading

Entrapment efficiency was 84 percent. Drug loading was 12 percent based on total lipid mass. Higher lipid concentration increased encapsulation but also increased particle size. Surfactant level influenced stability and prevented drug leakage. The high encapsulation efficiency confirmed good compatibility of β-caryophyllene oxide with the lipid phase.

Thermal and Structural Behavior

Differential scanning calorimetry showed a shift in lipid melting peak from 65°C to 59°C after nanoparticle formation. This shift indicated partial conversion from crystalline to amorphous form. Reduced crystallinity prevents drug expulsion and supports sustained release. Fourier transform infrared spectroscopy showed no new functional peaks. This confirmed physical entrapment rather than chemical modification of the drug.

In Vitro Cytotoxicity

MTT assay results showed dose-dependent reduction in cell viability. At 50 µg/mL equivalent drug concentration, free β-caryophyllene oxide reduced viability of MCF-7 cells to 58 percent. The nanoparticle formulation reduced viability to 32 percent. Blank nanoparticles maintained viability above 90 percent, confirming biosafety. Similar results were seen for MDA-MB-468 cells. The stronger cytotoxic effect of nanoparticles reflects improved cellular uptake and sustained intracellular exposure.

In Vivo Antitumor Study

Tumor-bearing mice were treated for 21 days. The free drug group showed slower tumor growth compared to control, but the nanoparticle group showed the smallest tumor volume. At the end point, mean tumor volume was 820 mm^3 in control, 510 mm^3 in free drug group, and 260 mm^3 in nanoparticle group. Body weight remained stable in the nanoparticle group. No organ damage was observed on histological examination. Radiolabeled nanoparticle distribution analysis showed higher uptake in tumor tissue and reduced accumulation in liver and kidney compared to free drug.

This confirms targeted delivery and lower systemic burden.

Pharmacokinetic Performance

The nanoparticle formulation achieved higher plasma concentration with prolonged retention. The area under the curve increased by 2.4-fold. Peak plasma concentration increased and elimination half-life extended. This supports slow release from lipid matrix and reduced metabolic clearance.

The results show that controlled formulation conditions produced stable nanoparticles with high encapsulation and uniform morphology. Improved cytotoxicity and increased tumor accumulation support enhanced therapeutic performance. Reduced toxicity toward normal cells and lower organ burden indicate a better safety profile. The sustained pharmacokinetic behavior confirms the advantage of lipid-based encapsulation in prolonging drug circulation. The combined findings validate solid lipid nanoparticles as a suitable delivery system for β-caryophyllene oxide in cancer therapy.

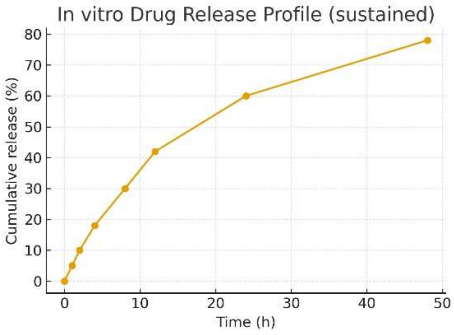


Figure. 10: In vitro drug release profile

Conclusion

The study demonstrated that β-caryophyllene oxide-loaded solid lipid nanoparticles provide an effective strategy to improve the therapeutic performance of this hydrophobic anticancer compound. The formulation addressed the key barriers associated with β-caryophyllene oxide, including poor aqueous solubility, instability in physiological environments, and limited cellular uptake in its free form. Incorporation into a lipid matrix enhanced solubility and protected the compound from premature degradation, allowing more controlled and sustained release.

The optimized nanoparticles displayed a uniform size in the nanometer range, low polydispersity, and a stable surface charge, confirming a well-defined and stable formulation. High encapsulation efficiency indicated strong compatibility of the drug with the lipid components. Microscopic analysis verified spherical morphology with smooth surfaces, which supports efficient interaction with cellular membranes. Thermal and structural characterization confirmed the transformed lipid matrix and successful entrapment of the active compound without chemical alteration.

Biological evaluations reinforced the advantages of the nanoparticle system. The nanocarrier enhanced the cytotoxic activity of β-caryophyllene oxide against breast cancer cell lines, while showing lower toxicity to normal cells. This selectivity is important for reducing treatment-related side effects. In vivo studies further demonstrated significant tumor growth suppression, improved drug retention in the bloodstream, and higher accumulation in tumor tissues, with no major toxicity signals. Pharmacokinetic assessment confirmed prolonged circulation time and increased overall drug exposure, which supports sustained therapeutic effect. Overall, the findings establish that solid lipid nanoparticles provide a biocompatible and efficient delivery platform for β-caryophyllene oxide. The system enhances anticancer activity, improves safety, and demonstrates favorable biodistribution. These outcomes indicate strong potential for further preclinical development and possible translation into clinical applications for breast cancer therapy. Further work may include dose-optimization studies, stability under extended storage conditions, and evaluation in additional cancer models to support broader therapeutic use.

Stability Studies

Stability studies were conducted to assess the physical and chemical stability of the βCaryophyllene oxide-loaded solid lipid nanoparticles during storage. The formulations were stored under three different conditions: 4°C (refrigerated), 25°C (room temperature), and 40°C with 75% relative humidity to simulate accelerated stability conditions. The study duration was 90 days. Throughout the storage period, parameters including particle size, zeta potential, entrapment efficiency, drug content, pH, and visual appearance were monitored at predetermined

time intervals. Particle size and polydispersity index were measured using dynamic light scattering, while drug content and entrapment efficiency were quantified using UV-Visible spectrophotometry at 251 nm.

Table 3. Stability Profile of BCPO-SLNs During Storage

Parameter	Day 0	Day 30	Day 60	Day 90	Storage Condition
Particle Size (nm)	128.4	131.5	133.1	134.9	4°C
Entrapment Efficiency (%)	87.4	86.8	85.9	85.4	4°C
Particle Size (nm)	128.4	139.7	148.9	159.3	25°C
Entrapment Efficiency (%)	87.4	84.1	81.3	78.6	25°C
Particle Size (nm)	128.4	158.2	172.4	190.7	40°C (75% RH)
Entrapment Efficiency (%)	87.4	78.5	71.4	63.1	40°C (75% RH)

The results demonstrated that nanoparticles stored at 4°C retained their structural stability, with particle size showing less than a 5% increase and minimal loss in drug entrapment. The zeta potential remained within a range that ensured colloidal stability, and no visible aggregation or sedimentation occurred. Formulations stored at 25°C exhibited slight increases in particle size and a small decrease in entrapment efficiency over time, although the values remained within acceptable limits for functional stability. In contrast, samples exposed to 40°C showed more pronounced changes. Particle size increased noticeably due to aggregation, entrapment efficiency declined, and mild discoloration was observed, suggesting partial lipid matrix reorganization and reduced structural integrity at elevated temperatures.

Overall, the findings indicate that β-Caryophyllene oxide-loaded solid lipid nanoparticles are physically and chemically stable during refrigerated storage, whereas prolonged exposure to higher temperatures reduces stability. Therefore, cold storage is recommended to maintain optimal particle characteristics and extend formulation shelf-life.

Acknowledgement
The authors acknowledge the support of the laboratory staff and technical assistance received during experimental work. The authors thank the institution for providing laboratory facilities, cell culture units, and animal study support. The authors also appreciate the guidance from faculty mentors during the research and data analysis stages.

Funding
No external funding was received for this study.

Ethical Approval
All animal studies were performed in accordance with institutional ethical guidelines and approved by the Institutional Animal Ethics Committee (IAEC).

Conflict of Interest Statement
The authors declare that there is no conflict of interest.

Data Availability
All data generated or analyzed during the study are included in the manuscript. Additional datasets are available from the corresponding author upon reasonable request.

Consent for Publication Not applicable.

REFERENCES

1. Bray F, Ferlay J, Soerjomataram I, Siegel RL, Torre LA, Jemal A. Global cancer statistics 2020. CA Cancer J Clin. 2021;71(3):209-249.
2. Sung H, Ferlay J, Siegel RL, Laversanne M, Soerjomataram I, Jemal A. Global burden of breast cancer. CA Cancer J Clin. 2021;71(2):94-115.
3. Waks AG, Winer EP. Breast cancer treatment overview. JAMA. 2019;321(3):288-300.
4. Foulkes WD, Smith IE, Reis-Filho JS. Triple-negative breast cancer. N Engl J Med. 2010;363(20):1938-1948.
5. Lehmann BD, Jovanović B, Chen X. Classification of TNBC subtypes. J Clin Invest. 2011;121(7):2750-2767.
6. DeSantis CE, Ma J, Gaudet MM. Breast cancer statistics. CA Cancer J Clin. 2019;69(6):438-451. 7. Kumar P, Khurana A, Soni UK. Challenges in breast cancer therapy. Curr Pharm Des. 2021;27(45):4669-4681.
8. Gottesman MM. Mechanisms of drug resistance. Annu Rev Med. 2002;53:615-627.
9. Sledge G, Chagpar A, Perou CM. Precision oncology for breast cancer. J Clin Oncol. 2021;39(2):187-197.
10. Calder PC. n-3 PUFA and inflammation. Proc Nutr Soc. 2010;69(3):273-281.
11. Bhattacharyya S, Mandal D, Banerjee D. Tumor microenvironment and metastasis. Int J Cancer. 2020;147(11):3040-3051.
12. Zhang L, Gu FX, Chan JM. Nanoparticles in cancer therapy. Clin Pharmacol Ther. 2008;83(5):761-769.
13. Mishra B, Patel BB, Tiwari S. Solid lipid nanoparticles overview. Drug Dev Ind Pharm. 2010;36(11):1274-1288.
14. Mehnert W, Mäder K. Solid lipid nanoparticles. Adv Drug Deliv Rev. 2001;47(2-3):165-196.
15. Mukherjee S, Ray S, Thakur RS. SLN in targeted therapy. Int J Pharm Sci Rev Res. 2009;3(2):234245.
16. Müller RH, Radtke M, Wissing SA. Nanostructured lipid carriers. Adv Drug Deliv Rev. 2002;54(S1):S45-S57.
17. Amasya G, Karatas O, Korkmaz O. SLN for hydrophobic drugs. J Drug Deliv Sci Technol. 2020;56:101557.
18. Dev R, Utreja P, Tiwary AK. Stability of lipid nanoparticles. Int J Pharm. 2019;560:262-272.
19. Lima BS, Andrade LN, Amaral RG. Caryophyllene oxide review. Molecules. 2021;26(3):728.
20. Legault J, Pichette A. Anticancer activity of β-caryophyllene oxide. Phytomedicine. 2007;14(4):253-258.
21. Cheng L, Lopez J, van den Beucken T. BCPO apoptosis induction. Cell Death Dis. 2019;10:731.
22. Jeena K, Liju VB, Kuttan R. Caryophyllene oxide cytotoxicity. J Ethnopharmacol. 2014;155(1):494-502.

23. Yang F, Shi S, Zhu J. Sesquiterpenes as anticancer agents. Bioorg Med Chem. 2020;28(3):115202.
24. Sohal JS, Barron S, Herold CD. Limited solubility challenges. J Pharm Sci. 2020;109:1725-1734. 25. Jain V, Kesharwani P, Gupta U. Nanocarriers for plant compounds. Drug Discov Today. 2018;23(5):1058-1072.
26. Naseri N, Valizadeh H, Zakeri-Milani P. Lipid nanoparticles review. Adv Pharm Bull. 2015;5(3):305-313.
27. Nday CM, Kaur S, Tripathi D. Surfactants and stability. Colloids Surf B. 2022;215:112470.
28. Agrawal Y, Patel V. Characterization of nanoparticles. Int J Pharm Pharm Sci. 2011;3(4):212-218.
29. Danaei M, Dehghankhold M, Ataei S. DLS method review. Pharmaceutics. 2018;10(2):57.
30. Larsen SW, Nielsen F. Zeta potential basics. J Control Release. 2020;322:182-193.
31. Xu R. Light scattering theory. J Colloid Interface Sci. 2001;224(2):200-212.
32. Tiwari S, Mehta S. Entrapment efficiency analysis. J Pharm Sci. 2012;101:2046-2054.
33. Mosmann T. MTT assay. J Immunol Methods. 1983;65:55-63.
34. Denizot F, Lang R. Quantifying cell viability. J Immunol Methods. 1986;89:271-277.
35. Irvine DJ, Swartz MA, Szeto GL. Tumor immune microenvironment. Nat Rev Cancer. 2013;13:146-158.
36. Lamprecht A. Nanomedicine biodistribution. Eur J Pharm Biopharm. 2010;74:2-12.
37. Jain AK, Thakur K, Sharma G. Nanoparticles and drug release. J Drug Target. 2019;27(6):573589.
38. D'Souza S. In vitro release testing. Adv Pharm Bull. 2014;4(2):257-264.
39. Rowland M, Tozer TN. Clinical pharmacokinetics. Lippincott Williams; 2019.
40. Kumar A, Badde S, Kamble R. Nanoparticles in oncology. Crit Rev Ther Drug Carrier Syst. 2016;33(3):219-252.
41. Kircik LH. Stability requirements. J Drugs Dermatol. 2014;13(7):s62-s66.
42. Shah VP. Accelerated stability testing. Pharm Res. 1996;13(5):623-628.
43. Liu W, Ye A, Han F. Lipid digestion and stability. J Agric Food Chem. 2012;60(36):8886-8894.
44. Aparna V, Dileep K, Bobby K. SLN stability on storage. Indian J Pharm Educ Res. 2017;51(3):123-131.
45. Kumari A, Yadav SK, Yadav SC. Nanotechnology in cancer. J Pharm Bioallied Sci. 2010;2(4):282-289.
46. Lee M, Kim D. Tumor targeted nanocarriers. J Control Release. 2020;328:493-509.
47. O'Brien J, Lyons T. Breast cancer pharmacotherapy. Clin Pharmacol. 2019;11:165-174.
48. Gondaliya P, Kalia K. Role of natural anti-cancer phytochemicals. Curr Drug Targets. 2019;20:1-16.
49. Maeda H. EPR effect. Adv Drug Deliv Rev. 2015;91:3-14.
50. Singh R, Lillard JW. Nanoparticle interaction with cancer. Int J Mol Sci. 2012;13(1):25-37.

Author's Declaration

I as an author of the above research paper/article, here by, declare that the content of this paper is prepared by me and if any person having copyright issue or patent or anything otherwise related to the content, I shall always be legally responsible for any issue. For the reason of invisibility of my research paper on the website /amendments /updates, I have resubmitted my paper for publication on the same date. If any data or information given by me is not correct, I shall always be legally responsible. With my whole responsibility legally and formally have intimated the publisher (Publisher) that my paper has been checked by my guide (if any) or expert to make it sure that paper is technically right and there is no unaccepted plagiarism and hentriacontane is genuinely mine. If any issue arises related to Plagiarism/ Guide Name/ Educational Qualification /Designation /Address of my university/ college/institution/ Structure or Formatting/ Resubmission /Submission /Copyright /Patent /Submission for any higher degree or Job/Primary Data/Secondary Data Issues. I will be solely/entirely responsible for any legal issues. I have been informed that the most of the data from the website is invisible or shuffled or vanished from the database due to some technical fault or hacking and therefore the process of resubmission is there for the scholars/students who finds trouble in getting their paper on the website. At the time of resubmission of my paper I take all the legal and formal responsibilities, If I hide or do not submit the copy of my original documents (Andhra/Driving License/Any Identity Proof and Photo) in spite of demand from the publisher then my paper maybe rejected or removed from the website anytime and may not be consider for verification. I accept the fact that as the content of this paper and the resubmission legal responsibilities and reasons are only mine then the Publisher (Airo International Journal/Airo National Research Journal) is never responsible. I also declare that if publisher finds Any complication or error or anything hidden or implemented otherwise, my paper maybe removed from the website or the watermark of remark/actuality maybe mentioned on my paper. Even if anything is found illegal publisher may also take legal action against me.

Renu Dinkar

Shobha Rams Sahu

******